OHIO STATE UNIVERSITY
JUN 7 1960
LIBRARY

BULLETIN

OF THE

CHEMICAL SOCIETY OF JAPAN

Vol. 33 No. 4 April 1960

CONTENTS

CHEMISTRY HALL LIBRARY

General and Physical

T. TAKAGI and T. ISEMURA: Interaction of Surface Active Agent with Amylose 437

H. HOTTA, A. TERAKAWA and S. ŌNO: Oxidation of Ferrous Ions in the Aqueous Ferrous-Cupric System. I. Effect of Cobalt-60 Gamma-Rays 442

T. TANAKA: Vibrational Spectra of Methyltrimethoxysilane 446

A. HAYAKAWA and K. TANAKA: Detection of Chromatogram by Swelling of Adsorbent 452

K. MAEDA: Some Characteristics of Zinc Oxide Phosphor 456

M. NAKAGAKI: Theory on the Small Angle Scattering of Light to Determine the Shape, Size and Orientation of High Polymer Molecules in Flow. 476

T. NAKAI, S. YAJIMA, K. SHIBA, J. OSUGI and D. SHINODA: The Behavior of Fission Products Captured in Graphite Powder by Nuclear Recoil. I. The Stability of the Fission Products toward Nitric Acid Solution. 494

T. NAKAI, S. YAJIMA, K. SHIBA, J. OSUGI and D. SHINODA: The Behavior of Fission Products Captured in Graphite by Nuclear Recoil. II. The Diffusion of Xenon-135 in Graphite at a High Temperature 497

S. TOYODA: Expansion of Nakano's Results on High Frequency Titration using the Resistance-type Instrument 504

T. WATANABE: Studies on Thixotropy. II. On the Thixotropic Gel Structure of Bentonite. . . 523

Y. KUBOKAWA: Chemisorption on Hydrogen on Zinc Oxide. I. Rate of Desorption and Adsorption Isotherm. 546

Y. KUBOKAWA: Chemisorption of Hydrogen on Zinc Oxide. II. Rate of Chemisorption and Heterogeneity of the Surface of Zinc Oxide 550

Y. KUBOKAWA: Carbon Monoxide Chemisorption on Zinc Oxide. 555

Analytical and Inorganic

S. YAMADA, H. YAMAZAKI, H. NISHIKAWA and R. TSUCHIDA: Absorption Spectra of Metallic Complexes with Aromatic Molecules 481

T. ISHIMORI: The Nitrogen Isotopic Equilibrium between Ammonia and Ammonium Ion . . . 516

T. ISHIMORI: Nitrogen Isotopic Equilibria between Ammonia and Metal-ammine Complex Ions in Aqueous Solution 520

Organic and Biological

M. NAKAGAWA and T. AKAGAMI: Crystalline Adducts of Dicyclohexylamine with Di- and Triols. 433

F. MUKAWA: 5, 6-Epoxy-cholestane 450

T. MUKAI: Structure of Namakochrome. I. 453

M. NAKAZAKI: Twofold Wagner-Meerwein Type Rearrangement of 2, 3-Disubstituted Indoles . . 461

(Continued on inside cover)

Published by the Chemical Society of Japan

THE CHEMICAL SOCIETY OF JAPAN

(NIPPON KAGAKUKAI)

Founded in 1948

Successor to the former Chemical Society of Japan founded in 1878 and to the Society of Chemical Industry, Japan founded in 1898.

OFFICERS

Shoichiro NAGAI, *President*, Nihon University, Tokyo
Eiichi IWASE, *Vice-President*, Institute of Physical and Chemical Research, Tokyo
Wasaburo KIMURA, *Vice-President*, Nagoya University
Sojiro OKA, *Vice-President*, The University of Tokyo
Ichiro SAKURADA, *Vice-President*, Kyoto University
Hiroshi SOBUE, *Vice-President*, The University of Tokyo

BULLETIN OF THE CHEMICAL SOCIETY OF JAPAN

Editor: Yoshiyuki URUSHIBARA, The University of Tokyo, Tokyo
Assistant Editor: Saburo NAGAKURA, The University of Tokyo, Tokyo
Editorial Board:

Toshio ANDO	Ichiro MIYAGAWA	Tadashi SUEHIRO
Yoshié BANSHO	Masazumi NAKAGAWA	Kenzi TAMARU
Hidehiro GOTÔ	Koji NAKANISHI	Takeo WATASE
Yoshimasa HIRATA	Shigeo OKUMURA	Iwao YASUMORI
Kenichi HONDA	Kazuo SAITO	Tsuneo YOSHINO
Sunao IMANISHI	Naoyasu SATA	Koshiro YOSHIOKA

(*Continued from outside cover*)

M. NAKAZAKI, K. YAMAMOTO and K. YAMAGAMI: Mechanism of Plancher's Rearrangement. I. Twofold Wagner-Meerwein Type Rearrangement of Indolenines 466

M. NAKAZAKI: Mechanism of Plancher's Rearrangement. II. Twofold Wagner-Meerwein Type Rearrangement of Indolenium Compounds 472

M. IMOTO and M. KINOSHITA: Vinyl Polymerization. XLIII. Polymerization of Styrene with Vinylmagnesium Chloride 490

T. SATO: Conformation of Biaryls. Dipole Moment Measurements of *o*-Methylbiphenyls . . . 501

S. MORITA: Vapor Phase Oxidation of Methyl Naphthalenes 511

M. ITO: Hydrolysis of 7-Anilinobenzyl-8-quinolinol 527

K. YAMAGISHI, K. ARAKI, T. SUZUKI and T. HOSHINO: The Photochemical Addition Reaction. VI. The Mechanism of the Addition Reaction of *n*-Butyl Mercaptan to Vinyl Acetate 528

A. WATANABE: Synthesis and Physical Properties of Normal Higher Alcohols. II. Synthesis of Normal Higher Primary Alcohols of Odd Carbon Numbers from Heptacosanol to Heptatriacontanol 531

N. EBARA: Benzylideneaniline. I. Structure and Ultraviolet Absorption Spectrum of Benzylideneaniline 534

N. EBARA: Benzylidene aniline. II. Iodine Complexes of Benzylideneaniline and its Derivatives. 540

S. TANAKA, H. HATANO and O. ITASAKA: Biochemical Studies on Pearl. IX. Amino Acid Composition of Conchiolin in Pearl and Shell 543

Short Communications

H. OKUDA: Formation of Mullite from Kaolin Minerals at Low Temperature 560

H. HAMAGUCHI, J. HASHIMOTO, K. HOSOHARA and Y. NARUSAWA: A New Application of Neutron Activation Analysis to the Polarography of Holmium. 562

M. SENŌ, T. SAITŌ and T. YAMABE: Transport Behavior of Ferric, Aluminum and Cupric Ions across the Alginate and the Other Membranes. 563

S. OKAZAKI and T. SASAKI: Two Types of Antifoamers and their Cooperating Action. 564

T. HAYASHI and K. MAEDA: Preparation of a New Phototropic Substance. 565

S. NISHIMURA: Hydrogenation and Hydrogenolysis. III. Rhodium-Platinum Oxide as a Catalyst for the Hydrogenation of the Aromatic Nucleus. 566

H. SUGINOME and T. IWADARE: The Synthesis of the Pterocarpin Ring System 567

Crystalline Adducts of Dicyclohexylamine with Di- and Triols

By Masazumi NAKAGAWA and Takashi AKAGAMI*

(Received August 6, 1959)

It has been reported briefly in the literatures that dicyclohexylamine forms crystalline addition compounds with hydroxy compounds such as water[1], ethanol[1], cyclohexanols[2] and cyclohexanediols[2]. An accidental observation of the formation of a white precipitate by mixing dicyclohexylamine with ethylene glycol urged the present authors to a more detailed study on the adducts.

When an acetone solution of dicyclohexylamine was mixed with some di- or tri-hydroxy compounds in the same solvent, immediate precipitation of very fine silky needles accompanied by an evolution of heat was observed. The crystals thus obtained could be easily recrystallized from acetone to give a pure adduct. The melting points, the analytical data of nitrogen and the composition of the adducts with various glycols are summarized in Table I.

It is to be noted that in spite of the remarkable change in the structure of glycols, the composition of the adducts with glycols was always in a ratio of 1 : 2. These results are inconsistent with those of Winans[2] who reported the composition of the adducts with diols is 1 : 1 so far as he studied**.

The properties of the adducts with several kind of triols are listed in Table II together with its analytical data.

In these cases the molar ratio of the triol against the amine was found to be 1 : 3 excepting the case of glycerol in which it was found to be 2 : 3.

These adducts are readily soluble in common organic solvents and are especially easily recrystallized from acetone. The adducts are decomposed into the components by the addition of water. The most striking property of the

TABLE I. ADDUCTS OF DICYCLOHEXYLAMINE WITH GLYCOLS

Glycol	m. p. °C	N(%) Found	N(%) Calcd.	Molar ratio Glycol : Amine
Ethylene glycol	70	6.60	6.60	1 : 2
1,2-Propanediol	49～49.5	6.28	6.39	1 : 2
1,3-Propanediol	53	6.32	6.39	1 : 2
1,4-Butanediol	68～69	6.13	6.19	1 : 2
2,3-Butanediol	63.5～64.5	6.11	6.19	1 : 2
1,3-Butanediol	below room temp	5.96	6.19	1 : 2
2(*cis*)-1,4-Butenediol	49.5～51	6.14	6.22	1 : 2
2(*trans*)-1,4-Butenediol	68～69	6.22	6.22	1 : 2
2-Butyne-1,4-diol	59.5	6.14	6.24	1 : 2
1,5-Pentanediol	39.5～42	6.02	6.00	1 : 2
1,6-Hexanediol	59.5～60.5	5.68	5.83	1 : 2
2,4-Hexadiyne-1,6-diol	68.5～69	5.96	5.95	1 : 2
1,7-Heptanediol	58～59	5.72	5.67	1 : 2
Diethylene glycol	25～25.5	5.65	5.98	1 : 2
Hydrocinnamoin	151.5～152	4.63	4.45	1 : 2
1,4-Di-(β-phenyl-α-hydroxyethyl)-benzene	78.5～80	3.96	4.11	1 : 2

TABLE II. ADDUCTS OF DICYCLOHEXYLAMINE WITH TRIOLS

Triol	m. p. °C	N(%) Found	N(%) Calcd.	Molar ratio Triol : Amine
Glycerol	38.5～39.5	5.75	5.77	2 : 3
1,2,4-Butanetriol	46～47	6.44	6.46	1 : 3
(−)-1,2,5-Pentanetriol	27～28	6.09	6.34	1 : 3
1,2,6-Hexanetriol	49～50	6.04	6.20	1 : 3

* Sansuisoyushi Industrial Co., Ltd., Kyoto.

1) G. Fouque, *Compt. rend.*, **166**, 394 (1918).
2) G. F. Winans, *J. Am. Chem. Soc.*, **61**, 3591 (1939).

** Winans prepared the adducts using petroleum ether or ether as solvent.

CHEMISTRY MAIN LIBRARY

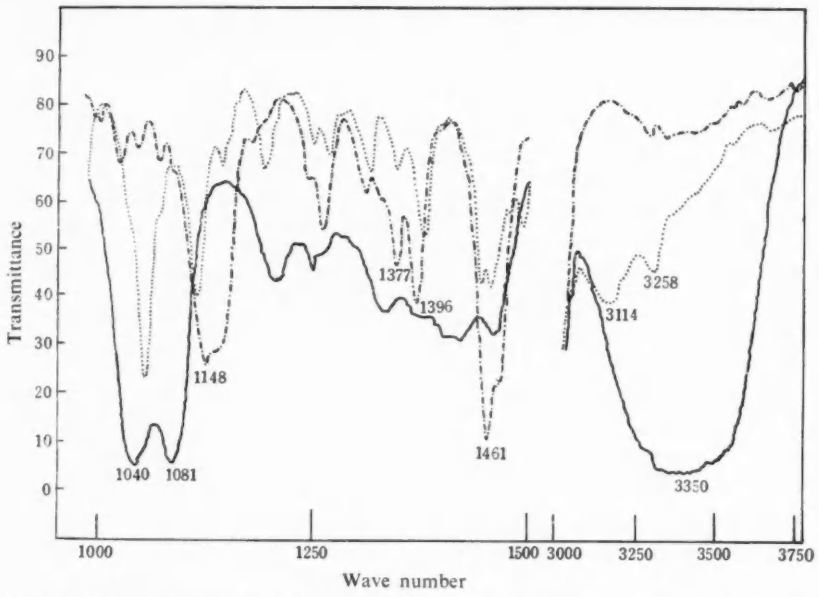

Fig. 1. The I. R. spectra of dicyclohexylamine (·-·-·), ethylene glycol (——) and the adduct with ethylene glycol (····).

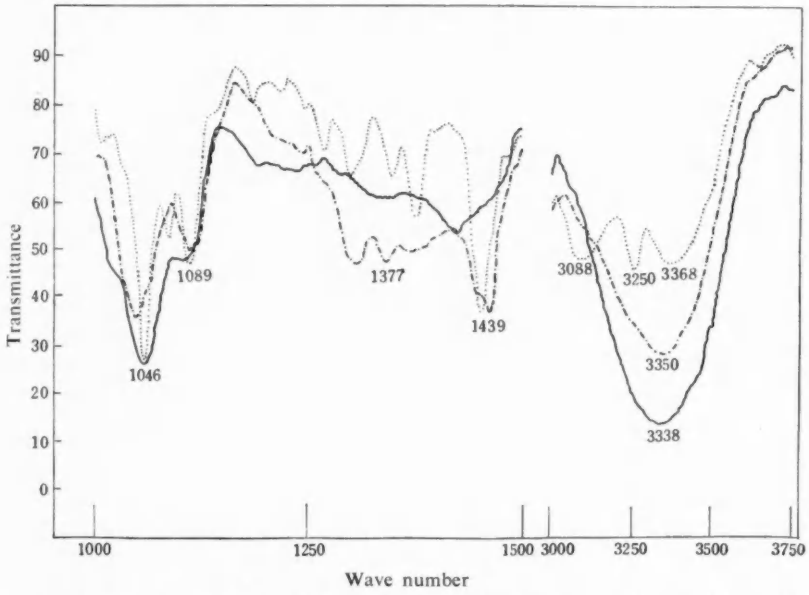

Fig. 2. The I. R. spectra of 1, 2, 4-butanetriol (——), the adduct with 1, 2, 4-butanetriol (····) and the adduct with glycerol (·-·-·).

adducts with diols is its tendency to sublime. When a crystalline adduct with a diol placed in an evacuated sealed tube is heated below its melting point, a rapid growth of beautiful silky needles on the cold wall of the tube can be observed.

The tendency of sublimation is characteristic of the adducts with glycols and can not be seen with the adducts with triols.

The existence of intermolecular polymeric association due to hydrogen bond in hydroxy compounds is well known, and the presence of this type of hydrogen bonds in ethylene glycol and in 1, 2, 4-butanetriol was revealed by the presence of a very broad absorption at 3350 and 3338 cm^{-1} in the infrared spectra of these alcohols as illustrated in Figs. 1 and 2. The diol and the triol also show a broad and strong absorption in the range of 1300～1440 cm^{-1} presumably arising from deformation of the associated hydroxy group or the streching of C–O of the associated hydroxy group. Also the infrared spectrum of dicyclohexylamine shows a broad absorption in the region of 3100～3500 cm^{-1} indicating the presence of associated N–H group. On the other hand, the infrared spectrum of the adduct with ethylene glycol showed two absorption peaks at 3114 and 3258 cm^{-1} instead of the broad absorption band of the glycol at 3350 cm^{-1} (Fig. 1).

Remarkable change in absorption was also observed in the range of 1300～1440 cm^{-1}. The broad absorption in the spectrum of ethylene glycol in this region disappeared in the spectrum of the adduct.

These spectroscopic evidences indicate that the formation of amine-glycol adduct is attributed to the formation of new strong intermolecular O—H···N hydrogen bonds destroying the original polymeric intermolecular hydrogen bonds which exist in ethylene glycol and in dicyclohexylamine. These arguments are consistent with the fact that the amine-diol adducts are easy to sublime. The formation of such a type of an "addition compound" in solution has been pointed out by several investigators[3]. The absorption band at ca. 3326 cm^{-1} in the infrared spectrum of the system of alcohol-amine-solvent was attributed to the formation of an amine-alcohol complex by Baker et al.[3c]

The situations are somewhat different in the cases of the adducts with triols. As illustrated in Fig. 2, the infrared spectrum of 1, 2, 4-butanetriol clearly indicates the presence of polymeric intermolecular hydrogen bonds in the triol. However, the infrared spectrum of the adduct with the triol exhibits three absorptions in the range of 3000～3400 cm^{-1} (3368, 3250 and 3088 cm^{-1}). Also the adduct with glycerol shows a broad and intense absorption at 3350 cm^{-1} (Fig. 2). These broad absorptions at 3368 or 3350 cm^{-1} seem to indicate the presence of remaining intermolecular polymeric hydrogen bonds in these amine-triol adducts. It is reasonable to conclude that some part of hydrogen bonds is used to associate the amine-triol adduct with each other, giving them the nature of non-sublimation.

Another point of interest in the physical property of the adducts is the oscillation of the melting points. As illustrated in Fig. 3,

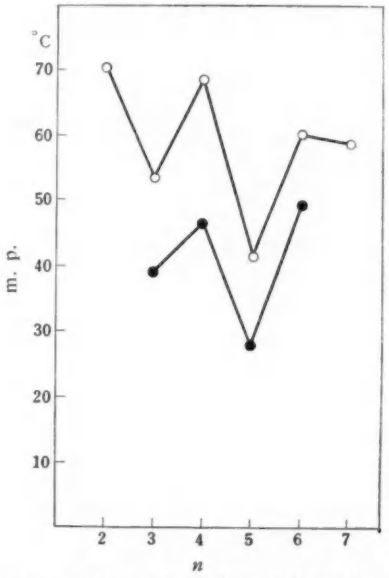

Fig. 3. The melting points of the adducts with α,ω-diols and α, β, ω-triols.
○—○ $HO\cdot(CH_2)_n\cdot OH$
●—● $HO\cdot CH_2CH\cdot(CH_2)_{n-2}\cdot OH$
$\quad\quad\quad

TABLE III. DISSOCIATION OF THE ADDUCTS IN SOLUTION

Alcohol component in adduct	Molecular weight			Degree of dissociation, %
	Calcd.	A.	B.	
Ethylene glycol	424	206 207	225	$\alpha_1=100$ or $\alpha_2=50$
1,4-Di-(β-phenyl-α-hydroxyethyl)-benzene	680	—	240	$\alpha_2=100$
1,2,6-Hexanetriol	677	—	214	$\alpha_3=100$ or $\alpha_4=70$

A. Cryoscopic method in benzene.
B. Isothermal distillation method in acetone solution.

isothermal distillation methods. The results summarized in Table III indicate the dissociation of the adduct in the solution. These results present no evidence on the nature of dissociation, but the calculated degree of dissociation is tabulated in Table III assuming the following types of dissociation.

$$\text{Diol}\begin{cases}(\text{amine})_2(\text{diol}) \overset{\alpha_1}{\rightleftarrows} (\text{amine})(\text{diol}) + (\text{amine}) \\ \text{or} \\ (\text{amine})_2(\text{diol}) \overset{\alpha_2}{\rightleftarrows} 2(\text{amine}) + (\text{diol})\end{cases}$$

$$\text{Triol}\begin{cases}(\text{amine})_3(\text{triol}) \overset{\alpha_3}{\rightleftarrows} (\text{amine})(\text{triol}) + 2(\text{amine}) \\ \text{or} \\ (\text{amine})_3(\text{triol}) \overset{\alpha_4}{\rightleftarrows} 3(\text{amine}) + (\text{triol})\end{cases}$$

As stated above, the formation of crystalline adduct with dicyclohexylamine is quite general for primary or secondary diols and triols, but it was found that the tertiary glycols such as 2,4-dimethyl-2,4-butanediol and 1,1′,4,4′-tetraphenyl-1,4-butynediol give no crystalline adducts. 2-Amino-ethanol, 1,8-terpin and (−)-menthol also gave no crystalline product even at the temperature in a refrigerator. The last two examples are remarkable as structurally related cyclohexanol itself gave a well defined adduct of m. p. 56~57°C with the composition of 1 : 1 (N, found : 4.87 ; calcd. for 1 : 1-adduct : 4.98%). These findings seem to suggest that the formation of crystalline adduct is influenced by the steric environment around the hydroxyl group.

Experimental***

Preparation of the Adducts.—A mixture of diol (1 mol.) and acetone (equal volume) was added to a solution of dicyclohexylamine (2 mol.) in acetone (equal volume). The mixture was kept for several hours in a refrigerator to complete the crystallization. The crystals formed were filtered and recrystallized from acetone. The molar ratio 1 : 3 (triol : amine) was used in the cases of the preparation of the adducts with triols.

Sublimation under reduced pressure was found as an excellent method of purification of the adducts with diols.

Measurement of the Infrared Spectra.—The spectrometer used was a Hilger H 800. The spectra of the hydroxy compounds and the amines were measured by the method of liquid film. The spectra of the adducts were measured employing KBr-disk method.

Determination of the Molecular Weight.—*(1) Cryoscopic method.*

a) Adduct with ethylene glycol : 0.01385 g.
Benzene : 2.637 g.
$\Delta T=0.130°$C. Mol. wt., 206

b) Adduct with ethylene glycol : 0.03859 g.
Benzene : 2.637 g.
$\Delta T=0.378°$C. Mol. wt., 207

(2) Isothermal distillation method.—A Signer molecular weight apparatus as modified by Clark was used using benzophenone as the standard and acetone as the solvent.

a) Adduct with ethylene glycol : 0.02878 g.
Benzophenon : 0.01220 g.
Final volumes : standard solution, 0.65 ml.
adduct solution, 1.24 ml.
Mol. wt., 225

b) Adduct with 1,2,6-hexanetriol : 0.00905 g.
Benzophenone : 0.00836 g.
Final volumes : standard solution, 1.12 ml.
adduct solution, 1.04 ml.
Mol. wt., 214

c) Adduct with 1,4-di-(β-phenyl-α-hydroxyethyl)-benzene : 0.01196 g.
Benzophenone : 0.01449 g.
Final volumes : standard solution, 1.00 ml.
adduct solution, 0.92 ml.
Mol. wt., 240

The authors are grateful to Professor S. Murahashi, Professor T. Kaneko and Mr. H. Katsura of Department of Chemistry of Osaka University and to Mr. H. Yamaguchi of the Nitto Institute of Chemical Research, Urawa for the gift of some of the hydroxy compounds. Acknowledgments are made to Messrs. T. Shiba and M. Okumiya and Miss K. Koike for performing the elementary analyses.

Department of Chemistry
Faculty of Science
Osaka University
Nakanoshima, Osaka

*** All melting points are not corrected.

Interaction of Surface Active Agent with Amylose

By Toshio TAKAGI and Toshizo ISEMURA

(Received August 17, 1959)

In the previous papers, one of the authors have reported the interaction of surface active agents with non-ionizable polymers[1] as well as with proteins[2,3]. It was found that the aspect of the interaction of surface active agents with non-ionizable polymers is entirely different from that of the interaction of surface active agents with proteins. Accidently, the authors have found that there is another way of the interaction of the surface active agent with polymer. Actually, they wished to examine the inactivation of Taka-amylase A by surface active agent using amylose as a substrate. As a matter of fact, it was found that amylose is precipitated by sodium dodecyl sulfate (SDS) even in a concentration as low as 0.007% from 0.05% amylose solution in 0.05 M sodium chloride. Accordingly, the cause of this precipitation of amylose was investigated thoroughly.

The precipitate was examined by the X-ray diffraction method and compared with the amorphous amylose precipitated by ethanol. A complex might be formed between amylose and SDS. It was interesting to examine whether such a complex might be formed even in a dissolved state under proper condition. So the possibility was examined from the two standpoints of view as will be described below. The effect of SDS on the coloration of amylose-iodine complex was investigated spectrophotometrically. As the viscosity of polymer solution is a function of the configuration assumed by the dissolved polymer molecules, the solution of amylose containing SDS was studied also by viscosity measurement. From all these experimental findings, the authors have concluded that the precipitation of amylose by the surface active agent should be due to the formation of an adduct between amylose and the surface active agent. The details of the present investigations and inferences based on them will be described hereafter.

Experimental

Amylose.—Amylose was prepared from potato starch by Schoch's butanol precipitating method[4] and was recrystallized three times. The purified amylose was dehydrated by methanol and then dried over calcium chloride in vacuo.

Amylopectin. — Amylopectin was precipitated by adding a large amount of methanol to the supernatant separated from amylose prepared by Schoch's method. The precipitate was suspended in methanol for some time to remove butanol and then dried over calcium chloride in vacuo.

Sodium Dodecyl Sulfate.—Sodium dodecyl sulfate was prepared by Dreger's method[5] and was recrystallized three times from aqueous butanol.

X-ray Diffraction Measurement. — The sample for X-ray diffraction study was prepared as will be described below. One gram of amylose was dissolved in 10 ml. of 1 N sodium hydroxide and kept in a refrigerator overnight to dissolve the amylose completely, and then diluted to about 50 ml. The solution was neutralized with 1 N hydrochloric acid and diluted with distilled water just up to 100 ml. A precipitate was formed by adding 25 ml. of 0.5% SDS solution to the amylose solution and the solution was stood overnight. The precipitate was gathered by centrifugation and dried over calcium chloride in vacuo. On the other hand, amylose was precipitated by adding excess ethanol to the amylose solution prepared just in the same way without the addition of SDS and after washing the precipitate with ether, it was dried over calcium chloride in vacuo. The amylose thus prepared was used as a reference sample without SDS for X-ray diffraction study.

X-ray diffraction patterns were taken by the powder method using "Norelco" recording X-ray diffractometer (Cu-K_α line was used).

Measurement of Absorption Spectrum of Amylose-iodine Complex.—Five milliliters of 0.1% solution of amylose which was prepared by Fuwa's method[6] was diluted to about 200 ml. with distilled water, to which the necessary volume of SDS solution was added to assure a desired final concentration and shaken thoroughly. After bringing out the color by the addition of 5 ml. of 0.2% iodine solution (containing 2% potassium iodide), the solution was diluted just up to 250 ml. After standing for about 30 min., the absorption spectra of the solutions were measured by a Hitachi spectrophotometer model EPU-2 or by a Beckman recording spectrophotometer model DK-2.

Measurement of Viscosity.—One gram of amylose was suspended in 10 ml. of 1 N sodium hydroxide, was kept in a refrigerator for 2 days and then was diluted with distilled water just up to 100 ml. This solution was diluted with 0.1 N sodium

1) T. Isemura and A. Imanishi, *J. Polymer Sci.*, **33**, 337 (1958).
2) T. Isemura and A. Imanishi, *Mem. Inst. Sci. Ind. Res., Osaka Univ.*, **15**, 173 (1958).
3) T. Isemura and T. Takagi, *J. Biochem.*, **46**, 1637 (1959).
4) T. J. Schoch, *J. Am. Chem. Soc.*, **64**, 2957 (1942).
5) E. E. Dreger et al., *Ind. Eng. Chem.*, **36**, 610 (1944).
6) H. Fuwa, *J. Biochem.*, **41**, 583 (1954).

hydroxide to obtain the solution of various concentrations in respect to amylose. Each solution was mixed with an equal volume of SDS solution of various concentrations. The solutions of various compositions were heated on a water bath at 60~80°C for about 30 min. and kept for 3 hr. in a thermostat at 30±0.05°C. Then, the viscosity of amylose solutions was measured by a viscosimeter of the Ostwald type in the same thermostat.

Viscosity of the amylopectin solutions was measured just in the same manner.

Results

Effect of SDS on the X-ray Diffraction Pattern of Amylose.—The X-ray diffraction pattern of amylose precipitated by SDS is shown in Fig. 1a, while that for amylose precipitated by ethanol in Fig. 1b. In the pattern for the former, two distinct diffraction peaks were found at $2\theta=13$ and 20° (θ=incident angle) which might be attributed to the helical structure of amylose[7-9], whereas in the pattern for the latter, only a broad peak was found which suggests an amorphous structure of amylose.

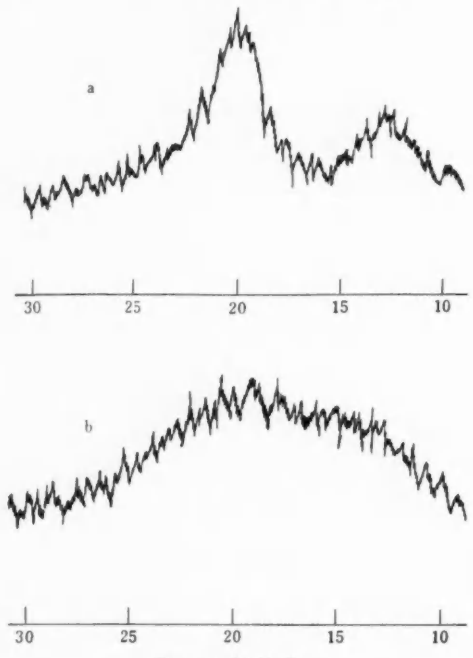

Fig. 1. X-ray diffractometer traces of SDS-treated and non-treated specimens of amylose.
a, precipitated by the addition of SDS.
b, precipitated by the addition of ethanol.

Effect of SDS on the Coloration of Amylose-iodine Complex.—If a helical complex is formed between amylose and SDS even in a dissolved state, it is expected that the coloration of amylose-iodine complex may be considerably affected in the presence of SDS. When an aqueous iodine solution was added to the amylose solution to which SDS was added previously, the solution appears at first light yellow assuming the color of I_3^- ion. Then the blue coloration of amylose-iodine complex comes out gradually. It needs about 30 min. to attain the steady coloration. All curves of

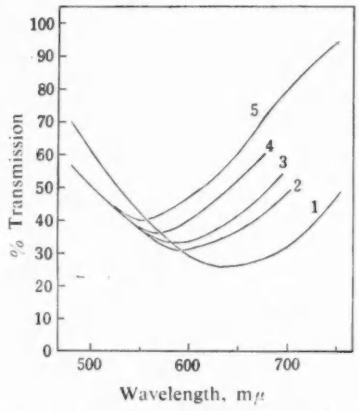

Fig. 2. The effect of the addition of SDS on the absorption spectrum of amylose-iodine complex.
1, 0 M; 2, 2.0×10^{-5} M; 3, 1.0×10^{-4} M; 4, 6.0×10^{-4} M; 5, 4.2×10^{-3} M. Amylose concentration, 2.0×10^{-3} g./l.

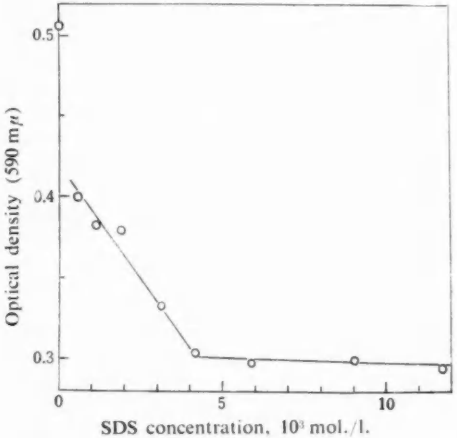

Fig. 3. The inhibitory effect of SDS on the coloration of amylose-iodine complex.

7) R. E. Rundle and D. French, *J. Am. Chem. Soc.*, **65**, 1707 (1943).
8) F. F. Mikus, R. M. Hixon and R. E. Rundle, ibid., **68**, 1115 (1946).
9) R. E. Rundle, ibid., **69**, 1769 (1947).

absorption spectra in Fig. 2 were measured after this steady state was attained. With the increase in the amount of added SDS, the absorption maximum shifts to a shorter wavelength side and the absorption decreases. If one examines the effect of the concentration of SDS by measuring the absorption at 590 mμ over a wide range of the concentration, the effect of SDS increases with the concentration up to 4×10^{-3} M, beyond which the change of the absorption spectra was not found as shown in Fig. 3. The concentration of SDS corresponds nearly to the critical micelle concentration of this surface active agent.

Effect of SDS on the Viscosity of Amylose Solution.—As is well known, the viscosity of polymer solution is a function of polymer configuration in solution. So the viscosity of an amylose solution might be profoundly affected by the addition of a small amount of SDS, if amylose changes its configuration from a random coil to a helical structure. The viscosity of amylose solution was measured in the presence of SDS in alkaline solution which is known as a good solvent for amylose and compared with that of amylose solution in the absence of SDS. As shown in Fig. 4., the effect of SDS on the viscosity of amylose solution is very remarkable. On the other hand, amylopectin which can not assume a helical structure because of its branched structure is expected to be scarcely affected by the addition of SDS. The experiment verifies that this is the case, as shown in Fig. 5.

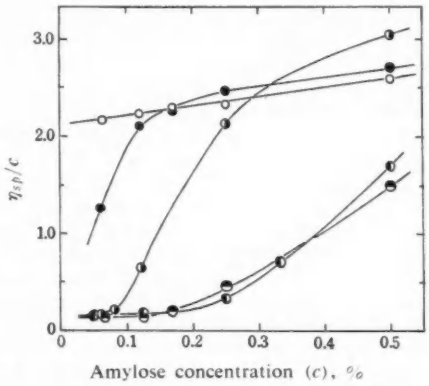

Fig. 4. The effect of the addition of SDS on the viscosity of amylose in 0.1 N KOH. SDS concentration, ○, 0 M; ●, 1.7×10^{-4} M; ◑, 3.5×10^{-4} M; ◐, 5.6×10^{-4}; ◓, 7.0×10^{-4} M.

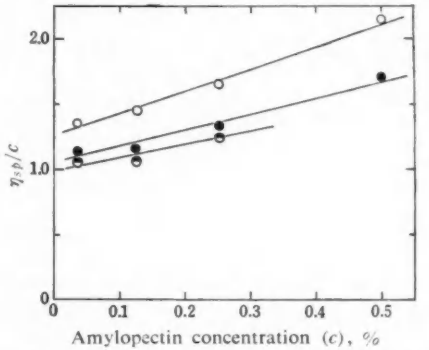

Fig. 5. The effect of the addition of SDS on the viscosity of amylopectin in 0.1 N KOH. SDS concentration, ○, 0 M; ◓, 3.5×10^{-4} M; ●, 7.0×10^{-4} M.

Discussion

As one of the authors have already reported[1], some surface active agents interact with some polymers causing oriented adsorption on the polymer molecules, often making insoluble polymers soluble. On the other hand, proteins interact with an ionic surface active agent at their ionic sites of the opposite sign[10]. Surface active agents precipitate proteins having opposite electric net charge, changing hydrophilic sites by covering with hydrocarbon chains. However, in the presence of excess surface active agents, surfactant ions are built up on the hydrocarbon tails of surfactant previously combined with protein molecules. Thus, the hydrophobic protein molecules which have been separated from the solution are turned to be hydrophilic again.

In the case of the interaction of amylose with an ionic surface active agent, the ion-ion interaction as in the case of proteins does not occur because of the lack of ionic sites. The oriented adsorption of surfactant ions as in the case of polyvinyl alcohol, as previously reported[1], might be excluded. Also, the dipole-ion interaction between hydroxyl groups of amylose and SDS ions as suggested by Fava and Eyring[11] in the case of adsorption of SDS on cellulose will be refused for the following reasons. In the present case, only an ion of SDS is sufficient to precipitate about 12 glucose residues in amylose. Moreover, it was found in the previous investigation[1] that the interaction of SDS with polyvinyl alcohol which has many hydroxyl groups in a molecule like amylose showed no sign of the insolubilization of the polymer. Further, the insolubilization of amylose can not be ascribed to the adsorption of SDS extending the hydrocarbon tails toward water as in the case of proteins, because of the

10) F. W. Putnam, *Advances in Protein Chem.*, **4**, 83 (1948).
11) A. Fava and H. Eyring, *J. Phys. Chem.*, **60**, 890 (1956).

lack of ionic sites as mentioned above. The precipitation of amylose is also caused by a cationic surface active agent such as cetylbenzyldimethyl amine bromide as well as SDS. On the other hand, the large excess of SDS, even as high as 12% in total concentration does not cause the redissolution of the precipitate. It is also to be noticed that no precipitate was formed by SDS with amylopectin which has a number of branched chains in the molecule.

According to X-ray diffraction study, the amylose precipitate formed by the interaction with SDS gave two distinct peaks at $2\theta = 13$ and 20° as shown in Fig. 1a. Rundle and his collaborators[7] concluded from their studies on amylose-iodine complex by X-ray diffraction that amylose forms an adduct with iodine, where amylose assumes a helical structure in which six glucose residues make a turn and iodine molecules lie along the axis of helix, which gives two distinct peaks in X-ray diffraction pattern at $2\theta = 13$ and 20°.

Later, they found that amylose forms similar adducts with some higher alcohols and normal fatty acids of moderate chain length[8,9]. As these two diffraction peaks are characteristic of the helical structure of amylose, the amylose precipitate formed by the addition of SDS should be an adduct of amylose including SDS ions in its helical structure. Although the mixture of amylose solution must be heated with higher fatty acid or alcohol at about 70°C and then cooled to obtain the adduct, only the addition of SDS to amylose solution at room temperature is enough in the present case. This difference might originate from the fact that SDS is much more soluble than higher fatty acid or alcohol.

There is another evidence for the formation of the adduct having a helical structure between amylose and surfactant. It is well known that when iodine was added to amylose solution, intensive blue color appears instantaneously. Now it is generally accepted that this characteristic coloration of amylose solution by iodine is caused by the change of an electronic state of iodine molecules lying along the axis of helix of the amylose-iodine complex[12]. The change of the electronic state should be caused by the large polarity of amylose in a helical structure due to the orientation of a large number of hydroxyl groups in glucose residues in a similar direction. As mentioned above, when iodine solution was added to amylose solution containing SDS, the blue color of amylose-iodine complex appears gradually instead of instantaneous coloration as in the case without SDS. It may be expected that it needs some time to exchange SDS ions with iodine in a helix of amylose.

As the authors have mentioned above, the absorption maximum shifts to shorter wavelength-side and absorption decreases with the concentration of SDS. The decrease in absorption is remarkable at the longer wavelength-side. Rundle et al.[13] studied the effect of the molecular weight of amylose on the coloration of amylose with iodine. They found that with the decrease in the molecular weight or the chain length of amylose, the absorption maximum shifts to the shorter wavelength side and the absorption decreases. This change of absorption is remarkable at the longer wavelength side. As iodine competes with SDS in intruding into a helix of amylose, the linear array of iodine molecules which intervened between SDS ions might become shorter with the increase of SDS concentration. The increase of SDS concentration might be assumed to have the same effect as the decrease of the chain length of the amylose molecule forming a helical complex with iodine. Parallel changes in the shift of absorption maximum and the decrease in absorption in both cases mentioned above might be explained in terms of the chain length concerning one continuous unit of the amylose-iodine-complex.

No more change was found in the absorption spectra of amylose-iodine complex, when the concentration of SDS exceeds about 4×10^{-3} M. This concentration almost exactly corresponds to the critical micelle concentration of this surfactant, so that this fact suggests that only the SDS ions are concerned with the formation of the helical complex.

According to the study of the absorption spectra mentioned above, amylose seems to assume a helical configuration in the presence of SDS even in a dissolved state. Viscosity measurments, as well known, give some insights into the configuration of polymer molecules in solution. As shown in Fig. 4., when the reduced viscosity η_{sp}/c of amylose solution in the absence of SDS was plotted against amylose concentration, the same linear relation was obtained as in the case of a typical non-electrolytic polymers. However, if SDS is present in the solution, η_{sp}/c decreases rapidly with the decrease in amylose concentration and converges to a definite value independent of the concentration of SDS in the low concentration of amylose. The larger the ratio of SDS to amylose is, the larger is the concentration of amylose from which the reduced viscosity begins to decrease. Accordingly, the ratio of SDS to amylose is evidently an important factor to the decrease of the reduced viscosity.

12) R. S. Stein and R. E. Rundle, *J. Chem. Phys.*, **16**, 195 (1948).

13) R. R. Baldwin. R. S. Bear and R. E. Rundle, *J. Am. Chem. Soc.*, **66**, 111 (1949).

In the case of amylopectin, the linear relation between η_{sp}/c and c was retained even in the presence of SDS. The line moves parallel, a little downward. Since the intrinsic viscosity of the polymers should be an indication of their volume in the dissolved state, the decrease in the reduced viscosity of amylose suggests the decrease in the effective volume of amylose when SDS was added to the solution. The cause of the decrease in viscosity should be attributed to the formation of a helical complex between amylose and SDS. Owing to the mutual compensation of the polarity of hydroxyl groups in the helical complex, the hydration of amylose might be decreased. This might be one of the reasons why the viscosity of amylose-surfactant-complex decreased.

The minor decrease in viscosity found with amylopectin in the presence of SDS might be caused by the contamination of a small amount of amylose, since the decrease of viscosity is almost the same with the solution containing 0.01% SDS and that containing 0.02% SDS.

In conclusion, it was found experimentally that there are at least three different ways of interaction between surface active agents and polymer, namely, (1) only by van der Waals' force, (2) by electrovalent bonding only or together with van der Waals' force, and (3) by a special combination found in the case of adduct formation. In the case of the interaction of a surface active agent with non-ionizable polymers such as polyvinyl formal or polyvinyl acetate[1], cooperative force between chains of surfactant is very significant. Accordingly, hydrophilic and lypophilic properties of surfactant must be appropriately balanced in this case. The cationic detergent shows poor interaction with polymers, probably because of its stronger hydrophility than that of the anionic detergent.

The electrovalent bonding of the surfactant with polymer is of course encountered with the polymers such as proteins which have ionic sites in the molecules[10]. The surface active agents which can act on the polymers should have the charge of the opposite sign to the polymer. After forming the envelope of the surface active agent of the thickness of a molecule, more layers of surface active agents can be built up on it by van der Waals' force.

The third class of interaction such as these encountered in the case of amylose and surface active agents, some specific steric conditions must be fulfilled. In this case, whether the surface active agent is anion or cation is out of the question. However, non-ionic detergents were found to have scarce interaction with the polymers throughout all these three types of interactions[14].

Summary

It was found that a specific precipitate is formed when some ionic surface active agents are added to amylose solution and it was confirmed by X-ray diffraction study that this phenomenon is due to the formation of the helical complex between amylose and a surface active agent.

It is also inferred that the same complex is formed even in the dissolved state from the study on the effect of the surface active agent on the viscosity of amylose solution and on the absorption spectrum of amylose-iodine complex.

The authors express their hearty thanks to Dr. S. Hizukuri of the Institute of Scientific and Industrial Research, Osaka Universiy for his valuable advice and cooperation in the X-ray diffraction measurements.

Division of Physical Chemistry
Institute for Protein Research
Osaka University
Kita-ku, Osaka

14) Preliminary experiments.

Oxidation of Ferrous Ions in the Aqueous Ferrous-Cupric System. I. Effect of Cobalt-60 Gamma-Rays

By Hiroshi HOTTA, Akira TERAKAWA and Shinichi ŌNO

(Received August 27, 1959)

An irradiation facility with a 10 kilocurie Co-60 gamma-ray source has been in operation at Japan Atomic Energy Research Institute since 1958[1]. Although the characteristics of the source, especially the distribution of radiation intensity around the hollow cylindrical source had to be measured for the public use of this facility, a chemical dosimeter for high dose, which was to be used as the standard, was not studied in Japan. The dose rate inside the present source is about 2×10^6 *r*/hr.

For this purpose, the properties of various aqueous solutions were examined to find a suitable chemical dosimeter for high doses. In general, a chemical dosimeter must have certain properties, namely, linearity, reliability, stability, easy standardization and so on[2]. It is concluded from the present experiments that a chemical dosimeter for high doses must have the following properties in addition to the above ones.

The first conclusion is that the oxygen-dependent reaction is not preferable, owing to the restriction of oxygen solubility like ferrous or benzene aqueous solution[3,4]. That is, all components of the system must have great solubility, which determines the upper limit of the appriciable dose. Moreover, the product to be measured should have no secondary reaction such as re-redox reaction and decomposition. Re-redox reactions are considered even for ferric[5] and cerous[6] ions, respectively. Since the temperature of solutions irradiated at a high dose rate is apt to be raised owing to the absorption of radiation energy, it is desirable for the *G*-value to be independent of temperature[7].

It is difficult to find an ideal system having all the above properties. The ceric dosimeter is usually recommended for this purpose, but demands the most careful distillation of water. Moreover, the reagent contains some rare earths occasionally. The ferrous-cupric dosimeter[8] is another one used for high doses. This dosimeter can easily be made from pure and cheap reagents, but this matter is not being so exhaustively studied at present. Therefore, the authors studied the aqueous ferrous-cupric system in detail, and give the results of some discussions concerning it in the present paper.

Experimental

Triply distilled water was used as usual, but chemical reagents of special grade were used without further purification. The aqueous solutions were irradiated in a test tube of hard glass (Hario Glass) by a 10 kilocurie Co-60 gamma-ray source at the Irradiation Laboratory of Japan Atomic Energy Research Institute at room temperature (ca. 25°C). The solutions were saturated with either oxygen or nitrogen, and sometimes irradiated without any treatment, which is called hereafter the non-treated solution. The concentration of oxygen in distilled water, which was treated similarly with the solution, was measured at 25°C by the Winkler method[9] as listed in Table I. The solubility of oxygen in water is 1.2×10^{-3} M in the handbook[10].

In the present experiment, as mentioned previously[4], the dose was changed not by the irradiation time, but by irradiation for one hour at

TABLE I. INITIAL CONCENTRATIONS OF OXYGEN AND FERRIC ION AT 25°C IN 10^{-3} M

Treatment	Oxygen in water	Ferric ion in ferrous-cupric system		
		(0)*	(10^{-3})*	(10^{-2})*
N_2-saturated	0.019	0.2	0.2	0.2
Non-treated	0.37	0.2	1.3	1.6
O_2-saturated	1.2	0.2	2.1	2.3

Note: The concentration of cupric ion is listed in ( )*.

1) A. Danno, M. Omura, H. Hotta, H. Hirakawa, G. Tsuchihashi and I. Yamaguchi, "The 7th Conf. Hot Lab. and Equipment", Session 6, Cleveland, Ohio, 1959.
2) G. V. Taplin, "Radiation Dosimetry", Ed. by G. J. Hine and G. L. Brownell, Chap. 8 Academic Press, New York (1956).
3) P. V. Phung and M. Burton, *Radiation Research*, 7, 199 (1957).
4) H. Hotta and A. Terakawa, This Bulletin, to be published.
5) T. Rigg, G. Stein and J. Weiss, *Proc. Roy. Soc.*, A211, 127 (1952).
6) J. T. Harian and E. J. Hart, *Radiation Research*, 9, 127 (1958).
7) H. Hotta and K. Shimada, This Bulletin, to be published.
8) E. P. Hart and P. D. Walsh, *Radiation Research*, 1, 342 (1954).
9) Am. Public Health Assoc., "Standard Methods for the Examination of Water, Sewage and Industrial Wastes", Am. Public Health Assoc., New York (1955), p. 252.
10) N. A. Lange, "Handbook of Chemistry", Handbook Publishers, Sandusky, Ohio (1956), p. 1093.

TABLE II. YIELD OF FERRIC ION IN VARIOUS SOLUTIONS

Run	Solute in M			Treatment	G-value	
	Ferrous ammonium sulfate	Cupric sulfate	Sulfuric acid		at low dose	at high dose
a	0.04	0	0.4	O_2-saturated	15.60±0.06	8.16±0.03
b	0.04	0	0.4	Non-treated	15.55±0.02	7.94±0.31
c	0.04	0	0.4	N_2-saturated	8.07±0.12	
d	0.04	0.001	0.4	O_2-saturated	14.2	6.44±0.2
e	0.04	0.001	0.4	Non-treated	6.50±0.15	
f	0.04	0.001	0.4	N_2-saturated	6.51±0.07	
g	0.04	0.01	0.4	O_2-saturated	2.60±0.14	
h	0.04	0.01	0.4	Non-treated	2.4 ±0.05	
i	0.04	0.01	0.4	N_2-saturated	2.34±0.08	

various positions, namely, various dose rates. Therefore, the abscissa of all figures gives a value of the dose in r as well as a value of the dose rate in r/hr. The deviation of the observed values from the curve is partially due to the uncertainty of the absolute dose rate at a respective position, for samples were not irradiated at a fixed position as is usually done. The absolute dose rate was determined by the ceric dosimeter, which was corrected up to about $1.4\times10^5 r$ by the oxygen-saturated ferrous dosimeter.

The amount of ferric ion was measured by optical density at 304 mμ (ε=2205 at 25°C). It should be noticed that the ferrous ion was fairly oxidized due to the addition of cupric ions in the presence of oxygen without irradiation as listed in Table I, in which the mean initial concentration of ferric ions in the irradiated solutions is shown[11].

Results

Ferrous Solutions.—The result of aqueous 0.04 M ferrous ammonium sulfate solution containing 0.8 N sulfuric acid and 0.001 M sodium chloride for a) oxygen-saturated, b) non-treated and c) nitrogen-saturated cases are shown in Fig. 1. Their G-value is listed with the composition of the solution in Table II. 0.001 M sodium chloride was added as a stabilizer as usual.

Ferrous-cupric Solutions.—The results of aqueous 0.04 M ferrous ammonium sulfate solution containing 0.8 N sulfuric acid and 0.001 M cupric sulfate for the above three treatments, d), e) and f), are shown in Fig. 2. Moreover, the results of the similar solution containing 0.01 M cupric sulfate for the same three treatments, g), h) and i), are shown in Fig. 3. Their G-value is also listed with the composition of the solution in Table II. The data below about $4\times10^4 r$ were unreliable.

The present results indicate that the non-treated solution is useful as a chemical dosimeter for high doses with good accuracy at

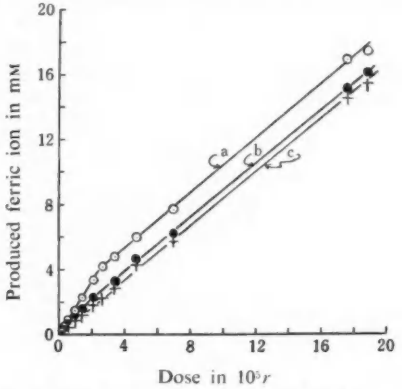

Fig. 1. The oxidation of ferrous ion in 0.04 M ferrous sulfate acidic aqueous solution for (a) oxygen-saturated, (b) non-treated and (c) nitrogen-saturated cases.

11) J. W. Mellor, "A Comprehensive Treatise on Inorganic and Theoretical Chemistry", Vol. XIV, Longmans, London (1935), p. 267.

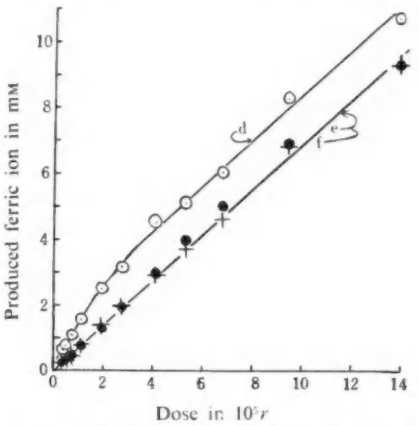

Fig. 2. The oxidation of ferrous ion in 0.04 M ferrous sulfate-0.001 M cupric sulfate acidic aqueous solution for (d) oxygen-saturated (•), (e) non-treated (●) and (f) nitrogen-saturated (+) cases.

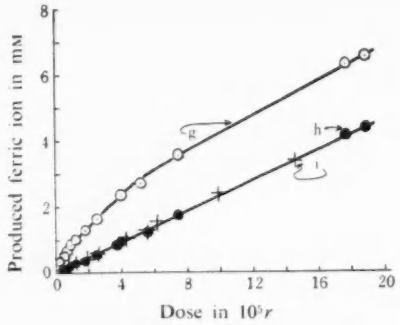

Fig. 3. The oxidation of ferrous ion in 0.04 M ferrous sulfate-0.01 M cupric sulfate acidic aqueous solution for (g) oxygen-saturated (⊙), (h) non-treated (●) and (i) nitrogen-saturated (+) cases.

least up to $2\times10^6 r$ from $4\times10^4 r$. However, the G-value is dependent on the composition of the solution[12].

Discussion

For the primary chemical effects of ionizing radiation on aqueous system,

$$H_2O \rightsquigarrow H_2,\ H_2O_2,\ H \text{ and } OH \qquad (0)$$

the yield of the above products per eV., namely, their G-value by Co-60 gamma-rays in the 0.8 N sulfuric acid aqueous system is considered to be $G(H_2)=0.39$, $G(H_2O_2)=0.78$, $G(H)=3.70$ and $G(OH)=2.92$, respectively[13]. The G-value of the following reactions, which is shown in parentheses at the right of each equation, is estimated from the above values. The suffix of G denotes the order of reactions included in the G-value. For example, $G_{2,1}$ means the total G-value of reaction 2 and reaction 1.

The action of OH and H_2O_2 in ferrous solution is

$$Fe^{2+}+OH=Fe^{3+}+OH^- \qquad (G_1=2.92) \qquad (1)$$

and

$$Fe^{2+}+H_2O_2=Fe^{3+}+OH^-+OH \qquad (G_{2,1}=2\times0.78) \qquad (2)$$

However, the action of the H atom is very different according to the condition as follows.

Yield of Ferric Ion in the Absence of Oxygen.—In the absence of oxygen, the action of the H atom in the acidic solution is

$$H+H^+=H_2^+ \qquad (G_3=3.70) \qquad (3)$$

and then

$$Fe^{2+}+H_2^+=Fe^{3+}+H_2 \qquad (G_4=3.70) \qquad (4)$$

Therefore, the total yield of ferric ion in the absence of oxygen is equal to $G_1+G_{2,1}+G_4=8.18$, as usual. In fact, the observed values at high dose for solutions a), b) and c) in Table I are in good agreement with this value.

In the presence of cupric ion, it reduces the yield of ferric ion by the reaction

$$Cu^{2+}+H=Cu^++H^+ \qquad (5)$$

and then

$$Fe^{3+}+Cu^+=Fe^{2+}+Cu^{2+} \qquad (G_5=G_6) \qquad (6)$$

Reaction 5 competes with reaction 4 within $G_4+G_5=3.70$. Even if the cuprous ion reacts with OH or H_2O_2 in addition to reaction 6, the effect of these reactions on the yield of the ferric ion is equivalent to reaction 6. Therefore, these effect are represented by G_6.

According to the above interpretation, the G_5 for solutions f) and i) are 0.85 and 2.9, respectively. On the assumption that

$$G_4/G_5=k_4K_3(H^+)(Fe^{2+})/k_5(Cu^{2+}) \qquad (i)$$

as pointed out by Hart[12], where k, K and parentheses denote rate constant, equilibrium constant and concentration, respectively, the ratios obtained, $k_4K_3(H^+)/k_5$ are 0.084 and 0.069 for solutions f) and i), respectively. If K_3 is assumed to be 100 l./mol. according to Hart[12], the ratio, k_4/k_5 is estimated to be about 10^{-3}. It is confirmed from this value that the cupric ion is very reactive for the H atom in comparison with the ferrous ion.

Yield of Ferric Ions in the Presence of Oxygen.—In the presence of oxygen, the action of H atom in the acidic solution is

$$H+O_2=HO_2 \qquad (7)$$

$$Fe^{2+}+HO_2=Fe^{3+}+HO_2^- \qquad (8)$$

and then

$$HO_2^-+H^+=H_2O_2 \quad (G_{7,8,9,2,1}=3\times3.70) \qquad (9)$$

Therefore, the total yield of ferric ions in the presence of oxygen is equal to $G_1+G_{2,1}+G_{7,8,9,2,1}=15.58$, as usual.

In the ferrous and cupric solution, reaction 8 competes with reaction 5 and the reaction

$$Cu^{2+}+HO_2=Cu^++H^++O_2 \qquad (10)$$

and the rate of the consumption of oxygen by reaction 8 is expressed by the equation

$$G(-O_2)_8=G(H)\times\frac{1}{1+\dfrac{k_5(Cu^{2+})}{k_7(O_2)}}\times\frac{1}{1+\dfrac{k_{10}(Cu^{2+})}{k_8(Fe^{2+})}} \qquad (ii)$$

as pointed out by Hart[12]. Therefore, the circumstance of these reactions is complicated.

On the other hand, if ΔG is considered to be the difference between the observed G-value, G°, and the ideal one, G^i, obtained on the

12) E. J. Hart, *Radiation Research*, **2**, 33 (1955).
13) A. O. Allen, 1st Intern. Conf. Peaceful Uses of Atomic Energy", Vol. 7, Geneva, (1956), p. 514.

assumption that cupric ion scavenges all H atoms, it is expressed as

$$\Delta G = G^{\circ} - G^{\mathrm{I}} = 4G_8 \qquad \text{(iii)}$$

and

$$G^{\mathrm{I}} = G_1 + G_{2,1} - G_{5+10} = 0.78$$

Therefore, the consumption of oxygen against the dose in solutions d) and g) is estimated from Eq. iii as shown in Fig. 4. The respective G-value of the elementary reactions at the initial stage for both solutions is obtained from the initial slope in Fig. 4 as listed in Table III.

TABLE III. YIELD OF ELEMENTARY REACTIONS AT THE INITIAL STAGE FOR OXYGEN-SATURATED FERROUS-CUPRIC SOLUTIONS

Run	Cupric ion	G_8	G_{5+10}	G°
d	10^{-3} M	3.34	0.34	14.22
g	10^{-2} M	2.64	1.06	11.34

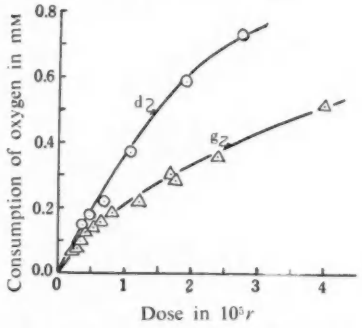

Fig. 4. The consumption of oxygen in oxygen-saturated 0.04 M ferrous sulfate acidic aqueous solution containing (d) 0.001 M and (g) 0.01 M cupric sulfate.

The linearity of the curve at the initial stage in Fig. 4 indicates that the ratios, $k_5(Cu^{2+})/k_7(O_2)$ and $k_{10}(Cu^{2+})/k_8(Fe^{2+})$ should be constant at this stage in Eq. ii, that is,

$$\frac{k_{10}}{k_8} = \frac{G_{10}(Fe^{2+})}{G_8(Cu^{2+})} \qquad \text{(iv)}$$

When the contribution of reaction 5 is assumed to be comparatively slight, $G_{10} \approx G_{5+10}$, in solution d), in which the concentration of cupric ions is low, the ratio, k_{10}/k_8 is estimated to be smaller than 4 from Eq. iv on using the values in Table III. According to Hart[12], the ratio, k_{10}/k_8 is about 50 for the aqueous solution of 10^{-3} M ferrous sulfate and 0.01 N sulfuric acid containing cupric ions between 10^{-6} M and 10^{-3} M. The disagreement between them may be the pH of the solution.

From the present experiment, 10^{-3} M cupric ion is sufficient to suppress the effect of oxygen dissolved naturally. However, it can not be concluded directly from this fact that oxygen is not concerned with the reaction in solution e). It is because the concentration of HO_2 radical should be sufficient for a ferrous ion to react with this radical from the result of solution b), and the G-value of reaction 10 is not so great as to suppress reaction 8 even in solution d) as listed in Table III. Therefore, it can not be understood why there is no difference between solutions e) and f) in spite of the above condition. However, if the cupric ion scavenges HO_2^- ion by the reaction

$$Cu^{2+} + HO_2^- = Cu^+ + HO_2 \qquad (11)$$

and then HO_2 radical or H_2O_2 molecule by reaction 9 reacts with ferrous and cupric ions as mentioned already, the effect of oxygen, namely, the difference between reactions 4 and 8 can be actually disregarded. The initial concentration of oxygen in solution e), supposed from Table I, is smaller than the concentration of oxygen at the bend point of solution a), supposed from Fig. 1 and Table I.

Summary

The oxidation of ferrous ion in ferrous-cupric acidic aqueous solution by Co-60 gamma-rays was studied in order to find a good chemical dosimeter for high doses. Consequently, it is found that the non-treated solution containing the 10^{-3} M cupric ion is useful for this purpose, for this amount of cupric ions is sufficient to suppress the effect of oxygen, and that the G-value of the ferrous-cupric system is dependent on the composition of the solution. The suppression can be explained by the scavenging of the HO_2^- ion by cupric ions. Furthermore, some discussions regarding the system are given in the present paper.

Japan Atomic Energy Research Institute
Tokai, Ibaraki-ken

Vibrational Spectra of Methyltrimethoxysilane

By Toshio TANAKA

(Received August 26, 1959)

The group frequency assignments have already been given for the infrared spectra of methyltrimethoxysilane and its higher homologues in the rock salt region[1]. This paper contains the Raman spectrum of methyltrimethoxysilane, the assignment of the observed frequencies and the calculation of the frequencies and the modes of the skeletal vibration. In the calculation a methyl group was regarded as one particle.

The normal coordinate treatment was carried out by the Wilson FG matrix method[2] with a Urey-Bradley potential function. The normal vibration has not yet been calculated for any $YM(XZ)_3$ type molecule.

Experimental

Material.—The preparation and the physical constants of methyltrimethoxysilane used in the present work have already been reported elsewhere[3].

Raman Spectrum.—The Raman spectrum has been obtained by a Yūki-gōsei Raman spectrograph. The observed frequencies are shown in Table II together with the infrared and the calculated frequencies.

Normal Coordinate Treatment

For the convenience of the calculation, it has been assumed that the molecule belongs to the point group C_{3v} and has the structure shown in Fig. 1, in which a C–Si–O–C plane and an O–Si–O plane including the same Si–O bond are assumed to have an interplaner angle of 120°. According to the group theory, this molecule has twelve skeletal vibrations, five of a_1, one of a_2 and six of e species. One of the six skeletal vibrations of the species e is the torsional oscillation of the (Si–)OCH_3 group*. All vibrations except the a_2 torsional mode are active both in infrared and Raman spectra.

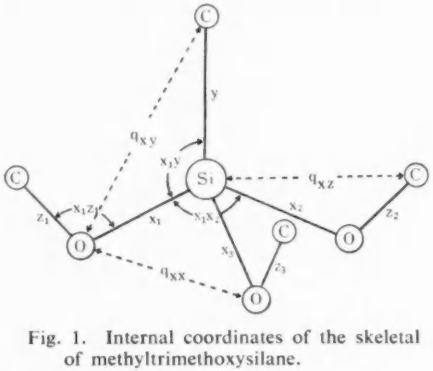

Fig. 1. Internal coordinates of the skeletal of methyltrimethoxysilane.

From the internal coordinates (Fig. 1), the following orthonormal symmetry coordinates have been found:

for the a_1 vibrations,

$$R_1 = \Delta(z_1+z_2+z_3)/\sqrt{3}$$
$$R_2 = \Delta y$$
$$R_3 = \Delta(x_1+x_2+x_3)/\sqrt{3}$$
$$R_4 = \Delta(x_1x_2+x_1x_3+x_2x_3-x_1y-x_2y-x_3y)/\sqrt{6}$$
$$R_5 = \Delta(x_1z_1+x_2z_2+x_3z_3)/\sqrt{3}$$

and for the e vibrations,

$$R_{7a} = \Delta(2z_1-z_2-z_3)/\sqrt{6}$$
$$R_{8a} = \Delta(2x_1-x_2-x_3)/\sqrt{6}$$
$$R_{10a} = \Delta(2x_1z_1-x_2z_2-x_3z_3)/\sqrt{6}$$
$$R_{11a} = \Delta(2x_1x_2-x_1x_3-x_2x_3)/\sqrt{6}$$
$$R_{12a} = \Delta(2x_1y-x_2y-x_3y)/\sqrt{6}$$

The numbering of these symmetry coordinates corresponds to the numbering of the fundamentals in Table II.

From the coefficients of the symmetry coordinates and the potential constants in a Urey-Bradley force field[4], the F matrix elements are obtained as follow:

for the a_1 vibrations,

$$F_{11} = K_z + s_{zx}^2F_{xz} + t_{zx}^2F_{xz}'$$
$$F_{13} = s_{xz}s_{zx}F_{xz} - t_{xz}t_{zx}F_{xz}'$$
$$F_{15} = (s_{zx}t_{xz}F_{xz} + s_{xz}t_{zx}F_{xz}')x$$
$$F_{22} = K_y + 3s_{yx}^2F_{xy} + 3t_{yx}^2F_{xy}'$$
$$F_{23} = \sqrt{3}\,(s_{xy}s_{yx}F_{xy} - t_{xy}t_{yx}F_{xy}')$$
$$F_{24} = -\sqrt{3/2}(s_{yx}t_{xy}F_{xy} + s_{xy}t_{yx}F_{xy}')x$$
$$F_{33} = K_x + 4s_{xx}^2F_{xx} + s_{xy}^2F_{xy} + s_{xz}^2F_{xz} + t_{xy}^2F_{xy}' + t_{xz}^2F_{xz}'$$

1) T. Tanaka, This Bulletin, 31, 762 (1958).
2) E. B. Wilson, Jr., *J. Chem. Phys.*, 7, 1047 (1939); 9, 76 (1941).
3) T. Tanaka, A. Tasaka, R. Ōkawara and T. Watase, *Technol. Repts. Osaka Univ.*, 7, 193 (1957).
* It represents the methoxy group attached to the silicon atom.
4) T. Shimanouchi, *J. Chem. Phys.*, 17, 245, 734, 848 (1949).

$$F_{34}=\sqrt{2}\,s_{xx}t_{xx}(F_{xx}+F_{xx}')x-(s_{xy}t_{yx}F_{xy}+s_{yx}t_{xy}F_{xy}')y/\sqrt{2}$$
$$F_{35}=(s_{xz}t_{zx}F_{xz}+s_{zx}t_{xz}F_{xz}')z$$
$$F_{44}=(H_{xx}+t_{xx}F_{xx}-s_{xx}^2F_{xx}')x^2/2+(H_{xy}+t_{xy}t_{yx}F_{xy}-s_{xy}s_{yx}F_{xy}')xy/2+3\kappa/\sqrt{8}$$
$$F_{55}=(H_{xz}+t_{xz}t_{zx}F_{xz}-s_{xz}s_{zx}F_{xz}')xz$$
$$F_{12}=F_{14}=F_{25}=F_{45}=0$$

and for the e vibrations,

$$F_{77}=K_z+s_{zx}^2F_{xx}+t_{zx}^2F_{xz}'$$
$$F_{78}=s_{xz}s_{zx}F_{xz}-t_{xz}t_{zx}F_{xz}'$$
$$F_{710}=(s_{zx}t_{xz}F_{xz}+s_{xz}t_{zx}F_{xz}')x$$
$$F_{88}=K_x+s_{xx}^2F_{xx}+s_{xy}^2F_{xy}+s_{xz}^2F_{xz}+3t_{xx}^2F_{xx}'+t_{xy}^2F_{xy}'+t_{xz}^2F_{xz}'$$
$$F_{810}=(s_{xz}t_{zx}F_{xz}+s_{zx}t_{xz}F_{xz}')z$$
$$F_{811}=s_{xx}t_{xx}(F_{xx}+F_{xx}')x/2$$
$$F_{812}=(s_{xy}t_{yx}F_{xy}+s_{yx}t_{xy}F_{xy}')y$$
$$F_{1010}=(H_{xz}+t_{xz}t_{zx}F_{xz}-s_{xz}s_{zx}F_{xz}')xz$$
$$F_{1111}=(H_{xx}+t_{xx}^2F_{xx}-s_{xx}^2F_{xx}')x^2+\kappa/\sqrt{8}$$
$$F_{1112}=\sqrt{2}\,\kappa/4$$
$$F_{1212}=(H_{xy}+t_{xy}t_{yx}F_{xy}-s_{xy}s_{yx}F_{xy}')xy+\kappa/\sqrt{8}$$
$$F_{711}=F_{712}=F_{1011}=F_{1012}=0$$

where the following abbreviations have been adopted:

$$s_{xx}=4x/3q_{xx} \qquad t_{xx}=\sqrt{8}\,x/3q_{xx}$$
$$s_{xy}=(3x+y)/3q_{xy} \qquad t_{xy}=\sqrt{8}\,y/3q_{xy}$$
$$s_{yx}=(3y+x)/3q_{xy} \qquad t_{yx}=\sqrt{8}\,x/3q_{xy}$$
$$s_{xz}=(x-z\cos\theta)/q_{xz} \qquad t_{xz}=z\cos\theta/q_{xz}$$
$$s_{zx}=(z-x\cos\theta)/q_{xz} \qquad t_{zx}=x\cos\theta/q_{xz},$$

and the symbols used for the equilibrium values of the interatomic distances and of the interbond angles are x=Si–O, y=Si–C, z=O–C, q_{xx}=O···O, q_{xy}=O···C, q_{xz}=Si···C and $\theta=\angle$SiOC.

The G matrix elements are obtained by the use of the table of Decius[5] and the method of Crawford[6]. Using the notations ρ_x, ρ_y and ρ_z for the reciprocals of Si–O, Si–C and O–C bond lengths, and μ_{Si}, μ_O and μ_C for the reciprocals of the masses of silicon and oxygen atoms and methyl group, respectively, the following G matrix elements have been obtained:

for the a_1 vibrations,

$$G_{11}=\mu_O+\mu_C$$
$$G_{13}=\mu_O\cos\theta$$
$$G_{14}=-\sqrt{2}\,\rho_x\mu_O\sin\theta$$
$$G_{15}=-\rho_x\mu_O\sin\theta$$
$$G_{22}=\mu_{Si}+\mu_C$$
$$G_{23}=-\mu_{Si}/\sqrt{3}$$
$$G_{24}=4\rho_x\mu_{Si}/\sqrt{3}$$
$$G_{25}=\sqrt{8/3}\,\rho_x\mu_{Si}$$
$$G_{33}=\mu_{Si}/3+\mu_O$$
$$G_{34}=-4\rho_x\mu_{Si}/3$$
$$G_{35}=-\sqrt{8}\,\rho_x\mu_{Si}/3-\rho_z\mu_O\sin\theta$$
$$G_{44}=2\rho_x^2(8\mu_{Si}/3+\mu_O)$$
$$G_{45}=8\sqrt{2}\,\rho_x^2\mu_{Si}/3+\sqrt{2}\,\rho_x(\rho_x-\rho_z\cos\theta)\,\mu_O$$
$$G_{55}=8\rho_x^2\mu_{Si}/3+\rho_z^2\mu_C+(\rho_x^2+\rho_z^2-2\rho_x\rho_z\cos\theta)\,\mu_O$$
$$G_{12}=0$$

and for the e vibrations,

$$G_{77}=\mu_O+\mu_C$$
$$G_{78}=\mu_O\cos\theta$$
$$G_{710}=-\rho_x\mu_O\sin\theta$$
$$G_{711}=-\rho_x\mu_O\sin\theta/4$$
$$G_{712}=\rho_x\mu_O\sin\theta$$
$$G_{88}=4\mu_{Si}/3+\mu_O$$
$$G_{810}=\sqrt{2}\,\rho_x\mu_{Si}/3-\rho_z\mu_O\sin\theta$$
$$G_{811}=-\sqrt{8}\,\rho_x\mu_{Si}/3$$
$$G_{812}=-\sqrt{2}\,(\rho_x/3+\rho_y)\mu_{Si}$$
$$G_{1010}=\rho_x^2\mu_{Si}/6+\rho_z^2\mu_C+(\rho_x^2+\rho_z^2-2\rho_x\rho_z\cos\theta)\,\mu_O$$
$$G_{1011}=-\rho_x^2\mu_{Si}/3+\rho_x(\rho_x-\rho_z\cos\theta)\,\mu_O/4$$
$$G_{1012}=-\rho_x(\rho_z+3\rho_y)\mu_{Si}/6-\rho_z(\rho_x-\rho_z\cos\theta)\,\mu_O$$

TABLE I. MOLECULAR AND POTENTIAL CONSTANTS OF METHYLTRIMETHOXYSILANE

Bond distance and angle	Potential constants	
	Type	md·Å
x=Si–O		
=1.64 Å[a]	K_x(Si–O)	3.25
y=Si–C		
=1.888 Å[b]	K_y(Si–CH_3)	3.03
z=O–C	K_z(O–CH_3)	4.88
=1.42 Å[a]	H_{xx}(O–Si–O)	0.13
	H_{xy}(O–Si–CH_3)	0.12
∠O–Si–O	H_{xz}(Si–O–CH_3)	0.22
=∠O–Si–C	F_{xx}(O···O)	0.13
=109°28′	F_{xy}(O···CH_3)	0.08
∠Si–O–C	F_{xz}(Si···CH_3)	0.21
=113°[a]	κ	0.25

a) Values in tetramethoxysilane, $Si(OCH_3)_4$; M. Yokoi, This Bulletin, **30**, 100 (1957).
b) Value in tetramethylsilane, $Si(CH_3)_4$; W. F. Sheehan, Jr. and V. Schomaker, *J. Am. Chem. Soc.*, **74**, 3956 (1952).

5) J. C. Decius, ibid., **16**, 1025 (1948).
6) B. Crawford, ibid., **21**, 1108 (1953).

TABLE II. RAMAN AND INFRARED DATA, CALCULATED WAVE NUMBERS AND THE ASSIGNMENT FOR METHYLTRIMETHOXYSILANE

ν. Obsvd.		ν. Calcd.	Assignment	Mode of vibration
Raman	Infrared			
150(0b)		165	$\nu_3(a_1)$	SiOC and $CSiO_3$ sym. def.
174(2b)		171	$\nu_{12}(e)$	SiO_3 rocking
268(3bb)		286	$\nu_{11}(e)$	SiO_3 nonsym. def.
336(0)		325	$\nu_4(a_1)$	$CSiO_3$ and SiOC sym. def.
374(0)		371	$\nu_{10}(e)$	SiOC nonsym. def.
425(3b)		—	$\nu_9(e)$	SiOC nonsym. torsion
628(7)		627	$\nu_3(a_1)$	Si–O sym. str.
748(2)		782	$\nu_8(e)$	Si–O nonsym. str.
800(3)	790(m)	829	$\nu_2(a_1)$	Si–C str.
860(3b)	845(m)			(Si–)CH_3 rocking
1072(6)	1089(s)	1069	$\nu_7(e)$	C–O nonsym. str.
		1073	$\nu_1(a_1)$	C–O sym. str.
	1110(sh)			
1148(4)				(O–)CH_3 rocking
	1192(m)			
1270(4)	1267(m)			(Si–)CH_3 and (O–)CH_3 def.
	1402(vw)			
1430(3)				
1461(4b)	1459(w)			
	2333(b)			
2795(1)	2825(m)			(Si–)CH_3 and (O–)CH_3 str.
2915(5)	2931(m)			
2954(5b)	2953(sh)			
2990(5b)				

$$G_{1111}=\rho_x^2(8\mu_{Si}/3+5\mu_O/2)$$
$$G_{1112}=\rho_x(\rho_x/3+\rho_y)\mu_{Si}-\rho_x^2\mu_O/4$$
$$G_{1212}=(\rho_x+3\rho_y)^2\mu_{Si}/6+\rho_x^2\mu_O+3\rho_y^2\mu_C/2$$

The geometrical and the potential constants used in the calculation are listed in Table I. As an aid in determining these potential constants, excepting H_{xz} and F_{xz}, the results in the previous investigations on tetramethylsilane[7], methoxychlorosilanes[8] and diethylether[9] have been used. However, somewhat lower and higher values for K_x and K_z, compared with the corresponding values in methoxychlorosilanes and diethylether, respectively, have been adopted, to obtain better agreement between the observed and the calculated frequencies. The value of K_x adopted here is rather close to that previously obtained in dichloromethylether[10]. The mean value of $H(CH_3\text{–}Si\text{–}CH_3)$ in $Si(CH_3)_4$[7] and H_{xx} in this paper, and that of $F(CH_3\cdots CH_3)$ and F_{xx} have been used as H_{xy} and F_{xy}, respectively. The value of $\varkappa$ has been derived by means of the proportional allotment from the intramolecular tension of silicon tetrahedron in $Si(CH_3)_4$[7] and that in $Si(OCH_3)_4$[8]. The values of H_{xz} and F_{xz} have been selected so as to give good agreement between the calculated and observed ones. Finally, the value of F' has been assumed to be equal to $-F/10$ by the usual way.

Assignment of Observed Frequencies

From the F and G matrix elements given above, the fundamental frequencies have been calculated by the use of the molecular and the potential constants listed in Table I, and the results are shown in Table II, together with the observed wave numbers of the Raman and the infrared bands. The skeletal vibrations have been assigned by the calculation of the potential energy distribution in the symmetry coordinates, and also the hydrogen vibrations have been tentatively assigned.

The L matrices and the distribution of potential energy in symmetry coordinates have been calculated for the skeletal normal modes; the results are shown in Table III and IV, respectively.

The calculated frequencies of the skeletal vibrations are in good agreement with their corresponding observed values, except for the Raman line at 425 cm^{-1}. This line may be classified as the (Si–)OCH_3 torsional oscillation of e species. As shown in Table IV some of

7) T. Shimanouchi, *J. Chem. Soc. Japan, Pure Chem. Sec.* (*Nippon Kagaku Zasshi*), **74**, 266 (1953).
8) H. Murata, ibid., **77**, 893 (1956).
9) M. Hayashi, ibid., **78**, 222 (1957).
10) Y. Morino and M. Katayama, *Reports of Research Institute of Radiation Chemistry, The University of Tokyo* (*Fukusyaken-hōkoku*), **4**, 1 (1947).

TABLE III. THE L MATRICES OF THE SKELETAL NORMAL VIBRATIONS OF METHYLTRIMETHOXYSILANE

a_1 Vibrations

	Q_1	Q_2	Q_3	Q_4	Q_5
R_1(C-O sym. str.)	1.13	0.05	0.08	−0.07	−0.01
R_2(Si-C str.)	0.00	−0.85	0.54	0.07	0.01
R_3(Si-O sym. str.)	−0.29	0.58	0.55	−0.15	0.03
R_4($CSiO_3$ sym. def.)	−0.44	−0.73	−0.13	−0.57	−0.32
R_5(SiOC sym. def.)	−0.27	−0.81	−0.56	−0.53	0.33

e Vibrations

	Q_7	Q_8	Q_{10}	Q_{11}	Q_{12}
R_7(C-O nonsym. str.)	1.11	−0.23	−0.03	−0.02	−0.01
R_8(Si-O nonsym. str.)	−0.42	−0.96	−0.07	−0.03	0.02
R_{10}(SiOC nonsym. def.)	−0.25	0.44	0.77	−0.29	0.24
R_{11}(SiO_3 nonsym. def.)	−0.03	0.26	−0.42	−0.85	−0.13
R_{12}(SiO_3 rocking)	0.39	0.23	−0.66	0.11	0.48

TABLE IV. POTENTIAL ENERGY DISTRIBUTION $F_{ii}L_{ia}^2/\lambda_a$ FOR THE NORMAL VIBRATION OF SKELETAL IN METHYLTRIMETHOXYSILANE

a_1 Vibrations

	ν_1	ν_2	ν_3	ν_4	ν_5
R_1(C-O sym. str.)	0.94	0.00	0.01	0.04	0.01
R_2(Si-C str.)	0.00	0.57	0.40	0.03	0.00
R_3(Si-O sym. str.)	0.04	0.31	0.49	0.14	0.02
R_4($CSiO_3$ sym. def.)	0.02	0.09	0.01	0.39	0.49
R_5(SiOC sym. def.)	0.00	0.11	0.09	0.32	0.48

e Vibrations

	ν_7	ν_8	ν_{10}	ν_{11}	ν_{12}
R_7(C-O nonsym. str.)	0.91	0.07	0.01	0.00	0.00
R_8(Si-O nonsym. str.)	0.09	0.90	0.03	0.01	0.01
R_{10}(SiOC nonsym. def.)	0.00	0.03	0.51	0.12	0.23
R_{11}(SiO_3 nonsym. def.)	0.00	0.01	0.13	0.87	0.05
R_{12}(SiO_3 rocking)	0.01	0.01	0.30	0.01	0.74

the symmetry coordinates of totally symmetric species are related to several normal modes to a considerable extent; the R_2 and R_3 coordinates to both modes of ν_2 and ν_3, and the R_4 and R_5 coordinates to both modes of ν_4 and ν_5. Especially, in the latter case, the symmetrical deformation of the $CSiO_3$ group and that of the SiOC groups have their equal share in the potential energy of the ν_4 normal mode, and also of the ν_5 mode.

The author wishes to express his sincere thanks to Professor T. Watase of this University, and Dr. H. Murata and Dr. K. Shimizu of Osaka Municipal Technical Research Institute for much valuable discussion.

Department of Applied Chemistry
Faculty of Engineering
Osaka University
Miyakojima-ku, Osaka

5,6-Epoxy-cholestane

By Fumikazu MUKAWA

(Received September 22, 1959)

Ruzicka et al.[1] have first obtained 5,6β-epoxy-5β-cholestane (II), m.p. 53°C, as a by-product of the reaction of cholest-5-ene (I) and peroxyacid. Recently Shoppee et al.[2] have reported that the melting point of 5,6β-epoxy-5β-cholestane (II) obtained by the above method was 55°C. Henbest and Wrigly[3] have prepared II, m.p. 58°C, $[\alpha]_D$ −9°, by the reduction of 5-bromo-5α-cholestan-6-one with lithium aluminum hydride, while Hallsworth and Henbest[4] have reported that the same epoxycholestane (II) prepared from 5,6β-diacetoxy-5α-cholestane by the method which was adopted in the preparation of 5,6β-epoxy-5β-cholestane 3β-ol from 3β,5,6β-triacetoxy-5α-cholestane[5] melted at 80°C and showed $[\alpha]_D$ +8°.

Mori and the present author[6] have investigated the addition reaction of hypochlorous acid (isocyanuric chloride-acetic acid) to 3-substituted-Δ^5-steroids and found that the products were 5α-chloro-6β-hydroxy derivatives which have been converted by base to 5β,6β-epoxides. In the same manner I was expected to be converted to II. However the intermediate 5-chloro-6β-hydroxy-5α-cholestane (III) was not produced but 5,6β-dichloro-5α-cholestane and oily substance were obtained.

Then, the author has turned to another route to obtain II. Thus, reduction of 5,6β-epoxy-5β-cholestan-3β-yl halide (I_a, halogen=Cl; I_b, halogen=Br) with lithium in liquid ammonia or zinc-copper alloy in ethanol has lead to II, m.p. 79°C, $[\alpha]_D$ +80° in 70% yield. The structure of II assigned was confirmed in the following way. Reduction of II with hydroiodic acid (55%) in acetone gave I, and reduction with lithium aluminum hydride in ether gave cholestan-6β-ol. Treatment of II with 1 N sulfuric acid in acetone gave 5,6β-dihydroxy-5α-cholestane.

It was interesting to notice that the oxide ring at $C_5 \sim C_6$ was indifferent to the lithium-ammonia reducing system. By the similar reduction 5,6α-epoxy-5α-cholestan-3β-yl halide (IV_a, halogen=Cl; IV_b, halogen=Br) yielded 5,6α-epoxy-5α-cholestan (V), m.p. 76°C, $[\alpha]_D$ −39.9°, which showed no melting point depression upon admixture with an authentic specimen.

It has been reported[7,8] that the reaction of the halohydrins of the steroid series with zinc dust and acetic acid yielded the unsaturated steroids, but 6β-halo (chloro and bromo)-5α-cholestan-3β,5-diol-3-monoester was exceptional. Thus, the latter was converted into the *trans*-triol 3,6-diester and Δ^5-derivative was not produced at all. It seems to be noteworthy that in the case of 6β-chloro-5α-cholestan-5-ol (VI), 6β-acetoxy-5α-cholestan-5-ol was obtained being accompanied by a small amount of I[9]. III was converted into I with zinc dust and acetic acid or lithium in liquid ammonia. I was also obtained by the reduction of VI with lithium in liquid ammonia.

Experimental**

Attempted Hypochlorous Acid Addition on Cholest-5-ene (I).—To a mixture consisting of 0.5 g. of I, 0.2 g. of isocyanuric chloride and 15 ml. of acetone were added five drops of 30% aqueous acetic acid. The whole was refluxed for five minutes. After cooling to room temperature, the mixture was poured with stirring into 10% aqueous sodium carbonate, and then extracted with ether. The extract was washed with water and dried over magnesium sulfate. After removal of the solvent, the residue was recrystallized from methanol to yield 0.18 g. of needles, m.p. 120~121°C. The compound did not depress the melting point on admixture with the authentic sample of 5,6β-dichloro-5α-cholestane. The filtrate was left to stand in a refrigerator for one month. However, only a gum was obtained.

5,6β-Epoxy-5β-cholestane (II).—*i) From 5,6β-epoxy-5β-cholestan-3β-yl chloride (I_a).*—To a well stirred mixture of 50 mg. of lithium and 30 ml. of liquid ammonia, 0.3 g. of I_a in 40 ml. of dry ether was added. After thirty minutes, the excess of

* Present address: Tsurumi Research Laboratory of Chemistry, Tsurumi-ku, Yokohama.

1) L. Ruzicka, M. Furter and G. Thomann, *Helv. Chim. Acta.*, **16**, 327 (1933).

2) C. W. Shoppee, R. H. Jenkins and G. H. R. Summer, *J. Chem. Soc.*, **1958**, 1657.

3) H. B. Henbest and T. I. Wrigly, ibid., **1957**, 4596.

4) A. S. Hallsworth and H. B. Henbest, ibid., **1957**, 4606.

5) M. Davis and V. Petrow, ibid., **1949**, 2536.

6) S. Mori, *J. Chem. Soc. Japan, Pure Chem. Sec. (Nippon Kagaku Zasshi)*, **64**, 981 (1943); F. Mukawa, ibid., **78**, 452 (1957).

7) S. Mori, ibid., **70**, 257, 303 (1949); L. Fieser and R. Ettorre, *J. Am. Chem. Soc.*, **75**, 1700 (1953) etc.

8) S. Mori and F. Mukawa, *Proc. Japan Acad.*, **31**, 532 (1955).

9) Cf. The reaction of epoxy-cholestane derivatives with boronfluoride etherate takes a different course when the substituent is persent at C_3. H. B. Henbest et al. *J. Chem. Soc.*, **1957**, 4765.

* All melting points are uncorrected.

lithium was destroyed by acetone. After two hours at room temperature, addition of water, extraction of ether and crystallization of the crude product from ethanol afforded II, m.p. 70~73°C, raised by crystallization from ethanol-*n*-hexane to 79°C, $[\alpha]_D$ +8°. It exhibited no absorption of hydroxyl band in the infrared spectrum.

Found: C, 83.85; H, 11.20. Calcd. for $C_{27}H_{46}O$: C, 83.87; H, 11.99%

A mixture of 0.3 g. of I_a, 0.2 g. of zinc-copper alloy and 20 ml. of alcohol was heated under reflux for 3 hr. But in this case only starting material was recovered.

ii) From 5,6β-epoxy-5β-cholestan-3β-yl bromide[10] *(I_b).*—To a well stirred mixture of 50 mg. of lithium and 30 ml. of liquid ammonia, 0.3 g. of I_b in 40 ml. of dry ether was added. There were obtained needles which melted at 79°C and did not depress the mixed melting point with the authentic 5,6β-epoxy-5β-cholestane (II). The infrared spectra of the two compounds were identical.

In another rum with 0.5 g. of I_b, 0.2 g. of zinc-copper alloy and 30 ml. of ethanol were heated under reflux for 3 hr. There were obtained 0.3 g. of needles with a melting point 78~79°C. There did not depress the mixed melting points with an authentic sample.

Structure of 5,6β-Epoxy-5β-cholestane (II).—The product obtained as described above was shown to be 5,6-β-epoxy-5β-cholestane (II) by the following series of reactions.

i) A solution of II (0.2 g.) in acetone (5 ml.) was treated with two drops of hydroiodic acid (55%). After being kept to stand at room temperature (21°C) for 24 hr., the solution was poured into water and was extracted with ether. The extract was washed with sodium thiosulfate solution (5%) and water, dried and evaporated. Crystallization of the residue from alcohol gave 0.1 g. of I, m.p. 90~91°C and mixed m.p. with the authentic specimen showed no depression.

ii) II (0.5 g.) dissolved in anhydrous ether (80 ml.) was added dropwise to lithium aluminum hydride (0.1 g.) in ether for 20 min. at room temperature (20°C) and then refluxed for 5 hr. Chromatography of the product over florisil and elution with ether-methanol gave 5α-cholestan-6β-ol, m.p. 81°C (plates from alcohol), undepressed in m.p. on admixture with the authentic specimen.

iii) A mixture of II (0.3 g.), two drops of sulfuric acid (10%) and 50 ml. of methanol was heated under reflux. After two hours, addition of water, extraction with ether and crystallization of the crude product from alcohol afforded 5α-cholestan-5,6β-diol, m.p. 60~73°C, raised by recrystallization from alcohol to 125°C, undepressed on admixture with the authentic sample.

5,6α-Epoxy-5α-cholestan-3β-yl Bromide (IV_b).—Cholesteryl bromide (0.5 g.) was added to a cold solution of perbenzoic acid (1.3 equiv.) in 20 ml. of chloroform, the reaction mixture briefly stirred and then allowed to stand at room temperature (18°C) for 48 hr. before pouring into a solution of sodium carbonate. The organic phase was separated, washed with water to neutrality, dried and evaporated. The product crystallized from alcohol to afford IV_b, m.p. 87~89°C, $[\alpha]_D = -21.2°$.

Found: C, 68.90; H, 9.70. Calcd. for $C_{27}H_{45}OBr$: C, 69.74; H, 9.75.

5,6α-Epoxy-5α-cholestane (V).—The procedure of II was followed. The product was recrystallized from methanol, yielded V, m.p. 76°C, $[\alpha]_D$ −39.9°. It was identified by mixed melting points with the authentic sample.

5-Chloro-5α-cholestan-6β-ol (III).—A solution of the epoxy-cholestan II (0.2 g.) in alcohol-free chloroform (2 ml.) was treated with a saturated solution of anhydrous hydrogen chloride in alcohol-free chloroform (10 ml.). After standing at 0°C for 4.5 hr., the solution was evaporated to dryness. The residue was recrystallized from aetone-water to give III, yield, 0.12 g., m.p. 121~123°C, $[\alpha]_D = -12°$.[11]

Found: C, 76.51; H, 11.45. Calcd. for $C_{27}H_{47}OCl$; C, 76.10; H, 11.29%.

i) With zinc dust.—A mixture of 0.1 g. of III, 0.2 g. of zinc dust, and 5 ml. of acetic acid was heated under reflux for 3 hr. The solids were filtered off and water was added to produce faint turbidity. The crystals were then crystallized from chloroform-methanol and melted at 91°C. The compound did not depress the melting point with the authentic sample of cholest-5-ene (I).

ii) With lithium in liquid ammonia.—The chlorohydrin (III) (0.3 g.) in dry ether was added with vigorous stirring to a solution of lithium (50 mg.) in liquid ammonia (50 ml.). After 30 min., excess lithium was destroyed by acetone. The reaction mixture was then diluted with ether and the ether solution was washed with cold hydrochloric acid solution (1%). Finally the solution was washed with water, dried sodium sulfate and the solvent removed. Crystallization of the product from methanol afforded I, yield, 0.2 g., m.p. 90~91°C, undepressed on admixture with the authentic sample.

Reduction of 6β-Chloro-5α-cholestan-5-ol (VI).—*i) With zinc dust.*—A mixture of 1 g. of VI, 0.5 g. of zinc dust and 50 ml. of acetic acid was heated under reflux for 1.5 hr. The solids were filtered off and diluted with water. The product was extracted with ether. The ether solution washed with sodium bicarbonate solution (5%) and then with water, dried, and evaporated. The residue was chromatographed on 20 g. of neutral alumina, the petroleum ether elute yielding, after crystallization from chloroform-methanol, 0.1 g. of I, undepressed on admixture with the authentic sample. Chromatography gave in the ether-methanol (1 : 1) fractions, 0.4 g. of 6β-acetoxy-5α-cholestan-5-ol, m.p. 80~82°C, $[\alpha]_D = -20°$, the melting point being raised by recrystallization from methanol to 108°C.

Found: C, 77.90; H, 11.00. Calcd. for $C_{29}H_{50}O_3$: C, 77.97; H, 11.28%.

ii) With lithium in liquid ammonia.—Reduction of 0.3 g. of VI with lithium in liquid ammonia under conditions described for the 5-chloro-isomer afforded 0.1 g. of I. It was identified by mixed melting point with the authentic sample.

10) S. Mori, *J. Chem. Soc. Japan, Pure Chem. Sec.* (*Nippon Kagaku Zasshi*), **74**, 89 (1953).

11) C. W. Shoppee et al., *J. Chem. Soc.*, **1958**, 1657, reported 108~109°C, $[\alpha]_D$ −22°.

The author wishes to express his sincere thanks to Professor K. Hata for his encouragement and to Assistant Professor Y. Nomura of the Universtiy of Tokyo for reading the manuscript. This work was supported in part by a Grant-in-Aid from the Ministry of Education.

Department of Chemistry
Faculty of Science
Tokyo Metropolitan University
Setagaya-ku, Tokyo

Detection of Chromatogram by Swelling of Adsorbent

By Akira HAYAKAWA and Kōji TANAKA

(Received September 17, 1959)

In the field of adsorption chromatography the column chromatography was devised for the first time by Tswett[1] about fifty years ago. Afterwards, in 1950, the chromatostrip as the modifier was introduced by Kirchner et al.[2] and more recently the larger strip called chromatoplate was used by Reitsema[3]. In these methods the adsorbent was sealed with a glass wall or hardened with a binder.

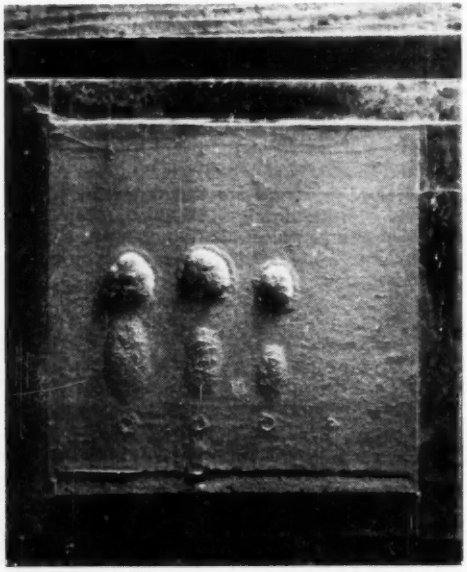

Fig. 1. Swelling of adsorbent by water vapor.
Developer: 10% ethylacetate in *n*-hexane
Adsorbent: Silica gel (about 200 mesh)
Sample : Benzaldehyde
The amount of sample is 15, 10, 5 and 1 drops from left to right, respectively.

Simplifying the operation of the above-mentioned chromatoplate, the authors used the adsorbent alone sprinkled on a glass plate without a binder. As an adsorbent was used silica gel of about 200 mesh. It was sprinkled on the glass plate in constant thickness (2 mm.) and the surface was smoothed with a glass rod. The commercially available pure benzaldehyde was used as a sample. It was developed by 10% ethylacetate in hexane and dried in air to remove the developer.

The present authors happened to discover that the adsorbent of the part of the spot made by benzaldehyde was upheaved by swelling when the plate prepared by the above-described process was left in an enclosed case of high humidity. In order to confirm this phenomenon, the authors left another plate prepared in quite the same way in the sealed case of 100% relative humidity and over a long time observed the change expected to be brought about on it. After 2 to 3 hr. an umbrella-shaped swelling of the adsorbent began to occur at the place of

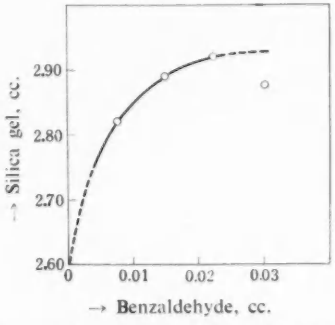

Fig. 2. The apparent volume of silica gel as a function of the amount of benzaldehyde added to 1 g. of silica gel.

1) M. Tswett, *Ber. deut. botan. Ges.*, 24, 384 (1906).
2) J. G. Kirchner and G. J. Keller, *J. Am. Chem. Soc.*, 72, 1867 (1950).
3) R. H. Reitsema, *Anal. Chem.*, 26, 960 (1954).

R_f about 0.5. After one day that of oval shape began to arise at R_f about 0.22 and after three days the rising of ring shape was found around the first one. The second swelling and the third one seem to be caused by derivatives of benzaldehyde or its oxidation products. In either case it is considered that polar groups in these compounds act on polar groups of silica gel and consequently the swelling by water vapor takes place. The condition of the plate after four days is shown in Fig. 1. The amount of the sample dropped on silica gel was 15, 10, 5 and 1 drops from left to right, respectively. In a drip of one drop hardly any upheaval is observed.

Fig. 2 was obtained by plotting the apparent volume of silica gel as a function of the amount of benzaldehyde added to 1 g of silica gel. As is seen in the figure the apparent volume of silica gel increased with the increasing amount of benzal dehyde until it came to 0.025 cc.

The swelling phenomenon was scarcely noted when the relative humidity in the enclosed case was decreased to below 40 or 50%.

So far the expression of the spot of chromatography has been two dimensional or superficial. But the use of the swelling phenomenon above described will make the three dimensional observation possible.

Department of Chemistry
Tokyo College of Science
Shinjuku-ku, Tokyo

*Structure of Namakochrome. I**

By Toshihiko MUKAI**

(Received September 16, 1959)

In a previous paper[1] of this series the isolation of namakochrome, which would be a new derivative of the polyhydroxynaphthoquinones, from *Polycheira rufescens* was reported.

Polycheira rufescens (in Japanese, Murasaki-kuruma-namako) is a sort of tiny sea cucumber, its body being dark purple in color. A crowd of the animals may be frequently found in the stony tidal zone. As preliminary examination assigned the purple coloration of the sea cucumber to a chromoprotein, some methods to isolate the prosthetic group of the protein had been undertaken, and namakochrome was obtained.

Twenty-eight thousand of the sea cucumbers were collected for material at a sea coast near the Amakusa Marine Laboratory, the Faculty of Science, Kyushu University. These animals were dipped into a dilute aqueous solution of acetic acid. The chromoprotein dissolved easily in the aqueous acid to give a red solution. To the red extract, diluted aqueous solution of sodium hydroxide was added till the color of the extract changed to dark purple. After the resulting opaque solution was allowed to stand overnight, a pale yellow supernatant liquid was decanted off and the remaining purple pasty precipitates were collected***. The precipitates were treated with concentrated hydrochloric acid, followed by extraction with ether. Two and thirty-six hundredths grams of crude, orange red pigment of the prosthetic group were obtained. Repeated recrystallization from glacial acetic acid afforded pure namakochrome, a pigment of crimson prisms, m. p. 218°C.

Namakochrome contains only three elements, namely, carbon, hydrogen and oxygen. Its molecular weight determination (by the micro-Rast method with camphorquinone) and elementary analysis yield the result which is in agreement with the molecular formula $C_{11}H_8O_8$. The ultraviolet (ethanol) and infrared (Nujol) absorption spectra are shown in Figs. 1 and 2, respectively. On heating, a greater part of namakochrome sublimes, leaving some carbonized matter. This pigment is easily soluble in solvents of high polarity. It is soluble in mineral acids, to which it is very stable; even in hot concentrated sulfuric acid a red color of the solution lasts for a considerably long time. It is unstable to the solution of weak alkali. With sodium bicarbonate solution it gives a light yellow color, changing gradually to colorless. On the other hand, it dissolves easily in

* "Pigments of Marine Animals", IX. VIII of this series: M. Yamaguchi, This Bulletin, 32, 1171, (1959).

** Present address: Yoshitomi Pharmaceutical Industries, Ltd., Yoshitomi Factory, Yoshitomi-cho, Chikujo-gun, Fukuoka-ken.

1) T. Mukai, *Mem. Fac. Sci., Kyushu Univ., Series C, Chem.*, 3, No. 2, 29 (1958).

*** The same precipitates could be obtained by the addition of methanol instead of aqueous sodium hydroxide, but this caused only imperfect precipitation, and its supernatant liquid still remained deep red.

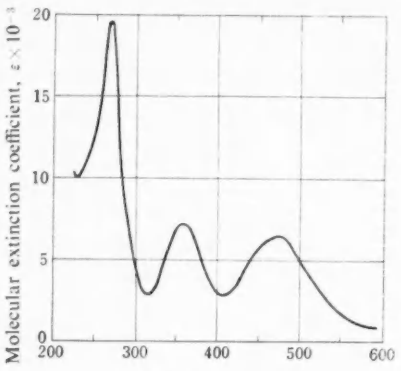

Fig. 1. Absorption curve of namakochrome: solvent, ethanol.

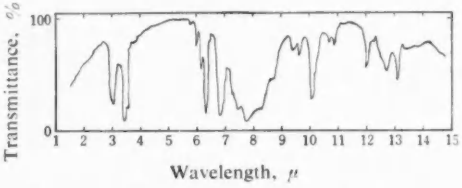

Fig. 2. Infrared spectrum of namakochrome.

dilute solution of strong alkali with orange red color, while with its more concentrated aqueous solution, it forms immediately purplish black salt, which is sparingly soluble in it. With heavy metals also, it gives the difficultly soluble black salts with purple luster. Namakochrome reduces silver nitrate, and gives a dark purple color with ferric chloride. It gives a purple precipitation with neutral lead acetate, a reddish purple precipitation with basic lead acetate, and a dark orange-yellow color with magnesium acetate. On adding zinc dust to a solution of namakochrome in an acetic anhydride pyridine mixture, an original red color soon changes to yellow, then the solution gradually turns colorless, and at last returns to yellow****. This yellow solution becomes red when warmed with concentrated sulfuric acid.

Now, the above-mentioned properties and the molecular formula would suggest that namakochrome is a derivative of polyhydroxynaphthoquinones. To obtain information on the basic structure of the molecular skeleton, zinc dust distillation of namakochrome was carried out, and naphthalene was isolated in a relatively good yield.

Brockmann[2] found that when most of quinone derivatives were hydrogenated in the presence of palladium catalyst on barium sulfate, in aqueous alkaline solution, only the quinone-system prevailed over the other reducible groups in the same molecule. He extended this selective hydrogenation method to a determination of a molecular weight of Actinorhodin, a new hydroxyquinone derivative, isolated from *Streptomyces coeli* color. This method was applied to catalytic hydrogenation of namakochrome, and the result showed that namakochrome shoud have a quinone-system in the molecule, as it absorbed one molecular equivalent of hydrogen. On coming in contact with the air, the resulting pale brown solution changed its color to original red.

In the presence of concentrated sulfuric acid as a catalyst, namakochrome reacts with acetic anhydride to yield a lemon yellow acetyl derivative, m. p. 158~163°C. The acetyl derivative is labile to alkali. When its ethereal solution is brought into contact with aqueous sodium bicarbonate solution even for a short time, decomposition of the acetate occurs and the original material, namakochrome, is isolated. In contrast with namakochrome, the acetate is easily soluble in benzene, sparingly soluble in cold ethanol, and recrystallization from ethanol is very easy. The analytical data[3] obtained for the acetate is in accordance with the formula, $C_{11}H_3O_8(COCH_3)_5$. The infrared absorption spectrum of the acetate is shown in Fig. 3.

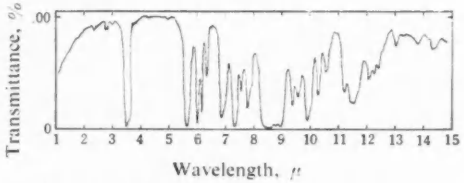

Fig. 3. Infrared spectrum of penta-acetyl namakochrome.

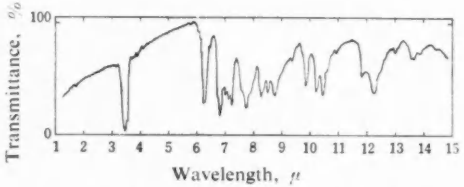

Fig. 4. Infrared spectrum of trimethyl ether of namakochrome.

**** There must be a leuco-acetyl derivative of namakochrome in the resulting yellow solution, but no crystalline product is obtained as yet.

2) H. Brockmann et al., *Ber.*, **88**, 781 (1955).

3) In the estimation of acetyl groups of the acetate, 5 N NaOH was emloyed as a saponifying agent. Namakochrome was also treated under the same saponifying condition, because there remained doubt whether this agent degrades namakochrome to acidic volatile substances. It was shown that under these conditions namakochrome which was liberated from the acetate by the saponification, did not suffer an undesirable change.

Since the formation of the acetate evidently shows many hydroxyl groups to be present in the namakochrome molecule, namakochrome was strongly methylated by the Kuroda's method[4]. The resulting ether is of brownish red long needles, melting at 185~187°C. Analysis of the ether yields results which are in accordance with the formula $C_{11}H_5O_5(OCH_3)_3$. The infrared absorption spectrum of the ether is shown in Fig. 4. In the trimethyl ether, two of the hydroxyl groups at the α-positions of naphthalene nucleus would, as usual, not be methylated and remain free. Furthermore, the following properties of the ether indicated that the positions of the three methylated hydroxyl groups would be located in 3-, 6- and 7-positions of the naphthalene nucleus. Such properties were of the color reactions, which were introduced by Kuroda[5], and were taken up in the work of Kuhn[6] on the structure of Echinochrome A. That is, namakochrome trimethyl ether, like naphthazarin and β-alkyl naphthazarin, dissolved in an aqueous solution of sodium hydroxide to give a purplish blue color[7], and did not dissolve in an aqueous solution of sodium bicarbonate. On the contrary, the color reaction and the precipitation reaction of namakochrome itself, already described, could be recognized it as the analogue of naphthopurpurin or β-alkyl naphthopurpurin.

Although, there is not, as yet, the clue given to the nature of one of the eight oxygen atoms in the namakochrome molecule, this oxygen atom should form a group together with the other remaining one carbon atom and three hydrogen atoms. The unascertained group would, therefore, be either a hydroxymethyl or a methoxyl group, which should locate at the β-position of the naphthalene nucleus. Namakochrome may be, anyhow, a new derivative of the naphthoquinones, possessing the following structure (I ↔ II).

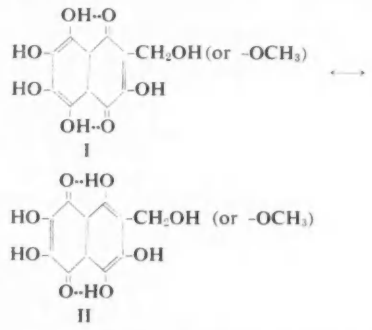

4) T. Kuroda, *Nat. Sci. Rep. Ochanomizu Univ., Tokyo*, **2**, 90 (1951).
5) T. Kuroda et al., *Proc. Imp. Acad.*, **12**, 239 (1936); ibid., **13**, 158 (1938).
6) R. Kuhn et al., *Ber.*, **72**, 1407 (1939).

Experimental

Distillation of Namakochrome with Zinc Dust.—Essentially the method of Ochiai and Tsuda[8] was followed for the distillation of namakochrome with zinc dust. Namely, one end of a glass tube (9 mm. in diameter and about 50 mm. in length) was drawn to a capillary about 2 mm. in diameter. A plug of clean asbestos was inserted at the point where the capillary began. Zinc dust was introduced into the tube so that it covered a length of about 10 mm. from the plug, and a mixture of namakochrome and zinc dust was introduced into the tube to fill a length of about 10 mm. of the tube. Zinc dust was last placed in the tube, which was then sealed at the open end. The mixture of 370 mg. of namakochrome and 7 g. of zinc dust was treated with seventeen of the above-mentioned apparatus. The tube containing the materials was heated from the open side to the closed side with continuous rotation, and was finally heated red hot. The distillates were three separate fractions. The first distillate was a waxy substance having a blue fluorescence near the asbestos plug. At a short distance, there was found the second distillate, colorless liquid over which the third colorless leaflets and white solid was lapped. The portions of the crystals and the solid were cut into sections (about 10 mm.) and packed at a sealed end of a glass tube (about 15 mm. in diameter). The other end of the tube had been drawn out to form a capillary, whose length and inside diameter were 70 mm. and 1.5~2 mm., respectively. Then the apparatus was emptied to about 20 mmHg from the open end of the capillary, which was then sealed off. The portion of the larger tube was horizontally inserted in an aluminum block maintained at 95°C, and a wet filter paper condenser was attached at a half of the capillary portion from its closed end. The part of the capillary where the colorless oil separated perfectly, was cut off, and the remainder portions of the capillary were handled again in the same manner as described. Repeated operations afforded the solid which is slightly contaminated with the oil. The solid was then purified by crystallization from ethanol. About 4 mg. of crystals, m. p. 80°C, were obtained. This was naphthalene, whose melting point was unaffected by admixture with an authentic sample.

Catalytic Hydrogenation.—In 4 ml. of 1 N sodium hydroxide, 7.65 mg. of namakochrome were hydrogenated in the presence of about 50 mg. of palladium on barium sulfate catalyst.

Found: 1.02 mol. of hydrogen.

Penta-acetyl Namakochrome.—One drop of concentrated sulfuric acid was, at room temperature, added to a suspension of namakochrome (50 mg.) in acetic anhydride (1.5 g.), to give a lemon yellow solution. After setting aside for two hours at room temperature, the resulting solution was poured into

7) When the trimethyl ether was catalytically hydrogenated by the Brockmann's method described above, the purplish-blue color caused by the alkali rapidly changed into nearly colorless and again backed to purplish-blue on exposure to air. At this time the trimethyl ether absorbed one molecular equivalent of hydrogen.
8) E. Ochiai and K. Tsuda, "Yuki Biryo Shyoryo Teiryo Bunsekiho", Nanzando, Tokyo (1940), p. 300.

ice water and extracted with benzene. The yellow extracts were concentrated to a small volume under the reduced pressure. The concentrate was filtered through a calcium carbonate column (3×16 cm.). Evaporation of the effluent under reduced pressure, and recrystallization of the resulting yellow residue from ethanol gave penta-acetyl namakochrome as lemon yellow needles (50 mg.), m. p. 158~163°C.

Found: C, 52.68; H, 3.93; AcO, 45.40. Calcd. for $C_{21}H_{18}O_{13}$: C, 52.73; H, 3.79; AcO, 44.99%.

Trimethyl Ether of Namakochrome.—A solution of diazomethane (prepared from 5 g. of *N*-methyl-*N*-nitroso-*p*-toluenesulfonamide) in ether (40 ml.) was added dropwise to crystalline namakochrome (300 mg.) spread on a large evaporating dish. When the violence of the reaction abated, and evaporation of the ether slowed, the solvent remaining in the evaporating dish was removed. Addition of the diazomethane solution was then continued. After the addition of the whole ethereal solution of diazomethane, the remaining solvent was evaporated as before. The resulting residue was dissolved in benzene, and filtered through a calcium carbonate column. The red effluent was evaporated to dryness under reduced pressure, and there remained brownish red, fine, long, needles, which, by recrystallization from a mixture of ethanol and benzene, gave trimethyl ether (279 mg.), m. p. 185~187°C.

Found: C, 54.17; H, 4.72. Calcd. for $C_{14}H_{14}O_8$: C, 54.20; H, 4.55%.

The author wishes to express his thanks to Professor Dr. Tokuichi Tsumaki under whose guidance this investigation has been carried out. The expenses of the work were partially covered by the Scientific Research Grant of the Ministry of Education.

Department of Chemistry
Faculty of Science
Kyushu University
Hakozaki, Fukuoka

Some Characteristics of Zinc Oxide Phosphor

By Keiji MAEDA

(Received August 31, 1959)

Zinc oxide is well known as a typical oxide semiconductor and many investigations have been made concerning it. Its characteristics are quite complex compared with those of other materials. It may be said that this complexity is due to the divalency of the constituting ions and the difficulty of preparing prefect crystals. Moreover, since zinc oxide is not a purely ionic crystal, one must take into account the homopolar nature of the binding. Although important progress has been made by the recent studies on the single crystal, there remain many ambiguities. A review of the present status has been given by Heiland, Mollwo and Stöckman[1].

On the other hand, zinc oxide has been used for many practical purposes, for instance, as a catalyst and photocatalyst for a series of chemical reactions, and as a phosphor with very fast decay time. In addition, it may play an important role in future in the "Electrofax" process of photographic duplication in which the photoconductivity of zinc oxide is utilized. These applications depend in a direct way on the electronic processes in zinc oxide. As a phosphor, zinc oxide has never been a subject of such extensive investigations as have been made on other similar materials, i.e. zinc and cadmium sulfides. In this report, several characteristics of zinc oxide phosphors will be described.

1) G. Heiland, E. Mollwo and F. Stöckman, "Solid State Physics", Vol. 8, Academic Press, New York (1959), p. 193.

Experimental and Results

Sample Preparation. — The samples were prepared by firing pure zinc oxide at several temperatures from 950 to 1200°C in an atmosphere of air, forming gas, hydrogen or oxygen for various durations. In some samples, many kinds of impurities were intentionally added before firing. Only the phosphors fired in reducing atmosphere give bright green luminescence. The phosphors fired in air emit yellowish green luminescence and those fired in an oxidizing atmosphere dark orange luminescence. Except in the case of a phosphor containing lead as an activator, effects of added impurities on the luminescence spectrum do not appear clearly. Neither chlorine nor bromine functions as a coactivator. A firing in hydrogen atmosphere at 1000°C for 3 min. produced a phosphor emitting intense luminescence. Because of the strong intensity of the green luminescence, one will be concerned with it in the experiments described below.

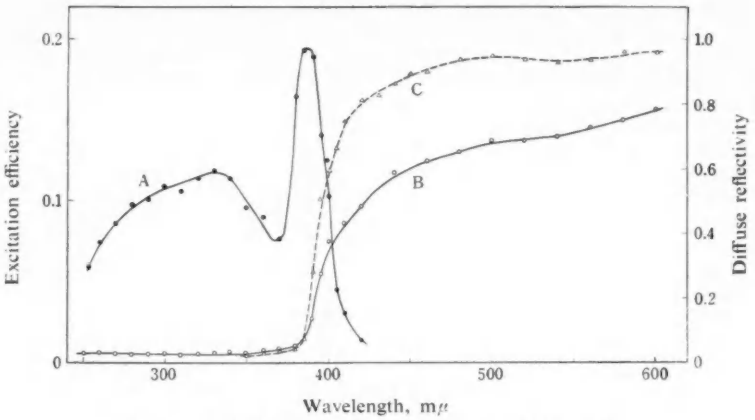

Fig. 1. Excitation and reflectivity spectra of zinc oxide.

A: Excitation efficiency of zinc oxide fired under reducing conditions.
B: Diffuse reflectivity of the same sample as A.
C: Diffuse reflectivity of zinc oxide fired under oxidizing conditions.

Luminescence Spectrum.—The luminescence spectrum was measured at both room and liquid air temperatures. The peak of the green luminescence is located at about 5050 Å and does not shift with temperature, but the spectral width decreases with decreasing temperature. This is in agreement with the published data[2].

Reflection and Excitation Spectra.—The reflection and excitation spectra were measured with the apparatus made in this laboratory[3]. As examples, some results are shown in Fig. 1. Here, the value of excitation efficiency is defined as the ratio of the number of luminescence photons to that of the incident exciting photons.

The absorption edge of zinc oxide is about 3900 Å at room temperature. The sample fired in an oxidizing atmosphere has a steep rise in reflectivity and a slight absorption at longer wavelengths. On the other hand, for the sample fired in a reducing atmosphere the rise in reflectivity is gradual and a notable absorption extends over the whole wavelength region measured. For the sample fired in stronger reducing condition, a larger absorption results.

There is a remarkable peak in excitation spectrum at the position of the absorption edge. The peak value of the excitation efficiency depends on the sample and amounted to 0.31 in the most efficient phosphor. It has no apparent correlation with the increment in absorption. The excitation decreases with decreasing wavelength of excitation and there are some structures. A similar behavior of excitation spectrum has been reported for zinc sulfide[4] and cadmium sulfide[5].

Temperature Dependence of Luminescence Intensity.—The temperature dependence of luminescence intensity was measured under excitation with both 2537 and 3650 Å radiation. As shown in Fig. 2, the characteristics are similar for the

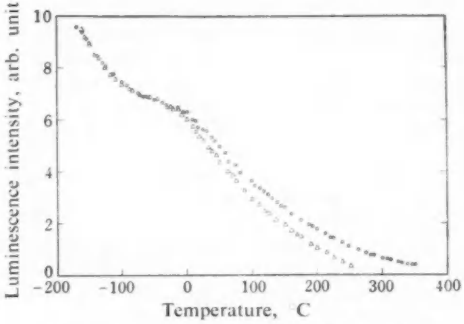

Fig. 2. Temperature dependence of luminescence intensity under 3650 Å excitation (○) and under 2537 Å excitation (△).

two sorts of exciting radiation. The intensity decreases with increasing temperature and the curves have an interesting shape in the neighborhood of 0°C. The author's results are different from those reported by Gobrecht et al.[6]

Decay of Luminescences.—The decay of luminescence was measured with an oscilloscope

2) F. J. Studer and L. Gaus, "Soild Luminescent Materials", John Wiley & Sons, Inc., New York (1948), p. 258.
3) Y. Uehara, I. Masuda and Y. Kobuke, to be published.
4) R. H. Bube, *Phys. Rev.*, **90**, 70 (1953).
5) C. C. Klick, ibid., **89**, 274 (1953).
6) H. Gobrecht, D. Hahn and K. Scheffer, *Z. Physik*, **139**, 365 (1954).

Tektronix Model 513D under pulse excitation of cathode ray and care was taken not to distort the fast signal. The luminescence decays very fast and exponentially with time constant of 0.4 μ sec., which is about an order of magnitude smaller than that reported by Gobrecht et at.[6]

After interruption of photoexcitation it was found a phosphorescence of very weak intensity but with long persistence. This phosphorescence is excited more strongly by 2537 than by 3650 Å radiation. The decay is neither simple monomolecular nor bimolecular type but is represented approximately by t^{-n} for a period of time between 1 and 20 min. following the interruption of excitation. Here n has the value 0.9 ± 0.1 depending on the sample and the condition of excitation. The phosphorescence intensity at one minute after interruption of excitation is smaller by more than three orders of magnitude than the steady state intensity under excitation.

Atmosphere Dependence of Luminescence Intensity.—It was found that the luminescence intensity under photoexcitation becomes stronger when the ambient atmosphere of the phosphor is evacuated with a rotary vacuum pump. Fig. 3 illustrates the change of luminescence intensity with time for the processes, excitation on, pumping start, admission of air and excitation off. Average values on several measurements are shown in Table I for the following quantities; the ratio of the luminescence intensity increase ΔI due to evacuation to the steady state luminescence intensity I, in air and the rise time T_r and the decay time T_d of the processes. It was ascertained that $\Delta I/I$ is larger for the weak excitation than for the strong excitation; that is, the proportionality between excitation and luminescence intensities is not satisfied. Here, the intensity ratio of strong to weak excitation is roughly 10. T_r is probably determined by the speed of the evacuating system, and T_d is in dependent on the exciting condition. It could not be detected the slow variation of luminescence intensity compared with T_r and T_d within the experimental accuracy. The light

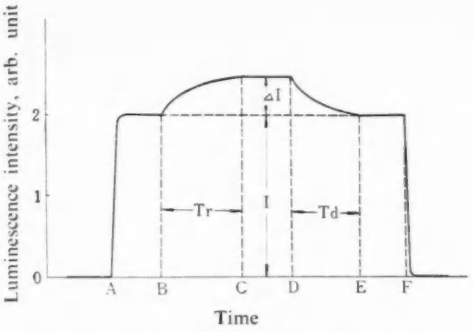

Fig. 3. Variation of luminescence intensity with ambient atmosphere.

A: Excitation on, B: pumping start, C: steady state luminescence intensity in vacuo, D: admission of air, E: steady state luminescence intensity in air and F: excitation off.

TABLE I

Excitation	$\Delta I/I$	T_r	T_d
Strong 2537 Å	0.14	1.7 min.	50 sec.
Weak 2537	0.18	1.8	54
Strong 3650	0.10	1.6	62
Weak 3650	0.17	1.3	44

intensity reflected from magnesia smoke placed at the same position as the phosphor is independent of the condition of evacuation. Therefore, the variation of luminescence intensity described above can not be attributed to any other causes than the phosphor itself.

Then the author investigated the relationship between the luminescence intensity and the ambient pressure under various kinds of simple atomospheres, such as hydrogen, oxygen, dry air, and mixed vapor of water and ethanol. Of these atmospheres, hydrogen, oxygen or dry air, when passed through a liquid air trap, exhibits no recognizable effect on luminescence intensity. On the other hand, water or ethanol vapor decreases the luminescence intensity

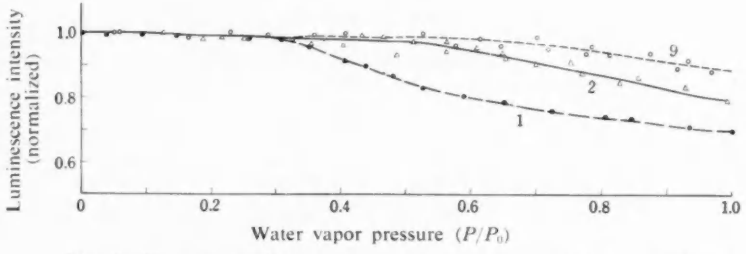

Fig. 4. Dependence of luminescence intensity on water vapor pressure for various exciting intensities (at 30°C). Relative exciting intensity is indicated in the figure and P_0 is the saturated vapor pressure.

considerably. Although the results are not always reproduced quantitatively, some of them are shown in Fig. 4 for three excitation intensities. From this figure it is seen that the luminescence intensity suffers quenching for the pressure P which is not so small compared with the saturated vapor pressure P_0. In the process of these measurements, photoadsorption or photodesorption of the vapor which gives an effect to luminescence intensity did not occur to a measurable extent.

Surface Potential.—It was expected that a change in the surface potential of the phosphor might be accompanied with the variation of the luminescence intensity under the ambient atmosphere. The author measured it by the well known Kelvin method using gold as a reference electrode. When dry or wet air is admitted, the surface potential of zinc oxide becomes more positive compared with that in vacuo.

X-ray Diffraction.—From the precise measurements of the lattice constants, it is concluded that the lattice constants are independent of the conditions of preparation within an experimental error. The numerical values are in complete agreement with those reported by Bunn[7].

Discussion

The green luminescence of zinc oxide is characteristic of phosphors fired under reducing conditions, and it has been reported[8] that a stoichiometric excess of zinc is detected by a chemical analysis from a sample prepared in this way. Although there would be many kinds of lattice defects in the green-emitting zinc oxide, interstitial zinc atoms and oxygen vacancies are considered to be the dominant defects. It is customarily said that the interstitial zinc atom is the luminescence center for the green luminescence. However, according to Mollwo[9], the green luminescence is quenched when the crystal is heated in zinc vapor below 1000°C and zinc atoms diffuse in it. On the contrary, Riehl and Ortman[10] have attributed the green luminescence center to the oxygen vacancy. The energies necessary for formation and migration of the oxygen vacancy would be greater than those of the interstitial zinc atom, since the binding between oxygen and zinc should be broken for the former processes. This consideration agrees with the various conditions for the preparation of the green-emitting phosphor. For example, the efficient phosphor should be fired at higher temperatures than those necessary for the introduction of interstitial zinc atoms.

The oxygen vacancy would be able to accomodate two electrons since it has two effective positive charges in the ionic model of zinc oxide. The same conclusion can be drawn from the covalent model. The first electron would be bound tightly in the vacancy but the second loosely. To be effective as the luminescence center, it would be necessary for the vacancy to have a specific charge. The quenching of green luminescence when the electric conductivity becomes great, for example, by the introduction of excess of zinc as cited above, might be explained by this model.

The ultraviolet emission, which is known to appear in zinc oxide fired under oxidizing conditions, is not observed for these samples. Although Kröger and Meyer[11] attributed this emission to exciton recombination, still more investigations are necessary to arrive at a definite conclusion.

The author has tried an analysis of the one-dimentional configurational coordinate curves[12] based on the experimental result that the peak position of the luminescence spectrum is independent of temperature. From this analysis one may expect an absorption band by the luminescence center in the long wavelength side of the absorption edge. Although an absorption in the expected wavelength region increases as a result of the firing under reducing conditions, one can not observe the excitation of luminescence by this absorption. In additon, the intensity of this absorption does not have any apparent connection with the luminescence efficiency of the phosphor. Therefore, it is considered that this absorption is probably caused by a change of the crystal lattice due to the presence of interstitial zinc atoms.

The decay of luminescence is exponential and the time constant is smaller by one order of magnitude than the reported value. It is considered[1] that the luminescence is emitted by the recombination of electrons at the luminescence center. If it is assumed that the density of the free electron is greater than that of the emptied luminescence center during excitation, the exponential decay and the dependence of time constant upon the sample can be understood.

It might be expected that the temperature dependence of luminescence intensity is different for the two sorts of excitation, i.e. 2537 and 3650 Å radiation, because the author found the structure in the excitation spectrum and the position of the absorption edge shifts toward longer wavelengths with increasing temperature at the

7) C. W. Bunn, *Proc. Phys. Soc.*, **47**, 835 (1935).
8) E. Mollwo and F. Stöckman, *Ann. Physik*, (6), **3**, 223 (1948).
9) E. Mollwo, *Z. Physik*, **138**, 478 (1954).
10) N. Riehl and H. Ortman, *Z. Elektrochem.*, **60**, 149 (1956).
11) F. A. Kröger and H. J. G. Meyer, *Physica*, **20**, 1149 (1954).
12) K. Maeda, *J. Phys. Soc. Japan*, **14**, 478 (1959).

rate of about 10^{-3} eV./deg[13]. However, the result is not in accord with the expectation. This suggests that the excitation spectrum changes its shape with temperature. From the temperature dependence shown in Fig. 2, one expects not a single but two kinds of activation energy for the nonradiative de-excitation. In the usual way, one obtains the activation energies of the order of 0.01 and 0.2 eV. by fitting the calculated curve with the observed. However, it is not clear to what process these activation energies correspond.

The slow phosphorescence decay indicates the existence of various metastable states. Considering the *n*-type conductivity of the phosphor, these states are probably deep hole traps.

The effect of atmosphere on the luminescence intensity has been reported only for a case of oxygen on cadmium sulfide[14]. In this case, the photoconductivity of cadmium sulfide is also reduced by the oxygen ambient. It is known that the photoconductivity of zinc oxide is decreased to a large extent by the adsorption of oxygen[15]. However, one found a quenching of luminescence intensity due to molecules having the hydroxyl group but not due to oxygen. Therefore, the above phenomenon seems to have a mechanism of quenching different from that found in cadmium sulfide. As stated in the preceding section, the surface potential of zinc oxide becomes positive when either dry or wet air is admitted relative to that in vacuo. Therefore, the change in the surface potential is not a cause of the luminescence quenching. The adsorbed molecule probably has an effect to accelerate nonradiative recombination of electrons and holes at the surface. Since the absorption constant in the fundamental absorption region is of the order of 10^5 cm^{-1}[16], electron-hole pairs are created by light absorption to a depth greater than that of a range influenced by surface conditions. Therefore, the amount of quenching is relatively small.

13) E. Mollwo, *Z. angew. Phys.*, **6**, 257 (1954).
14) S. H. Liebson and E. J. West, *J. Chem. Phys.*, **23**, 977 (1955); S. H. Liebson, ibid., **23**, 1732 (1955).
15) D. A. Melnick, *J. Chem. Phys.*, **26**, 1136 (1957).
16) E. Mollwo, *Ann. Physik*, (6) **3**, 230 (1948).

Summary

Zinc oxide phosphors were prepared under various conditions. From measurements on the characteristics of the green luminescence of the phosphors fired in reducing atmosphere, the following features were observed. (1) In the excitation spectrum, there is a sharp peak at the position of the absorption edge and a gradual decrease toward shorter wavelengths with some structures. The observed maximum value of excitation efficiency is 0.31. (2) The luminescence intensity decreases with increasing temperature. The plot of intensity against temperature has an unusual shape in the neighborhood of 0°C. (3) The decay of luminescence is exponential and the time constant, 0.4 μ sec., is smaller than that previously reported by an order of magnitude. Long persistent phosphorescence is observed indicating the presence of deep hole traps. (4) The luminescence intensity decreases in a gaseous ambient of molecules having the hydroxyl group.

Standing on the present experimental results, discussions have been undertaken on the luminescence center as well as on the theoretical explanation of the observed characteristics.

The author wishes to express his sincere thanks to Dr. Y. Uehara for his suggestion of this problem, to Mr. Y. Kobuke for the preparation of the samples and to Mr. Y. Hukao for the use of his X-ray apparatus.

Matsuda Research Laboratory
Tokyo Shibaura Electric Co.
Kawasaki

Twofold Wagner-Meerwein Type Rearrangement of 2,3-Disubstituted Indoles

By Masao NAKAZAKI

(Received August 31, 1959)

Among various interesting reactions of indoles, little attention has been paid to Fischer's rearrangement, which is as old as the discovery of indole itself. In 1888, Fischer and Schmidt[1] reported the conversion of 3-phenylindole (Ia) into 2-phenylindole (IIa) when heated with zinc chloride. Recently, Clemo and Seaton[2] demonstrated the same type of migration of substituents from 3-position to 2-position of indoles on 3-(2-pyridylmethyl) indole (Ib), 3-benzylindole (Ic) and skatole (Id), using aluminum chloride instead of zinc chloride.

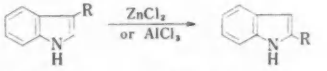

I a R = C_6H_5 II a R = C_6H_5
b R = 2-pyridylmethyl b R = 2-pyridylmethyl
c R = $CH_2C_6H_5$ c R = $CH_2C_6H_5$
d R = CH_3 d R = CH_3

Fig. 1

These researchers, however, did not dare to inquire into the possible exchange reaction of substituents between 2- and 3-position of 2,3-disubstituted indoles. This paper is concerned with the demonstration of such possibility.

As a simple representative of 2,3-disubstituted indoles, the reaction of 2-methyl-3-phenylindole (III) with aluminum chloride was initially investigated.

2-Methyl-3-phenylindole (III) was prepared from phenylacetone phenylhydrazone by Fischer's method employing zinc chloride[3] or borontrifluoride[4] as catalyst, but the melting point (78~79°C) was inconsistent with the reported melting point (59~60°C) by Trenkler[5] or Ockenden and Schofield[4]. Because of such a great discrepancy of the melting points, an attempt was made to determine the structure of the indole (m. p. 78~79°C) by ozonolysis.

The melting point of *o*-acetoaminobenzophenone (IVa) obtained by ozonolysis of the indole (m. p. 78~79°C) was found 86~88°C in our hands, but Ockenden and Schofield[4] reported it as 71~73°C. There have been disputes about the melting point of IVa: von Auwers and Meyerburg[5] reported that their sample prepared by the acetylation of *o*-aminobenzophenone showed m. p. 72°C, but from the mother liquor there were obtained other crystals melting at 88.5~89°C, although the latter were the only crystals obtained in the repetitions of their experiment by themselves[6] and by others[7].

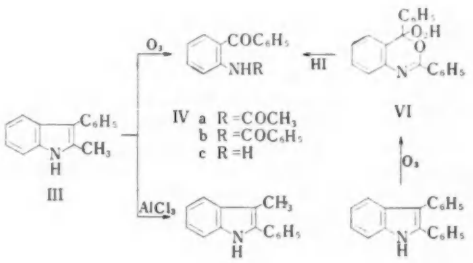

IV a R = $COCH_3$
b R = COC_6H_5
c R = H

III VII V VI

Fig. 2

To secure an authentic sample of *o*-acetoaminobenzophenone for comparison, IVa was synthesized by the process which involved the ozonolysis of 2,3-diphenylindole (V). Although Ockenden and Schofield[4] reported that 2,3-diphenylindole was converted into *o*-benzaminobenzophenone (IVb) (m. p. 85~86°C, 56% yield) when ozone was passed into a solution of V in ethyl acetate at 0°C, our result was found to be another contradiction with their finding.

In our hands, the ozonide VI[8] (m. p. 152

1) E. Fischer and T. Schmidt, *Ber.*, **21**, 1811 (1888).

2) G. R. Clemo and J. C. Seaton, *J. Chem. Soc.* **1954**, 2582. An excellent review about the rearrangement reactions of indoles and indolenines are to be found in P. L. Julian, E. W. Meyer and H. C. Pring, "The Chemistry of Indoles" in R. Elderfield, "Heterocyclic Compounds", Vol. 3, John Wiley & Sons, Inc., New York (1952), p. 1.

3) B. Trenkler, *Ann.*, **248**, 111 (1888).

4) D. W. Ockenden and K. Schofield, *J. Chem. Soc.*, 1953, 612.

5) K. von Auwers and V. Meyerburg, *Ber.*, **24**, 2384 (1891).

6) K. von Auwers, ibid., **29**, 1263 (1896).

7) A. Bishler and D. Barad, ibid., **25**, 3081 (1892); R. Camps, *Arch. Pharm.*, **237**, 683 (1899).

8) The stable ozonides of indole derivatives were first observed by G. Mentzer, D. Molho and Y. Berguer, *Bull. soc. chim.*, 555 (1950). For details see the exhaustive studies by Witkop on the ozonide of phenylskatole. B. Witkop and J. B. Patrick, *J. Am. Chem. Soc.*, **74**, 3855 (1952); B. Witkop, J. B. Patrick and H. M. Kissman, *Chem. Ber.* **85**, 949 (1952). Remembering that 2-aryl indoles usually afford stable ozonides, it seems rather surprising that Ockenden and Schofield[4] obtained *o*-benzaminobenzophenone (IVb) directly from V. The stable ozonide from 2-(dibenzylmethyl)-3-benzylindole which does not possess the 2-aryl group was reported by M. Nakazaki and K. Tanno, *J. Chem. Soc. Japan, Pure Chem. Sec.* (*Nippon Kagaku Zasshi*), **77**, 952 (1956).

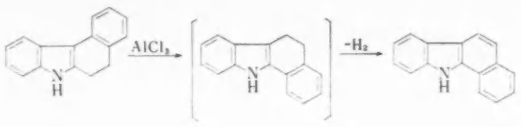

VIII IX X

Fig. 3

~154°C, decomp.) of 2, 3-diphenylindole was the only compound isolated following their procedure (in ethyl acetate) or in the ozonolysis in acetic acid. The ozonide VI showed typical reactions of ozonide, and reductive hydrolysis[9] with hydroiodic acid in acetic acid converted it into benzoic acid and *o*-aminobenzophenone (IVc) which was acetylated with acetic anhydride to give *o*-acetoaminobenzophenone (m. p. 86~88°C) which was found identical with IV from 2-methyl-3-phenylindole by mixed melting point determination and comparison of their infrared absorption spectra. Thus being established the structure, 2-methyl-3-phenylindole (III) was subjected to rearrangement by heating with aluminum chloride at 220~240°C for 20 min. The product obtained was found to be identical with 2-phenyl-3-methylindole[10] (VII).

5, 6-Dihydro-7-benzo[*c*]carbazole[11] (VIII) was the next indole derivative tried to demonstrate the analogous rearrangement reaction.

The tetrahydrocarbazole derivative VIII, which was provided from the phenylhydrazone of β-tetralone was heated at 220~240°C for 20 min. with aluminum chloride to give rise to 11-benzo[*a*]carbazole (X), apparently resulted by the dehydrogenation of the intermediate 5, 6-dihydro-11-benzo[*a*]carbazole (IX) with aluminum chloride.

Mechanistically, these rearrangements[12] can be explained by twofold Wager-Meerwein type rearrangement initiated by the electrophilic attack by the Lewis acid (A in Fig. 4.) on the 3-position of indoles (Fig. 4), and the equilibria XI ⇄ XII ⇄ XIII ⇄ XIV are completly parallel to the one to be found in rearrangement of indolenines[13] and Plancher's rearrangement of indolenium compounds[14].

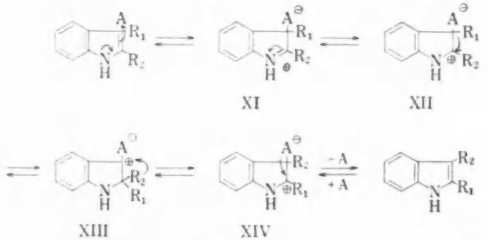

XI XII XIII XIV

Fig. 4

The *Spiro* type intermediate XV, analogous to the one postulated by Woodward[14] in the dienone-phenol rearrangement, would be the intermediate in the case of 5, 6-dihydro-7-benzo[*c*]carbazole.

Inspection of the ultraviolet spectra (Figs. 6, 7 and 8) and π-electron density in the indole

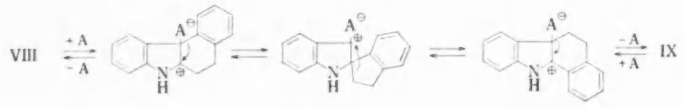

XV

Fig. 5

9) The reductive hydrolysis of the stable ozonide with hydrobromic acid in acetic acid was carried out on the ozonide of 2-(dibenzylmethyl)-3-benzylindole. M. Nakazaki and K. Tanno, Ref. 8.

10) The structure of 2-phenyl-3-methylindole was established by ozonolysis. B. Witkop and J. B. Patrick, *J. Am. Chem. Soc.*, **74**, 3861 (1952); cf. B. Witkop, J. B. Patrick and H. M. Kissman, *Chem. Ber.*, **85**, 949 (1952).

11) Dehydrogenation by heating with 5% palladium-charcoal at 250~260°C converted VIII into the known 7-benzo[*c*] carbazole, m. p. 135~136°C.

12) In Bishler's indole synthesis applied on α-bromo-β-phenylpropiophenone, there was found the formation of two isomeric indoles, i. e. 2-phenyl-3-benzylindole and 2-benzyl-3-phenylindole. [P. L. Julian, E. W. Meyer, A. Magnani and W. Cole, *J. Am. Chem. Soc.*, **67**, 1203 (1945); P. L. Julian and J. Pikl, ibid., **55**, 2105 (1953)]. But from a mechanistical standpoint which was worked out recently by Wygand and Richter[*Chem. Ber.*, **88**, 499 (1955)], it is highly improbable to assume the mutual interconversion of these two indoles under the reaction condition *after* they are formed.

13) See the author's papers on Plancher's rearrangement which follow.

14) R. B. Woodward and T. Singh, *J. Am. Chem. Soc.*, 72, 494 (1950). For the dienone-phenol rearrangements of the compounds possessing *spiro* structure, see R. T. Arnold, J. B. Buckley and R. M. Dodson, ibid., 72 3553 (1950); E. N. Marvell and A. O. Geiszler, ibid., 74, 1259 (1952). Also it is noteworthy to compare the smooth conversion of VIII into X with the dienone-phenol rearrangement of 2-keto-4a-methyl-2, 4a, 5, 6-tetrahydrobenzo[*c*] phenathrene in which the transformation which requires a *spiro* intermediate is inhibited. C. Djerassi and T. T. Grossnickle, *J. Am. Chem., Soc.*, **76**, 1741 (1954).

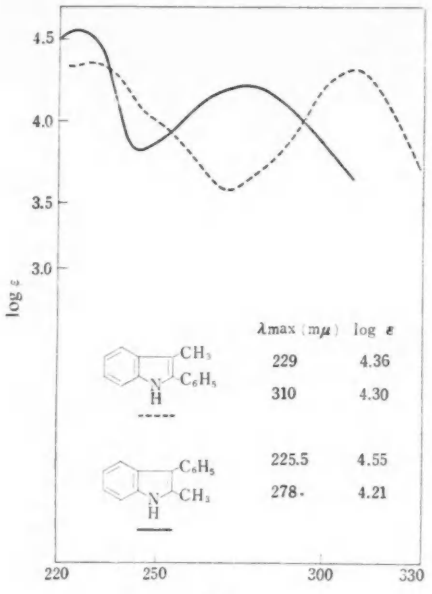

Fig. 6

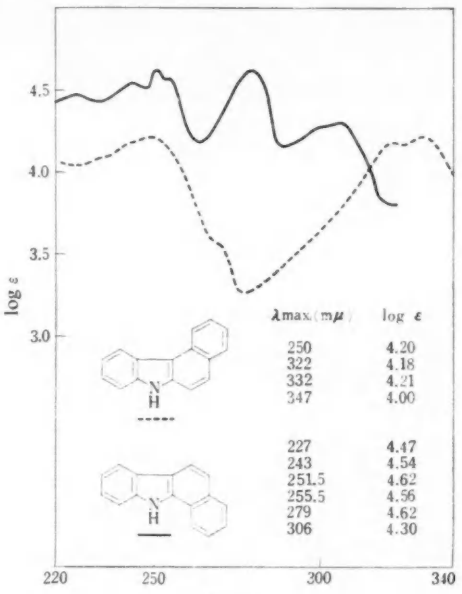

Fig. 8

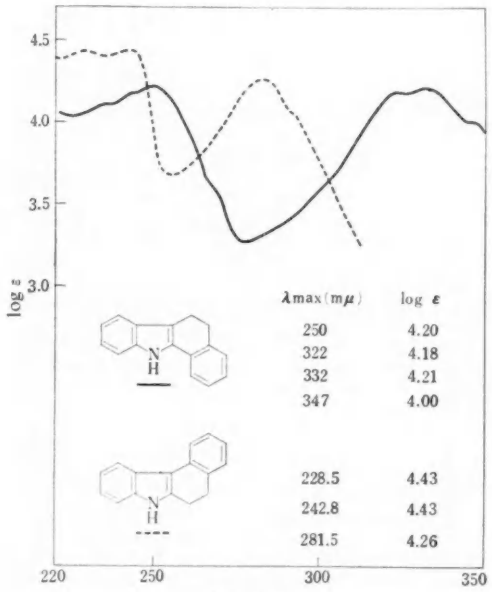

Fig. 7

nucleus[15] (1.059 at 2-position, 1.066 at 3-position) suggest that the driving force of these rearrangement reactions could be sought in the mesomeric stabilization of the products (VII, IX and X) by the phenyl group at 2-position rather than at 3-position.

The same reasoning could be applied to interprete Fischer's rearrangement[1] (migration of hydrogen anion), and the hyperconjugation effect[16] would be the stabilization factor in the case of the rearrangements of the indoles studied by Clemo and Seaton[2].

Experimental[17]

2-Methyl-3-phenylindole (III).—*By borontrifluoride etherate method*[4].—To a solution of 7.0 g. of phenylacetone phenylhydrazone (m. p. 82~83°C) in 70 cc. of acetic acid, 5.1 g. borontrifluoride etherate was added, and the mixture was refluxed on an oil bath for 3 hr. The color of the solution changed from yellow to brown→green→brown. Water was added into the reaction mixture and was extracted with ether. The ethereal extract was washed with water and dried over anhydrous sodium sulfate. Removal of the solvent gave a viscous brown

15) K. Higasi and H. Baba, "Quantum Organic Chemistry (Ryoshi Yuki Kagaku)", Asakura Publishers, Tokyo (1956), p. 406.

16) The formation of *spiro*-(cyclopentane-1, 3'-*pseudo*-2'-methyl-indole) instead of 11-methyltetrahydrocarbazole nine from *spiro*-(cyclopentane-1, 2'-*pseudo*indoxyl) by the action of methyl/magnesium iodide could be interpreted on the same reason. B. Witkop and J. B. Patrick, *J. Am. Chem. Soc.* **75**, 2572 (1953).

17) All melting points are not corrected. All ultraviolet spectra were measured by an EPS-2 Hitachi autorecording spectrophotometer and infrared spectra on a Perkin Elmer Model 12C. The analyses were performed in the Microanalytical Laboratory of the Institute of Polytechnics, Osaka City University.

liquid which was distilled in vacuo to afford a pale yellow liquid, b. p. 196~200°C/3 mmHg, 6.2 g. (57.5% yield). The distilate solidified gradually and was recrystallized from petroleum ether (b. p. 60°C) to give crystals, m. p. 78~79°C (literature[3,4]: 59~60°C).

Found: C, 86.77; H, 6.54. Calcd. for $C_{15}H_{13}N$: C, 86.99; H, 6.32%.

U.V. spectrum[18]: λ_{max} mμ (log ε), 225.5 (4.55), 278 (4.21). λ_{min} 245.5 mμ (log 3.82) in methanol (Fig. 6). I.R. spectrum: 2.95 μ.

The picrate was recrystallized from ethanol to give brown needles, m. p. 139~140°C (literature[3,4]: 141~142°C).

Found: C, 57.42; H, 3.84; N, 12.25. Calcd. for $C_{21}H_{15}O_7N_4$: C, 57.80; H, 3.70; N, 12.84%.

By zinc chloride method.— Following Trenkler's procedure[3], III was obtained in a yield of 34.6%, m. p. 78~79°C.

Ozonolysis of 2-Methyl-3-phenylindole (III)[4].—To a mixture of 0.7 g. of 2-methyl-3-phenylindole and 35 cc. of acetic acid, a stream of ozone (approximately 5%) was passed for 45 min. at room temperature, during which time the color of the solution was observed to change from yellow to red and then pale yellow again. After water was added, the solution was extracted with ether thrice and the combined ethereal extract was washed with water followed by 5% sodium carbonate solution and saturated sodium chloride solution. Removal of the solvent yielded a viscous residue which could be brought to crystallization by trituration. The crystals were collected and recrystallized from petroleum ether to give crystals melting at 70~72°C (0.291 g.). The melting point was raised to 86~88°C by further recrystallization from water-ethanol.

Found: C, 75.20; H, 5.78. Calcd. for $C_{15}H_{13}O_2N$: C, 75.30; H, 5.48%.

Stable Ozonide of 2, 3-Diphenylindole VI. — *In acetic acid solution.*—A stream of ozone (approximately 5%) was passed into a mixture of 1.4 g. of 2, 3-diphenylindole (V) and 40 cc. of acetic acid for 1 hr. at room temperature. Completion of the reaction was estimated by the usual color change of the reaction mixture: yellow→red→yellow. Water was added to the reaction mixture to precipitate crystals which were collected and washed with water.

Recrystallization from water-ethanol and ethanol gave colorless crystals (0.47 g.) which darkened in color at 140°C and decomposed at 152~153°C. On the addition of solid potassium iodide to a solution of VI in acetic acid, the formation of iodine was observed.

In ethyl acetate solution[4]. — Into a mixture of 2.7 g. of 2, 3-diphenylindole and 75 cc. of ethyl acetate, a stream of ozone (approximately 5%) was passed for 1.5 hr. at 0°C. The color of the solution changed from yellow to brown and then to yellow again. After the excess of ozone was blown out by a stream of nitrogen, the solvent was removed in vacuo to give a viscous residue which crystallized by trituration with ethanol.

The crude ozonide (decomp. 148°C) weighed 1.5 g., and was recrystallized from ethanol to afford crystals which decomposed at 152°C.

Found: C, 75.37; H, 5.12; N, 4.54. Calcd. for $C_{20}H_{15}O_3N$: C, 75.69; H, 4.72; N, 4.41%.

Reductive Hydrolysis of the Ozonide VI. — A mixture of 1.50 g. of the ozonide VI, 30 cc. of acetic acid and 10 cc. of constant boiling hydroiodic acid solution was refluxed for 5 hr. After water was added, the reaction mixture was extracted with ether, to separate basic and acidic fractions.

Acidic fraction.—The ether layer was washed with sodium thiosulfate solution to discharge the color of iodine, and was extracted with 2 N sodium hydroxide solution. The alkaline solution was acidified with 2 N hydrochloric acid solution to precipitate benzoic acid, 0.381 g. Recrystallization from water gave crystals which melted at 120~121°C, alone and admixed with an authentic specimen of benzoic acid.

Basic fraction.—The aqueous layer was washed with ether, and was made basic with 2 N sodium hydroxide solution to precipitate *o*-aminobenzophenone (IVc). Extraction with ether afforded 0.81 g. of golden yellow crystals, m. p. 101~104.5°C, which was recrystallized from ethanol-water to give yellow prisms, m. p. 103~105°C (literature[5-7]: 105~106°C).

Found: C, 78.88; H, 5.68. Calcd. for $C_{13}H_{11}ON$: C, 79.16; H, 5.62%.

***o*-Acetoaminobenzophenone (IVa).**—After a mixture of 0.287 g. of *o*-aminobenzophenone (IVc) and 3 cc. of acetic anhydride was heated on a water bath for 2 hr., water was added to the reaction mixture and was allowed to stand overnight. The precipitate was collected (0.270 g., m. p. 70~75°C) and was recrystallized from ethanol-water to give crystals melting at 86~88°C, alone and admixed with *o*-acetoaminobenzophenone (m. p. 86~88°C) obtained by the ozonolysis of 2-methyl-3-phenylindole (III) mentioned above. The identity was further comfirmed by the comparison of their infrared spectra.

Rearrangement of 2-Methyl-3-phenylindole (III).—A mixture of 0.8 g. of 2-methyl-3-phenylindole, 0.8 g. of aluminum chloride and 0.1 g. of sodium chloride was heated at 220°C for 15 min. and at 220~240°C for 5 min. After water was added to the resulted brown solid mass, the mixture was extracted with ether and the ether extract was washed with water and dried over anhydrous potassium carbonate. After the removal of the solvent, the residue was distilled in vacuo to afford 0.482 g. of a viscous oil, b. p. 194~195°C/2 mmHg., which crystallized on standing. Recrystallization from ethanol-water gave crystals, m. p. 89~90°C, which were found identical with 2-phenyl-3-methylindole[19] by mixed melting point determination and the comparison of infrared

18) Ultraviolet spectrum of phenylskatole: λ_{max}(log ε), 229 mμ (4.36), 310 mμ (4.30), λ_{min}271.5 mμ (3.58) in ethanol (Fig. 6). Cf. R. Huisgen and I. Ugi, *Ann.*, **610**, 57 (1957); B. Witkop and J. B. Patrick, *J. Am. Chem. Soc.*, **74**, 3855 (1952).

19) Prepared from propiophenonephenylhydrazone. Fischer's method employing zinc chloride was found to give better yield than the polyphosphoric acid method and borontrifluoride method. [H. M. Kissman, D. W. Farnsworth and B. Witkop, *J. Am. Chem. Soc.*, **74**, 3948 (1952); B. Witkop and J. B. Patrick, ibid, **74**, 3858 (1952)].

spectrum with an authentic specimen. Also, the picrate, m. p. 144~145°C (from ethanol) was prepared to confirm their identity.

5,6-Dihydro-11-benzo[*a*]carbazole (IX)[20].—5,6-Dihydro-11-benzo[*a*]-carbazole was synthesized following the procedure of Organic Syntheses, **30**, 90 (1950), m. p. 163~164°C (from methanol).

U. V. specrum. λ_{max} (log ε), 250 mμ (4.20), 332 mμ (4.21); λ_{min} (log ε), 227 mμ (4.04), 276 mμ (3.26) in ethanol (Fig. 7).

The picrate was recrystallized from ethanol to give black needles, m. p. 153~154°C.

Found: N, 12.79. Calcd. for $C_{22}H_{16}O_7N_4$: N, 12.50%.

11-Benzo[*a*]carbazole (X)[20].—A mixture of 0.5 g. of 5,6-dihydro-11-benzo[*a*]carbazole and 0.1 g. of 5% palladium-charcoal was heated at 250~260°C for 20 min. 11-Benzo[*a*]carbazole which resulted was recrystallized from benzene to yield crystals melting at 227~229°C. (literature[21]: 225°C).

U.V. spectrum[21]: λ_{max} mμ (log ε), 227 (4.47), 243 (4.54), 251 (4.62), 279 (4.62), 306 (4.30). λ_{min} mμ (log ε), 234 (4.42), 248.5 (4.51), 263 (4.18), 289 (4.17) in ethanol (Fig. 8).

5,6-Dihydro-7-benzo[*c*]carbazole (VIII)[20].—Considerable generation of heat was observed when 15 cc. of acetic acid was added to a mixture of 2.9 g. of β-tetralone[22] and 2.2 g. of phenylhydrazine, and the reaction mixture was refluxed for 1 hr. After being kept at room temperature overnight, the crystals precipitated were filtered and washed with methanol. Recrystallization from methanol gave 2.4 g. of crystals, m. p. 102~103°C.

Found: C, 87.91; H, 6.15; N, 6.31. Calcd. for $C_{16}H_{13}N$: C, 87.64; H, 5.98; N, 6.39%.

U.V. spectrum: λ_{max} mμ (log ε), 228.5 (4.43), 281.5 (4.26); λ_{min} 253.5 mμ (log ε 3.68) in ethanol (Fig. 7).

The picrate was recrystallized from ethanol to give black needles, m. p. 129~132°C.

Found: C, 59.11; H, 3.76; N, 12.82. Calcd. for $C_{22}H_{16}O_7N_4$: C, 58.93; H, 3.60; N, 12.50%.

7-Benzo[*c*]carbazole[20].—A mixture of 0.5 g. of 5,6-dihydro-7-benzo[*c*]carbazole and 0.1 g. of 5% palladium-charcoal was heated at 250~260°C for 30 min. The reaction mixture was extracted with boiling benzene. After the solvent was removed, the residue was recrystallized from benzene-ligroin to give 0.27 g. of crystals, m. p. 135~136°C (literature[23]: 135°C). U.V. spectrum: λ_{max} mμ (log ε), 265 (4.69), 285.5 (4.02), 326 (4.09), λ_{min} mμ (log ε), 237 (4.21), 282 (3.86), 295 (3.45) in ethanol (Fig. 8).

Rearrangement of 5,6-dihydro-7-benzo[c]carbazole (VIII).—A mixture of 1.0 g. of VIII, 1 g. of aluminum chloride and 0.1 g. of sodium chloride was heated at 220°C for 10 min. and at 220~240°C for 5 min. Water was added to the reaction mixture and extracted with ether. The yellow ethereal solution, which exhibited green fluorescence, was washed with water followed with sodium bicarbonate solution and was dried over anhydrous magnesium sulfate. Distillation of the solvent gave a residue which was recrystallized from carbon tetrachloride to give 0.206 g. of crystals, m. p. 210°C. Recrystallization from benzene improved the melting point to 227~228°C which was undepressed when admixed with an authentic specimen of 11-benzo[*c*]carbazole. The identity was further confirmed by the comparison of their infrared spectra which could be overlapped in every detail.

The author is very grateful to Dr. Itaru Mita for his generous supply of phenylacetone. He also feels indebted to Mr. Satosi Kamei for his technical assistance; to Mr. Sachihiko Isoe who kindly measured the ultraviolet absorption spectra.

Institute of Polytechnics
Osaka City University
Kita-ku, Osaka

20) Nomenclature followed A. M. Patterson and L. T. Capell, "The Ring Index", Reinhold Publishing Corp., New York (1940), p. 331.
21) R. Huisgen and I. Ugi, *Ann.*, **616**, 63 (1957).
22) M. D. Soffer et. al., "Organic Syntheses", Vol. 32, John Wiley & Sons, Inc., New York (1952), p. 97.
23) F. R Japp and W. M. Maitland, *J. Chem. Soc.*, **83**, 270 (1903); H. T. Bucherer and F. Seyde, *J. Prakt. Chem.*, (2) **77**, 406 (1908); S. G. P. Plant and S. H. Oakeshott, *J. Chem. Soc.*, **1928**, 1843.

Mechanism of Plancher's Rearrangement. I. Twofold Wagner-Meerwein Type Rearrangement of Indolenines

By Masao NAKAZAKI, Koji YAMAMOTO and Kikuo YAMAGAMI

(Received August 31, 1959)

Although, Plancher's rearrangement, which was described as early as 1898, has been much discussed[1], it is unfortunate that there are found many misunderstandings about the scope of this rearrangement, because of lack of definitive studies. In 1898, Plancher[2] obtained a indolenium iodide, m. p. 237°C, from 2-ethyl-3-methylindole (I) and 2-methyl-3-ethylindole (II) by heating with methyliodide at 120°C.

He assigned the structure of 1, 2, 3-trimethyl-3-ethylindolenium iodide (III) to the indolenium iodide, on a non-confirmative chemical base, but whatever structure it has, migration of the subsituents has to be assumed, in order to explain the formation of the same indolenium iodide, m. p. 237°C, from both I and II.

Another type of rearrangement was established when Plancher[3] obtained two indolenium iodides, m. p. 186° and 232°C, from 2-isopropyl-3-methylindole (IV) by heating with methyliodide at 85~90°C for 2 days.

He posturated the formation of the two intermediate indolenines VII and VIII which would give corresponding indolenium iodides V and VI with methyliodide. Although the structure of the indolenium iodides (V or VI) remained unestablished, the conversion of the indolenium iodide, m. p. 186°C, into the isomeric indolenium iodide, m. p. 232°C, was achieved by heating at 180~190°C for 10 min. From these and other experiments, Plancher could draw the following conclusion[4]: 1) The indolenium iodide with the lower melting point can be converted into the isomeric indolenium iodide with the higher melting point. 2) The heavier substituent migrates to the β-position. However, his conclusion 2) can be hardly justified without further strenuous studies, since the structures of these indolenium iodides were only presumed on nothing but some analogies, except on one occasion; i.e. 1,2,3-trimethyl-3-phenylindolenium iodide (X). By heating 2-phenylindole (IX) with methyliodide at 120°C, Plancher[5] obtained an indolenium iodide, m. p. 226~227°C, which

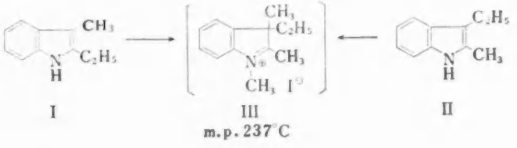

Fig. 1.

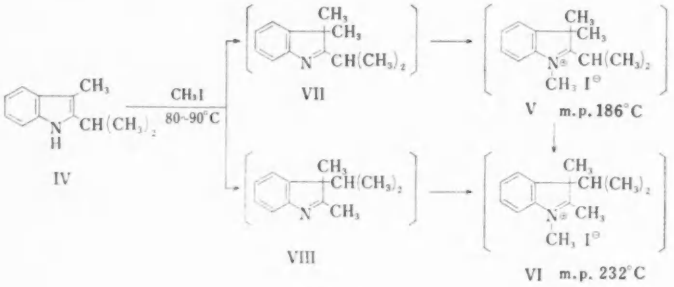

Fig. 2.

1) For general discussion of Plancher's rearrangement and other related rearrangement reactions, see P. L. Julian, E. W. Meyer and H. C. Pring, "The Chemistry of Indoles" in R. Elderfield, "Heterocyclic Compounds", Vol. 3, John Wiley & Sons., Inc., New York (1952), p. 1.

2) G. Plancher, *Gazz. chim. ital.*, **28**, II, 374 (1898); *Chem.-Zentr.*, **1899**, I, 282.

3) G. Plancher, *Atti. accad. Lincei*, (5), **11**, II, 182 (1902); *Chem.-Zentr.*, **1902**, I, 1322.

4) G. Plancher, *Atti. acced. Lincei*, (5), **9**, 115 (1900), *Chem.-Zentr.*, **1900**, I, 867. See also a brief discussion of Julian, Ref. 1.

5) G. Plancher, *Gazz. chim. ital.*, **28**, II, 391 (1898); *Chem.-Zentr.*, **1899**, I, 283.

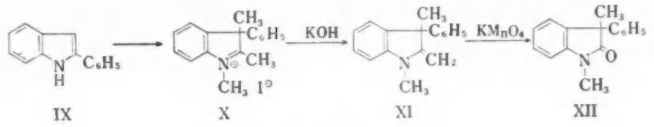

IX X XI XII

Fig. 3.

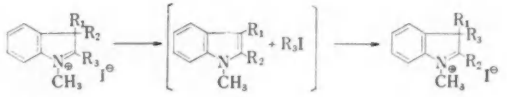

XIII XIV XV

Fig. 4.

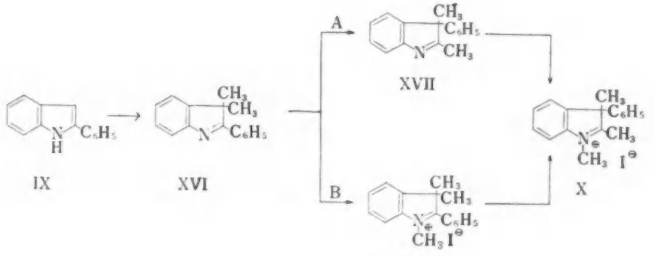

IX XVI XVII XVIII X

Fig. 5.

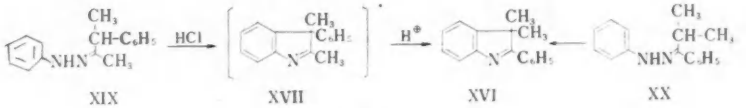

XIX XVII XVI XX

Fig. 6.

he thought to be 1, 2, 3-trimethyl-3-phenylindolenium iodide (X) as the result of rearrangement involving an exchange of methyl with phenyl group. But the structure of this indolenium iodide was left to be determined by chemical means until Boyd-Barrett[6] (1932) repeated Plancher's experiment and oxidized the product with alkaline potassium permanganate (via the intermediate XI) to form 1, 3-dimethyl-3-phenyloxyindole (XII), the nitro derivative of which was found to be identical with the one obtained by the umambiguous synthetic route.

The mechanism of the rearrangement of indolenium compounds proposed by Plancher[7] is illustrated in Fig. 4. According to this mechanism, the formation of iodobenzene and its subsequent reaction with 1, 2, 3-trimethylindole to secure 1, 2, 3-trimethyl-3-phenylindolenium iodide (X), though it is highly improbable, is an inevitable consequence to explain the formation of X from 2-phenylindole. Julian[8] pointed out another conceivable route from IX to X, assuming that 3, 3-dimethyl-2-phenylindolenine (XVI) is the intermediate and that rearrangement involving an exchange of methyl with the phenyl group takes place at this point (Fig. 5, route A).

This Julian's alternative postulated the migration of the substituents of indolenine which has not been demonstrated in any indolenine with umambiguous constitution[9], and it is unfortunate

6) H. S. Boyd-Barrett, *J. Chem. Soc.*, **1932**, 321.

7) G. Plancher, *Atti, accad. Lincei*, (5), **11**, 183 (1932); *Chem.-Zentr.*, **1902**, I, 1322.

8) See Ref. 1, p. 106.

9) M. Garry, *Ann. chim.*, **17**, 5 (1942); *Chem. Abstr.*, **36**, 6875 (1942), obtained two indolenines; 3,3-diphenyl-2-methylindolenine, m. p. 145°C, picrate, m. p. 210°C, and isomeric indolenine presumingly 2, 3-diphenyl-3-methylindolenine, m. p. 108°C, picrate, m. p. 155°C, from 1-anilino-1-phenylethylketone by heating with aniline and aniline hydrochloride at 160~165°C, but unfortunately she did not mention their possible interconversion. According to Julian's description, "she apparently assumed, and let it to the reader to assume, that the shifts involved in her synthesis took place *before* cyclization to the indolenines". But the recent study of the mechanism of Bishler's indole synthesis seems to suggest that the skeleton change of the anilinoketone would not occur *during* or *before* the cyclization. [F. Weygand and E. Richter, *Chem. Ber.*, **88**, 499 (1955).]. From the present achievement, it is safely assumed that the first formed 3, 3-diphenyl-2-methylindolenine rearranges to give 2, 3-diphenyl-3-methylindolenine under the reaction condition.

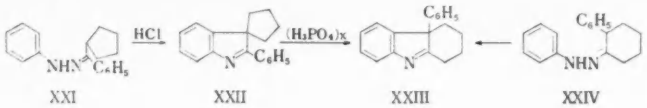

Fig. 7.

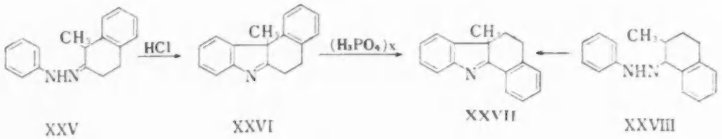

Fig. 8.

that sometimes Plancher's rearrangement was understood as this sort of rearrangement of indolenines only to cause many confusions[10].

This paper is concerned with demonstration of this migration of substituents of indolenines to elucidate the mechanism of Plancher's rearrangement. In order to obtain 2, 3-dimethyl-3-phenylindolenine (XVII), Fisher-Brunner's method was applied on 3-phenylbutane-2-one (XIX) under various conditions using zinc chloride, alcoholic hydrogen chloride and boron-trifluoride etherate as catalyst.

Even under very mild condition (with alcoholic hydrogen chloride at 0°C), all attempts failed only to afford 3, 3-dimethyl-2-phenylindolenine (XVI)[11], apparently resulting from the intermediate indolenine XVII by rearrangement reaction involving an exchange of the phenyl with the methyl group.

The view that 3-phenylbutane-2-one would rearrange to isobutyrophenone and then its phenylhydrazone (XX) would cyclize to XVI seems untenable, since the fact that the entirely reversed process is predominant in acidic condition was firmly established recently[12].

Also it is hard to find any reasonable sequence which would explain a possible migration of substituents in the cyclization steps of Fischer-Brunner's synthesis, which has a common feature with Fischer's indole synthesis extensively studied by Carlin et al.[13] At any rate, route A (Fig. 5) which assumes hypothetical rearrangement XVI → XVII has to be abandoned[14].

Although this is the first case, in which a rearranged indolenine is obtained in Fischer-Brunner's indolenine synthesis, the first example of the rearrangement of an indolenine to the other indolenine, both with established structures, was encountered in the isomerization of XXII to XXIII.

Spiro-(cyclopentane-1, 3'-*pseudo*-2'-phenylindole)[15](XXII) (λ_{max} 310 mμ)[16] which was synthesized from cyclopentylphenylketone phenylhydrazone (XXI) by Fischer-Brunner's synthesis by saturating its alcoholic solution with dry hydrogen chloride, was found to convert, when heated with polyphosphoric acid[17], into 11-phenylcarbazolenine (XXIII) which in turn was prepared from 2-phenylcyclohexanone phenylhydrazone (XXIV).

Another interesting rearrangement was demonstrated when 11b-methyl-5, 6-dihydro-11b-benzo-[*c*]carbazole[18] (XXVI) which could be prepared from α-methyl-β-tetralone phenylhydrazone (XXV), was heated with polyphosphoric acid

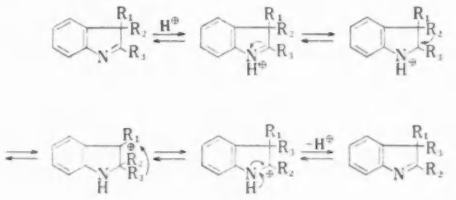

Fig. 9.

10) For example, B. Witkop and J. B. Patrick, *J. Am. Chem. Soc.*, **73**, 1358 (1951), discussed the rearrangement of indolenine as Plancher's rearrangement.

11) An attempt was made to prepare 2, 3-dimethyl-3-phenylindolenine (XVII) by alkylation of 2-methyl-3-phenylindole with sodium amide and methyliodide in liquid ammonia only to afford 1, 2-dimethyl-3-phenylindole. Also another attempt to obtain the indolenine XVII by Grignard synthesis from 2-methyl-3-phenylindole was found fruitless.

12) S. Barton and C. R. Portor, *J. Chem. Soc.*, **1956**, 2483.

13) R. B. Carlin, W. D. Henley and D. P. Carlson, *J. Am. Chem. Soc.*, **79**, 5712, (1957); and also his preceeding papers on the same subject.

14) The fact that the rearrangement actually takes place by route B (Fig. 5) was established by our experiment which follows. To avoid unnecessary confusion, the term of "Plancher's rearrangement" should be used to indicate solely the *rearrangement of indolenium compounds* such as illustrated XVIII→X (Fig. 5).

15) For the nomenclature of *spiro* compounds, see *Chem. Abstr.*, **39**, 5885, 5888 (1945).

16) U. V. spectrum of 3, 3-dimethyl-2-phenylindolenine: λ_{max} 306 mμ (log ε 4.177). B. Witkop, J. B. Patrick and H. M. Kissman, *Chem. Ber.*, **85**, 953 (1952).

17) When indolenine synthesis using polyphosphoric acid was applied on cyclopentylphenylketone-phenylhydrazone, 11-phenyltetrahydrocarbazolenine was formed directly.

18) According to the nomenclature of A. M. Patterson and L. T. Capell, "The Ring Index", Reinhold Publishing Corp., New York (1940), p. 331.

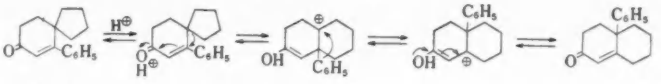

XXIX XXX

Fig. 10.

at 180°C for 5 min. The rearranged indolenine was found to be identical with 6a-methyl-5, 6-dihydro-6a-benzo[*a*]carbazole[18] (XXVII) provided from β-methyl-α-tetralone phenylhydrazone (XXVIII) by usual method.

The mechanism of the migration of the substituents of indolenines can be readily explained by twofold Wagner-Meerwein type rearrangement initiated by the attack of a proton on the nitrogen atom of the indolenine nucleus as formulated in Fig. 9[19-21].

Since undoubtedly all steps are in equilibrium, the thermodynamical stability of the products would be the predominant factor to determine the direction of the migration, and it would be safely assumed that mesomeric stabilization of the phenyl group is responsible in the case of XVII → XVI and XXVI → XXVII. The seemingly contradictory attitude of XXII toward acid can be reasoned when the inspection of its Stuart's model reveals that a considerable steric repulsion is observed between the phenyl group and the hydrogens of 3, 4-position of cyclopentyl group of XXII, i.e. this is the case where steric effects suppress mesomeric stabilization of the phenyl group[22].

Harmonious with this result is the smooth transformation[23] of 6-phenyl-*spiro*(4, 5)decen-6-one-8 (XXIX) to 10-phenyl-2-keto-$\Delta^{1,9}$-octahydronaphthalene (XXX) by heating with polyphosphoric acid.

Experimental[24]

3-Phenylbutane-2-one.—A mixture of 16.3 g. of methyliodide and 30 cc. of absolute ether was added dropwise to a mixture of 6.4 g. of magnesium and 30 cc. of absolute ether at room temperature. To the chilled Grignard solution, a mixture of 24.5 g. of α-methyl benzylcyanide[25] and 30 cc. of ether was added, and the reaction mixture was kept at room temperature for 4 hr. The Grignard complex was destroyed by the addition of diluted sulfuric acid and extracted with ether. The ethereal extract was washed with 5% sodium carbonate solution and water and dried over anhydrous sodium sulfate. Removal of the solvent afforded an oil which was distilled in vacuo to give 21.2 g. of 3-phenylbutane-2-one, b. p. 107~115°C/20 mmHg[26].

3, 3-Dimethyl-2-phenylindolenine (XVI) from 3-Phenylbutane-2-one Phenylhydrazone.—*By zinc chloride method*[27].—A mixture of 11.8 g. of 3-phenylbutane-2-one and 8.6 g. of phenylhydrazine was heated on a water bath for 40 min. The mixture became turbid and the separation of water drops was observed. Then the mixture was extracted with ether and dried over anhydrous sodium sulfate. After the solvent was evaporated completely, the residue was dissolved in 160 cc. of absolute ethanol and 80 g. of zinc chloride was added. The mixture was refluxed for 20 hr. and the alcohol was removed. The residue was made basic by the addition of concentrated ammonia solution to precipitate basic material. This was extracted with ether, and the ether extract was washed with water and dried over anhydrous potassium carbonate. Removal of the solvent afforded a residue which was distilled in vacuo to give 2.3 g. of a pale yellow liquid, b. p. 110~139°C/2 mmHg.

Found: C, 86.05; H, 7.27; N, 6.77. Calcd. for $C_{16}H_{15}N$: C, 86.84; H, 6.83; N, 6.33%.

The picrate was recrystallized to yield crystals, m. p. 170~172°C, which was found identical with the picrate of 3, 3-dimethyl-2-phenylindolenine, m. p. 167~168°C, prepared from an authentic 3, 3-dimethyl-2-phenylindolenine[28] (XVI), by mixed melting point determination.

19) An intermediate possessing *spiro* structure is to be assumed in the case of XXVI→XXVII, and it seems noteworthy to compare with the dienone-phenol rearrangement of 2-keto-4a-methyl-2, 4a, 5, 6-tetrahydrobenzo[*c*]phenathrene in which the transformation which requires a *spiro* intermediate is inhibited. C. Djerassi and T. T. Grossnickel, *J. Am. Chem. Soc.*, **76**, 1741 (1954). See also Ref. 14 in the preceeding paper on the rearrangement of 2, 3-disubstituted indoles.

20) A novel cleavage reaction of benzyl and *t*-butyl group is recently reported when R_1 (Fig. 9) is benzyl and *tert*-butyl, and the same sort of cleavage reaction was demonstrated on 11-benzyltetrahydrocarbazolenine and 11-*tert*-butyltetrahydrocarbazolenine. M. Nakazaki, S. Isoe and K. Tanno, *J. Chem. Soc. Japan, Pure Chem. Sec.* (*Nippon Kagaku Zasshi*), **76**, 1262 (1955).

21) The mechanism of Brunner-Robinson-Suginome's rearrangement (conversion of 3, 3-dimethylindolenine into 2, 3-dimethylindole) is the special case where R_3 is a hydrogen atom. K. Brunner, *Monatsh.*, **17**, 255 (1896); R. Robinson and H. Suginome, *J. Chem. Soc.*, **1932**, 298.

22) B. Witkop and J. B. Patrick, *J. Am. Chem. Soc.*, **73**, 1558 (1951), tried the rearrangement of 11-methyltetrahydorocarbazolenine in a hope to get *spiro*-(cyclopentane-1′, 3-*pseudo*-2′-methylindole) but in vain. This can be attributed to the stability of 11-methyltetrahydrocarbazolenine in respect of the steric effect as well as the small migration aptitude of the methyl group.

23) M. Nakazaki and S. Isoe, unpublished experiment.

24) All the melting points are uncorrected values. All ultraviolet spectra were measured with an EPS-2 Hitachi selfrecording spectrophotometer and infrared spectra on a Perkin Elmer Model 12C. The analyses were performed in the Microanalytical Laboratory of the Institute of Polytechnics, Osaka City University.

25) B. p. 106~112°C/11 mmHg or 71~79°C/2 mmHg. Prepared following the procedure of H. M. Crawford, *J. Am. Chem. Soc.*, **56**, 140 (1934).

26) W. D. Kumler, L. A. Strait and E. L. Alpen, *J. Am. Chem. Soc.*, **72**, 1463 (1950).

27) Following Leuch's procedure to synthesize 3, 3-dimethyl-2-phenylindolenine from isobutyrophenone phenylhydrazone. H. Leuchs, A. Heller and A. Hoffman, *Ber.*, **62**, 877, (1929).

28) B. p. 178~182°C/9 mmHg. Picrate, m. p. 167~168°C. Prepared by polyphosphoric acid method. H. M. Kissman, D. W. Farnsworth and B. Witkop, *J. Am. Chem. Soc.*, **74**, 3948 (1952).

By borontrifluoride etherate method[29].—To a mixture of 2.7 g. of 3-phenylbutane-2-one phenylhydrazone[30] and 30 cc. of acetic acid, 2.1 g. of borontrifluoride etherate was added and refluxed for 3 hr. After the solvent was removed in vacuo, the residue was dissolved in ether and basic material was extracted with 2 N hydrochloric acid solution. To the cooled acidic solution, 2 N sodium hydroxide solution was added to liberate the basic substance, and extracted with ether. After the ethereal solution was washed with water and dried over anhydrous potassium carbonate, the solvent was removed. The residue was distilled in vacuo to give a pale yellow oil, 1.2 g., b. p. 145~155°C/2 mmHg. The picrate, m. p. 168~169°C was prepared to be found identical with the picrate of 3,3-dimethyl-2-phenylindolenine (XVI) by mixed melting point determination.

Synthesis with hydrochloric acid in ethanol.—A solution of 2 g. of 3-phenylbutane-2-one phenylhydrazone[30] in 40 cc. of absolute ethanol was chilled in an ice bath and was saturated with dried hydrogen chloride. After being allowed to stand at room temperature for 2 days (15°C), the solvent was removed in vacuo (below 40°C). Water was added to the residue and extracted with ether. The aqueous layer was made basic by the addition of 2 N sodium hydroxide solution and extracted with ether. The ethereal extract was washed with water and dried over anhydrous potassium carbonate. After removal of the solvent, the residue was distilled to afford a liquid, b. p. 135~145°C/1.5 mmHg, infrared spectrum of which could overlap in every detail on that of 3,3-dimethyl-2-phenylindolenine. The identity was further confirmed by the mixed melting point determination of their picrates.

1,2-Dimethyl-3-phenylindole.—To a suspension of sodium amide prepared from 200 cc. of liquid ammonia and 0.78 g. of sodium, 5 g. of 2-methyl-3-phenylindole[31] was added with 10 cc. of ether. After a mixture of 3.4 g. of methyliodide and 10 cc. of ether was added dropwise in a period of 20 min., the reaction mixture was allowed to stand at room temperature overnight to evaporate the liquid ammonia. After 200 cc. of water was added, the mixture was extracted with ether. The ethereal extract was washed with 2 N hydrochloric acid to remove basic material (very small amount, discarded). After this has been washed with 5% sodium carbonate solution and water, the ether extract was dried over anhydrous sodium sulfate. Removal of the solvent gave crystals (4 g.), which were recrystallized from ethanol. m. p. 111~112.5°C.

Found: C, 87.38; H, 7.03; N, 6.33. Calcd. for $C_{16}H_{15}N$: C, 86.84; H, 6.38; N, 6.33%.

The picrate was recrystallized from ethanol to give brown black needles, m. p. 199~201°C.

Found: N, 12.40. Calcd. for $C_{22}H_{18}O_7N_4$: N, 12.44%.

***Spiro*-(cyclopentane-1,3'-*pseudo*-2'-phenylindole) (XXII).**—A mixture of 5 g. of cyclopentylphenylketone[32] and 3.4 g. of phenylhydrazine was heated on a water bath for 1 hr. and the water generated was removed by azeotropic distillation with benzene. After the benzene was removed completely in vacuo, the residue was dissolved in 60 cc. of absolute ethanol and the chilled solution was saturated with dry hydrogen chloride. Then 100 cc. of water was added to the semisolid mass, and washed with ether. The aqueous layer was made basic by the addition of 2 N sodium hydroxide solution, and extracted with ether. The ether extract was washed with water and dried over anhydrous sodium sulfate. After the solvent was evaporated, the residue was distilled at reduced pressure to give 4.9 g. of a pale yellow liquid, b. p. 164~167°C/1 mmHg. U. V. spectrum: λ_{max} mμ (log ε), 239 (4.28), 247(4.23), 310(4.28). λ_{min} 258 mμ(log ε 3.89) in ethanol (Fig. 11).

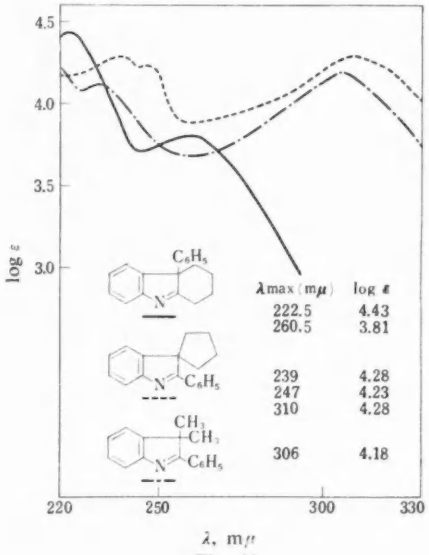

Fig. 11.

Found: C, 87.11; H, 7.21; N, 6.16. Calcd. for $C_{15}H_{17}N$: C, 87.41; H, 6.93; N, 5.55%.

The picrate was recrystallized from ethanol to give yellow crystals, m. p. 175°C.

Found: C, 61.18; H, 4.35; N, 11.74. Calcd. for $C_{24}H_{20}O_7N_4$: C, 60.50; H, 4.23; N, 11.76%.

11-Phenyltetrahydrocarbazolenine (XXIII).—*From 2-phenylcyclohexanone phenylhydrazone (XXIV).*—A mixture of 10 g. of 2-phenylcyclohexanone[33] and 7.3 g. of phenylhydrazine was

29) This attempt seems to be the first instance where borontrifluoride etherate was successfully employed for sythesis of indolenine, whereas this reagent has been frequently used for Fisher's indole synthesis. H. R. Snyder and C. W. Smith, ibid., **65**, 2454 (1943).

30) B. p. 160~176°C/2 mmHg; m. p. 76~78.5°C (from ethanol-water). Found: N, 11.83. Calcd. for $C_{16}H_{18}N_2$: N, 11.76%.

31) B. p. 194~196°C/3 mmHg; m. p. 78~79°C. Picrate m. p. 139~141°C. And also see the preceding paper.

32) B. p. 135~136°C/10 mmHg; m. p. of 2, 4-dinitrophenylhydrazone, 142°C, [prepared from cyclopentane carboxylic acid chloride by Friedel-Crafts synthesis. (D. H. Hey and O. C. Musgrave, *J. Chem. Soc.*, **1949**, 3156. B. p. 136~140°C/16 mmHg; m. p. of 2, 4-dinitrophenylhydrazone, 142~143°C).].

33) B. p. 140~146°C/10 mmHg (60% yield). Prepared following Newman's procedure. M. S. Newman and M. D. Frabman, *J. Am. Chem. Soc.*, **69**, 1550 (1944).

heated on a water bath for 1 hr. The water generated was removed by azeotropic distillation with benzene, and the benzene was removed by distillation in vacuo of a water pump. The residue was dissolved in 100 cc. of absolute ethanol, and saturated with dry hydrogen chloride. A considerable amount of ammonium chloride was observed to precipitate. After the reaction mixture was allowed to stand at room temperature for 10 hr., the solvent was removed in vacuo (below 40~45°C). The residue was dissolved in 250 cc. of water and washed with ether, and the aqueous layer was made basic by the addition of 2 N sodium hydroxide solution and extracted with ether. After the ethereal extract was washed with water and dried over anhydrous potassium carbonate, the solvent was removed to give crystals, which were recrystallized from ethanol-water, m. p. 126~127°C. I. R. spectrum: 6.3 μ. U. V. spectrum: λ_{max} mμ (log ε), 222.5(4.42), 260.5(3.81), λ_{min} 245 mμ (3.72) in ethanol (Fig. 11).

Found: C, 87.47; H, 7.02; N, 5.69. Calcd. for $C_{15}H_{17}N$: C, 87.41; H, 6.93; N, 5.66%.

The picrate was recrystallized from ethanol to give yellow prisms, m. p. 182~183°C.

Found: C, 60.48; H, 4.44; N, 11.78. Calcd. for $C_{24}H_{20}O_7N_4$: C, 60.50; H, 4.23; N, 11.76%.

From cyclopentylphenylketone phenylhydrazone (XXI).—To 29 g. of polyphosphoric acid, a mixture of 15 g. of cyclopentylphenylketone[32] and 9.8 g. of phenylhydrazine was added. The temperature of the reaction mixture rose spontaneously up to 150°C, and the reaction mixture was kept at this temperature for 10 min. in an oil bath. The viscous mass was dissolved in water and washed with ether. The acidic aqueous layer was made basic by the addition of 2 N sodium hydroxide solution, and was extracted with ether. After the ether extract was washed with water and dried over anhydrous sodium sulfate, the ether was distilled off. The residue was recrystallized from ethanol-water to give needles, m. p. 122~124°C (7.7 g.) which was proved identical with 11-phenyltetrahydrocarbazolenine (XXIII) prepared from 2-phenylcyclohexanone phenylhydrazone (XXIV).

From rearrangement of spiro-(cyclopentane-1,3'-pseudo-2'-phenylindole) (XXII).—A mixture of 1.4 g. of indolenine XXII and 7 g. of polyphosphoric acid was heated at 155°C for 10 min. in an oil bath. The reaction mixture was dissolved in water by warming on a water bath. The acidic aqueous layer was made basic by the addition of 2 N sodium hydroxide solution to precipitate needles (1.0 g.), which were collected and recrystallized from ethanol-water to give m. p. 124°C. The mixed melting point with 11-phenyltetrahydrocarbazolenine was 124°C.

11b-Methyl-5, 6-dihydro-11b-benzo[*c*]carbazole (XXVI).—A mixture of 8.1 g. of α-methyl-β-tetralone[34] and 5.5 g. of phenylhydrazine was heated on a water bath for 2 hr., and the generated water was removed by azeotropic distillation with benzene. After the solvent was removed in vacuo, the residue was dissolved in 70 cc. of absolute ethanol, and was saturated with dry hydrogen chloride. After being allowed to stand at 5°C overnight, the reaction mixture was poured into 350 cc. of ice water and washed with ether. The aqueous layer was made basic and was extracted with ether. The ether extract was washed with water and dried over anhydrous potassium carbonate. Removal of the solvent gave a viscous liquid, which was distilled in vacuo to afford 4.1 g. of a viscous pale yellow liquid, b. p. 159~163°C/1 mmHg. I. R. spectrum: 6.3 μ. U. V. spectrum: λ_{max} 248 mμ (log ε 4.02) in ethanol (Fig. 12).

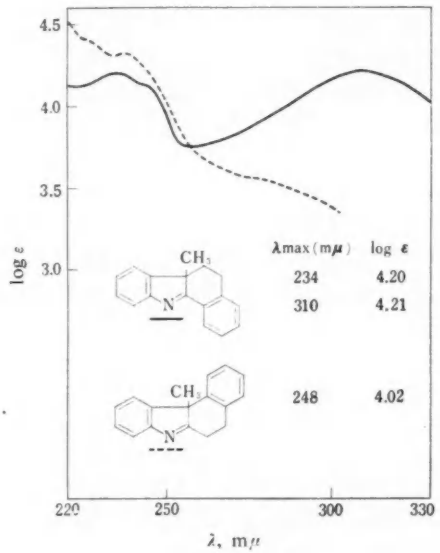

Fig. 12.

Found: C, 86.31; H, 6.83; N, 6.06. Calcd. for $C_{17}H_{15}N$: C, 87.51; H, 6.48; N, 6.00%.

The picrate was recrystallized from ethanol to give yellow prisms, m. p. 167~167.5°C.

Found: C, 59.91; H, 4.03; N, 12.31. Calcd. for $C_{25}H_{19}O_7N_4$: C, 59.74; H, 3.92; N, 12.12%.

6a-Methyl-5, 6-dihydro-6a-benzo[*a*]carbazole (XXVII).—When 30 g. of polyphosphoric acid was added to a mixture of 5.2 g. of β-methyl-α-tetralone[35] and 3.6 g. of phenylhydrazine, a considerable generation of heat was observed to cause the reaction temperature to rise to 165°C. After this rather violent reaction subsided, 200 cc. of water was added to dissolve the viscous reaction mass. The acidic aqueous solution was washed with ether, and was made basic to precipitate an oil, which was extracted with ether. The ether extract was washed with water and dried over anhydrous sodium sulfate. Removal of the solvent gave brown viscous residue which was distilled to give 3.4 g. of a pale yellow oil, b. p. 160~164°C/2 mmHg. I. R. spectrum:

34) B. p. 137~142°C/10 mmHg. Prepared following the procedure of J. English and G. Cavaglieri, *J. Am. Chem. Soc.*, 65, 1085 (1943).

35) B. p. 116~120°C/2 mmHg. Prepared following the procedure of W. E. Bachmann and D. G. Thomas, ibid., 63, 598 (1941).

6.5 μ. U. V. spectrum: λ_{max} mμ (log ε), 234(4.20), 310(4.21). λ_{min} 256 mμ (log ε 3.76) in ethanol (Fig. 12).

Found: C, 86.41; H, 6.69; N, 6.11. Calcd. for $C_{17}H_{13}N$: C, 87.51; H, 6.48; N, 6.00%.

The picrate was recrystallized from ethanol to give yellow prisms, m. p. 169~170°C. The mixed melting point with the picrate of 11b-methyl-5,6-dihydro-11b-benzo[*c*]carbazole (m. p. 167~167.5°C) was 156~159°C.

Found: C, 59.62; H, 4.12; N, 12.54. Calcd. for $C_{23}H_{15}O_7N_4$: C, 59.74; H, 3.92; N, 12.12%.

From rearrangement of 11b-methyl-5,6-dihydro-11b-benzo[c]carbazole (XXVI)—A mixture of 0.4 g. of the indolenine XXVI and 2 g. of polyphosphoric acid was heated at 180°C for 15 min. in an oil bath. After water was added, the aqueous solution was freed from a small amount of unsoluble resinous material by filtration.

The solution was made basic with 2 N sodium hydroxide solution, and the turbid mixture was extracted with ether. The ethereal extract was washed with water and dried over anhydrous sodium sulfate. After the ether wae removed, the residue was converted into picrate, without further purification, by the addition of ethanolic picric acid. The picrate was recrystallized from ethanol to give yellow prisms, m. p. 166~167°C, which was proved identical with the picrate of 6a-methyl-5,6-dihydro-6a-benzo[*a*]carbazole (m. p. 169~170°C) by mixed melting point determination.

The authors are very grateful to Mr. Muneo Sato for his technical assistance and to Mr. Sachihiko Isoe who kindly measured the ultraviolet absorption spectra.

Institute of Polytechnics
Osaka City University
Kita-ku, Osaka

Mechanism of Plancher's Rearrangement. II[1]. *Twofold Wagner-Meerwein Type Rearrangement of Indolenium Compounds*

By Masao NAKAZAKI

(Received August 31, 1959)

A novel conversion, by heating at 180~190°C, of an indolenium iodide, m.p. 186°C into an isomeric indolenium iodide, m.p. 232°C, both were obtained by the interaction of 2-isopropyl-3-methylindole and methyliodide was first described by Plancher[2], although the structures of these indolenium iodides were left unsettled.

But on only one occasion was the structure of the rearranged indolenium iodide established: Boyd-Barrett[3] oxidized the indolenium iodide III, obtained from 2-phenylindole (I) by heating with methyliodide at 120°C, to 1,3-dimethyl-2-phenyloxyindole, and thus confirmed the structure of the rearranged indolenium III proposed by Plancher[1].

Plancher[2] explained the formation of 1,2,3-trimethyl-3-phenylindolenium iodide (III) from 2-phenylindole (I) by the sequence of reactions: decomposition of the first formed 1,3,3-trimethyl-2-phenylindolenium iodide (II) into iodobenzene and 1,2,3-trimethylindole and a recombination of which together with iodobenzene to form III.

It is obvious that such mechanism is hardly tenable, and Julian[5] suggested another mechanism which assumed that 3,3-dimethyl-2-phenylindolenine is the first intermediate and its rearrangement involving an exchange of the phenyl with the methyl group would give 2,3-dimethyl-3-phenylindolenine. But the fact that the conversion of 3,3-dimethyl-2-phenylindolenine into 2,3-dimethyl-2-phenylindolenine, which would give III with methyliodide, however, was proved just opposite to the case[6], leaving only one possible mechanism remaining, i.e. the conversion of the intermediate 1,3,3-trimethyl-2-phenylindolenium iodide (II) into III, by a twofold Wagner-Meerwein type rearrangement formulated in Fig. 1. To testify this possibility, Leuch's experiment[7] was repeated in order to obtain 1,3,3-trimethyl-2-phenylindolenium iodide (II) from 3,3-dimethyl-2-phenylindolenine and methyliodide.

1) Part I: M. Nakazaki, K. Yamamoto and K. Yamagami, This Bulletin, 33, 466 (1960).
2) G. Plancher, *Atti. accad. Lincei*, (5) II, III, 182 (1902); *Chem.-Zentr.*, **1902**, I, 1322.
3) H. S. Boyd-Barrett, *J. Chem. Soc.*, **1932**, 321.
4) G. Plancher, *Gazz. chim. ital.*, **28**, II, 391 (1898); *Chem.-Zentr.*, **1899**, I, 283.
5) P. L. Julian, E. W. Meyer and H. C. Pring, "The Chemistry of Indoles", in R. Elderfield, "Heterocyclic Compounds", Vol. 3., John Wiley & Sons, Inc., New York (1952), p. 106. The introductory part of the preceding paper gives a brief historical survey of Plancher's rearrangement.
6) M. Nakazaki, K. Yamamoto and K. Yamagami, This Bulletin, 33 466 (1960).
7) H. Leuchs, A. Heller and A. Hoffmann, *Ber.*, **62**, 871 (1932).

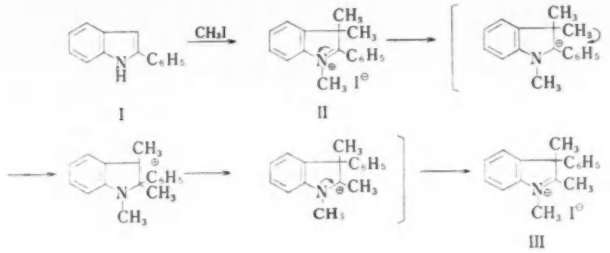

Fig. 1.

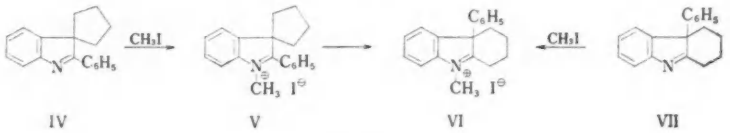

Fig. 2.

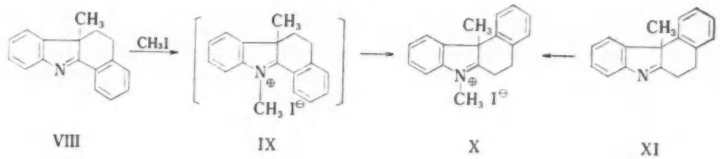

Fig. 3.

When a solution of 3, 3-dimethyl-2-phenylindolenine and methyliodide in methanol was heated at 100°C for 4 hr., there were obtained, in contrary to expectation, colorless prisms, m.p. 226~227°C[8], beside Leuch's indolenium iodide, yellow needles, m.p. 203°C, in about the same amount. Since the indolenium iodide with m.p. 226~227°C was proved to be 1, 2, 3-trimethyl-3-phenylindolenium iodide (III) by Boyd-Barrett's degradative experiment[3], the isomeric yellow indolenium iodide, m. p. 203°C which was a sole product Leuchs could isolate, was to be assigned the structure of 1, 3, 3-trimethyl-2-phenylindolenium iodide (II). These structure assignments were further confirmed by their ultraviolet absorption spectra, which show clearly a bathochromic shift (III, λ_{max} 276 mμ and II, λ_{max} 297 mμ) due to conjugation with the phenyl group (Fig. 5).

The conversion of II to III was realised when a methanolic solution of II was heated in a sealed tube at 120~150°C for 1/2 hr., and this is the first case where indolenium compound was rearranged into the isomeric indolenium compound both with known constitutions, exchanging substituents between 2- and 3-position of the indolenium nucleus. Another smooth isomerization was established when *spiro*-(cyclopentane-1, 3'-*pseudo*-2'-phenylindole) methoiodide (V), prepared from the corresponding indolenine IV, with methyliodide, was heated in methanolic solution at 160°C for 3 hr. in a sealed tube to give 11-phenyltetrahydrocarbazolenine methoiodide (VI), which could be prepared from 11-phenyltetrahydrocarbazolenin (VII) and methyliodide.

Although it was unsuccessful to obtain the methoiodide of 6a-methyl-5, 6-dihydro-6a-benzo-[*a*]carbazole (IX) in crystalline form, it could be isomerized by heating its methanolic solution at 150°C for 5 hr. to the isomeric 11b-methyl-5, 6-dihydro-11b-benzo[*c*]carbazole methoiodide (X) provided from the corresponding indolenine XI with methyliodide. The mechanism of these rearrangements of indolenium iodides can be sought in the twofold Wagner-Meerwein type rearrangement[9] illustrated in Fig. 4.

Situated between two substituents at 1- and 3-position of indolenium compounds the substituents at 2-position suffer a considerable steric repulsion from both sides and the most bulky group (R_3) would tend to migrate to 2-position,

8) In the repetition of Plancher's experimet, Boyd-Barrett (Ref. 3) obtained a yellow indolenium iodide, m. p. 196°C as a minor product. Apparently this is the intermediate 1, 3, 3-trimethyl-2-phenylindolenium iodide (II), but any structural study as well as its possible rearrangement III was not tried.

9) Twofold Wagner-Meerwein type rearrangement was also demonstrated in indolenines (ref. 6) and 2, 3-disubstituted indoles M. Nakazaki, This Bulletin, 33, 461 (1960) A *spiro* type intermediate has to be assumed in the case of the rearrangement IX→X.

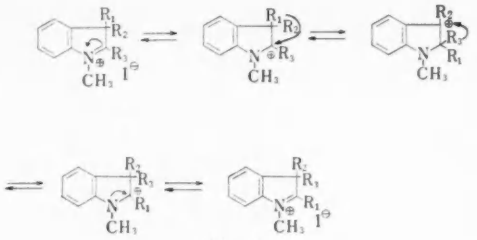

Fig. 4.

compelling the least bulky group (R_1) to 2-position (Fig. 4).

This steric effect would be strong enough[10] so as to compensate for the mesomeric stabilization effect of the phenyl group conjugated with the indolenium nucleus.

Experimental[11]

1, 3, 3-Trimethyl-2-phenylindolenium Iodide (II) and 1, 2, 3-Trimethyl-3-phenylindolenium Iodide (III).—A mixture of 12.7 g. of 3, 3-dimethyl-2-phenylindolenine[12], 24.2 g. of methyliodide and 77 cc. of methanol was heated at 100°C. for 4 hr. in a sealed tube. After the solvent was removed on a water bath, the residue was recrystallized from methanol-ethyl acetate. From the more soluble fraction yellow needles were obtained and recrystallization from water (aqueous solution was colorless, whereas the methanolic solution was yellow) gave 3.6 g. of yellow needles, m. p. 202~203°C. (literature[7]: 203°C). Ultraviolet spectrum of 1, 3, 3-trimethyl-2-phenylindolenium iodide: λ_{max} 297 mμ (log ε 3.97) in methanol (Fig. 5).

Found: C, 56.24; H, 5.07. Calcd. for $C_{17}H_{18}NI$: C, 56.21; H, 4.99%.

From the less soluble fraction, there were obtained colorless prisms which were recrystallized from methanol, m.p. 226~227°C (literature[8]: 227°C). This iodide is rather sensitive to air and gradually changes to pink in color. U. V. spectrum of 1, 2, 3-trimethyl-3-phenylindolenium iodide: λ_{max} 276 mμ (log ε 3.84) in methanol (Fig. 5).

Found: C, 56.73; H, 5.37. Calcd. for. $C_{17}H_{18}NI$: C, 56.21; H, 4.99%.

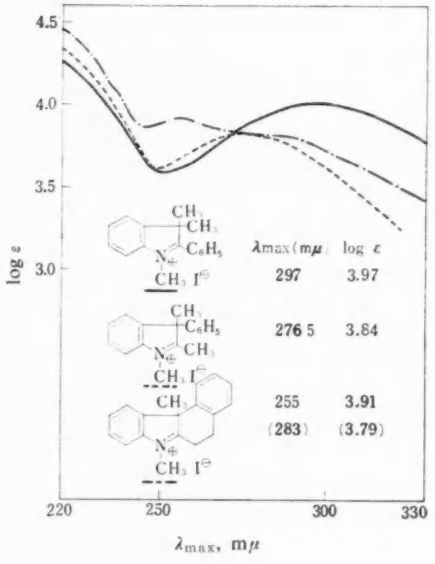

Fig. 5.

Rearrangement of 1,3,3-Trimethyl-2-phenylindolenium Iodide (II).—The indolenium iodide II (0.5 g.) was dissolved in 6 cc. of methanol and heated at 120~150°C for 3 hr., and then at 180°C for 1/2 hr. in a sealed tube. The original yellow color of the reaction mixture changed to violet-red. After removal of the solvent, the residue was dissolved in a small amount of methanol, and ethyl acetate was added to precipitate prisms (m.p. 222~224°C) with faint pink color, which was recrystallized from methanol to raise the melting point to 224~226°C. This was found identical with 1, 2, 3-trimethyl-3-phenylindolenium iodide (III) by mixed melting point determination and the comparison of infrared spectra.

***Spiro*-(cyclopentane-1, 3'-*pseudo*-2'-phenylindole)**

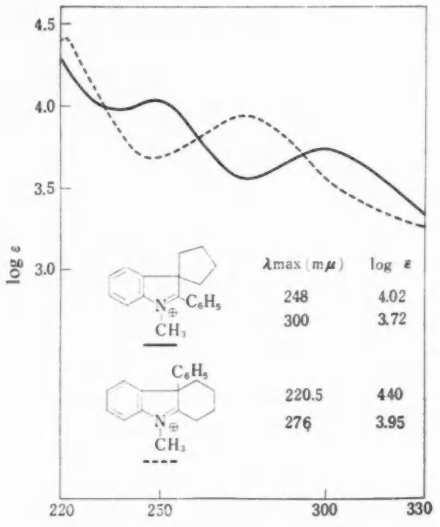

Fig. 6.

10) Even in the indolenine IV, without the repulsion from the substituent at 1-position, the steric strain is sufficient enough to be responsible for the smooth rearrangement of the isomeric indolenine VII (Ref. 6).

11) All the melting points are uncorrected values. All ultraviolet spectra were measured with an EPS-2 Hitachi autorecording spectrophotometer and infrared spectra on a Perkin Elmer Model 12C. The analyses were performed in the Microanalytical Laboratory of the Institute of Ploytechnics, Osaka City University.

12) B. p. 178~179°C/9 mmHg. Picrate, m. p. 167~168°C. Prepared following Witkop's procedure. [H. M. Kissman, D. W. Farnworth and B. Witkop, *J. Am. Chem. Soc.*, **74**, 3948 (1952)].

Methoiodide (V).—A mixture of 1 g. of *spiro*-(cyclopentane-1, 3'-*pseudo*-2'-phenylindole)[13], 1.0 g. of methyliodide and 10 cc. of methanol was heated at 100°C for 2 hr. in a sealed tube. After the solvent was removed from the dark green reaction mixture, the residue was recrystallized from ethanol to give yellow needles (0.55 g.), m.p. 186.5~188°C. U. V. spectrum: λ_{max} mμ(log ε), 248(4.02), 300 (3.72) in ethanol (Fig. 6).

Found: C, 58.51; H, 5.36; N, 3.59. Calcd. for $C_{19}H_{20}N$ I: C, 58.70; H, 5.18; N, 3.60%.

11-Phenyltetrahydrocarbazolenine Methoiodide (VI).—A mixture of 1.0 g. of phenyltetrahydrocarbazolenine[14] 1.0 g of methyliodide and 10 cc. of methanol was heated at 100°C. for 3 hr. in a sealed tube. After removal of the solvent, the green residue was dissolved in methanol and decolorized with sulfur dioxide.

Then small amount of water was added to precipitate needles, which were recrystallized from water to give colorless needles, m.p. 116~118°C (decomp.). U. V. spectrum: λ_{max} mμ(log ε), 220.5 (4.40), 276(3.95) in ethanol (Fig. 6).

Found: C, 56.26; H, 5.60; N, 3.67. Calcd. for $C_{19}H_{20}NI \cdot H_2O$: C, 56.03; H, 5.45; N, 3.44%.

Rearrangement of *Spiro*-(cyclopentane-1, 3'-*pseudo*-2'-phenylindole) Methoiodide (V).—A mixture of 0.4 g. of the indolenium iodide V and 6 cc. of methanol was heated at 160°C for 3 hr. and at 200°C for 15 min. in a sealed tube. After removal of the solvent, the green residue was extracted with boiling water. The aqueous solution was treated with Norit and was concentrated to give colorless needles which were recrystallized from water., m.p. 116~118°C. This was found identical with the 11-phenyltetrahydrocarbazolenine methoiodide (m.p. 116~117°C) by mixed melting point determination (m.p. 116~118°C).

11b-Methyl-5, 6-dihydro-11b-benzo[*c*]carbazole (X).—A mixture of 0.2 g. of the indolenine XI[15], 0.4 g. of methyliodide and 4 cc. of methanol was heated at 100°C. for 3 hr. in a sealed tube. After removal of the solvent, a small amount of ether was added to the residue and was allowed to stand with occasional trituration. The crystals precipitated were collected and recrystallized from ethanol to give m.p. 202~204°C. U. V. spectrum: λ_{max} 255 mμ(log ε 3.91) with a plateau at 283 mμ (3.79) in ethanol (Fig. 5).

Found: C, 57.81; H, 5.18; N, 4.20. Calcd. for $C_{15}H_{15}NI$: C, 57.61; H, 4.83 N, 3.73%.

Rearrangement of 6a-Methyl-5, 6-dihydro-6a-benzo[α]carbazole Methoiodide (IX).—A mixture of 0.5 g. of the indolenine VIII[16], 1.0 g. of methyliodide and 4 cc. of methanol was heated at 100°C for 3 hr. in a sealed tube. After the solvent was removed at reduced pressure, the residue was washed with ether. After various fruitless attempts to crystallize, the viscous residue was dissolved in 6 cc. of methanol and heated at 150°C for 5 hr. in a sealed tube. The solvent was evaporated and a small amount of ether was added to the residue and triturated. The crystals were collected, and recrystallized from ethanol to give crystals melting at 202~204°C, which was found identical with the indolenium iodide X by mixed melting point determination and the comparison of their infrared spectra.

The author is very grateful to Messrs. Keiji Inui, Koji Yamamoto, Muneo Sato and Kikuo Yamagami for their assistance to prepare various starting materials. He also feels indebted to Mr. Sachihiko Isao for measurement of ultraviolet absorption spectra.

Institute of Polytechnics
Osaka City University
Kita-ku, Osaka

13) B.p. 164~167°C/1 mmHg. Picrate, m.p. 175°C. Ref. 6.
14) M. p. 126°C. Picrate, m. p. 182~183°C. Ref. 6.
15) B. p. 160~165°C/2 mmHg. Picrate, m. p. 167~167.5°C, Ref. 6.
16) B. p. 160~194°C/2 mmHg. Picrate, m. p. 169~170°C. Ref. 6.

*Theory on the Small Angle Scattering of Light to Determine the Shape, Size and Orientation of High Polymer Molecules in Flow**

By Masayuki NAKAGAKI

(Received October 6, 1959)

As for the small angle scattering of light by high polymer moleculces in a solution at rest, the Zimm plot, that is a double extrapolation method devised by Zimm[1], has been used widely. On the other hand, a theory regarding the deformation of high polymer molecules in flow and on the light scattering by the deformed molecules has been developed by Peterlin, Heller and Nakagaki[2]. On the basis of this theory, it will be shown in the present paper that the Zimm plot can be used for the quantitative determination of the shape, size and orientation of high polymer molecules in flow, and that the photographic pattern of the small angle scattering can be used to determine the orientation of the molecules in flow.

Initial Slope of the Zimm Plot

The equation of light scattering derived by Debye[3] on the basis of fluctuation theory, and generalized by Zimm[1] is,

$$Kc/R_u(\vec{s}) = 1/MP(\vec{s}) + 2A_2c \tag{1}$$

where K is a constant, $R_u(\vec{s})$ is reduced scattering intensity, $P(\vec{s})$ is interference factor, and c, M and A_2 are concentration, molecular weight and the second virial coefficient of the polymer. The constant K is given by

$$K = (2\pi^2\mu_1^2/N_0\lambda_0^4)(\mathrm{d}\mu_{12}/\mathrm{d}c)^2 \tag{2}$$

where μ_1 is the refractive index of solvent, N_0 is the Avogadro number, λ_0 is wavelength of light in vacuo and μ_{12} is refractive index of solution. The reduced scattering intensity $R_u(\vec{s})$ is

$$R_u(\vec{s}) = (I_u(\vec{s})/I_0)/(1+\cos^2\theta) \tag{3}$$

where I_0 is the intensity of the unpolarized incident light, $I_u(s)$ is the intensity of light scattered in the direction designated by $\vec{s}$, and θ is the scattering angle. The scattering vector $\vec{s}$ is given by

$$\vec{s} = \vec{s'} - \vec{s_0} \tag{4}$$

where $\vec{s_0}$ and $\vec{s'}$ are unit vectors in the direction of the incident beam and scattered beam, respectively; and its absolute value, s, is

$$s = |\vec{s}| = 2\sin(\theta/2) \tag{5}$$

Here the scattering angle θ is the angle between $\vec{s_0}$ and $\vec{s'}$.

In the so called Zimm plot, (Kc/R_u) is taken as ordinate and $\sin^2(\theta/2)+kc$ is taken as abscissa, where k is a constant chosen arbitrarily. Therefore, the curve on the Zimm plot for the values extraporated to infinitely dilute concentration gives

$$[Kc/R_u(\vec{s})]_0 = 1/MP(\vec{s}) \tag{6}$$

as a function of σ defined by

$$\sigma = \sin^2(\theta/2) \tag{6a}$$

On the other hand, the theoretical expression for the interference factor of streaming polymer molecules derived by Peterlin, Heller and Nakagaki[2] is,

$$P(\vec{s}) = 2\int_0^1 (1-u)\exp[-X(u+\zeta u^2)]\,\mathrm{d}u \tag{7}$$

where

$$X = (8\pi^2/3\lambda^2)R^2\sin^2(\theta/2)\cdot\xi \tag{8}$$

and

$$\zeta = (2/3)\beta^2 \tag{9}$$

Here λ is the wavelength of light in the medium, R is the root-mean-square of the end-to-end distance of the polymer molecule at rest, and

$$\xi = \{1+[\beta^2+\beta(1+\beta^2)^{1/2}\cos 2\phi] \times\cos^2(\theta/2)\}/(1+2\beta^2/3) \tag{10}$$

Here β is a quantity proportional to the velocity gradient q defined by

$$\beta = (\pi a/6kT)\eta_i ZR^2 q = (M/N_0kT)[\eta]\eta_i q \tag{11}$$

where a is the hydrodynamic radius of segments, k is the Boltzmann constant, T is the absolute temperature, η_i is the viscosity, Z is the number of segments in a molecule, M is the molecular weight and $[\eta]$ is the intrinsic viscosity. The angle ϕ is concerned with the direction of observation as defined in Ref. 2 and will be described later (See Fig. 2).

* Presented before the 12th Annual Meeting of the Chemical Society of Japan, Kyoto, April, 1959.

1) B. H. Zimm, *J. Chem. Phys.*, **16**, 1099 (1948).
2) A. Peterlin, W. Heller and M. Nakagaki, ibid., **28**, 470 (1958).
3) P. Debye, *J. Appl. Phys.*, **15**, 338 (1944).
4) B. H. Zimm, *J. Chem. Phys.*, **16**, 1093 (1948).

The value of $[Kc/R_u(0)]_0$, that is the height of the ordinate at which the Zimm plot for infinite dilution intersects and the value of the initial slope of this Zimm plot are obtained by expanding $[Kc/R_u(\vec{s})]_0$ of Eq. 6 as a power series of σ of Eq. 6a. These values are:

$$[Kc/R_u(0)]_0 = 1/M \tag{12}$$

and

$$\begin{aligned}(\text{Initial slope}) &= [Kc/R_u(0)]_0 \times (8\pi^2R^2/9\lambda^2) \\ &\times [1+\beta^2+\beta(1+\beta^2)^{1/2}\cos 2\phi] \\ &\times (1+\beta^2/3)/(1+2\beta^2/3)\end{aligned} \tag{13}$$

If a parameter g defined by

$$g = (9\lambda^2/8\pi^2)\ (\text{Initial slope})/[Kc/R_u(0)]_0 \tag{14}$$

is used, the value is

$$\begin{aligned}g &= R^2[1+\beta^2+\beta(1+\beta^2)^{1/2}\cos 2\phi] \\ &\times (1+\beta^2/3)/(1+2\beta^2/3)\end{aligned} \tag{15}$$

Thus, the value of the ordinate at which the Zimm plot intersects is constant irrespective of whether the solution is streaming or not. From this value, the molecular weight may be determined on the basis of Eq. 12. On the other hand, the value of g depends on the velocity gradient or β. The value of g in the case of the solution at rest, designated by g_0, is obtained from Eq. 15 with $\beta=0$. The value is

$$g_0 = R^2 \tag{16}$$

Therefore, it is equal to the mean square end-to-end distance. The value of g for streaming solution depends on the direction of observation or ϕ as well as the velocity gradient or β.

At first, the observation plane is fixed and the variation of g with velocity gradient (or β) is considered. Since the angle ϕ is also a function of β, angle ω is used instead (see Fig. 2). The angle ω is the angle between the direction of flow and the plane of observation, and is related to ϕ by the equation:

$$\omega = \phi + 90^\circ - \chi \tag{17}$$

where χ is the extinction angle varying with β according to

$$\beta = -\cot 2\chi \tag{18}$$

Then, Eq. 15 is rewritten to

$$\begin{aligned}g/g_0 &= (1+\beta^2+\beta\sin 2\omega+\beta^2\cos 2\omega) \\ &\times (1+\beta^2/3)/(1+2\beta^2/3)\end{aligned} \tag{19}$$

The variation of g/g_0 due to β for several values of ω are shown in Fig. 1 with solid curves. Then, at a constant value of β, the maximum and minimum value of g/g_0 are calculated. The results are:

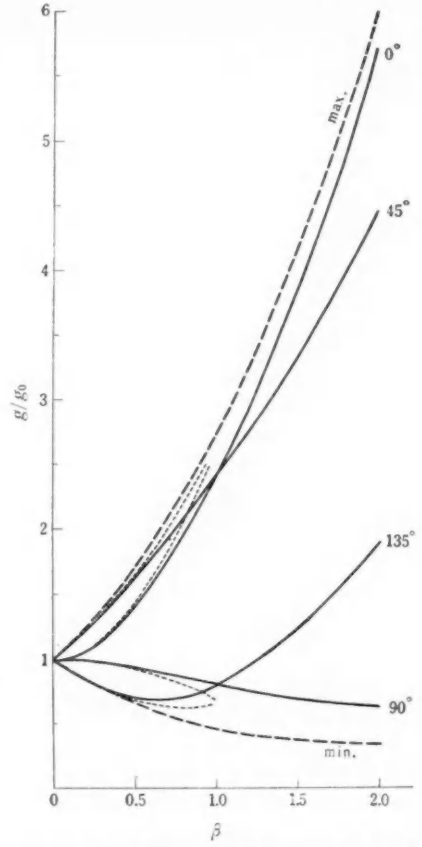

Fig. 1. The relationship between g/g_0 and β.

$$\left.\begin{aligned}g_{max}/g_0 &= [1+\beta^2+\beta(1+\beta^2)^{1/2}] \\ &\times (1+\beta^2/3)/(1+2\beta^2/3) \\ &\text{at}\quad \phi = 0^\circ,\ 180^\circ \\ g_{min}/g_0 &= [1+\beta^2-\beta(1+\beta^2)^{1/2}] \\ &\times (1+\beta^2/3)/(1+2\beta^2/3) \\ &\text{at}\quad \phi = \pm 90^\circ\end{aligned}\right\} \tag{20}$$

These values are shown in Fig. 1 with broken lines.

It may be instructive to estimate here the order of magnitude of β. If $[\eta]=100$, $\eta=1$ c.p.s., $M=3\times10^5$ and $q=1\times10^4$ sec^{-1}, the value of β calculated by Eq. 11 is 0.12. Therefore, the usual value of β seems to be smaller than unity. If $\beta \ll 1$, Eq. 19 is reduced to

$$g/g_0 \fallingdotseq 1+\beta\sin 2\omega+\beta^2(2/3-\cos 2\omega) \tag{21}$$

The error committed by this approximate equation is less than 5% as far as $\beta \leq 0.7$. The values calculated by this equation are shown in Fig. 1 with dotted curves.

As already mentioned, the quantity β is proportional to the velocity gradient q. When a concentric cylinder apparatus is used, β is, therefore, proportional to the rate of rotation $\Omega(\sec^{-1})$, that is

$$\beta = k_1 q = k_2 \Omega \tag{22}$$

with

$$k_2 = k_1(2\pi\rho/d) \tag{23}$$

where ρ is the radius of the rotating cylinder, d is the width of the gap of the concentric cylinder, and the value of k_1 is readily obtained from Eq. 11. Thus, there are three methods to determine the value of k_2 (or k_1). The first is to calculate the value of k_1 by Eq. 11. The second is to measure the extinction angle χ by a streaming double refraction measurement in order to obtain the value of β on the basis of Eq. 18. The values of β for various values of q or Ω will give the value of k_1 or k_2 by Eq. 22. The third and the most direct method for the present experiment is to use the equation derived from Eq. 21, that is:

$$(g/g_0 - 1)/\Omega = A + B\Omega \tag{24}$$

where

$$\left.\begin{aligned} A &= k_2 \sin 2\omega \\ B &= k_2^2(2.3 + \cos 2\omega) \end{aligned}\right\} \tag{25}$$

From the value of A or B determined experimentally, the value of k_2 will be obtained.

A Method for Measurement of the Semi-Major and Minor Axes of Flexible High Polymer Molecules

The extension of high polymer molecules in solution is expressed by the probability distribution of end-to-end distance, that is the probability ψ per unit volume to find one end of the high polymer molecule in a volume element when the other end is fixed at the origin. In the case of freely flexible high polymer molecules, it is well known that the function ψ is Gaussian:

$$\left.\begin{aligned} \psi &= (\mu/\pi)^{3/2} \exp(-\mu r^2) \\ \mu &= 3/2R^2 \end{aligned}\right\} \tag{26}$$

where r is the distance to the volume element from the origin and R is the root mean square end-to-end distance. On the other hand, it is often assumed that the distribution of segments around the center of gravity of the molecule is also Gaussian. The probability W to find a segment in a unit volume of a volume element is then:

$$\left.\begin{aligned} W &= Z(\mu^*/\pi)^{3/2} \exp(-\mu^* r^2) \\ \mu^* &= 6\mu \end{aligned}\right\} \tag{27}$$

where Z is the number of segments in one molecule, and r in this case is the distance between the volume element and the center of gravity. The relation between μ^* and μ shown in Eq. 27 is based on the fact established by Debye[5] that the root mean square distance S of a segment from the center of gravity of the molecule is

$$S = R/\sqrt{6} \tag{28}$$

On the other hand, Debye and Bueche[6] concluded from the study of intrinsic viscosity that the radius R_s of a high polymer molecule considered as a sphere should be

$$R_s = \sqrt{5/18}\ R \tag{29}$$

Now, by assuming that the distribution of segments is homogeneous in a sphere of radius R_s the root mean square distance of a segment from the center of gravity of the molecule is readily calculated and the result is

$$S = \sqrt{3/5}\ R_s \tag{30}$$

This result together with Eq. 29 yields a relation exactly the same as that of Eq. 28, the latter being obtained originally on the basis of the Gaussian distribution formulated in Eq. 27.

On the basis of these facts, one may say that the shape of a high polymer molecule in a solution at rest is a sphere with the radius of R_s. Then the value of W at the surface of the sphere (W_s) relative to the value of W at the center of gravity of the molecule (W_0) is,

$$W_s/W_0 = \exp(-5/2) = 0.082 \tag{31}$$

Therefore, to assume a high polymer molecule as a sphere of radius R_s corresponds to the assumption that the surface of the molecule is defined by the points at which $W_s/W_0 = 0.082$ in the Gaussian distribution.

Now, considering high polymer molecules in a streaming solution, Peterlin, Heller and

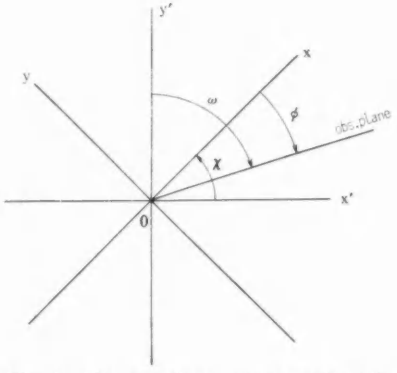

Fig. 2. The coordinate system and angles used.

5) P. Debye, ibid., **14**, 636 (1946).
6) P. Debye and A. M. Bueche, ibid., **16**, 573 (1948).

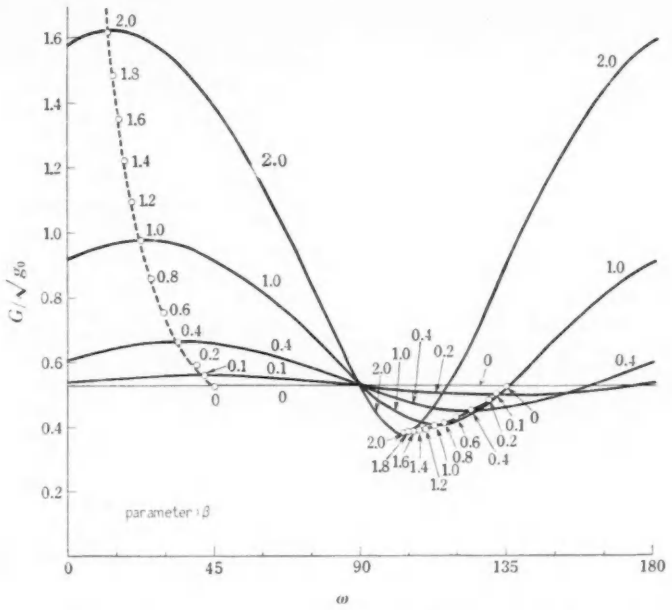

Fig. 3. The relationship between $G/\sqrt{g_0}$ and ω. Parameter: β.

Nakagaki[2] gave the probability distribution of end-to-end distance by the equation:

$$\psi=\frac{1}{abc}\left(\frac{\mu}{\pi}\right)^{3/2}\times\exp\{-\mu[(x/a)^2+(y/b)^2+(z/c)^2]\} \quad (32)$$

where

$$\left.\begin{aligned} a^2&=\sqrt{1+\beta^2}(\sqrt{1+\beta^2}+\beta)\\ b^2&=\sqrt{1+\beta^2}(\sqrt{1+\beta^2}-\beta)\\ c^2&=1\end{aligned}\right\} \quad (33)$$

Here, the coordinate system x, y, z is that obtained by rotating the coordinate system x', y', z by the angle χ around the z-axis, as shown in Fig. 2, x' and y' being the direction of velocity gradient and velocity, respectively. Eq. 32 is reduced to the usual Gaussian distribution (Eq. 26) when $\beta=0$.

The distribution of segments around the center of gravity of the molecule may then be assumed to be

$$W=\frac{Z}{abc}\left(\frac{\mu^*}{\pi}\right)^{3/2}\times\exp\{-\mu^*[(x/a)^2+(y/b)^2+(z/c)^2]\} \quad (34)$$

with $\mu^*=6\mu$, in analogy to Eq. 27. By the assumption that the surface of the molecule is defined by the points at which $W_s/W_0=\exp(-5/2)$, the molecule should be an ellipsoid expressed by the equation:

$$\mu^*[(x/a)^2+(y/b)^2+(z/c)^2]=5/2 \quad (35)$$

the semi-axes of the ellipsoid R_a, R_b, and R_c being in the direction of the coordinate axes x, y and z, respectively, and the values being[7]

$$\left.\begin{aligned} R_a&=\sqrt{5/18}\,aR\\ R_b&=\sqrt{5/18}\,bR\\ R_c&=\sqrt{5/18}\,cR\end{aligned}\right\} \quad (36)$$

When $\beta=0$,

$$R_a=R_b=R_c=R_s \quad (37)$$

since $a=b=c=1$.

In order to determine the values of R_a, R_b, and R_c experimentally, a quantity G defined by

$$G=\sqrt{(5/18)g(1+2\beta^2/3)/(1+\beta^2/3)} \quad (38)$$

is introduced. Here g is obtainable experimentally from the measurement of the initial slope by using Eq. 14, and β is obtainable experimentally by Eq. 22 as a quantity proportional to the rate of rotation Ω. Therefore, the quantity G is a measurable quantity. The theoretical expression for G may be obtained by using Eq. 15 and the result is:

$$G=\sqrt{5/18}\,R\sqrt{1+\beta^2+\beta\sqrt{1+\beta^2}\cos 2\phi} \quad (39)$$

Thus, G as a function of the direction of observation plane, ω, has one maximum and one

7) The quantity R is the root mean square end-to-end distance at rest. The value in flow is $\langle r^2\rangle=R^2(1+2\beta^2/3)$.

minimum in the range $\omega=0\sim180^\circ$. The maximum of G occurs at $\phi=0$, that is, $\omega=90^\circ-\chi$ or the direction of x-axis. The maximum value of G is

$$G_{max}=R_a \quad \text{at} \quad \omega_{max}=90^\circ-\chi \tag{40}$$

On the other hand, the minimum value of G occurs at $\phi=90^\circ$, that is the direction of y-axis, at which,

$$G_{min}=R_b \quad \text{at} \quad \omega_{min}=180^\circ-\chi \tag{41}$$

The value of χ can be predetermined theoretically by Eq. 18. Thus, the major and minor semi-axes of the ellipsoidal molecule, R_a and R_b, are obtained experimentally from the values of G_{max} and G_{min}, and the direction of the major and minor axes of the molecule coinside with ω_{max} and ω_{min}. The value of R_c is equal to the value of G for $\beta=0$, that is the value for the solution at rest:

$$G_0=R_c \tag{42}$$

The values of $G/\sqrt{g_0}$ are shown in Fig. 3, where g_0 is the value of g for the solution at rest. G_{max} and G_{min} are shown by open circles. The numerical values of $G_{max}/\sqrt{g_0}$ and $G_{min}/\sqrt{g_0}$ are shown in Table I for perfectly flexible molecules.

TABLE I. THE MAXIMUM AND MINIMUM OF G FOR PERFECTLY FLEXIBLE HIGH POLYMER MOLECULE

β	ω_{max}	$G_{max}/\sqrt{g_0}$	ω_{min}	$G_{min}/\sqrt{g_0}$
0	45.00°	0.52705	135.00°	0.52705
0.1	42.14	0.55540	132.14	0.50263
0.2	39.34	0.58784	129.34	0.48190
0.4	34.10	0.66475	124.10	0.45007
0.6	29.52	0.75642	119.52	0.42827
0.8	25.67	0.86032	115.67	0.41349
1.0	22.50	0.97388	112.50	0.40339
1.2	19.91	1.0948	109.91	0.39185
1.4	17.77	1.2212	107.77	0.39134
1.6	16.01	1.3518	106.01	0.38769
1.8	14.53	1.4857	104.53	0.38500
2.0	13.28	1.6221	103.28	0.38290

Expectation from Photographic Study of Small Angle Scattering

The shape of the pattern to be obtained by photographing the small angle scattering from a streaming solution will be discussed here. Let the distance from the specimen (a streaming solution) to the photographic plate be D, and the coordinate of one point P on the plate be (x', y'). Here the origin of the coordinate system is placed on the point where the primary beam hit the plate, the x'-axis being parallel to the direction of the velocity gradient, $\vec{q}$, and the y'-axis being parallel to the direction of flow, $\vec{v}$, and the direction of the primary beam being perpendicular to the plate.

Since the small angle scattering only is considered here, $\theta \ll 1$ or $r/D \ll 1$. Therefore,

$$\left.\begin{aligned}\sin(\theta/2) &\fallingdotseq r/2D \\ \cos\theta &\fallingdotseq 1-r^2/2D^2\end{aligned}\right\} \tag{43}$$

The intensity I_u of light per unit solid angle scattered to the direction SP in Fig. 4 is

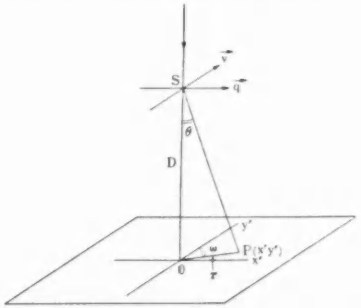

Fig. 4. Illustration of coordinate systems and angles.

$$I_u=I_0(1+\cos^2\theta)\,R_u \tag{44}$$

where I_0 is the intensity of the unpolarized incident light, and R_u is the reduced scattering intensity as defined by Eq. 3. Then, the intensity, I_u' of scattered light per unit area on the plate is

$$I_u'=I_u\cos\theta/(D^2+r^2) \tag{45}$$

Now, using Eq. 6 for sufficiently dilute solution, expanding the interference factor P in a power series of r/D and using Eq. 43,

$$I_u'=(2I_0KcM/D^2)\,[1-(r^2/2D^2)\{4+E\times(1+\beta^2+\beta\sqrt{1+\beta^2}\cos 2\phi)\}] \tag{46}$$

where

$$E=(4\pi^2R^2/9\lambda^2)\,(1+\beta^2/3)/(1+2\beta^2/3) \tag{47}$$

The contrast to be obtained on the photographic plate is probably not very great, although it will be the greater, the greater the value of R/λ is. Let us, however, expect that the contrast can be emphasized sufficiently by using adequate photographic technique. Here, the shape of the pattern obtained by connecting the points of equal blackness on the plate is discussed. Since I_u' is constant for these points, the value of h defined by

$$h=1-(D^2/2KcM)\,(I_u'/I_0) \tag{48}$$

is constant. Now changing the coordinate system from (x', y') to (x, y) shown in Fig. 2,

$$x^2/\{2D^2h/[4+E(1+\beta^2+\beta\sqrt{1+\beta^2})\}+y^2/\{2D^2h/[4+E(1+\beta^2-\beta\sqrt{1+\beta^2})]\}=1 \tag{49}$$

is obtained from Eqs. 46 and 48. Therefore, the shape of the pattern to be obtained on the plate is an ellipse. The direction of the major axis of the ellipse is parallel to the direction of the minor axis of the molecule (y-direction) and the direction of the minor axis of the pattern is parallel to the direction of the major axis of the molecule (x-direction). Thus, the orientation of the flexible high polymer molecules in flow can be determined by photographing the small angle scattering of light.

Summary

Small angle scattering of light by streaming flexible high polymer molecules is studied theoretically. It is concluded that the position at which the Zimm plot for infinite dilution cuts the ordinate does not change with the velocity gradient and is equal to $1/M$. The initial slope of the Zimm plot, however, varies with the velocity gradient as well as the direction of the observation plane. The quantity g proportional to the initial slope varies with the rate of rotation Ω of a concentric cylinder apparatus according to the approximation equation:

$$(g/g_0-1)/\Omega = A+B\Omega$$

where g_0 is the value of g at $\beta=0$, and A and B are parameters depending upon the direction of observation.

Now, when a quantity G:

$$G=\sqrt{(5/18)\ g\ (1+2\beta^2/3)/(1+\beta^2/3)}$$

(where β is a quantity proportional to the velocity gradient, the proportionality constant being obtained from the value of A or B) is measured, the value of G_{max} is equal to the length of the semi-major axis of the molecule, the observation plane for this G_{max} being parallel to the direction of the major axis of the molecule, while the value of G_{min} is equal to the length of the semi-minor axis of the molecule, the observation plane for this value being parallel to the direction of the minor axis of the molecule.

The pattern to be obtained by photographing the small angle scattering from a streaming solution of high polymer is discussed. The pattern is expected to be an ellipse, the orientation of the pattern is expected to be rotated by exactly 90° from the orientation of the molecule.

Faculty of the Science of Living
Osaka City University
Nishi-ku, Osaka

Absorption Spectra of Metallic Complexes with Aromatic Molecules

By Shoichiro YAMADA, Hiroshi YAMAZAKI[1], Hiroaki NISHIKAWA and Ryutaro TSUCHIDA

(Received September 30, 1959)

Ever since the first preparation of bis-(benzene)-chromium[2] and confirmation with X-rays of the sandwish structure of this compound[3], a number of metallic complexes with aromatic molecules have been synthesized. The study of these compounds is thought to be interesting because of the peculiar bonding involved in the compounds which may be quite similar to that in the ferrocene-type compounds. Many articles have been presented concerning various properties of the compounds, but there have been very few reports available which discuss their absorption spectra in relation to the bonding[4].

In the present work, the authors have determined quantitatively absorption spectra of some chromium compounds containing aromatic molecules and discussed the results of the measurements in relation to the bonding involved in the metal-arenes in general.

Experimental

Materials. — Bis-(benzene)-chromium(I) iodide was prepared in yellow crystals from bis-(benzene)-chromium(0), which was obtained according to the method of Fischer[2]. Dichroism of the compound was reported in the earlier paper[4].

Bis-(toluene)-chromium(I) iodide was prepared

1) Present address: Institute of Scientific and Industrial Research, Osaka Univ., Kitahanada-cho, Sakai-shi, Osaka.
2) E. O. Fischer and W. Hafner, *Z. Naturforsch.*, **10b**, 665 (1955).
3) E. Weiss and E. O. Fischer, *Z. anorg. u. allgem. Chem.*, **286**, 142 (1956).
4) S. Yamada, H. Nakamura and R. Tsuchida, This Bulletin, **30**, 647 (1957).

by the method of Fischer and Seus[5] from bis-(toluene)-chromium(0). The yellow, prismatic crystals of the compound show a straight extinction and a slight but definite dichroism on the well-developed prism face.

Monobenzene-chromium tricarbonyl was prepared in yellow, plate-like crystals by the method of Fischer and Öfel[6] from chromium hexacarbonyl and bis-(benzene)-chromium(0) in a sealed tube. The crystals show a slight dichroism on the face, on which the dichroism measurement was carried out.

Chromium hexacarbonyl was prepared in colorless crystals according to the method of Natta et al.[7]

Measurements. — Dichroism in the visible and ultraviolet regions of $Cr(C_6H_6)(CO)_3$ was determined on the above-mentioned face with Tsuchida and Kobayashi's microscopic method[8] using polarized light.

Ultraviolet absorption spectra in solution were determined with a Beckman DU spectrophotometer.

Infrared spectra of the compounds in Nujol mulls and in potassium bromide discs were determined in the rock salt region with a Hilger H800 infrared spectrophotometer.

The notations in the present paper are the same as those used in the former papers of this series.

Results and Discussion

Ultraviolet Absorption Spectra of Metal Carbonyls. — Absorption spectra of chromium hexacarbonyl in various solvents have been determined in the present work, and are shown in Fig. 1. The present measurement indicates that there is a very weak absorption band at about 50×10^{13} sec^{-1}, which was not reported by the previous investigators[9]. The weak absorption band of this sort, which is observed in the absorption spectra of $Cr(C_6H_6)(CO)_3$, $[Cr(C_6H_6)_2]^+$ and $[Cr(C_6H_5CH_3)_2]^+$, may belong to a "spin-forbidden absorption band" and is discussed in the later part of the present paper.

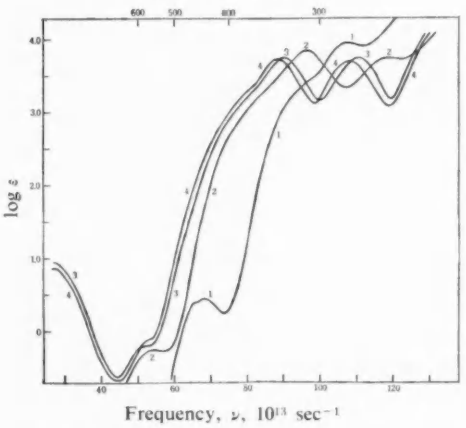

Fig. 1. Ultraviolet absorption spectra: 1, $Cr(CO)_6$ in methanol; 2, $Cr(C_6H_6)(CO)_3$ in methanol; 3, $Cr(C_6H_6)_2I$ in water; 4, $Cr(C_6H_5CH_3)_2I$ in water.

Milazzo and Scheibe[9] believed that most of the intense absorption bands of $Cr(CO)_6$ in the shorter wavelength, excepting the first inflation which they regarded as due to the carbonyl molecule itself, might be due to the decomposition products formed by photo-dissociation from the original molecule. Their conclusion was based upon the absence of a fine structure in the absorption curve. In the opinion of the present authors, however, the absence of a fine structure alone seems to be insufficient for such a conclusion. Such a flat absorption curve may be ascribed rather to the extraordinary nature of the ligand or, in other words, of the metal-to-ligand bond. Flat absorption curves similar to the spectrum of chromium hexacarbonyl are often exhibited; for example, by complexes of transition elements with ligands such as cyanide, isonitriles, ethylene, dimethylglyoxime and so forth.

Generally speaking, absorption spectra of carbonyls of transition elements may be regarded as a superposition of "ligand field absorption bands", due mainly to the metal under the field of the CO molecules, and absorption bands due to the electronic transitions which are closely related with the CO-groups under the field of the metal atom with which they are linked. Thus, the inflation at about 92×10^{13} sec^{-1} of $Cr(CO)_6$, which is found in Fig. 1, may be regarded as corresponding to a "ligand field band", and the absorption bands in shorter wavelength may be due to the electronic transitions closely related with the CO-groups under the field of the central metal. Absorption bands of the latter type, however, can not be ascribed to the CO-groups alone, since the present measurement shows that the absorption bands of $Cr(CO)_6$ undergo a slight "red shift" on changing a solvent from a less polar to a more polar one, whereas the carbonyl-group in ketones, for example, suffers a "blue shift"[10]. The authors are inclined to assume that the bands may most probably be due to electronic transitions from a level related principally with

5) E. O. Fischer and D. Seus, *Chem. Ber.*, **89**, 1809 (1956).
6) E. O. Fischer and K. Öfel, ibid., **90**, 2532 (1957).
7) G. Natta, R. Ercoli, F. Calderazzo and A. Rabizzoni, *J. Am. Chem. Soc.*, **79**, 3611 (1957).
8) R. Tsuchida and M. Kobayashi, This Bulletin, **13**, 619 (1938); "The Colour and the Structure of Metallic Compounds" (Kinzokukagobutsu no Iro to Kozo), Zoshindo, Osaka (1944), p. 180.
9) G. Milazzo and G. Scheibe, *Z. physik. Chem.*, **B31**, 431 (1936).
10) G. Scheibe, *Ber.*, **58**, 587 (1925).

the metal to excited levels of the CO-groups in the metallic complex.

In connection with the chromium hexacarbonyl, it seems to be interesting to discuss here about the absorption spectrum of $Co_2(CO)_8$. Hieber et al.[11] reported the absorption spectrum of the compound in solution, only pointing out that the binuclear complex showed an absorption spectrum different from that of the corresponding mononuclear complexes. The spectra of the compound in the gaseous and solution states were later determined and discussed in combination with the infrared spectrum, the bibridged structure being regarded as most probable[12]. On re-examination of the ultraviolet spectra reported by the former investigators, it is readily recognized that $Co_2(CO)_8$ exhibits absorption in the wavelength region much longer than the corresponding mononuclear $[Co(CO)_4]^-$ ion. It is known from data so far obtained that the absorption spectrum of bibridged complexes without special interaction between the two metal atoms may be regarded as a superposition of the two mononuclear complexes of which the binuclear complex is assumed to be composed. Thus, the absorption spectrum of the bibridged, binuclear complex is known to show no greatly bathochromic displacement from the spectrum of the corresponding mononuclear complexes. This may be recognized; for example, in comparing absorption spectra of dicobalt-μ, μ'-diol, diplatinum-μ, μ'-dichloro, dipalladium-μ, μ'-dichloro and dichromium-μ,-μ'-diol complexes with the spectra of the corresponding mononuclear complexes[13]. The displacement of the absorption spectrum of $Co_2(CO)_8$ from that of $[Co(CO)_4]^-$ seems to be too great for an ordinary type of binuclear complex without special interaction. Thus, the appearance of the absorption in the enormously long wavelength region may be taken as evidence for the assumption of the direct interaction between the cobalt atoms in the $Co_2(CO)_8$.

Ultraviolet Absorption Spectra of Bis-(benzene)- and Bis-(toluene)-chromium(I) Iodide.— Ultraviolet absorption spectra of bis-(benzene)- and bis-(toluene)-chromium(I) iodide, which have been determined in the present work, are shown in Fig. 2 and Table I. The absorption spectrum of $[Cr(C_6H_6)_2]I$ in solution was formerly reported by the present authors, but the measurement has been extended to the longer wavelength region in the present work.

It is seen in Fig. 2 and Table I that the absorption spectrum of $[Cr(C_6H_5CH_3)_2]I$ bears

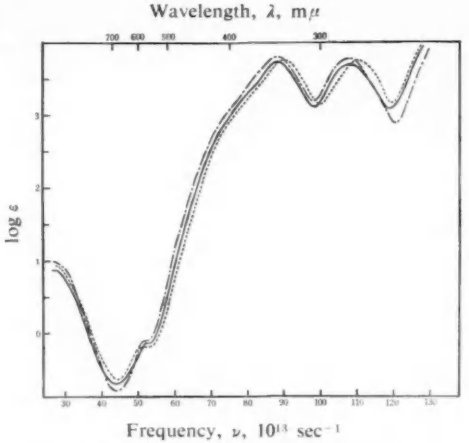

Fig. 2. Ultraviolet absorption spectra: ——, $Cr(C_6H_5CH_3)_2I$ in water; – – –, $Cr(C_6H_5CH_3)_2I$ in ethanol; ------, $Cr(C_6H_6)_2I$ in water.

a close resemblance to the spectrum of $[Cr(C_6H_6)_2]I$. Thus, between the two curves there is only a very slight difference in the wavelength and the intensity of the band maxima. In addition, the solvent effect on absorption bands is also the same for the two compounds, as seen in Table I. It may safely be concluded that the $[Cr(C_6H_5CH_3)_2]^+$ ion has the same structure and bonding as the $[Cr(C_6H_6)_2]^+$ ion. Both the complex ions may most probably have the sandwich structure.

Free benzene and toluene are known to show a characteristic band at about 260 mμ with a fine structure. On the contrary, both the $[Cr(C_6H_6)_2]^+$ and the $[Cr(C_6H_5CH_3)_2]^+$ ion are found to show no absorption bands of the above sort. The absorption bands of the chromium(I)-complexes in the corresponding wavelength region are much more intense than the band of benzene or toluene, and do not show such a fine structure as is observed in the spectra of the aromatic molecules themselves. Moreover, Bands II and III of the chromium(I)-complexes undergo a slight " blue shift ", whereas the absorption band of the benzene ring with a fine structure undergoes a slight " red shift ". These facts seem to show that the electronic state of the benzene rings in the chromium(I)-complexes is quite different from that of a benzene ring in the free benzene derivatives. The dichroism of the $[Cr(C_6H_6)_2]^+$ ion also seems to be consistent with this assumption[13]. If the aromaticity of the benzene rings in the chromium(I)-complex were comparatively remarkable, a dichroism similar to the benzene rings would be observed, just as in ordinary benzene derivatives. Since a dichroism of this

11) W. Hieber and K. K. Hofmann, *Z. anorg. u. allgem. Chem.*, **270**, 49 (1952).
12) R. A. Friedel, I. Wender, S. L. Shufler and H. W. Sternberg, *J. Am. Chem. Soc.*, **77**, 3951 (1955); J. W. Cable, R. S. Nyholm and R. K. Sheline, ibid., **76**, 3373 (1954).
13) S. Yamada and R. Tsuchida, unpublished.

TABLE I. ABSORPTION MAXIMA OF CHROMIUM COMPOUNDS WITH AROMATIC MOLECULES

Compound	Solvent	Band I′ ν(log ε)	Band I ν(log ε)	Band II ν(log ε)	Band III ν(log ε)
$[Cr(C_6H_5CH_3)_2]I$[a]	water	27(0.82)	75(2.9)	88.0(3.72)	108.1(3.69)
	ethanol	27(1.00)	76(3.0)	87.6(3.80)	107.8(3.77)
	solvent effect	very slight	very slight	slight blue shift	slight blue shift
$[Cr(C_6H_6)_2]I$[a,b]	water	26(0.95)	76(2.75)	90 (3.76)	110.6(3.75)
	solvent effect	very slight	very slight	slight blue shift	slight blue shift
	stronger component		Z	Z	Z
$[Cr(C_6H_6)(CO)_3]$[a]	methanol		80(3.3)	96.3(3.86)	118.3(3.74)
	ethanol		80(3.4)	96.1(3.54)	118.1(3.67)
	solvent effect		very slight	slight blue shift	slight blue shift
	stronger component		Z	Z	(Z)
$[Cr(C_6H_5\cdot C_6H_5)_2]I$	ethanol[c]			87.7(4.01)	120(3.39)
	——[d]			86.2(3.8)	120(4.5)
$[Cr(C_6H_5\cdot C_6H_5)_2](OC_6H_5)$	ethanol[c]			87.0(——)	121(——)
$[Cr(C_6H_6)(C_6H_5\cdot C_6H_5)]I$	ethanol[c]			87.5(——)	111(——)

ν : $10^{13}\times$ sec^{-1}

a) The present measurement.

b) Ref. 4 in the text.

c) Taken from H. H. Zeiss and M. Tsutsui, *J. Am. Chem. Soc.*, **79**, 3062 (1957).

d) Taken from Ref. 5, in which the solvent is not given. In the curve there is observed inflation at about 116×10^{13} sec^{-1} (log ε 4.3).

sort or a band with a fine structure characteristic of the free benzene derivatives is not observed, the electronic state of the benzene rings in this chromium(I)-complex seems to be comparatively far apart from the state of the free benzene molecule. It is most likely, as is shown in the later part of this paper, that the π-electrons on the benzene rings are attracted to a considerable extent toward the central chromium ion to form firm linkage with it.

The present measurement also indicates that both $[Cr(C_6H_6)_2]I$ and $[Cr(C_6H_5CH_3)_2]I$ exhibit an absorption band (Band I′) in the near-infrared region. Since it is known that neither free benzene, toluene nor iodide ion in solution has any absorption bands of this sort, Band I′ in the infrared region can be ascribed to the $[Cr(C_6H_6)_2]^+$ and $[Cr(C_6H_5CH_3)_2]^+$ ion. Band I′ may be characteristic of the chromium(I)-complexes, since the present measurement indicates that $Cr(C_6H_6)(CO)_3$ or $Cr(CO)_6$ has no absorption bands in the corresponding wavelength region.

It is known that, when a metal ion having an unfilled *d*-electron shell forms a complex-group with ligands, a few absorption bands of moderate intensity, rather characteristic of the metal ion, must generally appear in the visible or near-ultraviolet region. In terms of the "ligand field theory", these absorption bands, Bands I and I′, may be ascribed to electronic transitions between the energy levels which are produced by splitting the lowest levels of the free metal ion under the field of the ligands. The chromium(I) ion with a $3d^5$ configuration has an $^2F_2$ level as its lowest level in the very strong ligand field[14]. Therefore, a few ligand field bands should appear corresponding to electronic transitions from the lowest level to the upper levels of the metal with the same multiplicity which might be regarded, in approximation, as produced by splitting from the original ^2I of the free chromium(I) ion under the very strong ligand field[14]. Band I′ in the near-infrared region and the inflation at about 76 to 78×10^{13} sec^{-1} (Band I(of $[Cr(C_6H_6)_2]^+$ and $[Cr(C_6H_5CH_3)_2]^+$ seem to belong to this sort of absorption bands.

The appearance of the ligand field bands, rather characteristic of the metal in ordinary metallic coordination compounds, seems to show

14) Y. Tanabe and S. Sugano, *J. Phys. Soc. Japan*, **9**, 766 (1954).

that *the linkage between chromium and the aromatic molecules in the chromium-complexes discussed here is rather similar, at least essentially, to the linkage in complexes of transition elements of a Werner-type, so that the π-electrons on the benzene rings in these compounds are withdrawn to a considerable extent toward the central chromium.*

Bands II and III may be different in their origin from the ligand field bands, judging from their intensity, which seems to be rather too great for the ligand field bands. The two bands seem to be due most probably to electronic transitions closely related with the benzene rings, but may not be regarded as belonging to those bands that are quite identical in their origin to the typical absorption band of free benzene, since Bands II and III show a slight but definite "blue shift" when the solvent is changed from a less polar to a more polar one, whereas the band of free benzene rings is known to show a slight "red shift". It may be assumed that Bands II and III are due to electronic transitions from the orbital principally related with the central metal ion to the excited levels of the benzene rings in the complexes. The fact that the difference $\nu_{III}-\nu_{II}$ is nearly constant for the $[Cr(C_6H_6)_2]^+$ and the $[Cr(C_6H_5CH_3)_2]^+$ ion may be consistent with the assumption presented in this paper about the origin of these absorption bands. The assumption also is borne out by the observation in the present work that the value $\nu_{III}-\nu_{II}$ for $[Cr(C_6H_6)_2]^+$ and $[Cr(C_6H_5CH_3)_2]^+$ is nearly equal to the value for $Cr(C_6H_6)(CO)_3$. This will be reported in the next paragraph of the present paper.

Ultraviolet Absorption Spectra of Monobenzene-chromium(0) Tricarbonyl. — Ultraviolet absorption spectra of $Cr(C_6H_6)(CO)_3$ have been determined and are shown in Fig. 3 and Table I. Since the chromium(0) atom in $Cr(C_6H_6)(CO)_3$ with a $3d^6$ configuration has $^1A_1$ as its lowest level in the case of very strong ligand field, the chromium(0)-complexes are expected to show a few ligand field bands which are due to electronic transitions from the $^1A_1$ level to the upper levels of the metal atom with the same multiplicity. In fact, the present measurement indicates that no absorption bands of this sort are apparently observed in the absorption curve of $Cr(C_6H_6)(CO)_3$ in solution. In the opinion of the present authors, the ligand field bands of the compound are situated possibly in the comparatively short wavelength region and seem to be covered partly under the more intense absorption bands. The inflation at about 80×10^{13} sec^{-1} in the curve of the solution most probably represents a ligand field band superposed by more intense absorption bands. A distinct maximum corresponding to the ligand field band is recognized at about the same wavelength in the absorption curve of the crystal, as seen in Fig. 3.

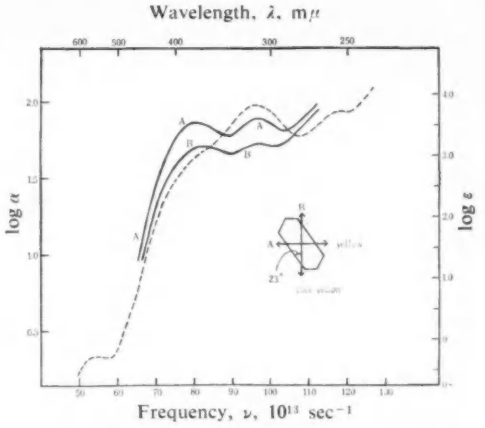

Fig. 3. Ultraviolet absorption spectra of $Cr(C_6H_6)(CO)_3$ in the crystalline state (——) and in methanol (------).

The ultraviolet absorption curve of $Cr(C_6H_6)(CO)_3$ bears a resemblance to that of the $[Cr(C_6H_6)_2]^+$ or the $[Cr(C_6H_5CH_3)_2]^+$ ion excepting that the absorption band in the infrared region, which is observed in the latter complexes, is absent in the former. Thus, the absorption bands at about 86 and 111×10^{13} sec^{-1} of $Cr(C_6H_6)(CO)_3$ in solution apparently correspond to Bands II and III of the $[Cr(C_6H_6)_2]^+$ or the $[Cr(C_6H_5CH_3)_2]^+$ ion, and are regarded as due to the electronic transitions from a level closely related with the central metal to two excited levels of the benzene rings in combination with the metal. It is found that *the difference $\nu_{III}-\nu_{II}$ is almost constant for $[Cr(C_6H_6)_2]I$, $[Cr(C_6H_5CH_3)_2]I$ and $Cr(C_6H_6)(CO)_3$*, it being in agreement with the present assumption about the origin of Bands II and III. The fact that $Cr(C_6H_6)(CO)_3$ shows absorption bands corresponding closely to those of $[Cr(C_6H_6)_2]I$, in spite of the oxidation state of chromium in the former compound which is different from the oxidation state in the latter, seems to indicate that *the linkage of chromium with the aromatic molecule is essentially alike in the above three compounds.* In fact, a recent study with X-rays[15] indicates that a molecule of $Cr(C_6H_6)(CO)_3$ has a structure similar to that of the $[Cr(C_6H_6)_2]^+$ ion having possibly the sandwich structure, the benzene ring in the molecule being parallel to the plane in which the three oxygen atoms are contained.

On the other hand, the absorption spectrum of

15) P. Corradini and G. Allegra, *J. Am. Chem. Soc.*, **81**, 2271 (1959).

$Cr(C_6H_6)(CO)_3$ is found to be quite different from the spectrum of $Cr(CO)_6$. Thus, the absorption bands in the ultraviolet region, which are rather characteristic of the metal carbonyls such as $Cr(CO)_6$ and may be due to the electronic transitions closely related with the excited levels of the CO molecules, are missing in $Cr(C_6H_6)(CO)_3$. This fact seems to show that *the linkage of chromium with the CO molecules in $Cr(C_6H_6)(CO)_3$ may be different in its nature from the corresponding linkage in $Cr(CO)_6$*. In connection with this, it may be worth noting that mixed carbonyls of wolfram and iron with some isonitriles show absorption spectra similar to those of $W(CO)_6$ and $Fe(CO)_5$, respectively. The linkage of the metal with the CO molecules in these mixed carbonyls is found to be rather similar to the linkage in the corresponding metal carbonyls.

TABLE II. CO STRETCHING FREQUENCIES

Compound	Freq. cm^{-1}
CO	2143[a]
$Cr(CO)_6$	2108, 2019, 2000[b] (1965, weak)[c]
$Cr(C_6H_6)(CO)_3$	1955[d]

a) Cf. L. J. Bellamy, "The Infra-red Spectra of Complex Molecules", Methuen & Co., London (1954).
b) N. J. Hawkins, H. C. Mattraw, W. W. Sabot and D. R. Carpenter, *J. Chem. Phys.*, **23**, 2422 (1955).
c) S. L. Shufler, H. W. Sternberg and R. A. Friedel, *J. Am. Chem. Soc.*, **78**, 2687 (1956).
d) The present measurement.

TABLE III. C-C SKELETAL VIBRATIONS OF BENZENE NUCLEUS

Compound	Skeletal vibr. cm^{-1}
$Cr(C_6H_6)(CO)_3$	1445[a]
$[Cr(C_6H_6)_2]I$	1428[b]
$Fe(C_5H_5)_2$	1410[c]
C_6H_6	1500[d]
C-C double	1600～1680[d]
C-C single	800～1200[d]

a) The present measurement.
b) Ref. 4 in the text.
c) L. Kaplan, W. L. Kester and J. Katz, *J. Am. Chem. Soc.*, **74**, 5531 (1952); E. R. Lippincott and R. D. Nelson, *J. Chem. Phys.*, **21**, 1307 (1953).
d) Cf. L. J. Bellamy, loc. cit.

As seen in Table II, comparison of a CO stretching frequency of $Cr(C_6H_6)(CO)_3$ with the corresponding values of its related compounds gives the following order: free CO > $Cr(CO)_6$ > $Cr(C_6H_6)(CO)_3$. Since the stronger linkage between the carbon and the chromium atom would loosen the linkage between the carbon and the oxygen atom more greatly, the above frequency shift seems to show, at least qualitatively, that *the metal-to-carbon bond in $Cr(C_6H_6)(CO)_3$ may be stronger than the corresponding bond in $Cr(CO)_6$*.

As seen in Table III, comparison of a skeletal C-C vibration of a benzene nucleus gives the following order: free C_6H_6 > $Cr(C_6H_6)(CO)_3$ > $[Cr(C_6H_6)_2]^+$. Since the displacement of the skeletal C-C vibration from the vibration of free C_6H_6 is less in $Cr(C_6H_6)(CO)_3$ than in $[Cr(C_6H_6)_2]^+$, *the linkage of the chromium atom with the benzene molecule may be stronger in the latter than in the former*.

The conclusion that the linkage between the chromium and the carbon of CO is stronger in $Cr(C_6H_6)(CO)_3$ than in $Cr(CO)_6$ is found to be in accordance with the fact that the Cr-C(in CO) distance is shorter in $Cr(C_6H_6)(CO)_3$[15] than in $Cr(CO)_6$[16]. It may also be worth noting that the Cr-C(in C_6H_6) distance is longer in $Cr(C_6H_6)(CO)_3$ than in the neutral molecule of $Cr(C_6H_6)_2$[17].

Dichroism of Monobenzene-chromium Tricarbonyl.—The results of the dichroism measurement are shown in Fig. 3. A preliminary report on the crystal structure of $Cr(C_6H_6)(CO)_3$ has recently been published, but the more detailed description of the crystal structure is not available. Comparison of the absorption spectra of $Cr(C_6H_6)(CO)_3$ with the spectra of $[Cr(C_6H_6)_2]I$, however, has enabled one to derive the main characteristics of the component absorptions of the former as referred to the principal axes of the molecule. Actually the molecules are not arranged in the crystal with their corresponding molecular axes completely parallel to each other. However, the dichroism of the crystal, as determined in the present work, may be thought to represent the main features of the component absorptions of the molecule.

The absorption band at about 80×10^{13} sec^{-1} of the crystal probably corresponds to the inflation at about the same frequency in the absorption curve of the compound in solution. This band may be regarded as corresponding to the absorption band at about 70×10^{13} sec^{-1} of $[Cr(C_6H_6)_2]I$ in the crystalline state, and may be assigned to one of ligand field bands. It is to be noted that Band II is found to be much weaker in the crystalline state than in solution, as was also found to be the case with $[Cr(C_6H_6)_2]I$.

16) L. O. Brockway, R. V. G. Ewens and M. W. Lister, *Trans. Faraday Soc.*, **34**, 1350 (1938).
17) E. Weiss and E. O. Fischer, *Z. anorg. u. allgem. Chem.*, **286**, 142 (1956).
18) The Z-direction refers to the threefold axis of the molecule of $Cr(C_6H_6)(CO)_3$.

The dichroism for Bands I and II of $Cr(C_6H_6)(CO)_3$ is found to be quite similar to that of $[Cr(C_6H_6)_2]I$ on suitable assumption of the crystal structure. Thus, if it is assumed that A- and B- absorptions in Fig. 3 represent, respectively, the main features characteristic of Z- and X, Y-absorption of the complex-molecule[18], the dichroism of $Cr(C_6H_6)(CO)_3$ seems to be coincident with the dichroism of $[Cr(C_6H_6)_2]^+$. The following relationship may be derived on the dichroism of $[Cr(C_6H_6)_2]I$ and $Cr(C_6H_6)(CO)_3$.

Z-absorption is stronger than X, Y-absorption for Bands I and II.

The absorption spectra and the dichroism of these compounds are evidently different from those of free benzene rings. If much aromaticity were kept in the benzene rings within the chromium-complexes, a dichroism similar to the dichroism of the free benzene rings would be observed, just as in most benzene derivatives. Since the dichroism characteristic of the free benzene rings or a band with a fine structure is not observed, the electronic state of the benzene rings in these compounds seems to be far from the state of the free benzene molecule.

The observation that Z-absorption is stronger than X, or Y-absorption for Bands I and II seems to be in good agreement with the concept that *the π-electrons on the benzene rings in $Cr(C_6H_6)(CO)_3$ are strongly withdrawn toward the chromium atom to form linkage with it.*

A similar type of dichroism was formerly reported with bis-(cyclopentadienyl)-iron(II) and cobalt(III) complexes, where Z-absorption is stronger than X- and Y-absorptions of the complexes for the two absorption bands in the long wavelength region[19]. This relationship also was taken as evidence that the π-electrons on the pentagonal rings are withdrawn considerably toward the metal atom to form firm bonds with it.

Weak Absorption Bands in the Long Wavelength Region.—The present measurement indicates that $Cr(CO)_6$, $[Cr(C_6H_6)_2]^+$ and $[Cr(C_6H_5CH_3)_2]^+$ all display a very weak band system in the long wavelength side. A part in the shorter wavelength region of the weak band is covered by much stronger absorption bands. It is theoretically known that the electronic transitions between levels with different multiplicities are strictly forbidden, appearing in most cases as very weak absorption bands. Thus, chromium(III)-complexes are known to display a spin-forbidden band with very small intensity to the long wavelength side of the ligand field absorption band[20]. In a similar way, the very weak absorption band systems of $Cr(CO)_6$ or $[Cr(C_6H_6)_2]^+$ may most probably correspond to the spin-forbidden bands which are due principally to chromium(0) or chromium(I). The spin-forbidden bands may tentatively be assigned to electronic transitions from the ground state $^1A_1$ to $^3F_1$ and $^3F_2$ in the case of chromium(0), and to transitions from the ground state $^3F_2$ to $^1F_1$ and $^1F_2$ in the case of chromium(I).

The solvent effect upon this type of the weak absorption bands has been examined, and is shown in Table IV. It is found that the band undergoes a slight "red shift" with the compounds examined here.

TABLE IV. SPIN-FORBIDDEN ABSORPTION BANDS

Compounds	Solvent	ν	$\log \varepsilon$
$[Cr(C_6H_6)_2]I$	water	52	$\bar{1}.80$
$[Cr(C_6H_5CH_3)_2]I$	water	52.5	$\bar{1}.90$
	ethanol	53	$\bar{1}.90$
$Cr(C_6H_6)(CO)_3$	methanol	53-4	$\bar{1}.8$
	ethanol	55-6	—
$Cr(CO)_6$	methanol	67.5	0.47
	ethanol	68.5	0.45

ν: 10^{13} sec^{-1}

The present measurement also indicates that the spin-forbidden bands are displaced to the shorter wavelength region, as the ligand field bands are displaced to the same direction in the following series: $[Cr(C_6H_6)_2]^+$, $Cr(C_6H_6)(CO)_3$, $Cr(CO)_6$.

Ultraviolet Absorption Spectra of Hein's Polyphenyl-chromium Compounds.— Hein[21] reported a number of polyphenyl chromium compounds with general composition of $Cr(C_6H_5)_n$ and $Cr(C_6H_5)_nX$, where n is equal to 3 or 4, and X denotes an anion such as iodide and anthranilate. It was only after the discovery of numerous compounds with a ferrocene-like structure that the suggestion was presented that Hein's compounds might contain chromium(I)-complexes having a sandwich structure with benzene, biphenyl, terphenyl or similar aromatic molecules[22]. Identificaion of one of Hein's compounds, $Cr(C_6H_5)_4I$, with the complex $[Cr(C_6H_5 \cdot C_6H_5)_2]I$, which was prepared from chromium-(III) chloride, aluminum and biphenyl as starting materials, was made by comparison of their infrared and ultraviolet absorption spectra, X-ray absorption edges and magnetic properties[5]. Absorption spectra as well as other properties

19) S. Yamada, A. Nakahara and R. Tsuchida, *J. Chem. Phys.*, **22**, 1620 (1954); This Bulletin, **28**, 465 (1955).
20) C. K. Jørgensen, *Acta Chem. Scand.*, **8**, 1502 (1954).
21) F. Hein et al., *Ber.*, **61**, 730 (1928); ibid., **62**, 1151 (1929); *Z. anorg. u. allgem. Chem.*, **273**, 209 (1953); etc.
22) H. H. Zeiss and W. Herwing, *Ann.*, **606**, 209 (1957); H. H. Zeiss and M. Tsutsui, *J. Am. Chem. Soc.*, **79**, 3062 (1957); H. H. Zeiss, M. Tsutsui and L. Onsager, "Abstr. 126th Meeting *Am. Chem. Soc.*", New York (1954), p. 29.

of Hein's compounds were formerly reported, but the detailed discussion about ultraviolet spectra of the compounds has not been presented up to the present. In the following, a brief discussion will be given about the absorption spectra of these compounds on the basis of the relationships which have been obtained in the present work.

It was reported in the earlier part of the present paper that the benzene rings in combination with chromium in the compounds having linkage characteristic of the sandwich molecules show two absorption bands, which are due presumably to electronic transitions from an orbital concerned mainly with the central chromium to the two excited levels of the benzene rings. In support of this idea seems to be the fact that the frequency difference between two such transitions is nearly constant for the chromium compounds with benzene rings.

When benzene is replaced by biphenyl in a similar type of compound, a similar type of relationship may exist about the frequency difference, if the sandwich structure is kept in the biphenyl-compounds. Thus, the magnitude of the corresponding frequency difference may be constant for the compounds of chromium with biphenyl, but different from the magnitude in the case of the chromium(I)-compounds with benzene rings. Based on the concept presented here, absorption spectra of Hein's polyphenyl compounds of chromium(I) seem to be understood well if it is assumed that they contain chromium(I)-complexes with aromatic molecules, having the sandwich structure of a ferrocene-type.

In the case of $[Cr(C_6H_6)(C_6H_5\cdot C_6H_5)]^+$, for example, which has both benzene and biphenyl in combination with chromium(I), electronic transitions to the two excited levels of benzene and to a few levels of biphenyl may be possible, their superposition being observed in the absorption curve of this compound. In fact, $\nu_{III}-\nu_{II}$ obtained from the observed curve[22] of $[Cr(C_6H_6)(C_6H_5\cdot C_6H_5)]^+$ is found to be nearly equal to the value for $[Cr(C_6H_6)_2]^+$, as seen in Table I. This observation may be readily understandable on the basis of the assumption presented in this paper. Thus, if it is assumed that the maximum frequency of Band III, ν_{III}, of the chromium compound is greater with biphenyl than with benzene rings, the difference $\nu_{III}-\nu_{II}$, which is obtained directly from the absorption spectrum of $[Cr(C_6H_6)(C_6H_5\cdot C_6H_5)]^+$, may correspond to the frequency difference between the two excited levels of the benzene ring in combination with the chromium. This is in agreement with the above-mentioned observation. The observation that $[Cr(C_6H_5\cdot C_6H_5)_2]^+$ shows larger $\nu_{III}-\nu_{II}$ than $[Cr(C_6H_6)_2]^+$ does may be understood in a similar way.

The fact that the absorption spectra of Hein's compounds may be explained in this way seems to indicate that *Hein's polyphenyl chromium-(I)-compounds have complex-ions with a sandwich structure similar to that of* $[Cr(C_6H_6)_2]^+$ *or* $[Cr(C_6H_5CH_3)_2]^+$.

It is to be noted that Hein's chromium(I)-complexes all show Band II at about 86 to 88×10^{13} sec^{-1}, which is very close to the value for Band II of $[Cr(C_6H_6)_2]^+$, $[Cr(C_6H_5CH_3)_2]^+$ and $Cr(C_6H_6)(CO)_3$. This seems to indicate that *the linkage of the aromatic molecules with the central chromium is remarkably alike in these complexes.*

It was found in the preceding part of the present paper that the chromium(I)-complexes with aromatic molecules exhibit a very weak absorption band, due possibly to spin-forbidden transitions, in the long wavelength region and one of the ligand field bands in the near-infrared. The former investigators did not report a very weak absorption band in the visible or an absorption band in the infrared region for Hein's polyphenyl compounds of chromium(I). In the opinion of the present authors, however, there is good reason to expect that the "polyphenyl compounds of chromium(I)" show a spin-forbidden absorption band at about 50 to 55×10^{13} sec^{-1}, and two of the ligand field bands, one in the infrared and the other as inflation at about 80×10^{13} sec^{-1}, just like the bis-(benzene)- and bis-(toluene)-chromium(I) complexes.

General Aspects of Absorption Spectra of Metal-arenes.—In the next place, the authors will discuss the general aspects of absorption spectra of metallic complexes with aromatic molecules and related compounds on the basis of these measurements with the aid of the data by the former investigators. It may be assumed that these compounds in general display "ligand field absorption bands", due mainly to the central metal under the strong ligand field surrounding it, and absorption bands corresponding to the electronic transitions to the excited levels of the ligand groups in combination with the metal. A part of the former is often covered by more intense absorption of the latter type. The absorption bands of the latter type seem to be rather dependent upon the ligand and sensitive to the nature of its linkage with the metal. Thus, in the case of the cyclopentadienyl-radical, the latter bands are found to undergo a marked shift as the central metal is exchanged, while little change in this type of bands is given rise to when a benzene molecule combined with chromium is replaced by a biphenyl molecule

in the chromium-arenes.

Besides these two types of absorption bands, there is usually observed a very weak absorption band system in the long wavelength region, corresponding to spin-forbidden bands due mainly to the central metal. A part of this band system is also covered by the other absorption bands with much greater intensity.

With an ordinary type of metallic complex, the order of ligands is known as the "spectrochemical series"[23], which represent the decreasing order as to the magnitude of their hypsochromic effect on the ligand field bands of the metallic complexes. In the following, discussion will be undertaken concerning metallic compounds with ligands which are coordinated to a metal atom through their carbon atom. Unambiguous assignments of absorption bands to particular electronic transitions are sometimes quite difficult, but a general trend concerning the above effect may be readily derived. Thus reviewing a series of compounds, $Cr(CO)_6$, $Cr(C_6H_6)(CO)_3$ and $Cr(C_6H_6)_2$, the authors may be able to obtain the following order as to the hypsochromic effect of the ligands: $CO > C_6H_6$. In a similar way, it is easily shown that CO has a greater hypsochromic effect than a cyclopentadienyl-radical: $CO > C_5H_5^-$. It is thus seen that CO stands extremely high in the spectrochemical series, probably even higher than CN^-. Comparison also reveals that $C_5H_5^-$ is very close to, but only a little higher than, C_6H_6 in the spectrochemical series. In summary, the following order may be derived: $CO > C_5H_5^- > C_6H_6$.

It is interesting to note that the following order also is derived from the previous data[24] about mixed carbonyls of iron and wolfram: $CO > CN{\cdot}CH_3 > CN{\cdot}C_6H_5$. Comparison of the isonitriles with C_6H_6 and $C_5H_5^-$ as to their hypsochromic effect seems to be difficult for the present.

With the same ligands, the order of transition metal elements as to their hypsochromic effect may also be derived in a similar way. With ligands such as CO, $C_5H_5^-$ and C_6H_6, light absorption is found to be displaced to a shorter wavelength, as the authors go down the periodic table for elements belonging to one and the same sub-group. More or less marked hypsochromic shift is observed when a metal atom is replaced by another which stands lower in the same sub-group for a series of elements such as (Cr, Mo, W), (Fe, Ru, Os) and (Co, Rh, Ir). Absorption maxima of all these compounds are not reported, but a difference in color seems to indicate the above trend without exception. The same trend was reported with many other ligands of an ordinary type[25].

Summary

Ultraviolet absorption spectra of $Cr(CO)_6$, $Cr(C_6H_6)(CO)_3$, $[Cr(C_6H_6)_2]I$ and $[Cr(C_6H_5CH_3)_2]I$ have been determined in various solvents. Dichroism in the visible and ultraviolet region of $Cr(C_6H_6)(CO)_3$ has been determined at room temperature by Tsuchida and Kobayashi's microscopic method with a single crystal of the compound.

The absorption spectrum of $Cr(C_6H_6)(CO)_3$ shows main features similar to those of the spectrum of the $[Cr(C_6H_6)_2]^+$ ion.

These compounds all show a weak absorption band to the long wavelength side of the intense absorption bands.

The results of the measurements have been discussed in relation to the bonding involved in these compounds. Discussion also has been undertaken about Hein's polyphenyl-compounds of chromium(I) on the basis of the present measurements. Absorption spectra of Hein's compounds of chromium(I) seem to be in agreement with the assumption of the sandwich structure.

Department of Chemistry
Faculty of Science
Osaka University
Nakanoshima, Osaka

23) R. Tsuchida, This Bulletin, **13**, 395 (1938); *J. Chem. Soc. Japan, Pure Chem. Soc.* (*Nippon Kagaku Zasshi*), **59**, 586, 731, 819 (1938); R. Tsuchida and Y. Shimura, This Bulletin, **25**, 49 (1953).

24) W. Hieber and D. von Pigenot, *Chem. Ber.*, **89**, 616 (1956).

25) C. K. Jørgensen, "Technical Report on Absorption Spectra of Complexes of Heavy Metals", U. S. Depratment of the Army, Contract No. DA-91-508-EUC-247, FTR No. 1 (1958), p. 50.

Vinyl Polymerization. XLIII. Polymerization of Styrene with Vinylmagnesium Chloride

By Minoru IMOTO and Masayoshi KINOSHITA

(Received September 21, 1959)

It was reported by Beaman[1] and others that Grignard reagents could polymerize some vinyl monomers. Recently, a synthetic method of Grignard reagent from vinyl chloride was published[2]. In this paper the authors prepared vinylmagnesium chloride after Ramsden[2] and carried out the kinetic study of the polymerization of some vinyl monomers.

Experimental

Materials.—Commercial tetrahydrofuran (THF) was refluxed over potassium hydroxide and then over sodium. After distillation it was stored in the presence of lithium aluminum hydride. Before use, it was redistilled in a stream of nitrogen. Commercial vinyl chloride was dried with potassium hydroxide, calcium chloride and then with phosphorus pentoxide.

Vinylmagnesium Chloride.—Vinyl chloride gas was passed into THF (507 g.) until 144 g. were absorbed. Ethyl bromide (2 ml.) was dropped into a mixture of 44 g. of magnesium turnings and 15 ml. of the vinyl chloride-THF solution was then added as rapidly as possible. After the reaction was completed, excess vinyl chloride was distilled out and the unreacted magnesium was filtered off. The homogeneous solution of vinylmagnesium chloride was stored in a brown bottle. The Grignard solution thus obtained had a concentration of 2.07 mol./l. by Gilman's titration[3] (81% yield). After a month, the concentration decreased to 2.01 mol./l. From these values it was considered that the concentration of the reagent might be kept constant throughout the experiment.

Change of Vinylmagnesium Chloride into Acrylic Acid.—A solution of vinylmagnesium chloride in THF was added into a large excess of powdered dry ice. After being acidified, the organic layer was distilled to give an acid, having a stimulus odor, and boiling at 84~88 C/82 mmHg, ($n^{20}=1.4223$). The acid could be polymerized easily. From these facts, it was confirmed that the acid was acrylic acid (in literature 4, b.p.$_{85}$=81°C, $n^{20}=1.4224$) and the Grignard reagent was vinylmagnesium chloride.

Polymerization.—Styrene and methyl methacrylate were polymerized in a sealed glass tube, and acrylonitrile in a 3-necked flask equipped with a stirrer and a nitrogen inlet tube.

In the case of glass tube method, the tube was first substituted with dry nitrogen and fed with Grignard reagent from a burette, into which the reagent had been fed with the aid of nitrogen pressure. Then, the monomer and solvent were charged. The usual degassing procedure followed. These tubes were set in a water bath at constant temperature and shaken during polymerization. The reacted mixture was poured into methanol, containing excess hydrochloric acid. Polystyrene and polymethyl methacrylate were purified by reprecipitation from benzene solution by methanol. To obtain a sample of polymethyl methacrylate for infrared absorption spectrum, a freezing technique was used.

When acrylonitrile was contacted with the Grignard reagent, so much heat was evolved that the following procedure was used. To a cold mixture of Grignard reagent and a large volume of solvent (THF), the monomer was added through a long glass tube surrounded by dry ice. These operations were carried out under the atmosphere of dry nitrogen.

The intrinsic viscosities shown in Table I are the values at 30 C measured in benzene solution, using a Ubberohde viscometer.

Results and Discussion

Polymerization of Vinylmagnesium Chloride.—As shown in Table I, vinylmagnesium chloride could not be polymerized by the usual methods.

Table I. Porymerization of vinylmagnesium chloride

Initiator	VMgCl* ml.	THF** ml.	T°C	Time hr.	Polymer
AIBN***	50	0	60	10	None
BPO****	50	0	60	10	None
None	50	0	60	10	None
UV 3600 A	50	0	30	10	None

* Vinylmagnesium chloride
** Tetrahydrofuran
*** 2,2'-Azobisisobutylonitrile
**** Benzoylperoxide

Copolymerization of Vinylmagnesium Chloride with Styren or Methyl Methacrylate.—The white polymers obtained from the systems consisting of styrene and vinylmagnesium chloride had the same analytical results with styrene or methyl methacrylate homopolymer within the limit of experimental error (Table II). To introduce carboxyl groups to the copolymer, the polymerization mixtures were poured onto a large

1) R. G. Beaman, *J. Am. Chem. Soc.*, **70**, 3115 (1949).
2) H. E. Ramsden, *J. Org. Chem.*, **22**, 1602 (1957).
3) H. Gilman, *J. Am. Chem. Soc.*, **51**, 1676 (1929).

TABLE II. POLYMERIZATION OF SOME VINYL MONOMERS WITH VINYLMAGNESIUM CHLORIDE

VMgCl	Monomer		THF	Temp.	Time	Polymer		
ml.	ml.		ml.	°C	hr.	g.	Yield, %	$[\eta]$*
60	Vinylchloride	10**	50	30	20			
90	Styrene	50	0	50	6	48	100	0.136
5	Styrene	10	0	50	6	8.7	96	
0	Styrene	10	5	50	6	0.16	1.7	2.9
0	Styrene	15	0	50	6	0.1	0.7	4.7
6	Styrene	5	0	50	5	2.9	65	0.26
30	Methylmethacrylate	20	50	−60	18	6.8	36	2.2
30	Methylmethacrylate	20	50	10	18	1.3	7.0	2.6
								N %***
20	Acrylonitrile	50	50	30	****	9.3	23	19.49
10	Acrylonitrile	10	0	30		4.4	55	16.83
30	Acrylonitrile	20	50	−10		8.4	52	13.07

* $[\eta]$ was measured in benzene at 30°C using a Ubberohde viscometer.
** Under UV irradiation, the mixture gave needle crystals gradually but no polymer.
*** By the Kjeldahl method. Calcd. value is 26.40%.
**** Dropping acrylonitrile into Grignard mixture, yellow polymer precipitated immediately.

Polystyrene Found: C, 92.09; H, 8.12.
Calcd. for C_8H_8: C, 92.27; H, 7.74%.
Polymethylmethacrylate Found: C, 59.78; H, 8.27.
Calcd. for $C_5H_8O_2$: C, 59.98; H, 8.05%.

excess of dry ice, acidified with hydrochloric acid and the polymer was reprecipitated. But the infrared aosorption spectra of the polymers had no absorption characteristic of the hydroxyl group in carboxylic acid and were identical to those of each homopolymer.

Polymerization of Vinyl Chloride Initiated by Vinylmagnesium Chloride. — The mixture of vinylmagnesium chloride and vinyl chloride was sealed in a glass tube and irradiated by ultraviolet ray of 3600 Å but no polymer was obtained.

Polymerization of Acrylonitrile Initiated by Vinylmagnesium Chloride. — Acrylonitrile polymerized vigorously to yellow powder which contained a much smaller quantity of nitrogen than polyacrylonitrile.

Polymerization of Styrene Initiated by Vinylmagnesium Chloride. — In the presence of vinylmagnesium chloride styrene hardly polymerized at room temperature, but did so easily above 40°C. Fig. 1 shows the process of polymerization. As the concentration of vinylmagnesium chloride increased, the rate of polymerization also increased. Figs. 2—4 are the time-conversion curves at 50, 60 and 70°C, respectively. Fig. 5 shows the dependence of rate on monomer concentration. At a monomer concentration, the rate becomes maximum but the reason is not clear.

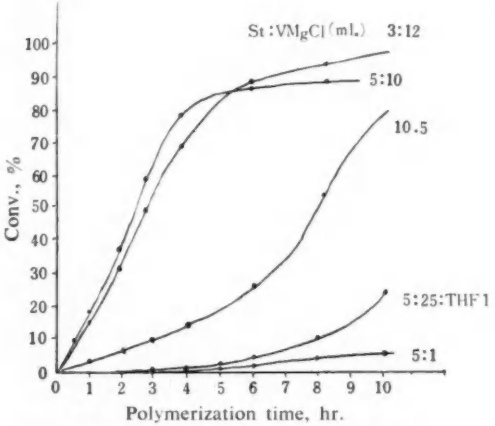

Fig. 1. Polymerization of styrene at 60°C.

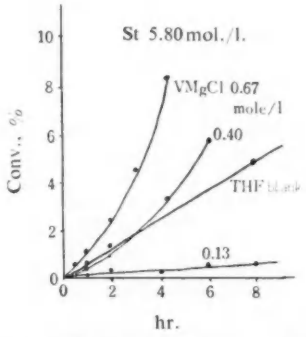

Fig. 2. Polymerization of styrene at 50°C.

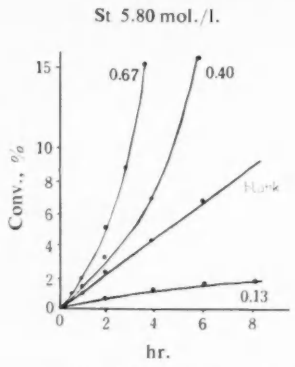

Fig. 3. Polymerization of styrene at 60°C.

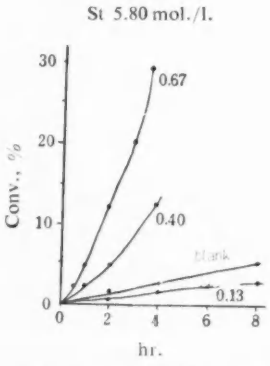

Fig. 4. Polymerization of styrene at 70°C.

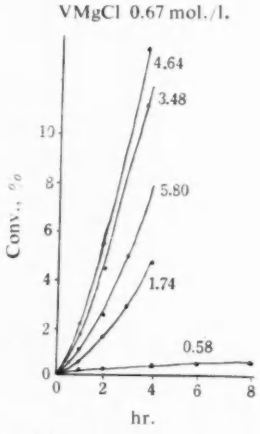

Fig. 5. Polymerization of styrene at constant initiator concentration at 50°C.

The rate of the polymerization of styrene in the absence of vinylmagnesium chloride was abnormally large, as shown in Figs. 2—4, as "blank test". The rapid rate was caused by the addition of THF instead of vinylmagnesium chloride solution. It may be considered that THF included THF-peroxide. In order to testify to this consideration, the THF above used was compared with oxygen absorbed THF. Oxygen was bubbled into THF under the irradiation of ultraviolet ray at room temperature for three days. The effects of the treatment was shown in Fig. 6. When the quantity of vinylmagnesium chloride was small, the rate decreased greatly. This was due to the consumption of the activities of Grignard reagent and peroxide by the mutual reaction.

Observation on the relation between the rate of polymerization and the concentration of vinylmagnesium chloride was carried out. As the curves for time vs. conversion were not straight, the conversions after two hours were plotted against the concentration of vinylmagnesium chloride. Straight lines were obtained as shown in Fig. 7. From the slope of these lines the following equation was derived.

$$Rp = k[C]^{1.4}$$

The overall activation energy of polymerization was about 12 kcal./mol. (Fig. 8).

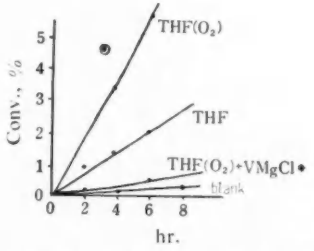

Fig. 6. Polymerization of styrene with O_2 treated tetrahydrofuran.
Double circle shows one carried out with the oily residue which was obtained by evaporation of THF treated with O_2.
* About 0.5 ml. VMgCl to 5 ml. THF(O_2).

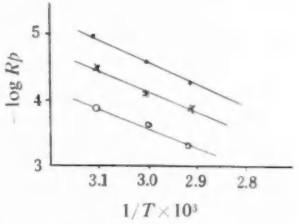

Fig. 7. The relation between the rate of polymerization and the concentration of vinylmagnesium chloride.
● 50°C × 60°C ○ 70°C

4) C. Moreau, M. Murat and N. Tampier, *Ann. chim.*, [9], **15**, 221 (1921).
5) R. Criege, *Angew. Chem.*, **62**, 120 (1950).

TABLE III. COPOLYMERIZATION OF STYRENE WITH METHYLMETHACRYLATE

No.	Styrene		Methylmethacrylate		Styrene	Time	Polymer	Styrene mol. % in copolymer
	ml.	mol. $\times 10^2$	ml.	mol. $\times 10^2$	mol. %	min.	g.	
1	10	8.70	0	0	100	710	0.134	100
2	9.5	8.26	0.53	0.49	94.4	570	0.029	70.46
3	9	7.83	1	0.94	89.3	380	0.088	19.75
4	8	6.96	2	1.87	78.8	150	0.141	4.80
5	7	6.09	3	2.80	68.5	70	0.339	4.80
6	6	5.22	4	3.74	58.3	60	0.492	2.50
7	5	4.35	5	4.67	48.2	60	0.612	2.09
8	4	3.48	6	5.61	38.3	50	1.404	0.71
9	3	2.61	7	6.54	28.5	50	1.556	2.47
10	2	1.74	8	7.48	18.9	50	1.108	0.48
11	1	0.87	9	8.41	9.38	20	0.996	1.99
12	0	0	10	9.36	0	20	1.095	1.58

Polymerization temperature ; 10°C.
Grignard concentration ; 0.67 mol./l.
Styrene contents in copolymer were calculated from the carbon contents.

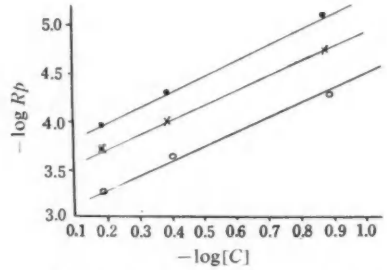

Fig. 8. Overall activation energy of polymerization.
● 50°C × 60°C ○ 70°C

Copolymerization of Styrene with Methyl Methacrylate.—In 1949, Beaman stated that the polymerization initiated by Grignard reagents proceeded through anionic mechanism. This idea has been generally accepted. To confirm the anionic mechanism in these systems, the authors carried out the copolymerization of styrene with methyl methacrylate at 10°C. From the carbon contents of copolymers their composition were calculated and plotted against the compositions in feed (Table III and Fig. 9). It was confirmed from the results in Fig. 9 that the polymerization initiated by vinyl magnesium chloride proceeded by anionic mechanism.

By the Beilstein test, it was found that no chlorine existed in the molecule of copolymer.

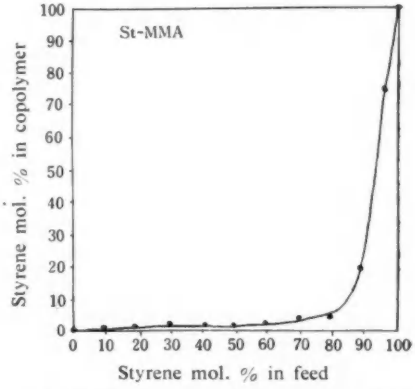

Fig. 9. The composition of styrene-methyl methacrylate copolymer.

From the results stated above, it was possible to state that the order of the rate of polymerization was as follows:

acrylonitrile > methyl methacrylate ≫ styrene > vinyl chloride = 0

Department of Applied Chemistry
Faculty of Engineering
Osaka City University
Kita-ku, Osaka

The Behavior of Fission Products Captured in Graphite Powder by Nuclear Recoil. I. The Stability of the Fission Products toward Nitric Acid Solution

By Toshio NAKAI, Seishi YAJIMA, Koreyuki SHIBA, Jiro OSUGI and Daisaburo SHINODA

(Received September 22, 1959)

In his pioneering study McMillan[1] placed a thin film of uranium oxide powder between filters or cigarette papers and irradiated it with cyclotron neutrons. He found that most of the fission products recoiled out of the film and were captured in the paper. This separation made it possible to identify the strong activity of neptunium 239 with a half life of 2.3 days that had been left behind.

If a fission reaction is caused to proceed in particles of uranium oxide with maximum dimensions smaller than the minimum range* of the fission products, these products will probably recoil out of the uranium oxide. On the other hand, heavier nuclei formed by neutron capture and beta decay will have a much shorter range and remain within the original particles. This means that in a suitable heterogeneous system the fission products will be completely separated from the actinide elements without complicated chemical treatment. Since McMillan's work appeared in a journal, several investigators studied the separation of the fission products and the actinide by nuclear recoil using several kinds of heterogeneous systems.

The authors have been investigating the possibility of the utility of the dispersion-type nuclear fuel element which consists of a mixture of graphite and uranium dioxide. In such a fuel, the behavior of fission products is most characteristic compared with the other solid-type nuclear fuels. If the dimensions of uranium oxide powder are smaller than the minimum range of fission products and the weight ratio of graphite powder to uranium oxide powder is great enough to prevent the penetration of the fission fragments into the neighboring uranium oxide particles and if uranium oxide particles are uniformly dispersed in graphite powder, the fission products produced in uranium oxide powder will be thoroughly recoiled out of them and captured by graphite powder. In the previous paper[2], it was made obvious that when the weight ratio of graphite (particle size is about 50 microns) to uranium dioxide (particle size is about 0.1 microns) was 10, approximately 70% of the overall fission product activity remained in graphite powder and that when the ratio was 30, approximately 95% was captured. Mixtures of graphite and uranium dioxide were irradiated with JRR-1 neutrons (Japan Research Reactor-1, a water boiler type) and after the addition of saturated zinc bromide solution (hydrochloric acid was slightly added), these mixtures were centrifuged. The graphite powder of these mixtures gathered on the upper layer and the uranium oxide powder settled at the bottom. The distribution of the fission products in these fractions was determined using gamma ray spectrometry. From the results, the possibility of a brief reprocessing of the dispersion-type spent fuel was suggested.

The present study was undertaken to investigate the variation of the gross gamma ray spectra of the fission products captured in graphite powder at various cooling times after irradiation, and the stability of the fission products captured in graphite toward nitric acid of several different concentrations at varying durations of immersion at a constant temperature.

Experimental

The Gross Gamma Ray Spectra of the Fission Products Captured in Graphite Powder. — *Procedure 1.*—Twenty milligrams of uranium dioxide (particle size, about 0.1 microns) was mixed with 600 mg. of natural graphite prepared by the Nippon Carbon Co., (particle size, about 50 microns), and the mixture was irradiated in the No. 16 experimental hole of JRR-1 under a thermal neutron flux of about 5×10^{11} neutrons/cm^2 sec. for about three minutes. The irradiated mixture was transferred to a centrifuging tube with 70 ml. of a saturated zinc bromide solution which contained a small amount of hydrochloric acid. After centrifugal separation, the graphite powder fraction which was collected on the upper side was transferred into a polyethylene tube (1.5 cm. in diameter and 7 cm. in length) and was gamma-assayed by the RCL

1) E. McMillan, *Phys. Rev.*, **55**, 510 (1939).

* The minimum range of the fission products in uranium dioxide is 8 microns.

2) T. Nakai and S. Yajima, *J. Chem. Soc. Japan, Pure Chem. Sec.* (*Nippon Kagaku Zasshi*), **79**, 1267 (1958).

256-channel gamma ray scintillation spectrometer with a welll-type sodium iodide crystal (2 in. ×1.75 in. diameter) as scintillator. The separation procedure was commenced after 20 min. cooling, and finished within 30 min. after irradiation. Gamma ray spectra were measured at appropriate intervals for two days.

Procedure 2.—Instead of the centrifugal separation, the irradiated mixture was treated for 5 min. with 50 ml. of 4 N hot nitric acid solution in order to dissolve uranium dioxide and neptunium formed by neutron capture and beta decay. The residual graphite powder was filtered and washed twice with 20 ml. of 0.1 N nitric acid solution, and then the graphite sample was gamma-assayed by the same method as above mentioned. In this case, the separation procedure was commenced after 20 min. cooling, and finished within 15 min.

Procedure 3.—The abundance of the fission nuclides contained in graphite powder varied with the cooling time, and also the state of each nuclide which was captured in a graphite crystal might vary. In this experiment, the irradiated mixtures were cooled for one day after irradiation and then submitted to the centrifugal separation or the nitric acid treatment. The obtained gamma ray spectra were compared with the spectra of the samples which were treated after 20 min. cooling and then cooled for 23 hr. Comparison of gamma ray spectra of the above mentioned treatments gave a good agreement.

Several gamma ray spectra of the gross fission products obtained by procedure 2 are shown in Fig. 1.

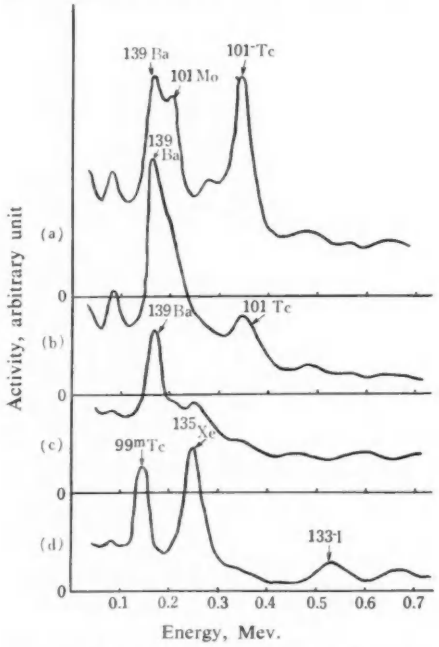

Fig. 1. Gamma ray spectrum of the fission products in graphite (a) at 26 min., (b) at 60 min., (c) at 160 min. and (d) at 20 hr. after irradiation.

The short lived nuclides in the fission products identified by these spectrodiagrams give a good agreement with those deduced from Peirson's experiment[3].

The respective abundance and the cross sections of uranium-238 and of uranium-235 are such that the irradiation of natural uranium by thermal neutrons leads to a temporary obliteration of the low energy portion of the fission products spectra by more intense X-rays and gamma rays emitted from neptunium-239 (half life 2.3 days). If a chemical treatment was used to eliminate the interfering neptunium-239, gaseous fission products such as xenon-135 would escape, and the complete spectrum of the gross fission products could not be obtained. For this reason, in Peirson's experiment[3] the gross gamma ray spectrum was measured by using a uranium, fifty times enriched in uranium-235. However, in this experiment the measurement of the gross gamma ray spectrum can be performed satisfactorily by using nautral uranium**.

The gamma ray spectrum of the fission products obtained by procedure 1 was similar to those obtained by procedures 2 and 3. From these results, it is evident that the centrifugal separation or the nitric acid treatment for such a short period can not affect the state of fission products captured in a graphite crystal. The effect of long time nitric acid treatment will be described in the next section.

Leaching of Fission Products out of Graphite by Nitric Acid Solution.—*Procedure.*—The graphite samples used in this experiment are artificial graphite

Table I. Particle size of graphite

Sample	Particle size, micron
Artificial graphite (A. G.)	30
Natural graphite (N. G.—1)	1
Natural graphite (N. G.—2)	50

Table II. Analytical data of impurities in graphite

Impurity	A.G.	N.G.-1	N.G.-2
Ash (total)	0.07%	0.3%	0.8%
SiO_2	250 p.p.m	220 p.p.m	3700 p.p.m
Al_2O_3	210 〃	60 〃	3500 〃
Fe_2O_3	130 〃	24 〃	300 〃
MgO	15 〃	24 〃	100 〃
CaO	70 〃	36 〃	300 〃
V_2O_5	— 〃	0.12 〃	0.5 〃
MnO	— 〃	— 〃	— 〃
Na_2O	20 〃	12 〃	25 〃
K_2O	15 〃	12 〃	20 〃
NiO	— 〃	0.06 〃	— 〃
ThO_2	— 〃	2.4 〃	— 〃
CuO	— 〃	— 〃	— 〃
B_2O_3	0.1 〃	0.02 〃	0.5 〃

3) D. H. Peirson, *Brit. J. Appl. Phys.*, 6, 444 (1955).

** It has been confirmed that the gaseous fission products captured in a graphite crystal did not diffuse at room temperature, and the results will be reported in the next article. The activity of fission products can not be recognized in the zinc bromide solution which has been used for the centrifugal separation.

TABLE III. LEACHING OF FISSION PRODUCTS

Conc. of HNO_3 (normality)	Digestion time hr.	120~160 keV. photo peak main nuclide Tc-99m leaching, %	490~580 keV. photo peak main nuclide I-133, La-140 leaching, %	630~720 keV. photo peak main nuclide I-132, Nb-97 leaching, %
Sample A.G. (not heated)				
	1	0.37		
0	2	0.37	0.25	
	4	0.38	0.27	0.31
	1	0.51	0.44	0.44
1	2	0.49	0.51	0.71
	4	0.68	0.51	0.85
	1	0.79	0.36	0.78
5	2	0.85	0.36	0.75
	4	0.97	0.36	0.54
	1	0.81		0.76
10	2	1.33		0.89
	4	1.57	0.36	0.73
Sample N.G.-1 (not heated)				
	1	0.64		
0	2			
	4	0.69		
	1	0.90		
1	2	1.01		
	4	0.88	0.76	
	1	1.26	0.86	
5	2	1.28	0.86	1.71
		1.26	1.15	1.71
	1	1.37	0.96	1.54
10	2	1.37	1.96	2.05
	4	1.39	2.29	2.05
Sample N.G.-2 (not heated)				
	1	2.03	0.52	0.74
0	2	1.90	1.03	
	4	1.90	1.03	
	1	2.33	1.03	
1	2			
	4			
	1			
5	2			
	4	3.71	1.55	1.97
	1	3.88	1.81	
10	2	3.79	1.55	3.94
	4			
Sample N.G.-1 (heated)				
	1	2.19	10.29	1.13
0	2	2.18	8.82	1.35
	4	3.06	6.40	1.58
	1	3.10	11.76	1.35
1	2	3.26	11.76	1.35
	4	3.93	12.94	2.70
	1	3.50	10.59	6.31
5	2	6.70	10.59	6.31
	4	6.53	14.12	8.11
	1	7.16	11.76	9.91
10	2	8.20	11.76	9.91
	4	8.71	9.41	9.01
Sample N.G.-2 (heated)				
	1	5.99	3.80	2.83
0	2	5.65	3.80	2.54
	4	5.54	5.06	2.83
	1	5.04	5.06	2.12
1	2	5.60	6.33	1.41
	4	4.05	3.80	7.76
	1	5.16	7.60	1.70
5	2	7.15	7.60	9.89
	4	8.09	5.06	9.89
	1	8.20	5.06	11.31
10	2	8.65	5.06	11.31
	4	8.87	5.06	14.13

made from petroleum coke, and two kinds of natural graphite. Grain sizes of the samples are shown in Table I and impurities contained in the samples in Table II.

A mixture of 5 g. of graphite and 0.5 g. of uranium dioxide was irradiated for one hour under the same condition mentioned above. The irradiated mixture was transferred into a centrifuging tube with a saturated zinc bromide solution which contained a small amount of hydrochloric acid. After a centrifugal separation, the graphite was washed rapidly with a diluted hydrochloric acid solution. After being dried at 70°C or heated at 1000°C for four hours in an argon gas stream, it was divided into portions of 100 mg. each. They were immersed in 30 ml. nitric acid solution of 0~10 N concentration at 80°C for a period of 1~4 hr. After the immersion, the solution were filtered the filtrates were evaporated to 3 ml.; this volume was suitable for gamma ray spectrometry. The gamma ray spectrum of fission products in filtrates and precipitates was measured by the RCL 256 channel gamma ray spectrometer with a well-type sodium iodide crystal (2 in.×1.75 in. diameter) as scintillator. By comparing the gamma ray spectra of the filtrates with their total spectra (filtrate + precipitate), the leaching of fission products in nitric acid solution was made clear.

Results

Experimental data are summarized in Table III. Based on these data the following results are elucidated.

1) Fission products captured in graphite are leached with difficulty in a nitric acid solution under various conditions of immersion; however, the leaching of all the nuclides is slightly increased with the nitric acid concentration.

2) There is no difference due to varying graphite samples.

3) When the samples were heated at a high temperature, the leaching of fission products increased with acid concentration. For example, 10% of the fission products was leached by 10 N nitric acid solution.

4) However, the fraction of the fission products leached is almost constant regardless of immersion time.

From the results, it is considered that fission products in graphite are very stable toward nitric acid and such stabilities are attributed to a hindrance effect because most fission products are captured in a graphite crystal. It is not yet clearly demonstrated that the leaching is increased with acid concentration when samples are heated at a high temperature.

The authors wish to thank Dr. Kenjiro Kimura for his encouragement.

Division of Chemistry
Japan Atomic Energy
Research Institute
Tokai, Ibaraki-ken
(T. N., S. Y. & K. S.)

Department of Chemistry
Faculty of Science
Kyoto University
Sakyo-ku, Kyoto
(J. O. & D. S.)

The Behavior of Fission Products Captured in Graphite by Nuclear Recoil. II. The Diffusion of Xenon-135 in Graphite at a High Temperature

By Toshio NAKAI, Seishi YAJIMA, Koreyuki SHIBA, Jiro OSUGI and Daisaburo Shinoda

(Received September 22, 1959)

In the previous study[1], it was shown that, when a mixture of uranium dioxide and graphite in a weight ratio of 1 : 30 was irradiated with JRR-1 (Japan Research Reactor-1) neutrons, about 95% of the fission products recoiled out of uranium oxide powder into graphite. The orbital electrons of the recoiled fission fragments are partially stripped, and the initial velocities of fission fragments are about 10^9 cm./sec. It has also been shown that they are highly ionized, bearing ionic charges of 20 or more. Because of this high velocity and the charge, the fission fragments interact readily with matter.

One of the practical problems connected with the operation of a reactor that employs a dispersion type fuel is the determination of the extent of diffusion of radioactive fission products from the fuel pellet when the mixture of graphite and uranium dioxide is pressed to give a density of about 1.8. Since the release of gaseous fission products from the fuel pellet will cause the destruction of the pellet and the radioactive contamination of the coolant and other establishments, it is important to study the behavior of gaseous fission products captured in graphite particles. Likewise the build-up of xenon-135 in a pellet is of some importance because of its abnormally large absorption cross section. In this case continuous elimination of xenon-135 from the pellet through some adequate process should be favorable in relation to the neutron economy of a reactor. Because of these reasons the firm retention and the continuous elimination of gaseous fission products would be of the greatest importance for the dispersion type fuel. Investigators of the North American Aviation Laboratory studied the diffusion of xenon-133 from graphite[2]. When discs of graphite, 0.84 cm. in diameter and 0.064～0.5 cm. in thickness, impregnated with uranium carbide to a concentration of about 520 mg./cc., were heated to 900～1500°C, the leakage rate of xenon varied from approximately 2% per 3 hr. of heating at 900°C to approximately 50% per 3 hr. at 1500°C.

However, an investigation of the state of

1) T. Nakai and S. Yajima, *J. Chem. Soc. Japan, Pure Chem. Sec.* (*Nippon Kagaku Zasshi*), **79**, 1267 (1958).

2) G. A. Cowan and C. J. Orth, *A/CONF.*, 15/p/613 (1958).

TABLE I. ANALYTICAL DATA OF IMPURITIES IN GRAPHITE

Impurity	Natural graphite-1 (N.G.-1)	Natural graphite-2 (N.G.-2)	Natural graphite-3 (N.G.-3)	Artificial graphite (A.G.)	Amorphous carbon (A.C.)
Particle size, micron	1	50	50	30	20
Ash (total)	0.3%	0.6%	0.8%	0.07%	0.1%
SiO_2	220 p.p.m.	2600 p.p.m.	3700 p.p.m.	250 p.p.m.	350 p.p.m.
Al_2O_3	60 〃	2300 〃	3500 〃	210 〃	100 〃
Fe_2O_3	24 〃	250 〃	300 〃	130 〃	250 〃
MgO	24 〃	80 〃	100 〃	15 〃	10 〃
CaO	36 〃	290 〃	300 〃	70 〃	150 〃
V_2O_5	0.12〃	5.5〃	0.5〃	— 〃	50 〃
MnO	— 〃	— 〃	— 〃	— 〃	— 〃
Na_2O	12 〃	15 〃	25 〃	20 〃	35 〃
K_2O	12 〃	17 〃	20 〃	15 〃	30 〃
NiO	0.06〃	— 〃	— 〃	— 〃	— 〃
ThO_2	2.4 〃	— 〃	— 〃	— 〃	— 〃
CuO	— 〃	— 〃	— 〃	— 〃	— 〃
B_2O_3	0.02〃	0.3〃	0.5〃	0.1〃	3 〃

gaseous fission products diffusing from the graphite particles is thought to be worth while. Consequently, the present work has been carried out to study the diffusion, at 400, 800 and 1200°C, of xenon-135 captured in several kinds of graphite powder.

Experimental

Preparation of Samples.—The mixture of 1 g. of graphite and 50 mg. of uranium dioxide was irradiated with thermal neutrons for about one hr. in an experimental hole (thermal neutron flux, about 5×10^{11} neutrons/cm^2 sec.), JRR-1. After irradiation, the mixture was washed with a hot 4 N nitric acid solution in order to dissolve uranium and neptunium, and dried at 70°C. The fission products captured in graphite particles were not leached with a 4 N nitric acid solution within the short time procedure[1]. The fission products in graphite were cooled for twenty hours after irradiation and used for the diffusion experiment. During such a cooling time iodine-135, which is the precursor of xenon-135, decayed sufficiently and the xenon-135 was predominantly built up. The graphite samples used in this experiment are tabulated in Table I.

Determination of the Diffusion of Xenon-135.—For the escape rate of xenon-135 from graphite powder to be determined at a high temperature, graphite samples into which fission products recoiled were heated in a stream of argon. The furnace, in which the heating in argon took place, consisted of a silicon carbide heater and a silica tube. The temperature of the furnace was measured with a platinum, platinum-rhodium thermocouple and controlled with a regulator. In the range 400 to 1200°C, the temperature of the furnace was found to remain constant within 10°C throughout the experiment. Argon gas was purified through sponge titanium at about 700°C and through phosphorous pentoxide to prevent the oxidation of the graphite surface. The flow rate of argon gas was checked with a glass capillary flow meter and maintained at a constant rate. The xenon released from graphite was trapped in a charcoal trap cooled with a dry ice-benzene mixture. At appropriate intervals the trap was replaced by a new one. Xenon-135 activity in the charcoal trap was determined with a gamma ray spectrometer. In this experiment an RCL 256 channel gamma ray scintillation spectrometer with a well-type sodium iodide scintillator (2 in. × 1.75 in. diameter) was used.

The gross gamma ray spectrum of fission products in graphite after twenty hours cooling, of the trapped xenon and of the fission products which remained in graphite after the diffusion run are shown in Fig. 1. The amount of the diffused xenon was determined by comparing the heights of

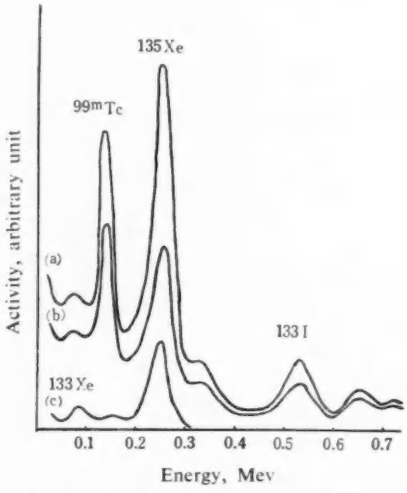

Fig. 1. Gamma-ray spectrum of the fission products in graphite.
(a) Fission products before diffusion.
(b) Fission products remained after diffusion.
(c) Trapped xenon.

the photoelectric peak of xenon-135 of the charcoal trap and of a standard graphite sample of a known weight which was not heat-treated.

Results

As already mentioned, the results were obtained from gamma ray spectra at appropriate time intervals. The photoelectric peak of gamma ray spectra is proportional to the amount of xenon that escaped from graphite. On the other hand, the initial amount of xenon in graphite was obtained from the gross gamma ray spectrum of the standard graphite sample. Therefore, the fraction of xenon which escaped can be calculated as a function of time. The diffusion rates of xenon-135 from the several kinds of graphite at 400, 800 and 1200°C are shown in Figs. 2—4, respectively.

To analyze these diffusion curves the relation between the logarithmic values of the remaining amounts of xenon-135 and the time intervals at 400, 800 and 1200°C was obtained and shown in Figs. 5—7, respectively.

From these figures it is seen that the curves consist of two fractions which are a steep slope

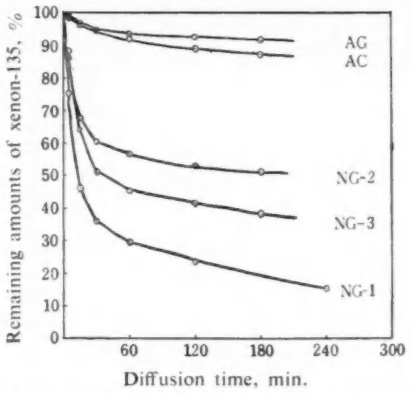

Fig. 4. Diffusion rates of xenon-135 at 1200°C.

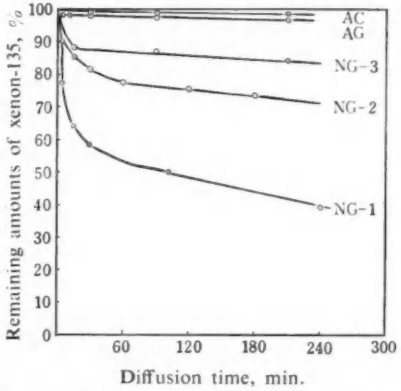

Fig. 2. Diffusion rates of xenon-135 at 400°C.

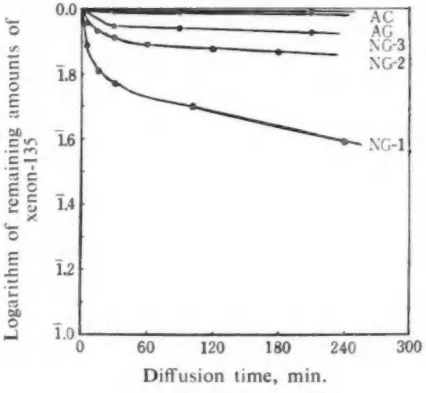

Fig. 5. Results at 400°C.

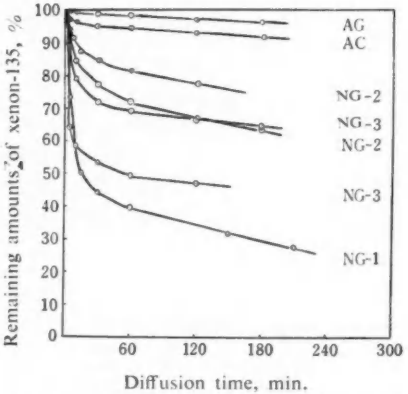

Fig. 3. Diffusion rates of xenon-135 at 800°C.

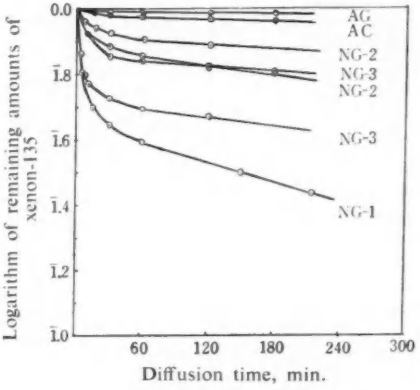

Fig. 6. Results at 800°C.

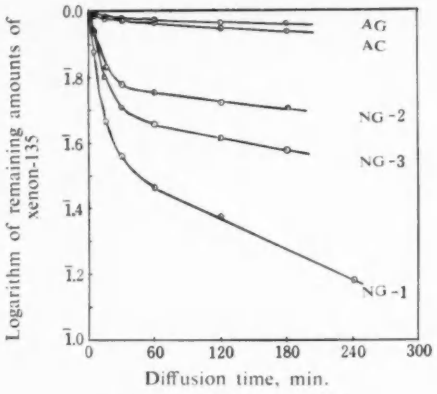

Fig. 7. Results at 1200°C.

curve for one hour and a slow inclination line after one hour. The results show that there are two mechanisms for diffusion in a graphite grain; they are a rapid and a slow diffusion.

The amounts of diffusion of xenon-135 for rapid diffusion are appreciably greater than those for slow diffusion and the amounts vary with the temperature and the kinds of sample. The amounts of diffusion from the natural graphite samples are appreciably greater than those from the artificial graphite or the amorphous carbon samples. The dependency of diffusion amounts on the kinds of sample will be discussed later.

The diffusion rate of a straight line fraction may be used to evaluate a diffusion constant of xenon-135 as shown in the following. In Figs. 5—7 the apparent inclination of a straight line fraction depends on the diffusion constant of xenon-135. Further, from the slope of the linear line for each sample, a diffusion constant is obtained, and they are summarized in Table II. Eq. 1 shows the relation between the diffusion constant and the activation energy, and from this equation the activation energy can be obtained as the inclination of the values of the logarithm of diffusion constants against the reciprocal of the absolute temperatures.

$$D = D_0 \exp\left(-\frac{\Delta H}{RT}\right) \qquad (1)$$

TABLE II. THE ACTIVATION ENERGY OF XENON-135

Sample	Inclination	Activation energy cal./mol.
Natural graphite-1	0.50×10^{3}	2.3×10^{3}
Natural graphite-2	0.50×10^{3}	2.3×10^{3}
Natural graphite-3	0.58×10^{3}	2.7×10^{3}
Artificial graphite	0.51×10^{3}	2.3×10^{3}
Amorphous carbon	1.06×10^{3}	4.9×10^{3}

where D: diffusion constant, D_0: diffusion constant at 0 of absolute temperature degree, R: gas constant, T: absolute temperature degree and H: activation energy.

The apparent activation energy of diffusion calculation from the slow inclination of these straight lines is shown in Table II.

Discussion

If one assumes that xenon diffuses along the interlaminar spaces in a perfect graphite crystal, the activation energy of diffusion can be calculated theoretically. An elementary process of xenon diffusion in graphite is the migration of xenon from position 1 to position 3 through position 2 in Fig. 8. As the activation energy is

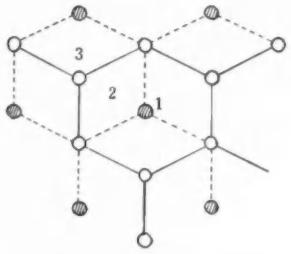

Fig. 8. A pertect graphite crystal.

represented to be the energy difference between position 1 and position 2, the activation energy can be obtained by use of the strain energy of each position. The strain energy is calculated by the interatomic force evaluated from an elastic constant as a specific heat at a low temperature. According to Suzuki[3], the activation energy calculated is about 2000 cal./mol. and is of the same order as the values obtained in this experiment. On the other hand, the calculated activation energy of diffusion across carbon layers is also about 200000 cal./mol. From this high value, the assumption that the diffusion occurs entirely along the interlaminar spaces is justified.

It is well known that graphite, in general, has a small mosaic, particularly in artificial graphite. Dislocation density in graphite is high along the boundary of mosaic structure. Xenon is trapped in trapping centers around a dislocation line rather than a interstitial site in a crystal at room temperature, because it is evident in the present experiment that the activation energy of xenon is fairly small. Therefore, the actual process of diffusion must be discussed with reference to the chemical potential of the trapping centers including the

3) H. Suzuki, private communication.

effect of a stress field as well as the concentration gradient in a sample.

The mosaic size of the graphite samples was determined by the X-ray diffraction method and the electron diffraction method. As a result, the mosaic size of the natural graphite is appreciably larger than those of the artificial graphite and of the amorphous carbon. It is evident that the dislocation density in the region of the mosaic boundary of the natural graphite is appreciably smaller than those of artificial graphite and of amorphous carbon. Therefore, in the case of the natural graphite, xenon-135 which was not captured by the trapping center, diffuses with a high concentration gradient. After that, xenon-135, which was captured by the center is successively released and slowly diffuses along the interlaminar space of a crystal. In this case, because the concentration gradient of xenon-135 in the sample is very small, it is very likely that the gradient is constant, and this warrants the calculation of activation energy.

Since the number of the trapping center of artificial graphite and of amorphous carbon and the amount of xenon-135 which was trapped in the trapping center are greater than those in the case of the natural graphite, the diffusion amounts of a rapid diffusion fraction of the amorphous carbon and the artificial graphite are relatively small.

The diffusion of gaseous fission products of dispersion type fuel will be related to the mosaic size of graphite material. It may be pointed out that, on the basis of the above discussion, the problem of xenon poisoning will be solved.

The authors wish to thank Dr. Kenjiro Kimura for his encouragement.

Division of Chemistry
Japan Atomic Energy
Research Institute
Tokai, Ibaraki-ken
(T. N., S. Y. & K. S.)

Department of Chemistry
Faculty of Science
Kyoto University
Sakyo-ku, Kyoto
(J. O. & D. S.)

Conformation of Biaryls. Dipole Moment Measurements of o-Methylbiphenyls

By Takeo SATO

(Received September 22, 1959)

Since the structure of biphenyl in crystals had been determined by X-ray crystal analysis[1], it was a subject of interest for many workers to elucidate the conformation of substituted biphenyls by using various physical methods. As the result of extensive works on biphenyl derivatives especially halogenobiphenyls, their conformations have been determined under various conditions. By X-ray method planar structure was advanced for 3, 3′-dichlorobenzidine[2] in accordance with the conclusion of Dhar on biphenyl itself, of which the result can be compared with a skew conformation found for 2, 2′-dichlorobenzidine[3]. For the knowledge of the free molecules, electron diffraction investigation was undertaken, and it was reported that the biphenyls without any substituent at position 2 were also non-planar[4,5] as well as 2, 2′-dihalogenobiphenyls[6]. Dipole moment measurements of 2-halogeno-[7,8], 2, 2′-dihalogeno-[7,9] and 3, 3′-dihalogenobiphenyls[9] were also reported and rotated molecular conformations were advanced for each case and the mean angles were calculated. It seemed, however, that the information on the structure of 2, 2′-dialkylbiphenyls were very limited, only two examples were reported, at present. Namely, Hargreaves et al.[10] have reported the X-ray

1) N. R. Dhar, *Indian J. Physics*, **7**, 43 (1932). Cf. J. Hengstenberg and H. Mark, *Z. Krist.*, **70**, 283 (1929); G. L. Clark and L. W. Pickett, *J. Am. Chem. Soc.*, **53**, 167 (1931); N. R. Dhar, *Proc. Nat. Inst. Sci. India*, **15**, 11 (1949).
2) J. Toussaint, *Acta Cryst.*, **1**, 43 (1948).
3) D. L. Smare, ibid., **1**, 150 (1948).
4) J. Karle and L. O. Brockway, *J. Am. Chem. Soc.*, **66**, 1974 (1944).
5) O. Bastiansen, *Acta Chem. Scand.*, **3**, 408 (1949).
6) Idem., ibid., **4**, 926 (1950).
7) G. C. Hampson and A. Weissberger, *J. Am. Chem. Soc.*, **58**, 2111 (1936).
8) A. C. Littlejohn and J. W. Smith, *J. Chem. Soc.*, 2456 (1953).
9) Idem., ibid., 2552 (1954).
10) F. Fowwether and A. Hargreaves, *Acta Cryst.*, **3**, 81 (1950); A. Hargreaves and W. H. Taylor, *J. Sci. Instruments*, **18**, 138 (1941).

crystal analysis of 2,2'-dimethylbenzidine dihydrochloride and found that the compound has a rotated angle of 70.6°. Suzuki[11] has also computed the interplanar angle of biphenyls with methyl groups at position 2 (and 2') based on the ultraviolet absorption spectra and found an angle of 70.5° for 2,2'-dimethylbiphenyl.

While, in the course of synthetic studies of estrogenic biphenyl derivatives, it has been reported that 2,2'-dimethylbiphenyls[12,13] failed to show a conjugation band of biphenyl system in the near ultraviolet region[14-16]. This result was explained by the steric interference of the two methyl groups which forced the benzene nuclei into non-planar arrangement, and the mean angle between the rings was assumed to be nearly perpendicular to each other.

In an effort to verify the above postulation, this communication records the results of the dipole moment measurement and the calculation of the interplanar angle of 2-methyl- and 2,2'-dimethylbiphenyls. Dipole moment of 2,2'-dimethylbiphenyl was reported to be 0.66 D[17]. The value, however, would not be large enough for the safer calculation of the angle, when one considered the small dipole moment found for toluene (0.34 D[18]) and the experimental error of this measurement. Thus for favorable compounds, 5,5'-disubstituted 2,2'-dimethylbiphenyls (II) were prepared from the corresponding iodocompound (I) by the Ullmann reaction. Suitable substituents at the meta positions will increase the moment of the system and alter it markedly according to the rotation around the axis of the biaryl without affecting the steric environment. The method of preparations were described in the *Experimental Part*.

The measurement was carried out for a benzene solution at 25°C. The values found for the dimethylbiphenyls are given in Table I. The moments of benzene component used for the calculations were 1.94 D for *p*-chlorotoluene[19] and 4.52 D for *p*-nitrotoluene[20]. The calculated values for *cis*-planar and perpendicular conformations are given in Table I. As can be seen, the observed values for compound II (X=Cl and NO_2) were essentially the same for the calculated ones for the perpendicular arrangement as long as the rings are coaxial. The present results is in good agreement with the assumption derived from the ultraviolet absorption spectra of 2,2'-dimethylbiphenyls[12,13].

It should, however, be pointed out that the calculated values would be modified in a minor degree by considering the induction effects[8,9,21-23], which comprised the effects already present in the component benzene, the effect of each dipole on the second ring and the moment induced at each dipolar substituent by the presence of the other. These inductive effects will be rather large when the polar groups are located at ortho positions as in the case of 2,2'-disubstituted biphenyls. Thus, the values of the angle for 2,2'-dichlorobiphenyl were 88° when all induction effects were ignored but 69~84° when they were considered[9]. However, as can be easily assumed, both values

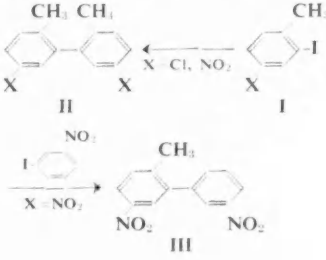

TABLE I. COMPARISON OF OBSERVED[a] WITH CALCULATED DIPOLE MOMENTS FOR 5,5'-DISUBSTITUTED 2,2'-DIMETHYLBIPHENYLS (II) AND 2-METHYL-3',5-DINITROBIPHENYL (III)

Compound	μ, D observed	μ, D, calculated: Rings *cis*-planar	μ, D, calculated: Rings perpendicular	Mean angle between planes of rings
II X=H	0.66[b]			
Cl	2.37	3.36	2.38	90°
NO_2	5.53	7.83	5.54	90°
III	4.55	7.35	5.21	104°

a) Benzene solution, at 25°C. b) See Ref. 17.

11) H. Suzuki, This Bulletin, **27**, 597 (1954).
12) T. Sato, ibid., **32**, 1130 (1959).
13) T. Sato and M. Ōki, ibid., **32**, 1289 (1959).
14) M. Ōki and T. Sato, ibid., **30**, 508 (1957).
15) T. Sato and M. Ōki, ibid., **30**, 859 (1957).
16) Idem, ibid., **30**, 958 (1957).
17) R. J. W. Le Fèvre and H. Vine, *J. Chem. Soc.*, **1938**, 967.
18) C. G. Le Fèvre, R. J. W. Le Fèvre and K. W. Robertson, ibid., 480 (1935).
19) L. Tiganik, *Z. physik. Chem.* **B13**, 425 (1931).
20) G. R. Paranjpe and D. J. Davar, *Indian J. Physics*, **15**, 173 (1941).
21) H. M. Smallwood and K. F. Herzfeld, *J. Am. Chem. Soc.*, **52**, 1919 (1930).
22) F. C. Frank, *Proc. Roy. Soc.*, **A152**, 171 (1935).
23) G. C. Hampson and A. Weissberger, *J. Chem. Soc.*, **1936**, 393.

were essentially the same for 3, 3'-disubstituted biphenyls[9], to which the present series are structurally related.

It is quite natural to consider that the conformation of 2-methylbiphenyl is located somewhat between 2,2'-dimethylbiphenyls (II) and biphenyl without ortho substituent owing to the decrease in steric hindrance given by the ortho substituent compared with compound II. The same measurement was applied to 2-methyl-3', 5-dinitrobiphenyl (III) of which preparation was illustrated in the diagram and described in the *Experimental Part*. For the calculation of the theoretical moment of the system, dipoles moments of nitrobenzene and *p*-nitrotoluene were taken as 3.96[24] and 4.52D[20], respectively.

The observed value, 4.55 D, is smaller than the calculated ones for the conformations in which both rings are in *cis*-planar and perpendicular arrangement. These facts suggest that the molecule takes conformation in which two benzene rings are twisted further from the perpendicular position to *trans*-relationship in respect to two nitro groups. The observed value agreed with the calculated one for the conformation with the rings inclined at an angle of 104°. Therefore, the molecule can be regarded to have a slightly *trans*-arrangement with inclined benzene rings at an angle of 76°. The present result might be compared with the value found for 3, 3'-dinitrobiphenyl, which was reported to have a non-planar structure with an interplanar angle of 106°[9]. The reduction in the rotation angle found in compound III compared with the dimethyl compounds (II) was quite reasonable, but it remained unexplained whether the preferred *trans*-conformation of compound III was given by the steric effect of ortho groups or by the presence of meta substituents.

Experimental[25]

2, 2'-Dimethyl-5, 5'-dinitrobiphenyl (II, X = NO_2).—It was obtained by the Ullmann reaction of 2-iodo-4-nitrotoluene, b. p. 138~140°C/3 mmHg, m. p. 58°C (reported melting point is 58°C[26]) according to the modified method given in the literature[27]. One hundred grams (0.38 mol.) of 2-iodo-4-nitrotoluene and 150 g. of dry clean sand were preheated to 215°C and to this mixture was added with good stirring 100 g. (1.6 atoms) of activated copper bronze during one hour while the temperature was maintained at 215~220°C. It was then heated to 250°C and kept at that temperature for one and a half hour. After the reaction was over the mixture was poured onto dry sand and extracted with ethanol. The extract was recrystallized from acetic acid or acetone for several times with the aid of active charcoal. Pale yellow needles, m. p. 177~178°C, were obtained in a low yield.

5, 5'-Dichloro-2, 2'-dimethylbiphenyl (II, X = Cl).—Sixteen grams (0.063 mol.) of 4-chloro-2-iodotoluene, b. p. 108~109°C/10 mmHg, n^{19} 1.6231 obtained from 4-chloro-2-toluidine[28] according to Wroblewski[29] or from 2-iodo-4-toluidine[30] by Sandmeyer reaction was heated at 240~250°C with stirring and 20 g. (0.32 atom) of activated copper bronze was added over a period of one hour. The reaction mixture was then heated and kept at 280~290°C for forty minutes. It was extracted with acetone and the extract was distilled to give an oil which boiled first at 140~155°C/4 mmHg, and then at 142~144°C/3 mmHg., n^{20} 1.5961 on redistillation. Yield was 4 g. or 50% of the theory.

Found: C, 66.75; H, 4.74. Calcd. for $C_{14}H_{12}Cl_2$: C, 66.95; H, 4.82%.

2-Methyl-3', 5-dinitrobiphenyl (III).—Under good stirring 15 g. (0.24 atom) of activated copper bronze was added to a mixture of 21 g. (0.080 mol.) of 2-iodo-4-nitrotoluene and 7.5 g. (0.030 mol.) of *m*-nitroiodobenzene in the course of thirty minutes, while the temperature was kept at 220~230°C. It was then heated to 240~250°C and kept for additional thirty minutes at that temperature. After the reaction was over, the mixture was extracted with acetone and the solution was treated with active charcoal. The solvent was evaporated and the remainder was recrystallized from ethanol for several times. Compound III was obtained as pale yellow plates, m. p. 145~146°C.

Found: N, 10.70. Calcd. for $C_{13}H_{10}O_4N_2$: N, 10.85%.

When the above reaction was conducted with an equimolar amount of iodo compounds the main product was found to be 3, 3'-dinitrobiphenyl.

The author wishes to express his hearty thanks to Drs. T. Chiba and T. Shimozawa, the University of Tokyo, for carrying out the measurements. The author's thanks are also due to Professors K. Hata, Tokyo Metropolitan University, and M. Ōki, the University of Tokyo, for their continued interest throughout this study.

Department of Chemistry
Faculty of Science
Tokyo Metropolitan University
Setagaya, Tokyo

24) R. Davis, H. S. Bridge and W. J. Svirbely, *J. Am. Chem. Soc.*, 65, 857 (1943).
25) All boiling and melting points are uncorrected. The author wishes to thank Mr. T. Mizushima for microanalyse and Mr. M. Fujii for preparations of the materials.
26) C. Willgerodt and B. R. Kok, *Ber.*, 41, 2077 (1908).
27) R. Pummerer, H. Puttfarcken and P. Schöpflocher, ibid., 58, 1808 (1925).
28) H. Goldschmidt and M. Hönig, ibid., 19, 2438 (1886).
29) E. Wroblewski, *Ann.*, 168, 147 (1873).
30) B. H. Nicolet and R. B. Sandin, *J. Am. Chem. Soc.*, 49, 1806 (1927).

Expansion of Nakano's Results on High Frequency Titration Using the Resistance-type Instrument

By Sadaharu TOYODA

(Received March 25, 1959)

There have been many papers[1-7] on high frequency titration. Many interesting results have been shown by Nakano's paper[8] on this subject. It was based on an experiment using the resistance-type instrument[9]. According to the experimental results of Figs. 2 and 4, which have been obtained by Nakano, the relation between the value of variable resistance, consisting of platinum wire and mercury column, and the concentration of solution shows a minimum point in a case of the condenser-type instrument, and minimum and maximum points in a case of the coil-type instrument. Nakano proved that there exists a relation $\omega C_0 R = 1$, at the minimum point for both cases of condenser-type and coil-type instruments. These results and others have been obtained by using the equivalent circuit without the variable resistance which makes a component of the resistance-type instrument. It is, therefore, significant to see if much more accurate results are obtained by using the equivalent circuit with the variable resistance. The present paper is concerned with the results of the calculation of the equivalent circuit containing the variable resistance.

Calculation for Condenser-type Instrument

Fig. 1 shows the equivalent circuit for the components of the portion containing the sample solution (refer to Fig. 7a). This equivalent circuit is the same as the one in Nakano's paper[5] except R_1 referring to the variable resistance of the platinum wire. Therefore, the physical meaning of C, C_0, R and L are omitted. If Z denotes the impedance for the condenser

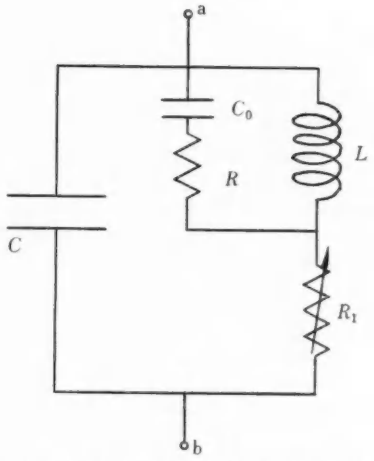

Fig. 1. Equivalent circuit for condenser-type.

element (C_0, R) and the coil (L), the following relation is obtained.

$$\frac{1}{Z}=\frac{(\omega C_0)^2 R}{1+(\omega C_0 R)^2}+\boldsymbol{j}\left\{\frac{\omega C_0}{1+(\omega C_0 R)^2}-\frac{1}{\omega L}\right\} \tag{1}$$

The total admittance between point a and point b in Fig. 1 is written as

$$Y=\boldsymbol{j}\omega C+\frac{1}{Z+R_1} \tag{2}$$

Putting the following expressions for the real and the imaginary parts of $1/Z$

$$A\equiv\frac{(\omega C_0)^2 R}{1+(\omega C_0 R)^2} \qquad B\equiv\frac{\omega C_0}{1+(\omega C_0 R)^2}-\frac{1}{\omega L} \tag{3}$$

and for those of Z

$$Z=\frac{A}{A^2+B^2}-\boldsymbol{j}\frac{B}{A^2+B^2}\equiv U-\boldsymbol{j}V \tag{4}$$

the real and imaginary parts of Y can be separated as follows:

$$Y_{\text{real}}=\frac{U+R_1}{(U+R_1)^2+V^2} \tag{5}$$

$$Y_{\text{imag}}=\frac{V}{(U+R_1)^2+V^2}+\omega C \tag{6}$$

1) W. J. Blaedel and H. V. Malmstadt, *Anal. Chem.*, **22**, 734 (1950).
2) K. Anderson, E. S. Bettis and D. Revinson, ibid., **22**, 743 (1950).
3) P. W. West, T. S. Burkhalter and L. Broussard, ibid., **22**, 469 (1950).
4) C. N. Reilley and W. H. McCurdy, Jr., ibid., **25**, 86 (1953).
5) S. Fujiwara and S. Hayashi, ibid., **26**, 239 (1954); S. Fujiwara and S. Hayashi, *J. Chem. Soc. Japan, Pure Chem. Sec.* (*Nippon Kagaku Zasshi*), **74**, 171 (1953).
6) K. Nakano, ibid., 74, 172 (1953).
7) T. Yano, S. Musya, T. Wada and T. Hino, *Chem. Eng.* (*Kagaku Kôgaku*), **20**, 339 (1956).
8) K. Nakano, *J. Chem. Soc. Japan, Pure Chem. Sec.* (*Nippon Kagaku Zasshi*), **75**, 776 (1954).
9) K. Nakano, ibid., **74**, 227 (1953); K. Nakano, R. Hara and K. Yashiro, *Anal. Chem.*, **26**, 636 (1954).

The frequency of oscillation is determined by the assumption that the imaginary part of Y is equal to zero as in the previous paper[8]. Substituting this condition into Eq. 5, one finds

$$(A^2+B^2)R_1=-\frac{Y_{\text{real}}}{\omega C}B-A \tag{7}$$

On the other hand, the change of plate current takes place by putting the beaker containing the aqueous solution into the condenser-type electrode or the coil. In the previous experiment the change of plate current is compensated by adjusting R_1. This manipulation suggests that the value of Y_{real} is kept constant. In the special case when the beaker is empty ($R=\infty$) the values of A and B are 0 and $-1/\omega_\infty L$, respectively. Applying these values to Eq. 7, Y_{real} is obtained as follows:

$$Y_{\text{real}}=R_{1\infty}\frac{C}{L} \tag{8}$$

where $R_{1\infty}$ and ω_∞ denote the variable resistance and the angular frequency in the special case, respectively. Thus Eq. 7 becomes

$$(A^2+B^2)R_1=-\frac{R_{1\infty}}{\omega L}B-A \tag{9}$$

Substituting the above equation into $Y_{\text{imag}}=0$, the following relation between ω and R will be easily obtained:

$$\omega C=-B\frac{1+(A/B)^2}{1+(R_{1\infty}/\omega L)^2} \tag{10}$$

Of course, both Eqs. 9 and 10 should be used simultaneously in order to find how R_1 and ω change with the concentration of solution.

The distributed capacity between the electrode and the solution, C_0, is determined by using the boundary conditions when the beaker is empty or full of the mercury as in the case of Nakano's experiment. From Eq. 10, one obtains

$$\begin{cases}\dfrac{1}{\omega_\infty^2 L}=C\left\{1+\left(\dfrac{R_{1\infty}}{\omega_\infty L}\right)^2\right\}\\[2ex] \dfrac{1}{\omega_0^2 L}=C\left\{1+\left(\dfrac{R_{1\infty}}{\omega_0 L}\right)^2\right\}+C_0\end{cases} \tag{11}$$

where ω_∞ and ω_0 are the angular frequency when $R=\infty$ and $R=0$, respectively, and $R_{1\infty}\approx 10\ \Omega$. Hence, the distributed capacity, C_0, is calculated by the following expression:

$$C_0\fallingdotseq\frac{1}{\omega_0^2 L}-\frac{1}{\omega_\infty^2 L} \tag{12}$$

which means the same as the method shown in the previous paper[8]. Referring to Table I, of course, it is clear that the following term can be neglected, if $R_{1\infty}$ is 100 Ω and C is 60 $\mu\mu$F:

$$C\left(\frac{R_{1\infty}}{\omega_0 L}\right)^2-\left(\frac{R_{1\infty}}{\omega_\infty L}\right)^2<0.012\ \mu\mu\text{F} \tag{13}$$

Thus the average value of C_0 is 2.3 $\mu\mu$F.

Eq. 9 can be rearranged as follows:

$$\left\{1-\frac{2\omega^2LC_0}{1+(\omega C_0R)^2}+\frac{(\omega^2LC_0)^2}{1+(\omega C_0R)^2}\right\}R_1 =R_{1\infty}\left\{1-\frac{\omega^2LC_0}{1+(\omega C_0R)^2} -\frac{\omega C_0R}{1+(\omega C_0R)^2}\frac{\omega C_0\omega^2L^2}{R_{1\infty}}\right\} \tag{14}$$

Since the variation of frequency is fairly small as shown by the experiment[10], the frequency can be taken as constant. With this assumption, one differentiates Eq. 14 with respect to R, then puts it equal to zero, and finally obtains the condition which gives the minimum point of R_1

$$R\fallingdotseq\left(1-\alpha+\frac{\alpha}{\beta}\right)\frac{1}{\omega C_0} \tag{15}$$

where $\alpha\equiv\omega^2LC_0$ and $\beta\equiv\omega C_0\omega^2L^2/R_{1\infty}$.

Neglecting α and α/β which are much smaller than unity according to Table II, one obtains the condition, $\omega C_0R=1$, which is the conclusion of the previous paper[8]. The depth of R_1 at minimum point predominantly depends upon the third term in the right-hand side of Eq. 14. Substituting the condition, $\omega C_0R=1$, into the third term, it becomes $\beta/2$. Then, the following results can be easily found. (a) Using the same coil, the depth of R_1 at minimum point increases with the increase of frequency. (b) Using the same frequency, which is approximately determined by the expression, $\omega^2LC=1$, the depth increases with the increase of L/C. (c) Even though the same frequency is used, the concentration of aqueous solution at the minimum point varies with the salts in solution.

Investigating the results of Fig. 2 in detail, it is noticed that R_1 of curve 9 or 10 is a little larger than $R_{1\infty}$ when the concentration increases.

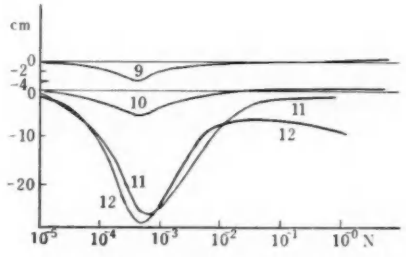

Fig. 2. Relation (Ref. 8) between change of length (resistance) of platinum wire and concentration of salt in aqueous solution for condenser-type.
9, 10, 11 : Ammonium nitrate solution.
12 : Sodium chloride solution.

10) K. Nakano, private communication.

TABLE I

Nos. of turn of coil	Material in beaker	Freq. Kc	$\omega_\infty^2/\omega_0^2$	$100^2/\omega_\infty^2L^2$ $100^2/\omega_0^2L^2$	$10^{12}/\omega_\infty^2L$ $10^{12}/\omega_0^2L$	C_0 p
100 ($L=4.3\times10^{-4}$H)	air	1050	4.35×10^{13}	1.24×10^{-3}	53.4_4	2.1_1
	mercury	1030	4.19 〃	1.29 〃	$55\cdot5_3$	
70 ($L=2.9\times10^{-4}$H)	air	1280	6.47 〃	1.84 〃	53.3_1	2.6_1
	mercury	1250	6.17 〃	1.93 〃	55.9_2	
40 ($L=1.3\times10^{-4}$H)	air	1872	1.38×10^{14}	4.28 〃	55.6_2	2.2_6
	mercury	1835	1.33 〃	4.45 〃	57.8_9	

TABLE II

No. of curve	Salt	Nos. of turn of coil	L henry	Freq. cycle	ω	α	α/β	$\omega C_0\omega^2L^2/2\times10$
9	NH_4NO_3	100	4.3×10^{-4}	1.12×10^6	7.037×10^6	4.90×10^{-2}	3.30×10^{-3}	7.40
10	〃	40	1.3×10^{-4}	1.27 〃	7.979 〃	1.90 〃	9.64 〃	0.986
11	〃	40	〃	1.88 〃	1.181 〃	4.17 〃	6.51 〃	3.20
12	NaCl	70	2.9×10^{-4}	1.26 〃	7.916 〃	4.18 〃	4.35 〃	4.79

This fact is attributed to the second term in the left-hand side of Eq. 14, though the right-hand side of Eq. 14 contains half the value of the same term. It is very desirable to calculate the value of R_1 at the minimum point, which is nearly equal to $R_{1\infty}(1-\beta/2)$. According to Table II, however, they should have a negative value except in the case of curve 10 and this is hard to be explained. Therefore, it is necessary to examine the equivalent circuit again more in detail and the results will be discussed later.

Calculation for Coil-type Instrument

Fig. 3 is considered as the equivalent circuit for the coil-type instrument (refer to Fig. 7b). This equivalent circuit except when including R_1 is the same as the one in the previous paper[8] which contains the element KLR showing the effect of eddy current. According to the same consideration of the equivalent circuit, the following results may be obtained:

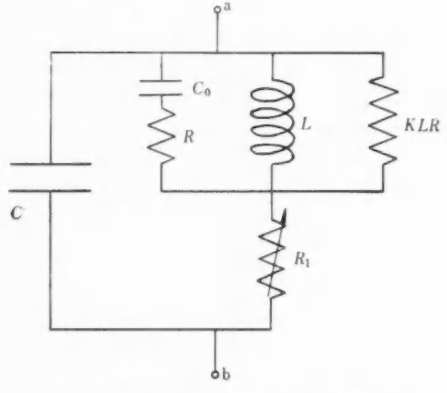

Fig. 3. Equivalent circuit for coil-type.

$$\frac{1}{Z}=\left\{\frac{(\omega C_0)^2R}{1+(\omega C_0R)^2}+\frac{1}{KLR}\right\}+\boldsymbol{j}\left\{\frac{\omega C_0}{1+(\omega C_0R)^2}-\frac{1}{\omega L}\right\}\equiv A+\boldsymbol{j}B \tag{16}$$

$$(A^2+B^2)R_1=-\frac{R_{1\infty}}{\omega L}B-A \tag{17}$$

$$\omega C=-B\frac{1+(A/B)^2}{1+(R_{1\infty}/\omega L)^2} \tag{18}$$

As it is rather difficult to determine the distributed capacity of coil, C_0, by these relations, the value shown in the previous paper[8] will be used in the following discussions.

As mentioned above, the change of frequency is expected to be caused by the change of R. But it is neglected, as the change of frequency was experimentally[10] found to be not so large. After the rearrangement of Eq. 17, it is written as

$$\left\{1-\frac{2\omega^2LC_0}{1+(\omega C_0R)^2}+\left(\frac{\omega L}{KLR}\right)^2+\frac{(\omega^2LC_0)^2(1+2/KL)}{1+(\omega C_0R)^2}\right\}R_1=R_{1\infty}\left\{1-\frac{\omega^2LC_0}{1+(\omega C_0R)^2}-\frac{\omega C_0R}{1+(\omega C_0R)^2}\frac{\omega C_0\omega^2L^2}{R_{1\infty}}-\frac{1}{KLR}\frac{\omega^2L^2}{R_{1\infty}}\right\} \tag{19}$$

As the first order approximation, the following expression to show the behaviors of all curves for the coil-type instrument is obtained:

$$R_1=R_{1\infty}\left\{1-\frac{\omega C_0R}{1+(\omega C_0R)^2}\frac{\omega C_0\omega^2L^2}{R_{1\infty}}-\frac{1}{KLR}\frac{\omega^2L^2}{R_{1\infty}}\right\} \tag{20}$$

The conditions which give the minimum and the maximum points are the same as the one

TABLE III

No. of curve	Nos. of turn of coil	Freq. cycle	ω	C_0 p	α	$\frac{\omega C_0\omega^2L^2}{2\times10}$
2	40	1.45×10^6	9.111×10^6	0.0665	7.18×10^{-4}	0.0425
3	70	〃	〃	0.126	3.03×10^{-3}	0.401
4	100	1.46×10^6	9.173×10^6	0.50	1.81×10^{-2}	3.57
5	100	7.575×10^5	4.759 〃	〃	4.87×10^{-3}	0.498
6	70	9.05 〃	5.686 〃	0.126	1.18×10^{-3}	0.0973
7	40	1.40×10^6	8.796 〃	0.0665	6.69×10^{-4}	0.0382

in the previous paper[8]

$$R=\frac{1}{\omega C_0}\sqrt{\frac{KL-2\pm\sqrt{(KL-2)^2-4(KL+1)}}{2(KL+1)}} \tag{21}$$

where positive and negative signs show minimum and maximum, respectively.

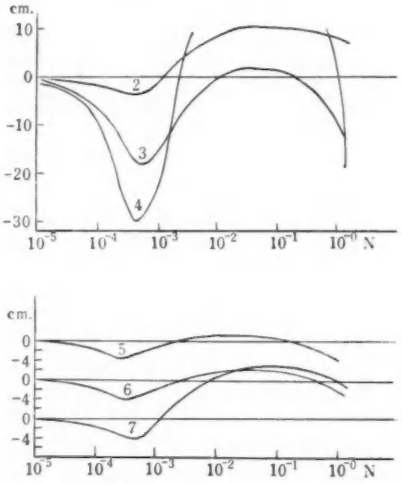

Fig. 4. Relation (Ref. 8) between change of length (resistance) of platinum wire and concentration of sodium chloride in aqueous solution for coil-type.

Investigating the curve in Fig. 4, it is noticed that the maximum value of R_1 is larger than the initial value $R_{1\infty}$. This fact should be ascribed to the second terms of the two sides in Eq. 19. But the value of $\alpha(\equiv\omega^2LC_0)$ in Table III is too small for this conclusion. In Table III the values of $\beta/2$ $(\equiv\omega C_0\omega^2L^2/2R_{1\infty})$ which cause the minimum points are smaller than unity except in the case of curve 4.

Re-examination of Equivalent Circuit

It is difficult to understand, for the condenser-type and the coil-type instruments, why the value of $\beta/2$ is greater than unity. The question arises, thus, whether the resistance value of platinum wire at high frequency would be much greater than the value at direct current or not. Even if only the coil-type is taken up, it is difficult to consider that the value at about one megacycle becomes greater than four times the value at direct current. Now, let us consider the loss of coil itself. Assuming that the low resistance, R_l, is connected in series with the inductance of the coil, L, the equivalent circuit for the coil-type instrument becomes Fig. 5, in

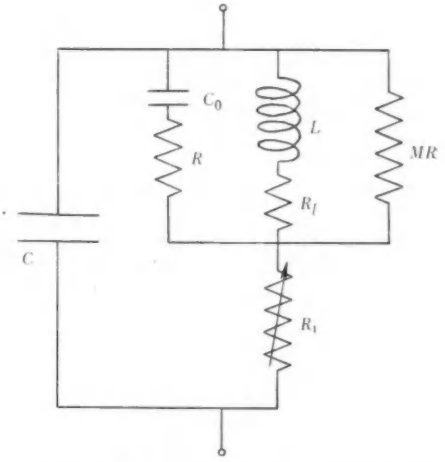

Fig. 5. Equivalent circuit with low resistance showing loss of coil.

which notation, M, means KL. The equivalent circuit for the condenser-type instrument is easily obtained by setting $M=\infty$. Repeating the calculation as before, one obtains

$$\frac{1}{Z}=\left\{\frac{(\omega C_0)^2R}{1+(\omega C_0R)^2}+\frac{R_l}{(\omega L)^2+R_l^2}+\frac{1}{MR}\right\}+j\left\{\frac{\omega C_0}{1+(\omega C_0R)^2}-\frac{\omega L}{(\omega L)^2+R_l^2}\right\}\equiv A+jB \tag{22}$$

$$(A^2+B^2)R_1=-\frac{Y_{real}}{\omega C}B-A \tag{23}$$

$$\omega C=-B\frac{1+(A/B)^2}{1+(Y_{real}/\omega C)^2} \tag{24}$$

where

$$Y_{\text{real}}=\frac{C}{L}(R_{1\infty}+R_l)$$

After the rearrangement, Eq. 23 is written as follows:

$$\left\{1-\frac{2\alpha}{1+x^2}+\frac{2\alpha xQ^{-1}}{1+x^2}+\frac{2\alpha Q^{-1}}{Mx}+\frac{\alpha^2(1+Q^{-2})}{(Mx)^2}+\frac{\alpha^2(1+Q^{-2})(1+2/M)}{1+x^2}\right\}R_1$$
$$=R_{1\infty}\left\{1-\frac{\alpha(1+Q^{-2})(R_{1\infty}+R_l)}{(1+x^2)R_{1\infty}}-\frac{x}{1+x^2}\frac{\omega C_0(\omega L)^2(1+Q^{-2})}{R_{1\infty}}-\frac{\omega C_0(\omega L)^2(1+Q^{-2})}{MxR_{1\infty}}\right\} \quad (25)$$

where $x\equiv\omega C_0R$, $\alpha\equiv\omega^2LC_0$ and $Q^{-1}\equiv R_l/\omega L$.

In Eq. 25, the term which gives the minimum value for the resistance R_1 is the same as the one in Eq. 19 except for the factor, $1+Q^{-2}$, being greater than unity. Therefore, it seems impossible in this procedure to find that the term in question has a value smaller than unity.

Now, Fig. 6 is considered instead of Fig. 5. In Eq. 19, substituting as follows $R_1\to R_1+R_l$, $R_{1\infty}\to R_{1\infty}+R_l$, the following equation is obtained:

$$\left\{1-\frac{2\omega^2LC_0}{1+(\omega C_0R)^2}+\left(\frac{\omega L}{MR}\right)^2+\frac{(\omega^2LC_0)^2(1+2/M)}{1+(\omega C_0R)^2}\right\}(R_1+R_l)$$
$$=(R_{1\infty}+R_l)\left\{1-\frac{\omega^2LC_0}{1+(\omega C_0R)^2}-\frac{\omega C_0R}{1+(\omega C_0R)^2}\frac{\omega C_0\omega^2L^2}{(R_{1\infty}+R_l)}-\frac{\omega^2L^2}{MR(R_{1\infty}+R_l)}\right\} \quad (26)$$

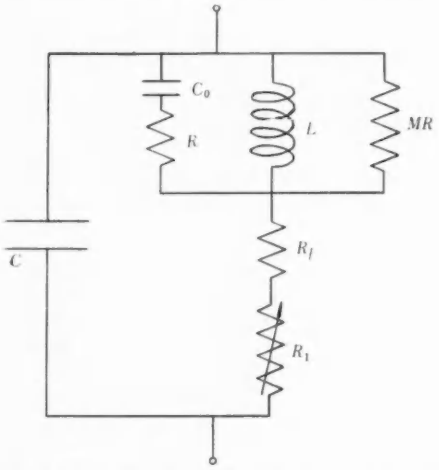

Fig. 6. Another equivalent circuit with low resistance showing loss of coil.

The Q of the coil shows $\omega L/R_l$ and then R_l is calculated from Q at the corresponding frequency. Two cases[10] are considered for the Q of the coil. One of them is to measure only the coil, and the other case is to measure the coil containing distilled water. The former should be considered for the condenser-type instrument, whereas the latter for the coil-type instrument with the assumption that the loss by distilled water is contained in $Q(=\omega L/R_l)$. In Table IV the values of the terms in question for the coil-type instrument are less than unity. The resistance value of platinum wire is 0.2 Ω/cm. and $M\approx10^3$ as shown in the previous paper[5]. The calculated values of the depth at minimum point agree with the experimental values in the case of curves 3 and 6 in Table IV. But the values of curves 4 and 5 are too great in comparison with the experimental ones, though the values of curves 2 and 7 are not discussed.

The calculated values for the condenser-type instrument are shown in Table V. In this case, the values of the terms in question become smaller than the previous value, but some of them are still greater than unity. Therefore, this equivalent circuit seems not to be useful

TABLE IV

No. of curve	ωL	Q*	R_l	$\frac{\omega C_0\omega^2L^2}{2(R_{1\infty}+R_l)}$	Depth** of curve Ω	cm.	Exp. value
2	1186	68.0	17.4	0.0155	−0.415	−2.07	−4.0
3	2642	77.5	34.1	0.0908	−3.95	−19.7	−18.5
4	3944	91.5	43.1	0.672	−35.7	−179	−31
5	2046	119.5	17.1	0.184	−4.94	−24.7	−3.5
6	1648	88.0	18.7	0.0339	−0.956	−4.78	−4.0
7	1143	68.0	16.8	0.0143	−0.374	−1.87	−4.5

* According to K. Nakano[10]

** $(R_1)_{\min}-R_{1\infty}\fallingdotseq(R_{1\infty}+R_l)\left\{\frac{\alpha}{2}-\frac{\omega C_0\omega^2L^2}{2(R_{1\infty}+R_l)}\right\}/(1-\alpha)$

for the calculation of the depth of the condenser-type instrument, though Q is the value of the coil without the condenser-type electrode.

TABLE V

No. of curve	ωL	Q*	R_l	$\frac{\omega C_0 \omega^2 L^2}{2(R_{1\infty}-R_l)}$
9	3026	112.8	26.8	2.01
10	1037	71.5	14.5	0.403
11	1535	67.8	22.6	0.982
12	2296	88	26.1	1.33

* According to K. Nakano[10]

The calculation on high frequency titration has been extended on the basis of Nakano's paper[8]. As a result of calculation, the relation between the variable resistance, R_1, and the high frequency resistance, R, having some connection with the concentration of solution becomes clear in some degree, including the condition, $\omega C_0 R = 1$. The term $\omega^2 L C_0/1+(\omega C_0 R)^2$, seems to cause the fact that R_1 becomes greater than $R_{1\infty}$ in the case of concentrated solution. Some of the calculated values of depth at minimum point are considerably great in comparison with the experimental one in the case of the coil-type instrument and can not be obtained in the case of the condenser-type instrument. Hence, it seems necessary to take into account another factor in the calculation of the equivalent circuit in order to obtain better agreement with the experimental results.

The sample solution in the condenser-type electrode or the coil has the capacitance together with the resistance as shown in Nakano's paper[8]. The former was omitted in Nakano's paper, under the assumption that the effect of the former is negligible when the value of the latter is not so great. Now, let us consider the equivalent circuit (Fig. 8) on the basis of Figs. 7a and 7b. This equivalent circuit is of the same physical meaning as in the case of Fig. 5 except in the case of the capacitance, $\varepsilon' C_1$, C_2, which are visualized by Figs. 7a and 7b, where the notation ε' means the dielectric constant (real part) of the sample solution. As mentioned above, the sample solution in the condenser-type electrode or the coil has the capacitance, which is shown by the notation $\varepsilon' C_1$ in Figs. 7a or 7b (and Fig. 8) instead of C_1 in Nakano's paper. The notation C_2 shows the rest of the capacitance of the condenser-type electrode in Fig. 7a and the rest of the self capacitance of the coil in Fig. 7b, which has also been shown by C_3 in the recent paper[11].

Again one repeats the similar calculation of this equivalent circuit containing another factor $\varepsilon' C_1$ and C_2. As a result of calculation, the following equation is easily obtained:

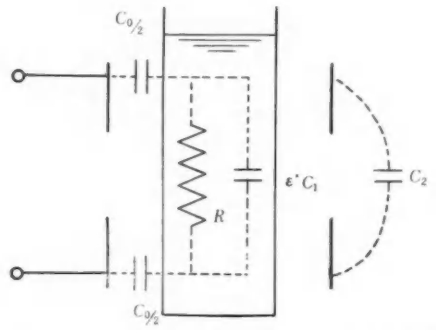

Fig. 7 (a). Relation between sample solution in condenser-type electrode and equivalent circuit.

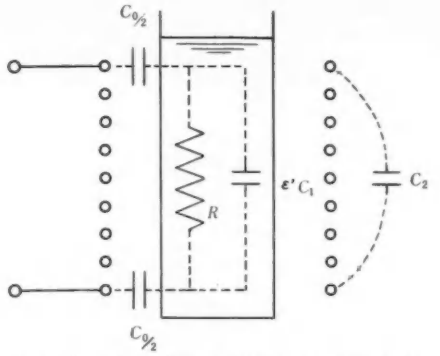

Fig. 7 (b). Relation between sample solution in coil and equivalent circuit.

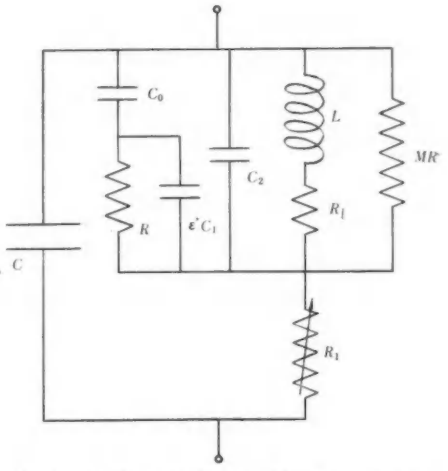

Fig. 8. Equivalent circuit taking into account another factor.

11) P. F. Knewstubb and T. M. Sugden, *Trans. Faraday Soc.*, **54**, 372 (1958).

$$\frac{1}{Z}=\left\{\frac{(\omega C_0)^2R}{1+\omega^2(\varepsilon'C_1+C_0)^2R^2}+\frac{R_l}{R_l^2+(\omega L)^2}+\frac{1}{MR}\right\}$$
$$+j\left[\frac{\omega C_0\{1+\omega^2\varepsilon'C_1(\varepsilon'C_1+C_0)R^2\}}{1+\omega^2(\varepsilon'C_1+C_0)^2R^2}\right.$$
$$\left.+\omega C_2-\frac{\omega L}{R_l^2+(\omega L)^2}\right]\equiv A+jB \qquad (27)$$

$$(A^2+B^2)R_1=-\frac{Y_{\text{real}}}{\omega C}B-A \qquad (28)$$

$$\omega C=-B\frac{1+(A/B)^2}{1+(Y_{\text{real}}/\omega C)^2} \qquad (29)$$

$$Y_{\text{real}}=\frac{C}{L}\frac{\{1-2\alpha_\infty+\alpha^2_\infty(1+Q^{-2}_{\infty 1})\}R_{1\infty}+R_l}{1-\alpha_\infty(1+Q^{-2}_{\infty 1})} \qquad (30)$$

where $Q_{\infty 1}\equiv\omega_{\infty 1}L/R_l$, $\alpha_\infty\equiv\omega^2_{\infty 1}L\left(C_2+\dfrac{C_0C_1}{C_1+C_0}\right)$, $\omega_{\infty 1}$ and $R_{1\infty}$ are the angular frequency ω and the variable resistance R_1, when $R=\infty$ and $\varepsilon'=1$, respectively. After the rearrangement of Eq. 28, it is written as the following expression corresponding to Eq. 25:

$$\left[1-2\alpha_2+\alpha_2^2(1+Q^{-2})-\frac{2\alpha(1+qx^2)}{1+x^2}\right.$$
$$+\frac{2\alpha pxQ^{-1}}{1+x^2}$$
$$+\frac{2\alpha\{\alpha_2(1+qx^2)+p\omega L/M_0\}(1+Q^{-2})}{1+x^2}$$
$$+\frac{\alpha^2(1+Q^{-2})\{(px)^2+(1+qx^2)^2\}}{(1+x^2)^2}$$
$$\left.+\frac{2Q^{-1}\omega L}{M_0x}+\left(\frac{\omega L}{M_0x}\right)^2(1+Q^{-2})\right]R_1$$
$$=\frac{\xi R_{1\infty}+\eta_l R_l}{1-\eta}\left[1-\frac{\xi R_{1\infty}+R_l}{\xi R_{1\infty}+\eta_l R_l}\left\{\alpha_2+\frac{\alpha(1+qx^2)}{1+x^2}\right\}\right.$$
$$\left.\times(1+Q^{-2})-\left(\frac{\alpha px\omega L}{1+x^2}+\frac{\omega^2L^2}{M_0x}\right)\frac{(1+Q^{-2})(1-\eta)}{\xi R_{1\infty}+\eta_l R_l}\right] \qquad (31)$$

where

$$x\equiv\omega(\varepsilon'C_1+C_0)R,\ Q\equiv\omega L/R_l,$$
$$M_0\equiv M/\omega(\varepsilon'C_1+C_0)$$
$$p\equiv\frac{C_0}{\varepsilon'C_1+C_0},\quad q\equiv\frac{\varepsilon'C_1}{\varepsilon'C_1+C_0}$$
$$\alpha\equiv\omega^2LC_0\qquad\alpha_2\equiv\omega^2LC_2$$
$$\xi\equiv1-2\alpha_\infty+\alpha^2_\infty(1+Q^{-2}_{\infty 1}),\ \eta_l\equiv\alpha_\infty(1+Q^{-2}_{\infty 1})$$

Thus, the term in question becomes

$$\frac{\alpha px\omega L}{1+x^2}\frac{1+Q^{-2}}{R_{1\infty}} \qquad (32)$$

assuming that ξ and η_l are approximately equal to unity and zero, respectively. It seems that the condition giving the minimum point is almost entirely determined by this term taking the rest into account. This term contains the significant factor p, which contains $\varepsilon'C_1$ and C_0, as compared to the corresponding term in Eq. 25. The capacitance of the sample solution, $\varepsilon'C_1$, will be comparable to or larger than C_0, when the sample solution is an aqueous solution which has a large value of dielectric constant, though C_1 is considerably smaller than C_0. Thus, it is possible to find the possibility that the factor p has a value somewhat smaller than unity, since the capacitance of the sample solution, $\varepsilon'C_1$, can not be neglected in comparison with the capacitance C_0. It seems likely that the consideration of the factor, $\varepsilon'C_1$, is helpful for the solution of the problem being discussed in this paper.

The author desires to thank Dr. K. Nakano for his support and advice. His numerous suggestions and interest have contributed much to this investigation. The author also desires to thank Dr. H. Honda for his kind encouragement throughout the investigation.

Shigengijutsu-Shikenjo
Resources Research Institute
Kawaguchi-shi, Saitama

Vapor Phase Oxidation of Methyl Naphthalenes[1]

By Shigeru MORITA

(Received September 23, 1959)

In 1916, Wohl[2] and Gibbs & Conover[3] discovered that, in the presence of vanadium pentoxide, naphthalene is oxidized to phthalic anhydride at 350 to 550°C. The ever-increasing demand for phthalic anhydride has in recent years stimulated the search for alternative raw materials. A patent claim was made that phthalic anhydride appears in the products of the catalytic air oxidation of methyl naphthalenes and phenanthrene. Methyl naphthalene oil[4] (a mixture of methyl naphthalene isomers, naphthalene and others) gave phthalic anhydride in the yield of 50~60%, but both pure 1- and 2-methyl naphthalenes[5] produced it in 30~40%. This yield is very low, in comparison with that from naphthalene (60~80%)[6]. The cause has not been studied. Reaction heat from methyl naphthalenes to phthalic anhydride is 605 kcal./mol. and is larger than that from naphthalene (450 kcal./mol.). Some investigators[7] accordingly proposed that the catalyst zone was superheated and phthalic anhydride once produced was decomposed, and the yield was lowered as a consequence.

The author studied the reaction mechanism of the vapor phase oxidation of methyl naphthalenes and related compounds and clarified the cause of the low yield.

Experimental

Apparatus.—It is the same as that reported before[8].

Experimental Conditions.—The air rate was 150 l. per hour, the feed rate 1.5 g. per hour; the range of reaction temperatures was 350~500°C, and the catalyst volume was 50 ml.

The method of preparing the catalyst[8] was also reported before (V_2O_5-MoO_3-pumice stone).

The physical constants of reactants are listed in Table I.

Results and Discussion

Vapor Phase Oxidation of Methyl Benzenes.—Methyl naphthalenes have two benzene rings condensed, whereas phthalic anhydride has one. Therefore, in order for methyl naphthalenes to produce phthalic anhydride by vapor phase oxidation, one of the two benzene rings of methyl

TABLE I. PHYSICAL CONSTANTS OF MATERIAL USED FOR VAPOR PHASE OXIDATION

Materials	°C	°C
Naphthalene	m.p. 80.3	
1-Methyl naphthalene	f.p. −32.0	b.p. 245.0
2-Methyl naphthalene	m.p. 32.0	b.p. 241.6
o-Xylene	f.p. −26	b.p. 143~144
1, 2, 3-Trimethyl benzene	f.p. −19.8	b.p. 173.4~174.5
1, 2, 4-Trimethyl benzene	b.p. 168.0~168.5	d_4^{20} 0.8755
1, 2, 4-Benzene-tricarboxylic acid	b.p. 216~217	
Naphthalene-1-carboxylic acid	m.p. 160.5	
Naphthalene-2-carboxylic acid	m.p. 183.5~184.0	
Tetralone	$b.p._{13}$ 127	d_4^{20} 1.092
2-Methyl-1, 4-naphthoquinone	m.p. 34.2	
2, 6-Dimethyl naphthalene	m.p. 109.5~110.0	
2, 7-Dimethyl naphthalene	m.p. 95.5~96.5	
Dimethyl naphthalene oil	b.p. 260~268	
Acenaphthene	m.p. 94.5	

1) This is a summary of reports published in *J. Chem. Soc. Japan, Pure Chem. Sec.* (*Nippon Kagaku Zasshi*), **80**, 509, 514 (1959).
2) A. Wohl, Ger. Pat., 379,882 (Sep. 4, 1916).
3) H. D. Gibbs and C. Conover, Brit. Pat., 119,518 (Oct. 1, 1918).
4) J. Shelmerdine et al., *J. Appl. Chem.*, **3**, 513 (1953); T. Yatagai, *J. Japan. Tar Ind. Assoc.* (*Coal Tar*), **9**, 648, (1957).
5) R. Norris et al., *Ind. Eng. Chem.*, **35**, 279 (1943); C. R. Kinney et al., ibid., **43**, 3880 (1951).
6) L. F. Marek and D. A. Hahn, "The Catalytic Oxidation of Organic Compound in the Vapor Phase", American Chemical Society Monograph No. 61., Chemical Catalog Co., New York (1932), p. 404.
7) H. Sasayama, *J. Chem. Soc. Japan, Ind. Chem. Sec.* (*Kogyo Kagaku Zasshi*), **46**, 1225 (1943).
8) S. Morita, This Bulletin, **33**, 309 (1960); O. Hibino and S. Morita, *J. Chem. Soc. Japan, Pure Chem. Sec.* (*Nippon Kagaku Zasshi*), **78**, 1766 (1957).

TABLE II. VAPOR PHASE OXIDATION OF METHYL BENZENES AND THE RELATED COMPOUNDS

Materials	Reaction temp. °C	Products: Phthalic anhydride mol. %	Maleic anhydride mol. %	Benzene tricarboxylic acid	Material unreacted
o-Xylene	400	66	7	0	0
1, 2, 3-Trimethyl benzene	400	0	3	trace	0
1, 2, 4-Trimethyl benzene	400	0	3	trace	0
1, 2, 4-Benzene-tricarboxylic acid	400	0	5	0	0

naphthalenes has to be cleaved to form benzene containing two side chains, followed by oxidation to the acid. The author studied the behavior of the side chains of the benzene ring during the vapor phase oxidation.

Toluene, *o*-xylene, 1, 2, 3- and 1, 2, 4-trimethyl benzenes were oxidized in vapor phase under the same conditions mentioned earlier. The results are listed in Table II.

As shown in Table II, phthalic anhydride was produced from *o*-xylene, and benzoic acid from toluene. Therefore, it is apparent that the methyl group is oxidized to carboxylic acid before the benzene ring is cleaved. Sasayama[9] reported that oxidation of trimethyl benzene proceeded stepwise as follows:

trimethyl benzene → benzene-tricarboxylic acid → phthalic anhydride → benzoic acid → benzene → maleic anhydride.

The results obtained by the author showed that both 1, 2, 3- and 1, 2, 4-trimethyl benzenes, on vapor phase oxidation, gave maleic anhydride (in 3% yield) and carbon dioxide, accompanied by very small amounts of 1, 2, 3- and 1, 2, 4-benzene-tricarboxylic acids, respectively, but gave neither phthalic anhydride nor benzoic acid. Furthermore, 1, 2, 4-benzene-tricarboxylic acid gave no phthalic anhydride, but only maleic, anhydride (in 5% yield) and carbon dioxide and no unreacted material was found. The yield of maleic anhydride in this case was comparable with that from 1, 2, 4-trimethyl benzene; therefore, benzene-tricarboxylic acid was presumably formed as an intermediate in the oxidative degradation of trimethyl benzene. However, decarboxylation of the extra carbonyl group did not ensue and the benzene ring was cleaved by the oxidation to form maleic anhydride and carbon dioxide.

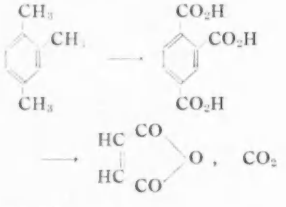

9) H. Sasayama, *J. Chem. Soc. Japan, Ind. Chem. Sec.* (*Kogyo Kagaku Zasshi*), **56**, 281 (1953).

Vapor Phase Oxidation of Methyl Naphthalenes and their Related Compounds.—The mechanism[10] of the vapor phase oxidation of naphthalene is described as follows:

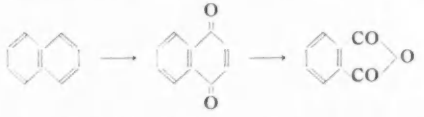

Meanwhile, Pongratz[11] proposed the following route:

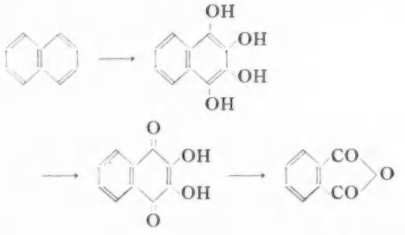

In either case, a carbon-hydrogen bond in one of two benzene rings is broken and a new carbon-oxygen bond is formed in its place, and then the benzene ring containing oxygen is cleaved.

Two benzene rings of naphthalene are equivalent reaction-wise but those of methyl naphthalenes are not, due to the presence of the methyl group in one ring.

Pongratz[11] studied the vapor phase oxidation of chloro-, nitro-, and hydroxy-naphthalenes and found that both 1- and 2-chloronaphthalenes produced phthalic anhydride and monochlorophthalic anhydride. These results show that chlorinated as well as unsubstituted benzene rings were cleaved, but he also obtained phthalic anhydride from 1, 5-dichloronaphthalene and concluded that dechlorination took place during the oxidation.

So far, no report has been made on the mechanism of vapor phase oxidation of methyl naphthalenes. The author examined four conceivable mechanisms (**a**, **b**, **c** and **d**) of vapor phase oxidation of methyl naphthalenes.

Mechanism ***a***.—Kato[12] and coworkers obtained naphthalene-carboxylic acids in 86% yield

10) C. R. Downs, *J. Soc. Chem. Ind.*, **46**, 383 T(1927).
11) A. Pongratz, *Angew. Chem.*, **54**, 22 (1941).
12) S. Kato et al., "Abstracts of the 11th Annual Meeting of Chem. Soc. Japan", Tokyo (1958), p. 18.

by heating methyl naphthalenes to 250°C with an aqueous solution of sodium dichromate in an autoclave. Pickering[13] et al. obtained the acid by oxidation of alkyl naphthalene with barium permanganate. In the same manner, in the vapor phase methyl naphthalene would first be oxidized to naphthalene-carboxylic acid, and then phthalic anhydride is produced as follows:

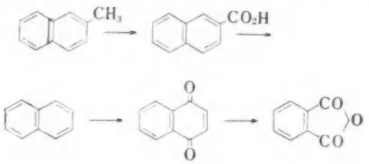

or

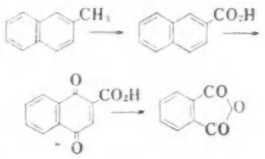

Mechanism ***b***.—Madison[14] obtained naphthalene by one-hour pyrolysis of 1- or 2-methyl naphthalene at 475°C, whereas Kynaston[15] obtained the same compound by passing acenaphthene with steam over a catalyst such as zinc oxide, chromium oxide or alumina. In the same way, methyl naphthalene would produce naphthalene by demethylation as an initial step and naphthalene would then be oxidized to phthalic anhydride:

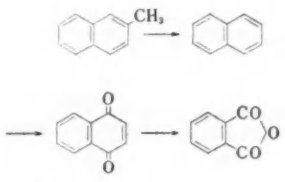

Mechanism ***c***.—Unsubstituted benzene ring (I) of methyl naphthalene would be oxidized and produce phthalic anhydride with the concomitant decarboxylation of one of the three carboxyl groups.

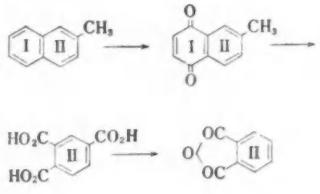

Mechanism ***d***.—Benzene ring bearing the methyl group would be cleaved by oxidation and produce phthalic anhydride:

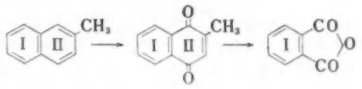

The author will discuss these four mechanisms.

On mechanism ***a***.—2-Methyl naphthalene was catalytically oxidized in the vapor phase under the same conditions at 350°C and the product contained 2-methyl-1, 4-naphthoquinone (identified as 2, 4-dinitrophenyl-hydrazone; m.p. 274°C uncor., no depression in mixed m.p.) but no naphthalene carboxylic acid. This result agrees with that obtained by Fieser[16].

Since decarboxylation is assumed in this mechanism, the possible occurrence of decarboxylation was examined. Naphthalene-1- or 2-carboxylic acid was passed through a reaction tube filled with pumice stone containing no vanadium pentoxide under the same conditions as in vapor phase oxidation (temperature, feed rate and air rate). The product did not contain naphthalene at all. In the same way, the acids were passed through the oxidation catalyst zone with a stream of carbon dioxide instead of air under the same conditions, but naphthalene was not obtained. Therefore, decarboxylation does not occur in the oxidation of naphthalene-carboxylic acid. This result is similar to the one obtained in the case of benzene-tricarboxylic acid.

From these results, it is supposed that mechanism **a** is incorrect.

On mechanism ***b***.—In order to check the assumption of demethylation, the following reaction was performed: methyl naphthalene was passed through a pumice stone zone with air or through an oxidation catalyst zone with carbon dioxide instead of air under the same conditions as in the vapor phase oxidation (temperature, feed rate and gas rate).

The products were carefully distilled, but naphthalene was not found. The density and refractive index of the product were identical with those of the starting material.

Madison's experiment[14] showed the formation of naphthalene from methyl naphthalenes but the heating period in his case was more than one hour. In vapor phase oxidation, the contact time was less than one second, and it is assumed that naphthalene was not formed in such a short time.

13) G. B. Pickering et al., *Rec. trav. chim.* **69**, 535 (1950); *Chem. Abstr.*, **44**, 838 (1950).
14) J. J. Madison et al., *Ind. Eng. Chem.*, **50**, 237 (1958).
15) W. Kynaston, *J. Soc. Chem. Ind.*, **68**, 225 (1949).
16) L. F. Fieser, *J. Am. Chem. Soc.*, **75**, 4377 (1953).

TABLE III. VAPOR PHASE OXIDATION OF METHYL NAPHTHALENES AND THEIR RELATED COMPOUNDS

Materials	Reaction temp. °C	Products: Phthalic anhydride mol. %	Maleic anhydride mol. %	Benzene tricarboxylic acid	Others	Material unreacted
Naphthalene	450	68	7	0	—	0
1-Methyl naphthalene	400	26	4	trace	a)	0
2-Methyl naphthalene	450	42	6	trace	b)	0
Naphthalene-1-carboxylic acid	400	27	21	—	—	4
Naphthalene-2-carboxylic acid	400	36	16	—	—	2
Tetralone	400	62	8	0	—	0
2-Methyl-1, 4-naphthoquinone	400	65	8	0	—	0
7-Methyl tetralone	400	0	3	trace	—	0

a) Trace of quinones
b) Trace of 2-methyl-1, 4-naphthoquinone

On mechanism **c**.—If the oxidation proceeds according to mechanism **c**, 1, 2, 4-benzene-tricarboxylic acid must produce phthalic anhydride. Consequently mechanism **c** is unlikely. To ascertain this conclusion, 7-methyl tetralone and tetralone were catalytically oxidized in the vapor phase under the same conditions. Tetralone produced phthalic anhydride in the same yield as that from naphthalene, but 7-methyl tetralone did not (Table III). The hydrogenated benzene ring of tetralone has an oxygen atom, and, on oxidation, this ring must have been cleaved in order to form phathalic anhydride. If the reaction proceeds similarly in the case of 7-methyl tetralone, the hydrogenated ring containing oxygen would be cleaved. This is the same course which 2-methyl naphthalene follows when it is oxidized through mechanism **c**.

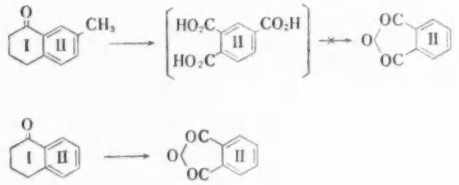

The oxidation products of 2-methyl naphthalene and 7-methyl tetralone caught in the hot part of an air condenser (collector of product) contained a trace of 1, 2, 4-benzene-tricarboxylic acid, which was identified by its melting point and neutralization equivalent. Thus, it is obvious that the benzene ring of methyl naphthalenes having no methyl group was cleaved, but no phthalic anhydride was produced.

On mechanism **d**.—If the benzene ring (II) of methyl naphthalenes having the methyl group is cleaved first and the resulting benzene ring (I) containing two side chains is oxidized, phthalic anhydride would be produced in the same way as from *o*-xylene. The benzene ring (II) of 2-methyl-1, 4-naphthoquinone which has a methyl group, contains two oxygen atoms. Therefore, by catalytic vapor phase oxidation, the benzene ring (II) is cleaved and the reaction follows only mechanism **d**.

The experiment showed that 2-methyl-1, 4-naphthoquinone produced phthalic anhydride in the yield of 65% which is the same as that obtained in the case of naphthalene and *o*-xylene. Accordingly, it is obvious that methyl naphthalenes produce phthalic anhydride only when it is oxidized through mechanism **d**.

From these experimental results it is seen that methyl naphthalenes do not produce phthalic anhydride by mechanism **c** but produce it in 60~70% yield by mechanism **d**.

The yield of phthalic anhydride obtained from methyl naphthalenes is about 30~40% by the catalyst used in these experiments (V_2O_5–MoO_3-pumice), German catalyst (V_2O_5–K_2SO_4–silica gel) or American catalyst (V_2O_5–alumina) and is about one half of that from naphthalene. It is conceivable that both reactions through mechanism **c** and **d** occur simultaneously to the same extent, as the presence of a trace of benzene-tricarboxylic acid was confirmed in the products.

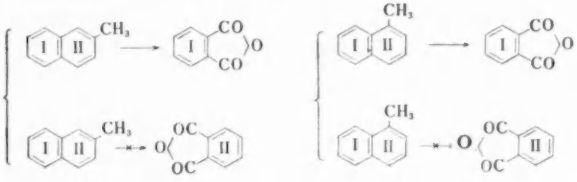

TABLE IV. VAPOR PHASE OXIDATION OF DIMETHYL NAPHTHALENES AND OTHERS

Materials	Reaction temp. °C	Products			
		Phthalic anhydride mol. %	Maleic anhydride mol. %	Naphthalic anhydride mol. %	Benzene tricarboxylic acid
2, 6-Dimethyl naphthalene	450	0	18	0	trace
2, 7-Dimethyl naphthalene	450	0	20	0	trace
Acenaphthene	450	0	14	39	0
Dimethyl naphthalene oil	400	15	8	0	trace
2, 3-Dimethyl naphthalene[a]	375	43	7	0	—

a) This result was obtained by Kinney et al. (V_2O_5–K_2SO_4–silica gel).

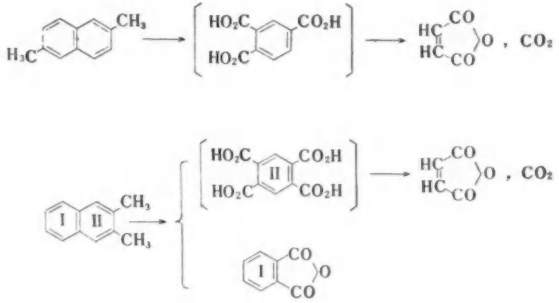

If it is desired to produce phthalic anhydride in high yield from methyl naphthalenes, it is necessary to find the catalyst that is capable of cleaving only the benzene ring of methyl naphthalenes which have a methyl group.

Vapor Phase Oxidation of Dimethyl Naphthalenes and Others.—Kinney[5] and coworkers obtained phthalic anhydride from 2, 3-dimethyl naphthalene in yields of 43% and 28% by the American and the German catalysts, respectively. Furthermore they obtained the anhydride in a 30% yield from a fraction (boiling in the 235～270°C range) of coal tar.

The author oxidized 2, 6- and 2, 7-dimethyl naphthalenes and obtained no phthalic anhydride but maleic anhydride in yields of 18 and 20%, respectively, and very small amounts of benzenetricarboxylic acid. He also obtained phthalic anhydride in a 15% yield by vapor phase oxidation of dimethyl naphthalene oil (boiling range, 260～268°C) of coal tar (Table IV).

Each of the two benzene rings of 2, 6-dimethyl naphthalene has one methyl group. Therefore, when either of them is cleaved by the oxidation, the resulting benzene ring has three side chains, and no phthalic anhydride would result according to the above-mentioned mechanism **c**. This conclusion agrees with the experimental results.

In the case of 2, 3-dimethyl naphthalene, one (II) of the two benzene rings has two methyl groups, and the other (I) has none. Therefore, when the benzene ring (II) which has two methyl groups is cleaved by vapor phase oxidation, phthalic anhydride would be produced by mechanism **d**, but when a benzene ring having no methyl group is cleaved, no phthalic anhydride would be produced by mechanism **c**. This conclusion agrees with the experimental results obtained by Kinney et al.

Acenaphthene is the compound that has an ethylidene group connecting positions 1 and 8 of naphthalene. Therefore, it is not conceivable that phthalic anhydride is formed. The author obtained naphthalic and maleic anhydrides but no phthalic anhydride.

From all the experiments mentioned above, it is concluded that the stability of rings and substituents against vapor phase oxidation in the decreasing order is as follows:

benzene ring > methyl group
> naphthalene ring > ethylidene group

The author is particularly indebted to Professor S. Kimura of Kyoto University, Dr. T. Yoshida, Superintendent of Tobata Chemical Works, and Mr. O. Hibino, Manager of Laboratory Department of the Yawata Chemical Industry Co., Ltd.

Tobata Works
Yawata Chemical Industry Co., Ltd.
Yawata-shi, Fukuoka

*The Nitrogen Isotopic Equilibrium between Ammonia and Ammonium Ion**

By Tatsujiro ISHIMORI

(Received September 21, 1959)

A number of studies have been reported on the enrichment of ^{15}N with the isotopic exchange reaction between ammonia gas and aqueous ammonium ion. The fractionation factor for this exchange reaction has been reported[1-3]. A separation of nitrogen isotopes has been made by the use of cation exchange resins[4]. One of the equilibria involved in the separation process is the equilibrium of nitrogen isotopes between ammonia and ammonium ion in aqueous solution. This paper is a report on the investigation of the equilibrium by the use of cation exchanger. The equilibrium constants and enthalpy of the reaction have been measured. It is found that the use of ion exchanger will be useful to study such an equilibrium existing in aqueous solution. Further, the measurement of the equilibrium of nitrogen isotopes between ammonia gas and ammonium ion of its solid chloride has been carried out and is described in this paper.

In an aqueous solution of ammonia and ammonium ion at isotopic equilibrium with the ammonium ion adsorbed on a cation exchange resin, the equilibria involved are described by the equations:

$$^{15}NH_{3(aq)} + {}^{14}NH_{4(aq)}^{+} = {}^{14}NH_{3(aq)} + {}^{15}NH_{4(aq)}^{+} \qquad K_1 \quad (1)$$

$$^{15}NH_4R + {}^{15}NH_{4(aq)}^{+} = {}^{15}NH_4R + {}^{14}NH_{4(aq)}^{+} \qquad K_2 \quad (2)$$

$$^{14}NH_4R + {}^{15}NH_{3(R)} = {}^{15}NH_4R + {}^{14}NH_{3(R)} \quad (3)$$

$$^{15}NH_{3(aq)} + {}^{14}NH_{3(R)} = {}^{14}NH_{3(aq)} + {}^{15}NH_{3(R)} \quad (4)$$

where NH_4R represents ammonium ion taken up into the cation exchanger phase by ion-exchange mechanism and $NH_{3(R)}$ ammonia adsorbed on an ion exchange resin. Equilibria 3 and 4 can be neglected in a solution of low pH, while they exist with the solution of high pH. However, the concentration of $NH_{3(R)}$ is small compared to that of NH_4R when the concentration of $NH_{3(aq)}$ is low. The amount of $NH_{3(R)}$ is also smaller than that of $NH_{3(aq)}$ if the volume of the exchanger is smaller than that of the solution. Thus, the fractionation factor between the exchanger and solution phase may not greatly involve the contribution by $NH_{3(R)}$. Further, the equation

$$^{14}NH_4R + {}^{15}NH_{3(aq)} = {}^{15}NH_4R + {}^{14}NH_{3(aq)} \quad (5)$$

which is the sum of Eqs. 3 and 4, results also from Eqs. 1 and 2. Hence, Eqs. 1 and 2 are enough to represent the equilibria involved in the system of an aqueous solution of ammonia and ammonium ion, and an exchanger of ammonium ion form.

The following quantity can be measured conveniently:

$$\frac{(^{15}N/^{14}N)_{solution} - (^{15}N/^{14}N)_{exchanger}}{(^{15}N/^{14}N)_{exchanger}} = \delta \quad (6)$$

where $(^{15}N/^{14}N)_{exchanger}$ and $(^{15}N/^{14}N)_{solution}$ are the nitrogen isotope ratios in the exchanger and solution phase, respectively. The fractionation factor between the exchanger and solution phase is defined as follows:

$$K = \frac{(^{15}N/^{14}N)_{exchanger}}{(^{15}N/^{14}N)_{solution}} = \frac{1}{1+\delta} \quad (7)$$

This value can be obtained experimentally. Let the following concentrations be represented by the associated symbols:

$$(^{15}NH_{3(aq)}) = a', \ (^{15}NH_{4(aq)}^{+}) = b', \ (^{15}NH_4R) = c'$$

$$(^{14}NH_{3(aq)}) = a, \ (^{14}NH_{4(aq)}^{+}) = b, \ (^{14}NH_4R) = c$$

Then, the following relationship between K_1, K_2 and K can be readily derived:

$$\frac{1}{K} = \frac{a}{a+b}\left[\frac{1}{K_1K_2} + \frac{b}{aK_2}\right] \quad (8)$$

The value of $a/(a+b)$ and b/a can be calculated from the dissociation constants of ammonia and water: K_{dis} and K_w; if the pH value of the solution is known:

$$\frac{b}{a} \simeq \frac{b+b'}{a+a'} = \frac{K_{dis}}{K_w}(H^+) \quad (9)$$

$$\frac{a}{a+b} \simeq \frac{1}{1+\frac{K_{dis}}{K_w}(H^+)} \quad (10)$$

* This study has been done in the Chemistry Department of the University of Arkansas, Arkansas, U. S. A.

1) H. G. Thode, R. L. Graham and J. A. Ziegler, *Can. J. Research*, **B23**, 40 (1945).

2) E. W. Becker and H. Baumgartel, *Z. Naturforsch.*, **1**, 514 (1946).

3) I. Kirshenbaum, J. S. Smith, T. Crowell, J. Graff and R. McKee, *J. Chem. Phys.*, **15**, 440 (1947).

4) F. H. Spedding, J. E. Powell and H. J. Svec, *J. Am. Chem. Soc.*, **77**, 6125 (1955).

It is assumed that $a \simeq a+a'$ and $b \simeq b+b'$ are held since nitrogen with natural isotopic abundance is used and the ^{15}N content is about 0.36%[5]. The numerical value of K_{dis}/K_w is 1.04×10^9 at 30°C[6].

If the pH of the solution phase is less than 5, the concentration of $NH_{3(aq)}$ is negligibly small. Hence,

$$K = K_2 \qquad (11)$$

for the low pH. The value of K_1 can be calculated from Eq. 8, using the values of K_2, K and pH value.

If the value of K is measured at high pH, the concentration of ammonium ion is very low: $b \ll a$. Hence, Eq. 8 can be written as

$$K_1 = K/K_2 \qquad (12)$$

for the value of K at high pH of the solution. This relation gives approximately the value of K_1. Spedding, Powell and Svec[4] have evaluated the fractionation factor, K, in the above-mentioned condition.

Experimental

The ammonia solution was purified by distillation. The other chemicals were of analytical grade. The cation exchange resin used was Dowex 50, X-8.

The conventional water bath for a constant temperature was used. The temperature was controlled within ±0.2°C at the vicinity of the room temperature. The air bath was used to keep the elevated temperatures constant at 200°C to 275°C within ±2°C.

The mass spectrometer used was a Nier type, 60° sector, double collecter instrument designed to measure small differences in isotopic ratio as described by McKinney et al.[7] and Dole[8]. Measurements were made on the ions of mass 28 and 29 ($^{14}N^{14}N^+$ and $^{15}N^{14}N^+$). The result of each isotopic analysis is estimated to have a precision of ±0.0003 in the quantity of δ.

A solution of ammonium chloride and ammonia was added to the cation exchange resin of the ammonium ion form. This mixture was allowed to stand for ten to twelve hours in the constant temperature bath with shaking and brought to isotopic equilibrium. Then, the solution phase was pipetted and acidified with sulfuric acid solution. The resin was separated from the solution by suction filtration. In each experiment, the solution or resin phase contained one to two milligram equivalents of nitrogen. Ammonium ion was converted to nitrogen gas by the oxidation with sodium hypobromite[9]. The resulting nitrogen gas was purified by repeatedly passing the gas over copper oxide at 800°C and through the liquid air[10]. A set of nitrogen gases from the solution and resin phase was analyzed with a mass spectrometer.

The isotopic equilibrium between gaseous ammonia and solid ammonium chloride was measured. The containing vessel was made of Pyrex glass and had two 200 ml. bulbs (Bulbs A and B). A vacuum stopcock (Stopcock 1) connected Bulbs A and B. On the opposite side of Stopcock 1, Bulb A had a well to insert a thermometer and Bulb B had another vacuum stopcock (Stopcock 2). The silicon grease used in the stopcocks was satisfactory at 200 to 275°C. Water vapor and gaseous ammonia were added, at 20 to 25 mmHg and 200 to 275 mmHg, respectively, to 50 to 100 mg. ammonium chloride in Bulb A and allowed to stand for 13 to 62 hr.

It was difficult to know whether or not isotopic equilibrium had been established. The equilibrium was considered to be established if the equilibrium constant did not increase with a longer period of standing at the same temperature. The vapor pressure of ammonium chloride is 117 mmHg at 275°C and 6 mmHg at 200°C[10]. Extra gaseous ammonia was added to get a large enough sample of gas phase for analysis. Water vapor was added to help isotopic equilibrium to be established[11].

After the establishment of isotopic equilibrium, the gas phase was collected in the evacuated Bulb B through Stopcock 1. The stopcock was turned through the window of the air bath. The vessel was taken out of the air bath and cooled with water. A sufficient amount of sulfuric acid was introduced into Bulb B through Stopcock 2 and gaseous ammonia was collected as ammonium ion in aqueous solution. Bulb A was disconnected and the ammonia gas in it was evacuated and replaced with air. Then, the solid ammonium chloride was dissolved with water.

Experimental Results

The experimental fractionation factors between resin and the solution phase are listed in Table I with the pH values of the solution phases. The value of K_1 is calculated by Eq. 8 using the values of the experimental fractionation

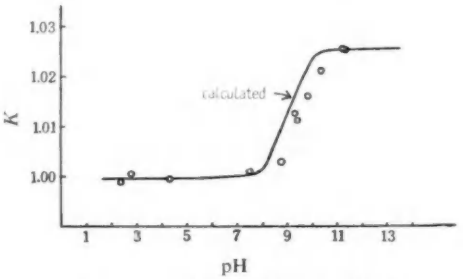

Fig. 1. Fractionation factor and pH.

5) K. T. Bainbridge and A. O. Nier, *Natl. Research Council (U. S.) Prelim. Rept.* 9, (1950).
6) W. M. Latimer, "Oxidation Potential", Prentice-Hall, Inc., New York (1953), Chaps. 3 and 7.
7) C. R. McKinney, J. M. McCrea, S. Epstein, H. A. Allen and H. C. Urey, *Rev. Sci. Instr.*, **21**, 724 (1950).
8) M. Dole, *Chem. Revs.*, **51**, 263 (1952).
9) D. Rittenberg, "Preparation and Measurement of Isotopic Tracers", Edwards Bros., Ann Arbor, Michigan (1947), p. 31.
10) T. C. Hoering, *Science*, **122**, 1233.
11) W. H. Rodebush and J. C. Michalek, *J. Am. Chem. Soc.*, **51**, 752 (1929).

TABLE I. EFFECT OF pH OF THE SOLUTION PHASE ON THE FRACTIONATION FACTOR BETWEEN THE RESIN AND SOLUTION PHASE, K, AT 30°C

Run	pH	Concentration of solution ($NH_3+NH_4^+$) mol./l.	Fractionation factor K
1	11.3	0.496	1.0255
2	11.3	0.496	1.0250
3	11.2	0.196	1.0257
4	11.2	0.196	1.0253
5	10.3	0.196	1.0210
6	10.3	0.196	1.0208
7	9.76	0.496	1.0163
8	9.76	0.496	1.0156
9	9.72	0.496	1.0160
10	9.34	0.196	1.0112
11	9.28	0.516	1.0125
12	8.66	0.516	1.0029
13	7.47	0.196	1.0010
14	7.46	0.196	1.0010
15	4.30	0.483	0.9997
16	2.75	0.196	1.0007
17	2.72	0.196	0.9997
18	2.35	0.196	0.9992
19	2.34	0.196	0.9992
20	1.17	0.516	0.9999

TABLE II. EFFECT OF THE CONCENTRATION OF THE SOLUTION ON THE FRACTIONATION FACTOR BETWEEN RESIN AND SOLUTION PHASE AT 30°C

Run	pH	Concentration of solution ($NH_3+NH_4^+$) mol./l.	Fractionation factor K
15	4.30	0.483	0.9997
21	4.40	0.0966	1.0000
22	5.40	0.0097	1.0000
23	basic	3.23	1.0279
24	basic	1.29	1.0269
25	basic	0.515	1.0265
26	basic	0.208	1.0257

"basic" shows that pH value is larger than 11.2.

factor of Run 1 to 4:

$$K_1 = 1.0256 \pm 0.0006 \text{ at } 30°C$$

The error shown is the average deviation. The fractionation factors of Run 1 to 20 are plotted against their pH values of the solution phase in Fig. 1, on which the calculated line is drawn by Eq. 8 using the K_1 and K_2 obtained.

The effects of the concentration of the solution phase are shown in Table II.

The effects of temperature on the fractionation factor between the resin and solution phase are shown in Table III. The equilibrium constants, K_1, are calculated by Eq. 12 with the fractionation factors at the solution of low pH value,

TABLE III. EFFECT OF TEMPERATURE ON THE FRACTIONATION FACTOR BETWEEN RESIN AND SOLUTION PHASE, K

T°C	Acidic solution (pH less than 6) $(NH_{4(aq)}^+)=0.107$ M			Basic solution (pH=11.2) $(NH_{3(aq)})=0.196$ M		
	Run	$\delta\times1000$	K	Run	$\delta\times1000$	K
50	27	0		32	−21.9	
	28	−0.5	1.0002	33	−21.9	1.0224
40	29	0	1.0000	34	−22.3	
				35	−23.1	1.0232
30	*		0.9997	36	−24.7	
				37	−25.0	1.0255
0.2	30	−0.8		38	−25.0	
	31	+0.3	1.0003	39	−25.8	
				40	−25.2	1.0260

* Average of Run 15 to 20 in Table I.

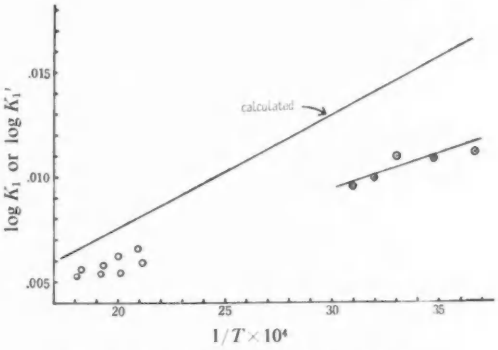

Fig. 2. Equilibrium constant and $1/T$.
○ Represents the equilibrium constant measured for the exchange reaction between gaseous ammonia and solid ammonium chloride.
◉ Represents the average value of the equilibrium constant measured for the exchange reaction between ammonia and ammonium ion in an aqueous solution.

and the logarithms of the equilibrium constants are plotted against the reciprocal of the absolute temperature, $1/T$, to get the heat of the exchange reaction 1 in Fig. 2:

$$\Delta H = -13.8 \text{ cal./mol.}$$

The effect of temperature on the fractionation factor between gaseous ammonia and solid ammonium chloride is shown in Table IV with the experimental conditions. In this case, these fractionation factors are the equilibrium constant of the equation:

$$^{15}NH_{3(gas)} + {}^{14}NH_4Cl_{(solid)} = {}^{14}NH_{3(gas)} + {}^{15}NH_4Cl_{(solid)} \qquad K_1' \quad (13)$$

The logarithms of the equilibrium constants are

Table IV. Effect of temperature on the fractionation factor between ammonia gas and solid ammonium chloride

Run	NH_4Cl[1] mg.	NH_3[2] mmHg	T°C	Period hr.	Fractionation factor, K_1'
41	100	100	275	27	1.0123
42	50	200	274	22	1.0130
43	50	255	245	13	1.0135
44	50	250	248	21	1.0124
45	50	200	247	62	1.0132
46	50	200	227	18	1.0144
47	50	260	224	38	1.0125
48	50	250	203	21	1.0137
49	50	300	206	49	1.0155

1: Amount of ammonium chloride used
2: Pressure of ammonia added at room temperature.

also plotted against the reciprocal of the absolute temperature in Fig. 2. The equilibrium constant between ammonia and ammonium ion, both in the gaseous state, has been calculated by Urey[12]. The calculated values are also plotted in Fig. 2.

Discussion

The equilibrium constant for the equation

$$^{15}NH_{3(gas)} + {}^{14}NH_{4(aq)}^{+} = {}^{14}NH_{3(gas)} + {}^{15}NH_{4(aq)}^{+} \quad (14)$$

has been measured and found to be 1.034 at 25°C by Kirshenbaum et al.[3] The equilibrium constant for the equation

$$^{14}NH_{3(aq)} + {}^{15}NH_{3(gas)} = {}^{15}NH_{3(aq)} + {}^{14}NH_{3(gas)} \quad (15)$$

has been obtained and found to be 1.005 at 25°C[3]. From the data by Kirshenbaum et al. the equilibrium constant for Eq. 1 is calculated to be 1.029 at 25°C. The value of K_1 obtained by the author compares well with the values reported in literature. Further, Fig. 1 shows that Eq. 8 is well satisfied by the experimental fractionation factors and Eqs. 1 and 2 are enough to represent the equilibria involved in the aqueous ammonia-ammonium ion solution and the exchanger of ammonium ion form.

In the equations which involved ammonia in aqueous solution the unionized ammonium hydroxide, NH_4OH, is assumed not to exist in the aqueous solution. Instead, $NH_{3(aq)}$ is assumed to represent ammonia in the aqueous solution. There is some uncertainity in regard to the interpretation of "ammonium hydroxide". However, the relatively weakly basic character of "ammonium hydroxide" solution is interpreted recently as resulting simply from the fact that the ammonia molecule is a weaker than the hydroxide ion. There must be a hydrogen bond between the nitrogen of ammonia in aqueous solution and hydrogen of solvent water.

The value of the equilibrium constant K_1 is smaller than that of the calculated equilibrium constant with the gaseous partition functions of the isotopic ammonia and ammonium ion as shown in Fig. 2. This difference may be chiefly contributed by the difference of ammonia in the aqueous state from the gaseous state. The equilibrium constant for Eq. 14 by Kirshenbaum et al.[3]: 1.005; is considered to be large enough to explain the difference of the isotopic equilibrium constant K_1 from the calculated values. There may not be a large isotope effect on the difference between the gaseous and aqueous ammonium ions, since the nitrogen atom is surrounded by the hydrogen atoms and the nitrogen isotope effect on the solvation in the aqueous ammonium ion may be very small.

The effect of the concentration of the solution phase on the fractionation factor between resin and solution phase (Table II) shows that there is no effect upon acidic solution or ammonium ion and that the concentration of ammonia in the aqueous solution has the tendency to increase the value of the fractionation factor.

The slope of $\log K_1$ versus $1/T$ gives $\Delta H = -13.8$ cal. per mole for the exchange reaction 1. The measurements of the equilibrium constants K_1' for the gas-solid exchange reaction have some difficulty in separating phases at elevated temperatures. The data are not sufficient to determine the accurate value of the heat of the exchange reaction.

In Fig. 2, it is seen that the equilibrium constants measured are located below the line of the calculated equilibrium constants. However, the differences between the measured and the calculated values at the same temperature are smaller with the measured values of the gas-solid exchange reaction than with those of the exchange reaction in aqueous solution. This fact may be partly understood by the presence of the hydrogen bond of ammonia molecules in aqueous solution.

This work was made possible by the support of the U.S. Atomic Energy Commission. The invaluable advice and encouragement from Dr. T. C. Hoering are acknowledged with thanks.

Department of Chemistry
College of Science
Rikkyo University
Toshima-ku, Tokyo

12) H. C. Urey, *J. Chem. Soc.*, **1947**, 562.

*Nitrogen Isotopic Equilibria between Ammonia and Metal-ammine Complex Ions in Aqueous Solution**

By Tatsujiro ISHIMORI

(Received September 21, 1959)

The isotopic exchange of ions or molecules dissolved in solution with those coordinated in complex ions have been studied on the carbon isotopes between carbonate or bicarbonate ion and the carbonate coordinated in the cobalt complex ions[1,2], the oxygen isotopes between water as solvent and that in cobalt complex ion[3], and the nitrogen isotopes between ammonia as solvent and metal-ammine complex ions in liquid ammonia[4]. These studies have given data on the nature of the bond in complex ions. This paper reports on the nitrogen isotope effect in the formation of a series of metal-ammine complex ions with ammonia in aqueous solution. Copper-, zinc-, cadmium-, silver- and nickel-ammine complex ions were studied. The experimental method using ion exchangers[5] has been employed. A theoretical relation has been derived between the isotopic equilibrium constant and the first dissociation constant of the complex ion of the stable form.

Experimental

Using the nitrogen compound with natural isotopic abundance, the equilibrium to be measured is written as

$$\mathrm{M(^{14}NH_3)_{n-1}(^{14}NH_3)^{+p}} + \mathrm{^{15}NH_{3(aq)}} = \mathrm{M(^{14}NH_3)_{n-1}(^{15}NH_3)^{+p}} + \mathrm{^{14}NH_{3(aq)}} \qquad K_1 \quad (1)$$

where $\mathrm{M(NH_3)_n^{+p}}$ represents a metal-ammine complex ion, K_1 the equilibrium constant. The cation exchanger of the metal-ammine complex ion form can be brought to isotope equilibrium with the metal-ammine complex ion or ammonia in solution The equilibria are written by the equations:

$$\mathrm{M(^{14}NH_3)_{n-1}(^{15}NH_3)^{+p}} + \mathrm{M(^{14}NH_3)_{n-1}(^{14}NH_3)R} = \mathrm{M(^{14}NH_3)_{n-1}(^{14}NH_3)^{+p}} + \mathrm{M(^{14}NH_3)_{n-1}(^{15}NH_3)R}, \qquad K_2 \quad (2)$$

$$\mathrm{M(^{14}NH_3)_{n-1}(^{14}NH)R} + \mathrm{^{15}NH_{3(aq)}} = \mathrm{M(^{14}NH_3)_{n-1}(^{15}NH_3)R} + \mathrm{^{14}NH_{3(aq)}} \qquad K_3 \quad (3)$$

where $\mathrm{M(NH_3)_nR}$'s represent the metal-ammine complex ions adsorbed on the cation exchanger, K_2 and K_3 the equilibrium constant for Eqs. 2 and 3, respectively.

The following quantity can be measured conveniently:

$$\delta = \frac{(^{15}N/^{14}N)_{solution} - (^{15}N/^{14}N)_{resin}}{(^{15}N/^{14}N)_{resin}} \qquad (4)$$

where $(^{15}N/^{14}N)_{resin}$ and $(^{15}N/^{14}N)_{solution}$ are the ratio of the nitrogen isotopes in resin and solution, respectively. The value of δ for Eq. 2 can be measured directly for the system of the complex ion adsorbed on the resin and the solution of the complex ion, if the complex ion is stable without free ammonia or with a negligible amount of the excess ammonia. The equilibrium constant for Eq. 2 can be written

$$K_2 = \frac{\mathrm{M(^{14}NH_3)_{n-1}(^{15}NH_3)R}}{\mathrm{M(^{14}NH_3)_{n-1}(^{14}NH_3)R}} \Big/ \frac{\mathrm{M(^{14}NH_3)_{n-1}(^{15}NH_3)^{+p}}}{\mathrm{M(^{14}NH_3)_{n-1}(^{14}NH_3)^{+p}}} \simeq (^{15}N/^{14}N)_{resin}/(^{15}N/^{14}N)_{solution} = 1/(1+\delta_2) \qquad (5)$$

Eq. 3 describes the equilibrium of the complex ion adsorbed on the resin with excess ammonia in aqueous solution. Using the symbols δ_3 for this case, the equilibrium constant of Eq. 3, K_3, is given by the following equation:

$$K_3 = \frac{\mathrm{M(^{14}NH_3)_{n-1}(^{15}NH_3)R}}{\mathrm{M(^{14}NH_3)_{n-1}(^{14}NH_3)R}} \Big/ \frac{\mathrm{^{15}NH_{3(aq)}}}{\mathrm{^{14}NH_{3(aq)}}} \simeq n(^{15}N/^{14}N)_{resin}/(^{15}N/^{14}N)_{solution} = n/(1+\delta_3) \qquad (6)$$

In this equation, $(^{15}N/^{14}N)_{resin}$ is assumed to represent the isotope ratio in only the exchanged complex ions, since the amount of the free ammonia in the resin is negligibly small compared with that of ammonia coordinated in the exchanged compelx ions. It is not necessary to consider ammonium ion in this equilibrium if the pH of the aqueous solution is high.

Now, K_1 is given with δ_2 and δ_3;

$$K_1 = \frac{\mathrm{M(^{14}NH_3)_{n-1}(^{15}NH_3)^{+p}}}{\mathrm{M(^{14}NH_3)_{n-1}(^{14}NH_3)^{+p}}} \Big/ \frac{\mathrm{^{15}NH_{3(aq)}}}{\mathrm{^{14}NH_{3(aq)}}} = K_3/K_2 = n(1+\delta_2)/(1+\delta_3)$$

The value of the fractionation factor, $(1+\delta_2)/(1+\delta_3)$, can be experimentally obtained.

The metal-ammine complex ion may undergo successive dissociations. However, many of the complex ions, in general, have one stable form

* This study has been done in the Chemistry Department of the University of Arkansas, Arkansas, U. S. A.

1) D. R. Stranks and G. W. Harris, *J. Chem. Phys.*, **19**, 257 (1951); *J. Phys. Chem.*, **56**, 906 (1952).

2) P. E. Yankwich and J. E. McNamara, *J. Chem. Phys.*, **20**, 1325 (1952).

3) A. Rutenberg and H. Taube, ibid., **20**, 825 (1952).

4) H. U. D. Wiesendanger, W. H. Jones and C. S. Garner, ibid., **27**, 668 (1957).

5) T. Ishimori, This Bulletin, **33**, 516 (1960).

TABLE I. FRACTIONATION FACTORS OF NITROGEN ISOTOPES BETWEEN METAL-AMMINE COMPLEX IONS AND AMMONIA IN AQUEOUS SOLUTION AT 30°C

Complex ion	Composition of solution, M		$\delta \times 10^3$	$\frac{K_1}{n}$
	Complex ion	Ammonia		
(I) Experiments using cation exchanger				
$Cu(NH_3)_4^{2+}$	0.259	0.00024	$\delta_2 = -0.4 \pm 0.1$	
	0	0.236	$\delta_3 = -11.9 \pm 0.4$	1.0117
$Zn(NH_3)_4^{2+}$	—	—	$\delta_2 \equiv 0$	
	0	0.270	$\delta_3 = -11.5 \pm 0.4$	1.0116
$Cd(NH_3)_4^{2+}$	—	—	$\delta_2 \equiv 0$	
	0	0.270	$\delta_3 = -10.2 \pm 0.9$	1.0103
$Ag(NH_3)_2^{2+}$	0.250	0	$\delta_2 = -0.1 \pm 0.3$	
	0	0.237	$\delta_3 = -9.3 \pm 0.6$	1.0093
(II) Experiments by salting out complex ions				
$Cu(NH_3)_4^{2+}$	0.0455	0.276	$\delta = -11.9 \pm 0.4$	1.0120
$Ni(NH_3)_n^{2+}$	0.250	0.540	$\delta = -7.4 \pm 0.3$	1.0076

which exists predominantly in aqueous solution. In such a case, the isotopic equilibrium constant measured will present the equilibrium constant of the stable form of the complex ion.

Copper quadrammine sulfate was prepared[6] and its solution was made by dissolving the prepared crystal in a very dilute ammonia solution. The other complex solutions: zinc, cadmium and silver complex solution were made by dissolving the slight excess of metal sulfate in an ammonia solution and filtering the insoluble residue out. The cation exchanger used was Dowex 50, X-8. The exchanger of a complex ion form was made by passing the metal-ammine complex- ammonia solution through the exchanger column. The exchangers were washed with ammonia solution on the glass filter with a suction of water jet pump.

The general procedures were the same as described in the previous report[5]. The exchanger of the complex ion form was added to the solution of the complex ion or ammonia and allowed to stand in the constant temperature bath at 30°C over one or two nights. The periods may be long enough for the attainment of the equilibria of the exchange reactions in this experiment, which are supposed to be rapid by the rapid exchanges of ammonia between solvent liquid ammonia and copper-, silver- or nickel-ammine complex ion[4]. After the attainment of the equilibria, the exchangers were separated from the solution with suction filtration, and washed with a limited amount of water to avoid the hydrolysis of the exchanged complex ions. The washed exchanger was put into the sulfuric acid solution to convert to the metal ion and ammonium ion. Then, the exchanger and the solution were poured on the exchanger column in the hydrogen form. The ammonium ion was recovered by eluting with 0.5 N potassium sulfate-0.5 M sulfuric acid solution. Through this process, the greater part of the metal ion was removed. The ammonia solution separated from the exchanger at equilibrium was acidified with sulfuric acid solution and used for the isotopic analysis. The complex ion solution was acidified with sulfuric acid solution and treated by the same procedure as described for the complex ion exchanged.

For copper and nickel complex ions, the complex ions were separated from the complex-ammonia mixed solutions by salting out the complex salts with the addition of the large amount of alcohol and centrifuging the complex salts. The isotopic measurements were carried out for the supernatant solution and complex salts centrifuged.

The isotope ratio measurements were made in the same way as described in the previous report[5].

Results

The experimental results are shown in Table I with the experimental conditions. In the experiments of cadmium and zinc complex ion, the value of δ_2 could not be measured since these complex ions were not stable in aqueous solution without a large excess of ammonia. Their equilibrium constants were calculated by assuming the value of δ_2 to be zero. This assumption seems to be reasonable since the equilibrium constant of isotopic ions between the exchanger and solution phase is nearly unity.

The experiments were carried out by the technique of salting out the complex ion from the complex ion-ammonia mixture solution with the addition of alcohol for copper and nickel complex ions. In this technique, the equilibrium constant can be readily obtained from the measured value of δ:

$$\delta = [(^{15}N/^{14}N)_{solution} - (^{15}N/^{14}N)_{salt}] / (^{15}N/^{14}N)_{salt}$$

The results are also shown in Table I. Both the techniques of using cation exchanger and

6) G. Brauer, "Handbuch der Praeparativen Anorganischen Chemie", Ferdinand Bnke Verlag, Stuttgart (1954), p. 757.

salting out the complex ion gave a good agreement on the value of K_1. The agreement shows that the technique with cation exchanger can be efficiently used in measurements of this kind.

Theoretical and Discussion

A theoretical relationship can be derived between the isotopic equilibrium constant of Eq. 1, K_1, and the first dissociation constants of the stable ammine complex ions, k and k' for the dissociations:

$$\mathrm{M}(^{14}\mathrm{NH_3})_{n-1}(^{15}\mathrm{NH_3})^{+p} = \mathrm{M}(^{14}\mathrm{NH_3})_{n-1}{}^{+p} + {}^{15}\mathrm{NH}_{3(aq)} \qquad k \quad (8)$$

$$\mathrm{M}(^{14}\mathrm{NH_3})_{n-1}(^{14}\mathrm{NH_3})^{+p} = \mathrm{M}(^{14}\mathrm{NH_3})_{n-1}{}^{+p} + {}^{14}\mathrm{NH}_{3(aq)} \qquad k' \quad (9)$$

The value which is defined as a ratio of the partition functions of isotopic molecules by Biegeleisen and Mayer[7], is written as,

$$\frac{s}{s'}f = 1 + \Sigma_i G_i \Delta u_i \qquad (10)$$

where s and s' are the symmetry number of isotopic molecules. The primed notation refers to the light molecule. The G function relates to the difference in free energy of the formation of isotopic molecules from the isolated gaseous atoms[7]:

$$\frac{\Delta F^0 - \Delta F^{0\prime}}{RT} = -\Sigma_i G_i \Delta u_i + \ln \frac{s}{s'} \qquad (11)$$

The following equation can be obtained from Eqs. 10 and 11:

$$f = \frac{s'}{s}\left(1 - \frac{\Delta F^0 - \Delta F^{0\prime}}{RT} + \ln \frac{s}{s'}\right) \qquad (12)$$

Then Eq. 12 is applied to the isotopic complex ions in aqueous solution, the ratio of their symmetry numbers, s'/s, can be replaced by the number of the ammonia molecules coordinated in the stable complex ions. Further, if Eqs. 8 and 9 are compared the difference of the free energies of formation of the complex ions becomes

$$\Delta F^0{}_c - \Delta F^{0\prime}{}_c = \Delta F^0{}_a - \Delta F^{0\prime}{}_a - RT \ln(k'/k) \qquad (13)$$

where the subscripts c and a refer to the complex ion and ammonia, respectively. The f function of the complex ion is written as

$$f_c = n\left(1 + \ln k'/k - \frac{\Delta F^0{}_a - \Delta F^{0\prime}{}_a}{RT} - \ln n\right) \qquad (14)$$

For the isotopic ammonia molecules, the ratio of the symmetry numbers is one and its f function is given by

$$f_a = 1 - \frac{\Delta F^0{}_a - \Delta F^{0\prime}{}_a}{RT} \qquad (15)$$

With Eq. 15, the f function of the complex ion is rewritten as

$$f_c = n(\ln k'/k + f_a - \ln n) \qquad (16)$$

Now the equilibrium constant, K_1, which is the ratio of the f function of the complex ion to that of ammonia, can be expressed with the dissociation constants of the stable complex ions, k and k':

$$K_1 = n\left[1 + \ln\left(\frac{k'}{n} \Big/ k\right)\Big/ f_a\right] \qquad (17)$$

The quantity of k'/n in this equation is equivalent to k if the probabilities of the dissociations of the isotopic complex ions are taken into account. Both k'/n and k are a measure of the strength of the bond between metal and nitrogen in the complex ions which appeared at the first dissociation.

The measured fractionation factors can be compared with the relationship of Eq. 17, provided a form of the complex ion among the successively dissociated ions is predominantly stable. The successive dissociation constants have been measured[8]. The values of the dissociation constants are listed with the measured fractionation factors in Table II. Copper, zinc, cadmium and silver complex ions have one stable form. However, in the case of nickel complex ion, the successively dissociated ion may exist with comparable concentrations and they effect the value of the measured fractionation factor as an average.

Table II. Fractionation factors and the first dissociation constants of complex ions

Complex ion	$\frac{K_1}{n}$	$\log k'$	$\log \frac{k'}{n}$
$Cu(NH_3)_4^{2+}$	1.0117	−2.13	−2.73
$Zn(NH_3)_4^{2+}$	1.0116	−2.15	−2.75
$Cd(NH_3)_4^{2+}$	1.0103	−0.93	−1.53
$Ag(NH_3)_2^{+}$	1.0093	−3.83	−4.13
$Ni(NH_3)_n^{2+}$	1.0076	−0.03 for $n=6$	−0.81
		−0.75 for $n=5$	−1.45
		−1.19 for $n=4$	−1.79

In Table II, the tendency is noted that the smaller value of k' causes the greater fractionation factor or the greater value of the ratio of k'/n to k. An exception is in the case of the silver complex ion although the reason is not clear. The greater isotope effect is found in the more tightly bound complex ion which agrees with the general rule of the isotope effects.

7) J. Biegeleisen and M. C. Mayer, *J. Chem. Phys.*, **15**, 261 (1947).

8) J. Bjerrum, *Chem. Revs.*, **46**, 381 (1950).

This work was made possible by the support of the U. S. Atomic Energy Commison. The invaluable advice and encouragement from Dr. T. C. Hoering are acknowledged with thanks.

Department of Chemistry
College of Science
Rikkyo University
Toshima-ku, Tokyo

*Studies on Thixotropy. II.**[1] *On the Thixotropic Gel Structure of Bentonite*

By Takehiko WATANABE

(Received August 10, 1959)

There are two kinds of structure which are currently taken as a model for thixotropic gel of bentonite. One of them is the structure in which dispersed plate-like particles are linked together at a short distance to build up a network. The other[2,3] is the structure in which particles are regularly oriented to each other at a considerable distance. According to the latter structure, however, it was difficult to explain the process of thixotropic gel formation which proceeds in two steps as described in the previous paper[1]. By making light-scattering, birefringence and viscoelastic studies on mono-disperse sol of Wyoming Bentonite, M'Ewen et al.[4] have suggested that particles are oriented edge-to-edge in the form of flat ribbons. Olphen[5] has also concluded from the results obtained by the study of the surface conductance of bentonite suspension that particles are linked with each other at a short distance. These results show that the former structure, e. g. "house of cards" structure[6] in which the particles are linked at

TABLE I. RELATIONS BETWEEN RHEOLOGICAL PROPERTIES AND CONCENTRATION

Investigator	Apparatus or Method	Relation presented	Relation derived by the present author
Braune et al.[7]	Kämpf viscometer	$A_\infty \propto C^2$	
Peter et al.[8]	Couette viscometer	$\tau_B \propto C^2$	at low concn. $\tau_B \propto C^2$ at high concn. $\tau_B \propto C^4$
Olphen[9]	Stormer viscometer	$\tau_B \propto (C-C_m)^2$	at low concn. $\tau_B \propto C^2$ at high concn. $\tau_B \propto C^4$
	Shear propagation	$\mu \propto (C-C_m)^3$	$\mu \propto C^6$
Packter[10]	Stormer viscometer	$S_\infty \propto C^6$	
Watanabe[1]	Torsion balance	$\begin{cases} A_{1\infty} \propto C^2, \\ A_{2\infty} \propto C \end{cases}$	
		or $\begin{cases} A_{1\infty} \propto C^4, \\ A_{2\infty} \propto C^2 \end{cases}$	

A_∞: max. yield value; τ_B: Bingham yield stress; μ: modulus of elasticity; S_∞: max. gel strength: $A_{1\infty}$ and $A_{2\infty}$: max. yield value for the first and the second step of gel formation, respectively; C: concentration; C_m: a constant.

* Presented at the 12th Annual Meeting of the Chemical Society of Japan, Kyoto, April, 1959.

1) Part I: T. Watanabe, This Bulletin, **33**, 347 (1960).
2) E. A. Hauser and D. S. LeBeau, *J. Phys. Chem.*, **45**, 54 (1941); E. A. Hauser, "Silicic Science", D. van Nostrand Co., Inc., Princeton, New Jersey (1955), p.36.
3) E. Forslind, "Proceedings of the Second International Congress on Rheology", Butterworths Scientific Publications, London (1954), p. 50.
4) M. B. M'Ewen and M. I. Pratt, *Trans. Faraday Soc.*, **53**, 535 (1957); M. B. M'Ewen and D. L. Mould, ibid., **53**, 548 (1957).
5) H. van Olphen, *J. Phys. Chem.*, **61**, 1276 (1957); H. van Olphen and M. H. Waxman, "Fifth National Conference on Clays and Clay Minerals", Publ. 566, National Academy of Sciences, National Research Council, Washington (1958), p. 61.
6) U. Hofmann, *Kolloid-Z.*, **125**, 86 (1952).
7) H. Braune and I. Richter, ibid., **113**, 20 (1949).
8) S. Peter and I. Stolle, *Z. physik. Chem.* [*N. F.*], **11**, 251 (1957).
9) H. van Olphen, "Proceedings of the Fourth National Conference on Clays and Clay Minerals", Publ. 456, National Academy of Sciences, National Research Council, Washington (1956), p. 204.
10) A. Packter, *Kolloid-Z.*, **150**, 60 (1957).

a short distance, is favored. Therefore, in this report, discussions will be carried out on this structure on the basis of the rheological data.

Discussion and Proposal of Gel Structure

In Table I are collected the relations between the rheological properties and the concentration of thixotropic gel of bentonite presented by different investigators, and those derived by the present author using the data obtained by other authors. Furthermore, from the experimental data provided by Peter et al.[5] the relations between shearing stress (τ) and concentration (C) at a fixed rate of shear (q) are derived and given in Table II. The relation between τ and C is also dependent on C. Referring to the study of Enneking[11], in which he discussed experimental conditions similar to Peter's, in the range where the values of τ in Table II are proportional to C^n, the flow may be induced not in the whole but in a localized part of the gel. Therefore, it may be said that in the flowing part, the actual value of q is higher than those listed. Consequently, this high q is to be suddenly induced to the set gel. It may further be reasonable to assume that the experimental conditions, under which some of the measurements for Table I were carried out, must be essentially similar to those above stated. Therefore, μ and S_∞ can be proportional to C^n.

TABLE II. RELATIONS BETWEEN τ (SHEARING STRESS) AND C (CONCENTRATION) AT FIXED q (RATE OF SHEAR) VALUES, DERIVED FROM THE DATA OF PETER ET AL.[5]

Geisenheim Bentonite in Water

q(sec^{-1}) \ C(%)	1	2	3	3.47	3.92
4.16	$\tau \propto C^2$	$\tau \propto C^4$		$\tau \propto C^6$	
25.7	$\tau \propto C^2$			$\tau \propto C^6$	
102.9	$\tau \propto C^2$			$\tau \propto C^4$	
662	$\tau \propto C$		$\tau \propto C^2$		

Algeria Bentonite in water

q(sec^{-1}) \ C(%)	1.79	2.71	3.61	4.49	5.10	5.92
4.16	$\tau \propto C^2$				$\tau \propto C^6$	
6.44	$\tau \propto C^2$				$\tau \propto C^6$	
66.5	$\tau \propto C^2$				$\tau \propto C^4$	
411	$\tau \propto C$			$\tau \propto C^2$		

11) H. Enneking, *Rheologica Acta*, **1**, 234 (1958).

Tables I and II show that the relations between rheological properties (in the following, represented by "strength") and concentration are dependent on the condition of measurement, so that it may be expected that the particles constituting the gel do not orientate so regularly as ions in crystal lattice but link with each other at random to build up the gel structure. This leads to the conclusion that, in the gel, several kinds of agglomerated particle groups can coexist. It may also be expected that under a certain experimental condition, the gel strength is determined by a particular particle group in the gel. Namely, if the observed gel strength is proportional to C^p where p is a positive integer, there exists a particular particle group which performs the role of structural unit. And in this case, provided that the contribution to the gel strength is equal in each particle group of the same kind, it may be concluded that the number of the particle group per unit volume of the gel varies as C^p. In other words, the probability of the existence of this particle group is proportional to C^p. In the following discussion, a particle group such as stated above will be named structural unit-C^p (abbr. S. U.-C^p). If many kinds of particle groups which act as S. U.-C^p, exist in the system, the gel strength may be determined by one of them, or by a set of particle groups which make equal contribution to the gel strength in cooperation with each other.

Since the form of bentonite particle is plate-like, the association between particles may be classified into three types based on the steric condition of the junction point as described in the previous paper[1]. In the first type, two particles are linked with each other at one point (P-1 association); while, in the second, particles are linked at two or more points belonging to one straight line (P-2 association) and, in the third, particles are linked at three or more points belonging to one plane (P-3 association). Also the number of junction points in unit volume in which two adjacent particles are linked with P-1, P-2 or P-3 association is proportional to C, C^2 or C^3, respectively.

In the first place, it is assumed that, in the gel structure, all particles are linked to each other with P-1 association. In this case, consideration is made based on the experimental results with Yamagata Bentonite reported in the previous paper[1]. This sample shows the maximum yield value proportional to C^2, or C according to the first or the second gelation process, respectively. Therefore, it is concluded that S. U.-C^2 contributes to the gel strength in the first step and S. U.-C in the second. Furthermore, from the results discussed in the

previous paper[1], it has been ascertained that the particle group which acts as a structural unit in the first step does not disappear, but its contribution to the yield value diminishes in the second step under the experimental method employed. Considering the process of gel formation, the structure developed in the second step is doubtless more rigid than that of the first. S. U.-C^2 in the first step, is the cross-linkage in which two linear ribbons are linked to the hypothetical fixed particle which behaves as if it were restricted at a fixed position when the cross-linkage acts as structural unit. Therefore, in the second step, the existence of cross-linkage may be expected, of which more than two linear ribbons are linked to the fixed particle. Namely, there exists the S. U.-C^p where $p>2$ in the second step. Consequently, the structure which satisfies all the relations listed in Tables I and II, may be as follows. The structure is formed by cross-linking of the linear ribbons which are formed of the aligned particles linked by P-1 association. For the cross-linkage, there must coexist at least five kinds of cross-linkage in which two to six linear ribbons, respectively, are linked to the fixed particle.

Based on the above consideration on the structure, in the case of Yamagata Bentonite, the structural unit is S. U.-C, namely, the linear ribbons; since the maximum yield value developed in the second step ($A_{2\infty}$) varies as C. The result obtained with Volclay[1] where $A_{2\infty} \propto C^2$ and also with Braune's results, $A_\infty \propto C^2$, may be explained as follows. The structural unit is S. U.-C^2, that is, the cross-linkage formed by two linear ribbons linking to the fixed particle.

Next, it is assumed that all particles in structure are linked by P-2 association. In this case, the consideration must be made based on the results obtained with Volclay in the previous paper[1]. By treatment similar to that described above in completely set gel, there must exist S. U.-C^6 besides S. U.-C^2 and S. U.-C^4. S. U.-C^2 is the linear ribbons which are formed by the aligned particles linked by P-2 association. S. U.-C^4 or S. U.-C^6 is the cross-linkage in which two or three linear ribbons, respectively, link to the fixed particle. Using this model of structure, it is possible to explain all the experimental results listed in Tables I and II except that of Yamagata Bentonite. However, as to the S. U.-C^6 it is not enough to consider such a simple model as that mentioned above, it must satisfy the following requirements.

(1) Among the strengths of bentonite gel measured by various methods, the one proportional to C^6 has the largest value of p. Therefore, the particle group which acts as S.U.-C^6 must be the one which plays the part of constituting a rigid gel structure.

(2) Packter[10] has suggested that the rate of gel formation varies as C^6 in the case where the maximum gel strength S_∞ is proportional to C^6 as shown in Table I. To satisfy this fact, S. U.-C^6 must be the cross-linkage formed in the process where six adjacent particles which participate in the formation of separate linear ribbons, orientate to the fixed particle.

Considering the above requirements, the cross-linkage which acts as S. U.-C^6 will be as follows.

The fixed particle is linked to three linear ribbons composed of a certain number of particles, of which each one nearest to the fixed particle must be further linked to another different linear ribbon. The particle group formed in such a way as stated above is an overlapping assembly of the four particle groups, each of which is expected to act as S. U.-C^6.

Considering such a particle group, it is safely assumed that such a cross-linkage plays an important role in the rigid gel structure which satisfies requirement 1, and the rate of formation of the cross-linkage varies as C^6 and requirement 2 is also fulfiled.

In the above consideration, only the case of P-2 association is treated. However, provided that similar structural conditions exist in the case of P-1 association, it may be expected that a rigid gel structure is built up from the three kinds of particle groups which will be able to act as S. U.-C, S. U.-C^2 and S. U.-C^3, respectively.

Now, it is assumed that four states of particle agglomerate will appear in the course of thixotropic gel-sol-gel transformation. Possible

Table III. Structural units which exist in four rheological states of thixotropic gel-sol-gel transformation

Type of structure	Type of association	Rheological state			
		Rigid gel	Loose gel	Sol I	Sol II
I	P-1	S. U.-C S. U.-C^2 S. U.-C^3	S. U.-C S. U.-C^2	S. U.-C	Dispersed particles
II	P-2	S. U.-C^2 S. U.-C^4 S. U.-C^6	S. U.-C^2 S. U.-C^4	S. U.-C^2	Dispersed particles

S. U.-C^p which may contribute to the strength at each state is collected in Table III. In the state where two or more structural units exist, the strength is determined by one of them, depending on the experimental condition. S. U.-C in type I structure and S. U.-C^2 in type II are listed on both gel and sol states. These are the linear ribbons which participate in the structure in the gel state and are free in the sol state.

As described in the previous paper[1], during the first step of the thixotropic gel formation, the increase of the yield value of the gel in the loose gel state with setting time was measured and during the second step that of the gel in the rigid gel state was measured. In the case of the second step, experiments have been made to measure the yield value corresponding to the stress necessary to induce a fixed elastic deformation to the gel in which linear ribbons act as the structural unit. This deformation may be classified as a complete, recoverable, non-ideal one[12]. Therefore, the gel at this step shows retarded elasticity. Accordingly, if the deformation within the elastic limit has been induced gradually to the gel in rigid gel state of type II, its strength varies as C^2 since the linear ribbons act as the structural unit. On the contrary, when the deformation has been induced to the gel under the condition where the stress is suddenly applied to the system accompanying a fairly high rate of shear, the linear ribbons may not respond to this deformation, and as a result they come to play no role as the structural unit. The cross-linkage then comes to act as the structural unit so that the strength of the gel varies as C^6.

When experiments are carried out to obtain a flow curve, the rate of shear induced to the system is gradually increased and the stress corresponding to a given rate of shear is estimated. In this case, the observations are made on the variation of the state, starting from the rigid gel state and ending at the sol state II, listed in Table III. In the course of this experiment, a breakdown of the cross-linkage will occur at the initial stage and will be followed by the disintegration of the linear ribbons into individual particles at a later stage. Therefore, the results derived from the curve reported by Peter et al. or Olphen as shown in Tables I and II are explained as follows.

In these experiments, it may be expected that these systems take a structure of type II shown in Table III. From the results given in Table II, the relations between the stress and the concentration at a fixed rate of shear are dependent on the concentration of the system. Similar dependence on the above is also observed with the relation between the Bingham yield stress and the concentration as shown in Table I. It was observed in the previous experiment[1] that both the ratio of $A_{2\infty}$ to $A_{1\infty}$ and the difference between the values of $A_{2\infty}$ and $A_{1\infty}$ are larger in the case of the lower concentration. Therefore, it may be expected that in the gel which is in the rigid gel state, the ratio of the number of S. U.-C^2 to that of S. U.-C^4 or S. U.-C^6 of low concentration is larger than that of high concentration. Hence, at low concentrations, even the gel standing for a long period has a structure of either a loose gel state or a state not strictly distinguishable from sol state I. According to the above consideration, the relations listed in Table II may be elucidated with the concept given in Table III. The Bingham yield stress (τ_B) is obtained from the intersection of the extraporated straight line with the stress axis so that the relation between τ_B and concentration is determined by the kind of structural unit in the range in which a linear relationship between the rates of shear and stress is obtained.

There has been no information regarding the condition under which the particles take either the structure of type I or II. However, it may be assumed that if the dispersed bentonite particles are in the form of unit layer, they will constitute a structure of type I, and if the dispersed particles are composed of stacking of several unit layers, a structure of type II will be formed.

P-1 association may be represented typically by the edge-to-edge linkage and P-2 association by the edge-to-surface linkage.

Packter[10] has reported that the maximum gel strength is proportional to C^3 in non-heterocoagulated system where polyanion is added to the bentonite suspension. The results can be clearly explained by the assumption that the particles in the structure are linked by P-3 association. However, the gel structure which is formed by the particles linked by P-3 association is a very compact one compared with those listed in Table III and it is inadequate to accept this structure as that of thixotropic gel.

Summary

(1) Discussions are carried out on the structure of the thixotropic gel of bentonite on the basis of the relation between the gel strength and the concentration, and the steric conditions of the junction point between two particles participating in structure.

(2) The gel strength is determined by the

12) J. M. Burgers and G. W. Scott Blair, "Report on the Principles of Rheological Nomenclature", North-Holland Publishing Co., Amsterdam (1949), p. 49.

particular group of particles in the structure which acts as the structural unit.

(3) The particle group which plays the part of the structural unit is not limited to one kind but more than one may coexist in a system. The gel strength is determined by one kind of the particle groups according to the experimental method used.

(4) The structure of the thixotropic gel of bentonite is classified into two types according to the mode of association between particles. One of them is the structure in which linear ribbons, which act as structural units, are formed by the aligned particles linking each other at one point. The other is the structure in which linear ribbons are formed by the particles linking at two or more points on one straight line.

The author would like to express his gratitude to Professor Sôzaburo Ono for his kind guidance and discussion throughout this work.

Laboratory of Biophysical Chemistry
College of Agriculture
University of Osaka Prefecture
Sakai-shi, Osaka

Hydrolysis of 7-Anilinobenzyl-8-quinolinol

By Motoko Ito

(Received August 21, 1959)

On heating with 4 N hydrochloric acid 7-anilinobenzyl-8-quinolinol (I) gave 7-hydroxybenzyl-8-quinolinol (II) and aniline as major products. The formation of benzaldehyde was found to be very scanty at this reaction though a distinct odor of benzaldehyde was noticed, suggesting that dissociation into three components of the Mannich base proceeded only to a negligible extent. On further heating with hydrochloric acid, II produced neither 8-quinolinol nor benzaldehyde but gave undefined matter (m.p. 118~119°C, foaming at 125°C). The bromination of II produced 5, 7-dibromo-8-quinolinol and benzaldehyde.

The dissociation of I by 4 N hydrochloric acid was first studied by Phillips et al.[1], however, it was considered at that time that I dissociated into three components in one step.

Experimental

7-Hydroxybenzyl-8-quinolinol (II).—A hot solution of I (0.5 g.) in 4 N hydrochloric acid (10 ml.) was kept at around 85°C for 16 min. (when an odor of benzaldehyde was noticed). After being cooled, the solution was diluted with water (50 ml.) and then sodium acetate (6 g.) was added to it. The resulting precipitate was filtered after standing overnight (when no odor of benzaldehyde was noticeable). The filtrate gave a deep violet color with bleaching powder. The crude product was heated with ligroin (20 ml.) and filtered. From the filtrate on working up a colorless solid (0.15 g.), m.p. 88~100°C, foaming at 120~130°C, was isolated. This may be an impure bakelite-type condensation product.

The undissolved II was crystallized from five hundred times its weight of hot ligroin as colorless prismatic needles, m.p. 128°C.

Found: C, 76.52; H, 5.30; N, 5.20. Calcd. for $C_{16}H_{13}NO_2$: C, 76.49; H, 5.18; N, 5.58%.

When crystallized from benzene (20 ml.), it contained a mole of the solvent, m.p. 126~127°C; yield, 0.25 g. (66%) and when crystallized from carbon tetrachloride and dried in vacuo at room temperature, it also contained the solvent.

Found: C, 80.09; H, 5.65; N, 3.85. Calcd. for $C_{16}H_{13}NO_2 \cdot C_6H_6$: C, 80.24; H, 5.78; N, 4.26%.

Found: C, 53.84; H, 4.01. Calcd. for $C_{16}H_{13}NO_2 \cdot 0.8CCl_4$: C, 53.87; H, 3.47%.

The hydrochloride was obtained as colorless needles by the reaction of the base and hydrogen chloride, both in ethereal solution in the cold. It gave no definite m.p., began to sinter at 265°C and became a tar at 302°C.

Found: N, 4.73. Calcd. for $C_{16}H_{13}NO_2 \cdot HCl$: N, 4.87%.

The picrate was crystallized from benzene as prisms, m.p. 169°C.

Found: N, 11.50. Calcd. for $C_{16}H_{13}NO_2 \cdot C_6H_3N_3O_7$: N, 11.67%

Acetyl Derivatives.—A mixture of II (0.2 g.), freshly fused sodium acetate (0.2 g.), acetic anhydride (0.4 ml.) and ether (20 ml.) was allowed to stand at room temperature for 3 days, ether was evaporated and then water was added to the reaction mixture. The resulting precipitate was filtered; yield, 0.26 g.

The crude product was treated with ether (50 ml.) and the undissolved solid was crystallized from benzene as thick plates, m.p. 135°C. Analysis proved it to be a monoacetyl compound. It gave no color reaction with ferric chloride. This suggests that phenolic hydroxyl was acetylated.

Found: C, 73.89; H, 4.89; N, 4.71. Calcd. for $C_{18}H_{15}NO_3$: C, 73.72; H, 5.12; N, 4.78%.

1) J. P. Phillips and A. L. Duckwall, *J. Am. Chem. Soc.*, 77, 5505 (1955).

The crude product obtained from the ether extract by evaporating the solvent, was carefully recrystallized from ether as colorless prisms, m.p. 109~110°C. The analytical figures corresponded to those of the diacetyl derivatives.

Found: C, 71.49; H, 5.00; N, 4.06. Calcd. for $C_{20}H_{17}NO_4$: C, 71.64; H, 5.07; N, 4.18%.

II (m.p. 126~127°C) on heating with 4 N hydrochloric acid for 10 min. when no odor of benzaldehyde was noticed and further working gave a product m.p. 118~119°C foaming at 125°C.

5, 7-Dibromo-8-quinolinol.—*Method A.*—A mixture of the Mannich base (I) (0.33 g., 0.001 mol.) and 4 N hydrochloric acid (7 ml.) was treated in the same manner as that of Phillips[1]. The reaction mixture was neutralized with sodium acetate and the separated solid was filtered; yield, 0.65 g., m.p. 105~170°C. When it was crystallized from ethanol, it gave needles (0.17 g.) melting at 194~195°C alone or on admixture with a sample of 5, 7-dibromo-8-quinolinol which was prepared by bromination of 8-quinolinol.

Method B.—To a mixture of II (0.33 g. 0.001 mol.) and 4 N hydrochloric acid (7 ml.) after it was diluted with water (50 ml.), one half normal bromate-bromide solution (8 ml.) was added dropwise.

After standing for 2 hr., the resulting solid (80 mg.) was filtered and crystallized from ethanol to give colorless needles, m.p. with a sample of 5, 7-dibromo-8-quinolinol 194~195°C. A mixture of the filtrate of the crude product and an ethanolic solution of dinitro-phenylhydrazine (0.1 g.), on mild warming and long standing gave a solid, which crystallized from ethanol as orange elongated plates, m.p. 235~236.5°C and identified as benzaldehyde dinitrophenylhydrazone by mixed m.p. method.

The author wishes to thank Mr. Konomu Matsumura for help and advice throughout this work.

Chemical Laboratory
Kitasato Institute
Minato-ku, Tokyo

The Photochemical Addition Reaction. VI. The Mechanism of the Addition Reaction of n-Butyl Mercaptan to Vinyl Acetate

By Kazuo Yamagishi, Kunio Araki, Tadao Suzuki and Toshio Hoshino

(Received September 15, 1959)

Many synthetic investigations have been made on the addition reaction of mercaptans to olefins, yielding the products of β-alkylthioethyl derivatives with anti-Markownikov configuration under the influence of oxygen, peroxides and light[1]. It has been reported that, by the action of ultraviolet light, the addition of mercaptans to olefins such as vinyl acetate, vinyl chloride and allyl alcohol, proceeds according to the following overall reaction[2];

$$RSH + CH_2:CHR' \xrightarrow{h\nu} RSCH_2CH_2R' \quad (1)$$

Recently Sivertz et al.[3] studied the kinetics of the photosensitized addition reaction of a mercaptan to various olefins in order to explain the reaction mechanism kinetically, although the identification of the reaction products was not involved in their study.

The purpose of the present study is to elucidate the mechanism of the addition reaction of mercaptans to vinyl compounds. Attention has been paid to identifying the termination product as follows: In the presence of a large excess of mercaptan, butyldisulfide has been assumed as the termination product by Sivertz et al.[3] This compound, however, has been found to decompose under ultraviolet light, which was employed for the initiation of the reaction studied. It is impossible to assume that the disulfide is the final product. Hence, the formation of the cross termination product, α, β-dibutylthioethyl derivative could not be ignored. In this connection, the analysis of all the products in the reaction has been carried out. Vinyl acetate and *n*-butyl mercaptan were chosen as the reactants, because they form 1:1 adduct quantitatively with no teromer formation during the reaction.

The molar ratio of vinyl acetate to mercaptan in this experiment was 1:20. Samples were purified by vacuum distillation for the purpose of excluding water, oxygen and oxides. The reaction mixture was irradiated with ultraviolet light of 3660 Å for forty hours. The mixture

1) S. O. Jones and E. E. Reid, *J. Am. Chem. Soc.*, **60**, 2452 (1938); M. S. Kharasch, W. Nudenberg and G. J. Mantell, *J. Org. Chem.*, **16**, 524 (1951).

2) T. Hoshino, K. Yamagishi and Y. Ichikawa, *J. Chem. Soc. Japan, Pure Chem. Sec.* (*Nippon Kagaku Zasshi*), **74**, 510 (1953); K. Yamagishi and N. Nakajima, ibid., **75**, 1086, (1954).

3) R. H. Pallen and C. Sivertz, *Can. J. Chem.*, **35**, 723 (1957).

irradiated was first divided into gas (fraction I) and liquid at room temperature. By the distillation of the liquid fraction at 20°C (20 mmHg) it was futher divided into two parts (named fractions II and III). One was the distillate (fraction II) consisting of excessively used mercaptan and unreacted vinyl acetate, which were collected in a cold trap (−78°C), and the other was the residue (fraction III) consisting mostly of the main product, β-butylthioethyl acetate, and the termination product, α, β-dibutylthioethyl acetate.

The mass-spectroscopic analysis of fraction I showed the mass number 2 and 88, which correspond to hydrogen and ethyl acetate, respectively. By the rectification of fraction II ethyl acetate was isolated from the mixture of unreacted vinyl acetate and excessively used mercaptan. This ethyl acetate was identified by Dragendorff's xanthate color test.[4] It is, therefore, certain that the mercaptan decomposed directly under the influence of ultraviolet light, yielding hydrogen atom and thyl radical by the primary initiation reaction of Eq. 2.

Prim. init.

$$RSH \xrightarrow{h\nu} RS\cdot + H\cdot \qquad (2)$$

The hydrogen atom may subsequently react with vinyl acetate and mercaptan by the secondary initiation mechanisms a) and b).

a) When a hydrogen atom is added at the double bond of a vinyl acetate molecule, the acetoxyethyl radical is produced (Eq. 3) and the acetoxyethyl radical thus formed reacts with the mercaptan giving the thyl radical and the ethyl acetate (Eq. 4).

Sec. init. a)

$$H\cdot + CH_2{:}CHOAc \rightarrow CH_3\dot{C}HOAc \qquad (3)$$

$$CH_3\dot{C}HOAc + RSH \rightarrow RS\cdot + CH_3CH_2OAc \qquad (4)$$

b) When a hydrogen atom abstracts the hydrogen atom from a mercaptan molecule, a thyl radical and a hydrogen molecule are produced (Eq. 5).

Sec. init. b)

$$H\cdot + RSH \rightarrow RS\cdot + H_2 \qquad (5)$$

In either secondary initiation a) or b), the thyl radical is produced ultimately, and the radical initiates the propagation reaction of Eqs. 6 and 7.

Prop.

$$RS\cdot + CH_2{:}CHOAc \rightarrow RSCH_2\dot{C}HOAc \qquad (6)$$

$$RSCH_2\dot{C}HOAc + RSH \rightarrow RS\cdot + RSCH_2CH_2OAc \qquad (7)$$

By the rectification of fraction III, the main product, β-butylthioethyl acetate was obtained in a good yield with a small amount of heavy colorless liquid (b. p. 110°C at 2 mmHg), which was identical with the authentic sample of α, β-dibutylthioethyl acetate. The identification of α, β-dibutylthioethyl acetate was performed as follows: (a) The physical properties of the sample were compared with those of the authentic sample, which was prepared by the reaction of vinyl acetate with butyldisulfide under the irradiation of ultraviolet light of 3660 Å at room temperature for forty hours (Table I). (b) α, β-Dibutylthioethyl acetate was hydrolyzed to butylthioacetaldehyde. This gave the hydrazone (m. p. 63~64°C) with 2, 4-dinitrophenyl hydrazine and no depression of the melting point when mixed with the hydrazone of the authentic sample. The authentic sample of the aldehyde was prepared from bromacetaldehyde dimethyl acetal[5] and sodium mercaptid.

These facts indicate that β-butylthioethyl acetate is produced by the chain propagation reaction of Eqs. 6 and 7. The isolation of α, β-dibutylthioethyl acetate from the reaction mixture supports the view that termination reaction occurred by the mechanism shown in Eq. 8.

Term.

$$RS\cdot + RSCH_2\dot{C}HOAc \rightarrow RSCH_2CH(SR)OAc \qquad (8)$$

Further support of the initiation reaction was obtained by means of the experiment with oxygen as the quencher of atomic hydrogen. By the mass-spectroscopic analysis of fraction I, no ethyl acetate was identified, although traces of water and hydrogen were detected. This result suggests that the hydrogen atom combined with oxygen and the hydrogenperoxyl radical ($HO_2\cdot$) thus formed produced the thyl radical and hydrogen peroxide. More thyl radicals may be produced by H_2O_2 (Eq. 11).

$$H\cdot + O_2 \rightarrow HO_2\cdot \qquad (9)$$

$$HO_2\cdot + RSH \rightarrow RS\cdot + H_2O_2 \qquad (10)$$

$$H_2O_2 + RSH \rightarrow RS\cdot + H_2O \qquad (11)$$

Experimental

Materials.—*n-Butyl mercaptan.*—By the hydrolysis of *S*-butylthiuronium hydrobromide *n*-butyl mercaptan was obtained (b. p. 98°C)[5].

Vinyl acetate.—After removing the impurities in a commercial product by Matheson's prepolymerization method[6], the remaining monomer was

4) F. Feigl, "Spot Tests in Organic Analysis", Elsevier Publ. Co., Amsterdam (1956), p. 174.

5) H. Backer, *Rec. trav. chim.*, **51**, 289 (1932).

6) M. S. Matheson, E. E. Auer, E. B. Bevilacqua and E. J. Hart, *J. Am. Chem. Soc.*, **71**, 2610 (1949).

TABLE I.

α,β-Dibutylthioethyl acetate	Boiling point °C at mmHg	Refractive index n_D	Anal. Found C	H
The sample from reaction products	107/0.3	1.4958(20°C)	54.58	9.29
The authentic sample	109/0.3	1.4948(24°C)	54.22	9.25
Calcd. for $C_{12}H_{24}O_2S_2$:			54.53	9.15

fractionated and the fraction of b. p. 72.6°C was collected and the sample was stored in vacuo.

The purification of these two samples was effected at first by fractional distillation under nitrogen through a Steadmann type of glass column with 100 plates and the distillate was further purified of a high vacuum system. The out gassing of the liquid sample in the vacuum distillation was achieved by repeated freezing and pumping until no more non-condensible gas was evolved. The liquid sample in the system was then distilled into a vacuum reactor.

The purity of the vinyl acetate was checked by measuring the absorption spectrum. The original crude sample showed two bands at 2680 and 2590 Å, in which the band at 2590 Å was decided to be due to the acetaldehyde present in the sample. These impurity bands were completely removed by the purification described above and no band appeared between 2500 and 3000 Å in the spectrum of the purified sample. The purified sample showed no induction period in the polymerization initiated by 2,2'-azo-bis-*iso*-butyronitrile in the concentration of 10^{-4} mol. per liter. This is also an indication of the high purity of the sample.

Apparatus.—The parallel light from a Gleiter high pressure mercury lamp (SHL-200 W.) with a condenser was filtered with a Matsuda-UVD2 filter to obtain monochromatic light of 3660 Å. The intensity of the light was measured by a photoelectric tube and was kept constant by controlling the current through the lamp. The mass spectra were observed by a modified Hitachi RMA mass spectrometer. For the study of absorption spectra, a Beckman DU Spectrophotometer was used with 1 cm. cells.

Procedure.—The purified vinyl acetate (5.83 g.) and *n*-butyl mercaptan (122 g.) were measured in calibrated tubes and were mixed in a reaction cell in the molecular ratio of olefin to mercaptan 1 : 20.

The reaction cell with a reaction mixture was sealed off from the vacuum line and was irradiated with ultraviolet light of 3660 Å for forty hours. The irradiated mixture which was collected from three reaction cells, was first divided into gas (fraction I) and liquid at room temperature. By the distillation of the liquid fraction at 20°C (20 mmHg), it was further divided into two parts (named fractions II and III). One was the distillate (fraction II) consisting of excessively used mercaptan and unreacted vinyl acetate, which were collected in a cold trap (−78°C), and the other was residue (fraction III), consisting mostly of the main product, β-butylthioethyl acetate, and the termination product, α,β-dibutylthioethyl acetate.

The mass-spectroscopic analysis of fraction I showed the mass numbers 2 and 88, which correspond to hydrogen and ethyl acetate, respectively.

Fraction II was distilled fractionally with a Steadmann type glass column at an atmospheric pressure under nitrogen. One gram of crude ethyl acetate (b. p. 78.1～83.0°C) and 0.5 g. of unreacted vinyl acetate (b. p. 72.1～73.0°C) were obtained together with mercaptan. In order to confirm the existence of ethyl acetate, Dragendorff's xanthate color test[6] was carried out on the crude fraction (b. p. 78.1～83.0°C). The test showed violet color, the indication of ethoxyl residue. The same color test gave us no color with vinyl acetate and blue color with mercaptan.

Fraction III was fractionated under reduced pressure. Thirty-two grams of β-butylthioethyl acetate (b. p. 62°C at 0.7 mmHg n_D^{25} 1.4954) was obtained as the main product. Another product of α,β-dibutylthioethyl acetate (0.3 g.) was identified as follows.

(a) The physical properties of the sample were compared with those of the authentic sample (Table I). The authentic sample was prepared in 30% yield by the reaction of vinyl acetate (0.1 mol.) with butyldisulfide[7] (0.5 mol.) under the irradiation of ultraviolet light of 3660 Å at room temperature for forty hours.

(b) α,β-Dibutylthioethyl acetate was hydrolyzed to butylthioacetaldehyde by steam distillation with a drop of sulfuric acid. The aldehyde gave a hydrazone (m.p. 63～64°C) with 2,4-dinitrophenyl hydrazine and no depression of the melting point when mixed with the hydrazone of the authentic sample. The authentic sample was prepared as follows: The solution of sodium mercaptid (0.5 mol.) in ethanol (200 ml.) was added to the solution of bromoacetaldehyde dimethyl acetal[8] (0.5 mol.) in ethanol (30 ml.) at room temperature. After refluxing for half an hour, sodium bromide and ethanol were removed and *n*-butylthioacetaldehyde diethyl acetal (b. p. 75°C at 0.1 mmHg, n_D^{25} 1.4532) was obtained in the yield of 60.0%.

Found: C, 54.02; H, 10.43. Calcd. for $C_8H_{18}O_2S$: C, 53.91; H, 10.18%.

n-Butylthioacetaldehyde dimethylacetal was hydrolyzed by refluxing with dilute sulfuric acid. *n*-Butylthioacetaldehyde (b. p. 88°C at 24 mmHg) was obtained from the reaction mixture by steam distillation in the yield of 77.6%. The 2,4-dinitrophenyl hydrazone of this substance had m. p. 62.0～63.0°C.

Found: N, 17.53. Calcd. for $C_{12}H_{16}O_4N_4S$: N, 17.94%.

When oxygen was used as the quencher of atomic hydrogen the reaction mixture was exposed to dry air in the reaction cell before the irradiation and

7) L. D. Small, J. H. Bailey and C. J. Cavallito, ibid., **69**, 1711 (1947).
8) P. Z. Bedoukian, ibid., **66**, 651 (1944).

the cell was sealed off from the vacuum line at −78°C. By the analysis of fraction I no ethyl acetate was identified, although traces of water and hydrogen were detected.

The authors are indebted to Mr. Asaji Kondo for the elementary analyses and to Mr. Haruyoshi Sakurai for the mass spectroscopic analyses. The authors' thanks are also due to Dr. Shoji Shida and Dr. Saburo Fujii for their helpful discussions in carrying out this study.

Laboratory of Organic Chemistry
Tokyo Institute of Technology
Meguro-ku, Tokyo

Synthesis and Physical Properties of Normal Higher Alcohols. II. Synthesis of Normal Higher Primary Alcohols of Odd Carbon Numbers from Heptacosanol to Heptatriacontanol

By Akira WATANABE*

(Received August 17, 1959)

In continuation of the work described in the preceding paper[1], synthesis of the normal higher primary alcohols of odd carbon numbers containing from twenty-seven to thirty-seven carbon atoms were undertaken and gave the desired products as pure as practicable.

Heptacosanol was prepared by Bowman's method[2], which was outlined in the first paper[1], from arachidic acid and ethyl ε-bromocaproate. The reaction is shown in the following equations.

$$\underset{\text{(I)}}{C_2H_5O_2C(CH_2)_nBr} \xrightarrow{\text{Ethyl malonate}}$$

$$\underset{\text{(II)}}{C_2H_5O_2C(CH_2)_nCH(CO_2C_2H_5)_2} \xrightarrow{C_6H_5CH_2OH}$$

$$\underset{\text{(III)}}{C_6H_5CH_2O_2C(CH_2)_nCNa(CO_2CH_2C_6H_5)_2} \xrightarrow{RCOCl}$$

$$\underset{\text{(IV)}}{C_6H_5CH_2O_2C(CH_2)_nC(CO_2CH_2C_6H_5)COR} \xrightarrow{H_2}$$

$$\underset{\text{(V)}}{HO_2C(CH_2)_nC(CO_2H)COR} \xrightarrow{-CO_2}$$

$$\underset{\text{(VI)}}{RCO(CH_2)_{n+1}CO_2H} \xrightarrow{\text{Huang-Minlon}}$$

$$\underset{\text{(VII)}}{R(CH_2)_{n+2}CO_2H} \xrightarrow{C_2H_5OH}$$

$$\underset{\text{(VIII)}}{R(CH_2)_{n+2}CO_2C_2H_5} \xrightarrow{LiAlH_4} \underset{\text{(IX)}}{R(CH_2)_{n+3}OH}$$

By means of the same series of reactions but starting with higher fatty acids and ω-bromoacids, higher alcohols than heptacosanol were synthesized. Since the use of ω-bromoacids is restricted by the difficulty of their preparation in pure state when the carbon chain is considerably long, the author has used a series of long chain fatty acids along with the ω-bromoacids I where n is 5, 7 and 10.

The three bromoacid ethyl esters required for condensation with ethyl malonate were prepared by the following methods. Ethyl ω-bromocaproate was obtained by the method described in the first paper. Ethyl ω-bromooctanoate was prepared, with some modification, according to Hunsdiecker's method[3]. Silver salt of ethyl hydrogen azelaate was added to the carbon tetrachloride solution of bromine in reverse of the customary procedure. The yield was 80% which was better as compared with those of the analogous synthesis of Hunsdiecker (69.7%).

Ethyl ω-bromoundecanoate was obtained from undecylenic acid by addition of dry hydrogen bromide in the presence of benzoyl peroxide followed by exhaustive esterification, according to Jones' method[4].

Besides commercially available fatty acids, the long chain fatty acids such as arachidic (C_{20}), tricosanoic (C_{23}), tetracosanoic (C_{24}) and pentacosanoic (C_{25}) acids were synthesized from octadecyl bromide, heneicosyl bromide, and docosyl bromide by repetition of the modified malonic ester synthesis[5].

The condensation products of benzyl alkanetricarboxylates with acid chlorides were semisolid brown materials which were subjected to

* Some parts of this wark were performed at the Department of Chemistry, Faculty of Science, Kyoto University; Sakyo-ku, Kyoto.

1) A. Watanabe, This Bulletin, **32**, 1295 (1959).
2) R. E. Bowman, *J. Chem. Soc.*, **1950**, 174.
3) H. Hunsdiecker et al., *Ber.*, **75B**, 29 (1947).
4) R. G. Jones, *J. Am. Chem. Soc.*, **69**, 2350 (1947).
5) W. Bleyberg et al., *Ber.*, **64**, 2506 (1931).

TABLE I

Alcohols	Formula	Calcd. C	Calcd. H	Found C	Found H	m. p., °C	f. p. °C	t. p. °C
Heptacosyl	$C_{27}H_{56}O$	81.74	14.23	81.59	14.36	80.5(81.0)[a]	80.0	7.25
Nonacosyl	$C_{29}H_{60}O$	82.10	14.24	81.30	14.03	83.5(83.8)[b]	82.5	75.0
Hentriacontyl	$C_{31}H_{64}O$	82.22	14.25	81.97	13.95	87.0(87.0)[b]	85.8	78.5
Tritriacontyl	$C_{33}H_{68}O$	82.42	14.25	82.19	14.35	88.5(88.6)[b]	87.8	
Pentatriacontyl	$C_{35}H_{72}O$	82.60	14.26	82.83	14.01	91.2(91.5)[b]	89.5	
Heptatriacontyl	$C_{37}H_{76}O$	82.75	14.27	82.92	14.15	92.7	91.6	

Melting points are uncorrected.

When a sample is cooled below its freezing point, transition appears with change of the transparent waxy material into opaque crystalline state. Transition points of C_{33}, C_{35}, C_{37} alcohols could not be observed.

a) S. Shiina, *J. Soc. Chem. Ind. Japan* (*Kogyo Kwagaku Zasshi*), **39**, 345 (1936).

b) R. G. Johns, *J. Am. Chem. Soc.*, **69**, 2350 (1947).

TABLE II

Ethyl alkane-tricarboxylates	Acid chlorides	Cno.	Ketonic acids	m. p. °C	Fatty acids	m. p., °C
n-Hexane	Eicosanoyl(C_{20})	27	$CH_3(CH_2)_{15}CO(CH_2)_6CO_2H$	99.5	Heptacosanoic	86.6(87)*
	Docosanoyl(C_{22})	29	$CH_3(CH_2)_{20}CO(CH_2)_6CO_2H$	101	Nonacosanoic	98.7(89.2)*
n-Octane		31	$CH_3(CH_2)_{29}CO(CH_2)_8CO_2H$	105	Hentriacontanoic	92.5
	Tetracosanoyl(C_{24})	33	$CH_3(CH_2)_{24}CO(CH_2)_8CO_2H$	107	Tritriacontanoic	96.0
n-Undecane	Tricosanoyl(C_{23})	35	$CH_3(CH_2)_{21}CO(CH_2)_{11}CO_2H$	109	Pentatriacontanoic	98.0
	Pentacosanoic(C_{25})	37	$CH_3(CH_2)_{23}CO(CH_2)_{11}CO_2H$	110	Heptatriacontanoic	98.7

* S. Shiina, *J. Soc. Chem. Ind. Jap.* (*Kogyo Kwagaku Zassi*), **39**, 345 (1936).

TABLE III

Starting materials: Fatty acids	m. p. °C	Intermediates: Alcohols	m.p., °C	Bromides[a] m.p., °C	Malonic[b] acids m.p., °C	Products: Fatty acids[c]	m. p., °C	Yields to bromides %
Stearic	68.5	Octadecyl	58	28.5	109	Eicosanoic	75(75.5[d])	75
Behenic	79	Docosyl	71.5	44.0	125	Tetracosanoic	85(86.0[e])	50
Tricosanoic	78.5	Tricosyl	72.0	51.0	—	Pentacosanoic	83.5(85[e])	42

a) Bromination of the alcohols was modelled after Reid. [E. E. Reid et al., "Organic Syntheses" Vol. 15, John Willey & Sons, Inc., New York (1935), p. 26]. Hydrogen bromide was passed for 15 hr. in each alcohol.

b) Recrystallized from benzene.

c) The malonic acids were decarboxylated in vacuo and the resulting fatty acids were recrystallized from benzene.

d) F. Adam et al., *J. Chem. Soc.*, **1926**, 72.

e) P. A. Levene et al., *J. Biol. Chem.*, **59**, 921 (1924).

hydrogenation without purification, since it is known[2] that the compounds of this type can not be purified. Therefore, for the successful hydrogenation of the compounds, it is essential to purify the acid chlorides by distillation. However, since arachidyl and higher acid chlorides were found to decompose even under vacuum distillation at 2 mmHg, these acid chlorides were subjected to further reaction without distillation. In this case, oxalyl chloride proved to be superior for the preparation of acid chlorides to thionyl chloride because it furnished cleaner products. On hydrogenation considerable poisoning of the catalyst was found even when distilled acid chloride was used. After debenzylation and decarboxylation, the desired ketonic acids were obtained in low yield of about 35%, considerable amount of the starting fatty acids being recovered. Huang-Minlon reduction[6] of the ketonic acids took place readily to give the corresponding fatty acids which, after conversion to their ethyl esters, were led to the final products by reduction with lithium aluminum hydride.

6) Huang-Minlon, *J. Am. Chem. Soc.*, 68, 2487 (1946).

Repeated recrystallizations of the alcohols from benzene or toluene gave products having sharp melting points and excellent analytical values. For hentriacontanol $C_{31}H_{63}OH$ and higher alcohols high vacuum distillation as well as recrystallization was employed. In order to prevent thermal degradation during distillation, the pressure was reduced to 2×10^{-3} mmHg so as to maintain the bath temperature below 210°C.

Melting points, transition points and analytical data of these alcohols are given in Table I. Heptatriacontanol $C_{37}H_{75}OH$ has not been reported previously. All the transition points have been unknown. Combination of the starting materials and the melting points of the intermediate ketonic acids and fatty acids are given in Table II. The physical properties of these alcohols are being investigated and the results will be reported in a separated communication.

Experimental

Preparation of ω-Bromo Acids and their Condensation with Ethyl Malonate. — *Ethyl ε-bromocaproate.*—It was prepared from caprolactone by the method described in Part I[1]. The physical constants are as follows: b. p. 118°C/14 mmHg or 98°C/4.5 mmHg, n_D^{32} 1.4561.

Ethyl ω-bromooctanoate.—The procedure of Hunsdiecker[3] was followed with some modification to give increased yield. Pure azelaic acid (m. p. 104~106°C) obtained by repeated recrystallizations of commercial specimen from aqueous ethanol was converted to its ethyl ester by exhaustive esterification. Boiling point of the ester was 135~137°C at 6.5 mmHg (reported: 130~132°C at 5 mmHg)[7]. Above acid (130 g.) and its ethyl ester (98 g.) were treated in the same manner as described in Organic Syntheses[8] for the preparation of ethyl hydrogen sebacate and yielded 62 g. of the monoester; b. p. 161 ~ 163°C/1 mmHg (reported: 169 ~ 170°C/2 mmHg)[9]. Silver salt of the monoester was prepared by an analogous manner described in Part I[1] for the preparation of silver heneicosanoate. The thoroughly dried silver salt (85 g.) was added portionwise to a solution of 60 g. of bromine in 100 ml. of carbon tetrachloride under strict exclusion of moisture. A vigorous reaction ensued with evolution of carbon dioxide. When no more gas evolved, the solution was filtered, washed with water, aqueous solution of sodium hydroxide, again water, and dried over sodium sulfate. Following evaporation of the solvent the residue was distilled through a short Widmer column to give a liquid having a boiling point of 125°C at 3.5 mmHg. n_D^{27}, 1.4572: Yield, 53 g. (80%), (reported: 69.7% for methyl compound)[3].

Ethyl ω-bromoundecanoate. — The preparation of the corresponding acid was essentially the same as the method described by Jones[4]. The melting point of the acid was 48~49.5°C (reported: 49~50°C).

Ethylester of the acid was obtained in an almost quantitative yield by exhaustive esterification. b. p. 148~150°C/5 mmHg, m. p. 11.5~13.5°C, n_D^{20} 1.4651.

The three ethyl esters of ω-bromo acids mentioned above were condensed with sodiomalonic ester by an usual method to give ethyl alkanetricarboxylates in good yields. The constants are: *Ethyl n-hexane-1, 1, 6-tricarboxylate* (II where *n* is 5): b. p. 150~151°C/1 mmHg, n_D^{28} 1.4360. *Ethyl n-octane-1, 1, 8-tricarboxylate* (II where *n* is 7): b. p. 170~172°C/1.5 mmHg, n_D^{28} 1.4380. *Ethyl n-undecane-1, 1, 11-tricarboxylate* (II where *n* is 10): b. p. 187°C/1 mmHg, n_D^{28} 1.4435.

Preparation of Long Chain Fatty Acids.—Except heneicosyl bromide which was prepared from behenic acid by degradative bromination[1], a long chain alkyl bromides were made by the reduction of the corresponding acid esters to the alcohols by high pressure hydrogenation or using lithium aluminum hydride followed by treatment with hydrogen bromide. Further treatment of the alkyl bromides with sodiomalonic ester in butanol[3] in place of ethanol led to the acids of two additional carbon atoms. Since these reactions are relatively well known, detailed descriptions of the experiments were omitted and the results are summarized in Table III.

Preparation of Higher Alcohols. — General procedures of the synthesis are very similar throughout the series, so only an example for the preparation of heptatriacontanol $C_{37}H_{75}OH$ is described in detail.

Benzyl n-undecane-1, 1, 11-tricarboxylate. — To a suspension of sodium ethoxide (prepared from 0.38 g. of freshly cut sodium and 10 ml. of absolute ethanol) in benzene was added 6.15 g. of ethyl undecane-1, 1, 11-tricarboxylate. After the sodium ethoxide dissolved 5.35 g. of purified benzyl alcohol was added, the mixture was distilled through a Fenske column until the boiling point reached to 80°C. During this time an almost theoretical quantity of ethanol was removed.

13-Keto-heptatriacontanoic acid $C_{24}H_{49}CO(CH_2)_{11}\cdot CO_2H$.—To the benzene solution of the above tribenzyl esters was added gradually 6 g. of pentacosanoyl chloride in benzene (prepared from 5.8 g. of pentacosanoic acid and 7.5 g. of oxalyl chloride, and excess of the oxalyl chloride was removed under reduced pressure at 100°C). The reaction mixture was refluxed for 1 hr. After cooling, the solution was washed with ice water to neutral reaction and then dried over sodium sulfate. The solvent was removed under reduced pressure at 50°C of bath temperature to give a brown colored oil which solidified on standing at room temperature. Yield, 20 g. Hydrogenation of the above compounds in 60 ml. of ethyl acetate over Pd-C (5 g.) and Pd-$SrCO_3$ (5 g.) took place at a slightly positive hydrogen pressure, accompanying a considerable poisoning of the catalysts. A nearly theoretical amount of hydrogen was absorbed within 3 hr. The catalyst was filtered off, then the ethyl acetate solution was refluxed for 1 hr. to decarboxylate compound V. Upon cooling to room temperature, small crystals were separated. They were recrystallized twice from ethyl acetate to give the product

7) Jones et al., *J. Chem. Soc.*, **1928**, 68.
8) S. Swann, "Orgamic Syntheses", Vol. 19, John Wiley & Sons, Inc., New York (1938), p. 45.
9) M. Asano, *J. Pharm. Soc. Japan*, **504**, 8 (1924).

having a melting point of 105 to 107°C. Further recrystallizations from benzene gave a pure acid. m. p. 108~109°C. Yield, 3.2 g. (37%). From the mother liquor, 2.5 g. of the pentacosanoic acid was recovered.

Heptatriacontanoic acid $C_{36}H_{73}CO_2H$.—The Hung-Minlon reduction of long chain ketonic acid was found to be superior to the Clemmensen reduction[4], because of its effectiveness and simplicity. The experimental conditions were essentially the same as those described in the first paper. A mixture of 3 g. of the ketonic acid, 3 g. of potassium hydroxide, 3 ml. of 85% hydrazine hydrate and 25 ml. of diethylene glycol (b. p. 250°C) was refluxed for 1 hr. After removing the water formed, the temperature of the mixture was gradually raised to 200°C and the refluxing was continued at this temperature for 6 hr. When the mixture was cooled to about 80°C. it was poured into a 100 ml. of water containing 15 ml. of hydrochloric acid with stirring. A white solid separated was collected and washed with water, and then dried. Yield of the crude acid was nearly quantitative. Repeated recrystallizations from benzene and then toluene gave a pure product with little loss of the material, m. p. 97.5~98.5°C.

Found: C, 78.42; H, 13.10. Calcd. for $C_{37}H_{72}O_2$: C, 78.66; H, 12.85%.

Heptatriacontanol $C_{37}H_{75}OH$.—Ethyl heptatriacontanoate (2.5 g.) was readily reduced to the alcohol with lithium aluminum hydride in absolute ether[1]. The reaction mixture was hydrolyzed to remove the small amount of unchanged ester, but traces of alkali or soap could not be removed from the product by crystallization. Pure alcohol could be obtained by high vacuum distillation at 2×10^{-3} mmHg followed by repeated crystallizations from toluene, m. p. 92~92.7°C. Yield, 1.8 g.

The author expresses his sincere thanks to Professor Ryozo Goto, Kyoto University, for his kind guidance throughout this study. Thanks are also due to the Ministry of Education for a Grant-in-Aid for Scientific Research.

Department of Applied Chemistry
Himeji Technical College
Idei, Himeji

Benzylideneaniline. I. Structure and Ultraviolet Absorption Spectrum of Benzylideneaniline

By Nozomu EBARA

(Received July 31, 1959)

Benzylideneaniline has been believed to assume a planar structure without any experimental proof, as it has a similar molecular constitution as stilbene or azobenzene, of which the geometries are proved to be planar by the aid of X-ray diffraction method[1]. Benzylideneaniline, however, has many unusual properties which can not be accounted for by the planar structure.

1) Imoto[2] measured the pK values of the several carboxyl derivatives of substituted benzylideneanilines and found that the conduction of the effects of the substituents across the central C=N double bond is extraordinarily small. His data show that *N*-(substituted benzylidene)-*p*-aminobenzoic acid has the pK value almost equal to that of *p*-aminobenzoic acid.

2) Hertel and Schinzel[3] investigated the reaction of methyl iodide with the lone pair electron of N atom in benzylideneaniline and found that the substituents on the aniline ring exert remarkable effects on reaction velocity, while the effects of the substituents on the other ring are negligibly small.

3) The dipole moment of *p,p'*-dinitrobenzylideneaniline was reported to have the intermediate value between those expected for *trans* and *cis* forms[1].

4) Benzylideneaniline seems to show no geometrical isomerism, in contrast to stilbene, azobenzene and azoxybenzene, of which the two isomers can be detected and easily separated. Wyman[5], by means of the rotating-shutter technique, found that the solution of this substance does not show any spectral change when exposed to light. Gaouck and LeFèvre[6] investigated the polymorphic crystals of the derivatives of benzylideneaniline by means of

1) (a) J. M. Robertson and I. Woodward, *Proc. Roy. Soc.*, **162A**, 568 (1937). (b) J. M. Robertson, *J. Chem. Soc.*, 1939, 232.
2) E. Imoto et al., Presented at the 12th Annual Meeting of Chemical Society of Japan, Kyoto, April, 1959.
3) E. Hertel and M. Schinzel, *Z. physik. Chem.*, **B48**, 289 (1941).
4) K. A. Jensen and N. Hofman-Bang, *Ann.*, **548**, 106 (1941).
5) G. M. Wyman, *Chem. Revs.*, **55**, 625, (1955).
6) V. De Gaouk and R. J. W. LeFèvre, *J. Chem. Soc.*, 1938, 741.

the measurements of dipole moments and of absorption spectra, and concluded that these molecules exist exclusively in *trans* forms.

5) It has been shown[7] that the phase diagrams of the admixtures of benzylideneaniline with *trans*-stilbene, *trans*-azobenzene, phenanthridine or bibenzyl[8] involve discontinuous curves, while those of the admixtures between *trans*-stilbene, *trans*-azobenzene and bibenzyl speak for the perfect miscibility. This fact is likely to show that the structure of benzylideneaniline corresponds to neither *trans* nor *cis* form.

6) The shape of the ultraviolet absorption spectrum of benzylideneaniline is quite different from those of stilbene, azobenzene and azoxybenzene, which resemble each other very closely. Wiegand and Merkel[7] found that the spectrum of 2-phenylbenzimidazole (I) exhibits a similarity to stilbene and not to benzylideneaniline, while that of 2-phenylindene (II) is very much similar to that of stilbene, where I and II must have planar *trans* structures. They proposed a linear planar structure for benzylideneaniline, but it seems inadequate, as it has no theoretical basis and is energetically less favorable.

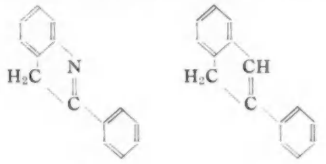

I II

7) Benzylideneaniline shows no $n-\pi^*$ transition at the longer wavelength region. Jaffé[9] has assumed that this transition is hidden under the long tapering end of the absorption curve of 315 mμ band, but it appears that the strong experimental support is lacking for this assumption.

These experimental facts are not consistent with the generally accepted stilbene-type structure, and yet very few works have been carried out with regard to the very nature of the benzylideneanilinemolecule. Therefore, series of experiments are now undertaken to explain some fundamental problems of benzylideneaniline.

Results and Discussion

Measurements were carried out on the ultraviolet absorption spectra of benzylideneaniline, stilbene, azobenzene and azoxybenzene in *n*-heptane, ethanol and 50% mixture of ethanol and concentrated hydrochloric acid, together with their variations caused by the substituent groups, and for comparison, spectra of some aromatic compounds were also measured. The results are shown in Tables I and II and in Fig. 1.

If benzylideneaniline assumes the stilbene-type planar structure, there must be some substantial similarity in behavior between the spectra of benzylideneaniline and of stilbene, azobenzene or azoxybenzene.

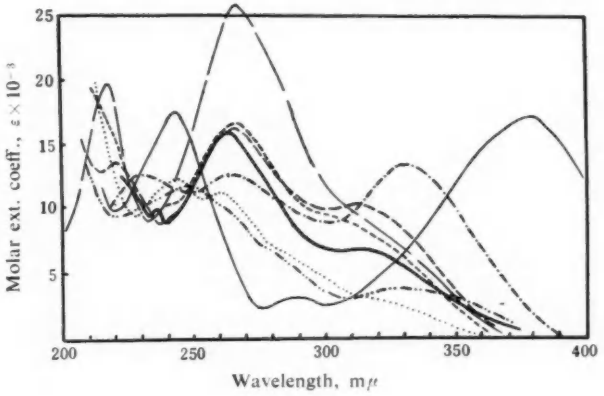

Fig. 1. Spectra of benzylideneanilines: (in C_2H_5OH)

R = —— H ; —— *p*-NO_2 ; —— *m*-NO_2 ; -·-· *p*-OCH_3 ; -···- *o*-OCH_3 ; —— *p*-Cl ; ------ *m*-Cl ; ····· *o*-Cl.

7) C. Wiegand and E. Merkel, *Ann.*, **550**, 175 (1942).
8) Bibenzyl is found to have the planar *trans* conformation (Ref. 1b).
9) H. H. Jaffé, S. Yeh and R. W. Gardner, *J. Molecular Spectroscopy*, **2**, 120 (1958).

Table I. Wavelengths and intensities of ultraviolet absorption maxima (in C_2H_5OH)

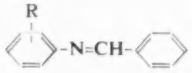

R	Free bases abs. max. λ, mμ	ε_{max}	Conjugate acids abs. max. λ, mμ	ε_{max}
H	236	10100	250	13900
	263	16400	290	2000
	315	6200	360	—
o-Cl	244	12400	220	7400
	260	11200	250	10300
	290	—	290	2800
	330	2700	360	—
m-Cl	240	10300	220	7200
	264	16900	250	13900
	310	8800	290	3200
			360	—
p-Cl	223	13800	220	8800
	264	16600	250	14600
	314	10400	290	2250
			360	—
o-OCH_3	246	11700	220	10800
	263	—	250	15700
	330	3850	290	—
			373	—
p-OCH_3	229	12900	223	11500
	264	13100	250	15500
	330	13300	290	—
			360	—
m-NO_3	218	19900	252	22900
	267	25900	290	—
	325	6730	355	—
p-NO_3	243	17300	252	22200
	290	3040	290	—
	380	16800	335	—

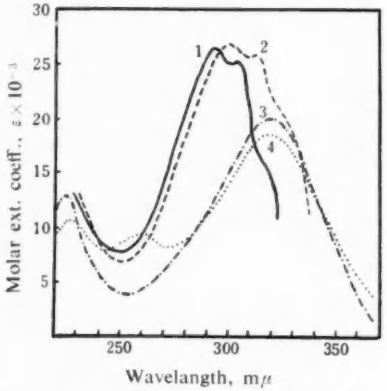

Fig. 2. Spectra of: 1, —— stilbene; 2, ---- *p*-methoxystilbene; 3, -·-· azobenzene; 4, ····· azoxybenzene. (in C_2H_5OH)

Table II. Wavelengths and intensities of some aromatic compounds (in C_2H_5OH)

R_1	R_2	λ, mμ	ε_{max}
Cl	H*	209.5	7400
		263.5	190
OCH_3	H	220	7020
		271	1830
NO_3	H*	268.5	7800
NH_2	H	235	8100
		285	1400
	o-Cl	238	8740
		292	2480
	m-Cl	245	9000
		295	2300
	p-Cl	239	11700
		290	1500
	o-OCH_3	235	10000
		285	3700
	p-OCH_3	235	8450
		300	2580
	o-NO_3	230	13100
		278	4220
		406	4250
	m-NO_3	234	14900
		282	3560
		373	1310
	p-NO_3	230	6600
		368	15200
CHO	H*	249.5	11400
		285	—
NH^+_3	H*	203	7500
		254	160
	p-Cl*	215.5	9200
		263	360
	p-NO_3*	208	7800
		258	8700

* L. Doub and J. M. Vandenbelt, *J. Am. Chem. Soc.*, **69**, 2714 (1947).

Stilbene, as well as azobenzene and azoxybenzene, shows an intense absorption maximum near 300~320 mμ, which has been interpreted to be the $\pi - \pi^*$ transition[9-12]. This band shifts toward longer wavelength when *p*-position is substituted. The spectrum of azobenzene in concentrated sulfuric acid was measured by several authors, and it was suggested that the band at 320 mμ in neutral solvent shifts to 420 mμ in acidic medium, whereby its intensity also increases considerably. This shift has been explained by Jaffé[9] in terms of the LCAO

10) P. P. Birnbaum, J. H. Linfold and D. W. G. Style, *Trans. Faraday Soc.*, **49**, 735 (1953).
11) H. Suzuki, This Bulletin, **25**, 145 (1952).
12) W. Maier, A. Saupe and A. Englert, *Z. physik. Chem., N. F.*, **10**, 273 (1957).

method by taking into account the increase of Coulombic integral of the nitrogen atom when proton attaches to it.

In the present experiment the activity of proton seems to be insufficient to convert the substance completely into its conjugate acid, and it can be inferred from Fig. 3 that there is

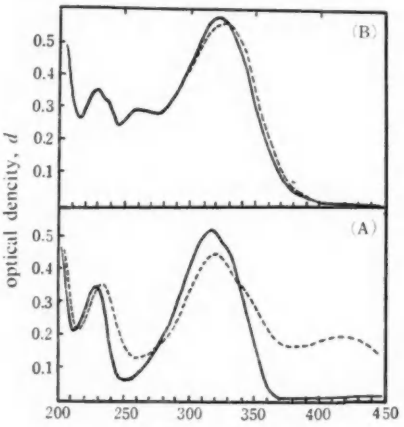

Fig. 3. Spectra of (A) azobenzene and (B) azoxybenzene in —— C_2H_5OH and in ------ C_2H_5OH+conc. HCl

an equilibrium between azobenzene and its conjugate acid. In the same condition, azoxybenzene does not undergo any remarkable change in spectrum. This fact may be explained by the consideration that owing to the inductive effect of N→O coordination, basicity of this molecule is greatly reduced compared with that of azobenzene. But the inspection of the shape of the spectrum is likely to tell that also in this case a red shift occurs when conjugate acid is formed.

Benzylideneaniline shows an intense band at 263 mμ and a weak band at about 315 mμ, the latter has been assigned as the $\pi-\pi^*$ transition which corresponds to that of stilbene near 300 mμ[9]. But it can hardly be accepted when one compares it with those of azobenzene or azoxybenzene, as the reduction of symmetry in benzylideneaniline would not reduce the intensity more than that of azoxybenzene. Also it is difficult to assume the 263 mμ band as this transition, as its wavelength is too short and the substituents on the ring exert too little effects upon this band as compared with stilbene or azobenzene. In addition to this, these interpretation can not account for the aforementioned spectrum of 2-phenylbenzimidazole (I), for which the planar *trans* structure is to be assumed. Moreover, acidic medium causes large

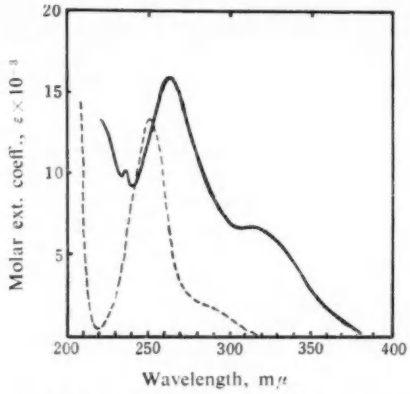

Fig. 4. Spectra of benzylideneaniline —— and its conjugate acid ---- (in C_2H_5OH)

unexpected change on these bands (Fig. 4): these bands become weak and shift toward shorter wavelengths, and the spectrum of free base diminishes completely. Measurements were made with various acid concentrations, but no change occurs unless acid concentration was reduced below 10^{-3} mol./l. (the base concentration remaining about 10^{-4} mol./l.). In addition to this, these shifted bands are at the same position even when the aniline ring is substituted. As there is no time-dependence in spectrum during the measurements, and the decomposition rate of this molecule is found to be not so large, this spectrum must be attributed to the conjugate acid.

To explain these experimental results, together with the peculiarities cited above, an alternative geometrical structure must be proposed for this molecule. One possible structure may be such that the benzene ring at the N side is nearly perpendicular to the rest of the molecule (which accounts for problem 5 cited above).

When this structure is assumed, there may be a strong aniline-type resonance interaction, and, as a result, the $n-\pi^*$ transition is necessarily missing (problem 7). In addition, the interaction of benzene rings across the C=N double bond would be reduced to a large extent (problem 1), and the ultraviolet absorption spectrum would become close to the superposition of those of its components, aniline-type and styrene-type (problem 6). Then the substituent on the aniline ring would exert a large influence upon the lone-pair electron, whereas that on the other ring would not (problem 2).

The absence of geometrical isomerism can also be explained with this model. The C-N-C bond angle may be 120° with sp^2 hybridization, 180° with sp hybridization or intermediate with higher order hybridization. If it is 180°, there can be no geometrical isomerism at all; if it is

120° or intermediate, there may be bending isomerization through intermediate *sp* structure, where the benzene ring would become absolutely perpendicular so as to reduce the energy of this state by the increase of resonance interaction between nitrogen non-bonding orbital and benzene π orbital, and this would permit the undetectably fast reaction (problem 4). Probably the hybridization and the angle of the twist of the benzene ring would be such as to minimize the energy of the molecule, and when the ring is almost perpendicular, the hybridization will be close to *sp*.

Whether this is the case or not may be inferred also from the examination of the absorption spectra.

The spectra of the conjugate acids must be similar to the superposition of those of substituted anilinium ions and the conjugate acid of *N*-benzylidene-alkylamine, with a slight modification caused by the small interaction between these two. In benzylideneaniline, the former should have the absorption maximum at 254 mμ, of which the intensity is so weak that it should be hidden under the intense band of the latter. The latter is isoelectronic with benzaldehyde and the bands of conjugate acids at 250 and 290 mμ can be compared with 249.5 and 285 mμ bands of benzaldehyde, respectively (247 mμ of benzylidene-methylamine). In the case of the conjugate acids of benzylidene-*m*- and -*p*-nitroaniline, 252 mμ band is very intense, perhaps owing to the overlap of the intense 268.5 mμ band of nitrobenzene component, as its extinction coefficient is just in the same magnitude as the sum of those of two components. For the conjugate acid of benzylidene-*o*- and -*p*-anisidine, there is an additional band at 220 mμ which coincides with 217 mμ band of anisole, intensified by the substituent ($-N^+=$). Also the 220 mμ band of chlorine-substituted conjugate acids can be compared with the 210 mμ band of chlorobenzene (216 mμ of *p*-chloranilinium ion).

The assignment of the bands near 360~370 mμ are not certain, but one tentative explanation is that they may be the transitions between orbitals of the two components, as their intensities are of the order of $n-\pi^*$ transition**.

The assignment of the spectra of free bases is more obscure, but the bands near 315 mμ experience considerable perturbation due to the introduction of substituents and can presumably be compared with the 285 mμ band of aniline (296 mμ of dimethylaniline). The latter is found to correspond with A_{1g}–B_{2u} transition of benzene at 260 mμ, allowed by the perturbation of the amino-substituent group, and becomes more intense and shifts toward red by successive substitution, because perturbation becomes larger. In the case of benzylideneanilines, the orbitals will mix to some extent with those of the other benzaldehyde-type part; therefore, one can probably expect that their positions and intensities may be such as these.

The band at 264 mμ is more difficult to interprete, but the absence of the effects of the substituents on this band is likely to show that this band comes from the styrene-type part; i.e. corresponds to the 250 mμ band. It seems at first unlikely that in the conjugate acid the band shifts toward shorter wavelength. However, this can probably be accepted when one assumes that the nitrogen valence orbital is nearly *sp* in free base but becomes sp^2 when conjugate acid is formed, and that the C=N bond length is longer in *sp* than in sp^2. Calculation was carried out for the transition energy of R–N=CH–C_6H_5 (R=alkyl) by the simple LCAO method, assuming that for the conjugate acid the Coulombic integral of N atom is $\alpha+\beta$, the exchange integral of C=N bond, which must have strong double bond character, 1.2β, and that of C–C_{ring}, which is predominantly single, 0.6β and for the free base, these integrals are $\alpha+\beta/2$, β and 0.6β, respectively; where α and β represent their usual meanings (Fig. 5). The

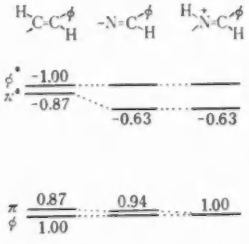

Fig. 5. Energy diagram (in β unit).

result shows that the effect of the change in C=N bond length offsets the reverse effect of the change in Coulombic integral of the nitrogen atom, and the hypsochromic shift will occur when conjugate acid is formed.

Other bands near 230~240 mμ may be attributed to the aniline-type part, as their positions coincide and their intensities are of comparable magnitude.

The spectrum of benzylidene-*p*-nitroaniline exhibits the striking feature that it changes greatly with the solvent, whereas those of chloro-, methoxy- or unsubstituted benzylideneaniline does not. The 380 mμ band in ethanol shifts to 320 mμ in *n*-heptane, and its intensity decreases. This is not the case in *p*-nitrostilbene or -azobenzene, and it is highly likely that this band corresponds to 370 mμ *p*-nitroaniline charge-transfer band, and that the band at 243

** Or it may be that they come from the decomposition products.

mμ is the superposition of 230 mμ of *p*-nitroaniline and 250 mμ of styrene-type part. Their intensities are also consistent with this assumption. In this case, owing to the large charge-transfer resonance interaction between nitro group and nitrogen non-bonding electron, the molecule would assume almost perpendicular conformation with the result that the spectrum of this molecule is much more similar to the superposition of those of components as compared with those of any other benzylideneanilines.

There are some experimental evidences which seem to contradict this assumption. For example, Raman spectra show that the frequencies of C=N stretching vibrations of R–C=N–R′ type compounds decrease in the order R–C=N–R′> R–C=N–Ar>Ar–C=N–Ar, where R and R′ denote alkyl groups—the fact which is parallel to that of the corresponding C=C compounds[13]. This fact is at first likely to show that benzylideneaniline has the planar conformation and the increase of the number of benzene rings causes the increase of resonance interaction, and therefore decreases the force constant of vibration. But in the present model, the resonance interaction will increase though to a smaller extent, and in addition to this, hybridization-change will occur when R′ is replaced by C_6H_5, which would also tend to reduce the force constant.

Another strong objection to this assumption is the evidence of photoisomerism of this substance at low temperature[14]. It is not certain whether this is *cis-trans* isomerism, but if it is so, one explanation is that the bending isomerization is frozen at low temperature.

Some question may arise why benzylideneaniline can assume this structure, while azobenzene can not, and why it does not return to the planar structure when proton attaches to it. In this respect, the author has the impression, though merely speculative at this stage, that azobenzene also behaves in somewhat like manner in solution, and its thermal *cis-trans* isomerization is the mixture of ordinary and bending ones, because it belongs to neither of the two types classified by Eyring[15]. This point will be investigated in future.

13) A. Kirrman and P. Laurent, *Bull. soc. chim. France*, **6**, 1657 (1939).
14) E. Fischer and Y. Frei, *J. Chem. Phys.*, **27**, 808 (1957).
15) J. L. Magee, W. S. Shand, Jr., and H. Eyring, *J. Am. Chem. Soc.*, **63**, 677 (1941).

Experimental

Benzylideneanilines were prepared by direct condensation of benzaldehyde with corresponding anilines. Stilbene and azobenzene were prepared by recrystallization of commercial substances. *p*-Methoxy-stilbene was kindly supplied by Mr. H. Suzuki. Azoxybenzene was prepared by treating nitrosobenzene with ethanol and sodium hydroxide.

Absorption spectra were measured by Cary self-recording spectrophotometer model 14 M using 1 cm. quartz cell.

Summary

The ultraviolet absorption spectra of benzylideneanilines, as well as of their conjugate acids, have been measured.

These spectra can not be explained with the ever believed stilbene-type planar structures of these molecules.

An alternative structure is proposed for benzylideneaniline with the benzene ring of aniline part nearly perpendicular to the rest of the molecule.

This structure also adequately explains many experimental evidences, which have been investigated previously but are not accounted for by the planar structure.

The author wishes to express his sincere thanks to Professor S. Nagakura for his kind instruction throughout this study. Thanks are also due to Professor K. Shiomi and to the members of his laboratory for their fruitful discussions.

Department of Chemistry
College of General Education
The University of Tokyo
Meguro-ku, Tokyo

Benzylideneaniline. II. Iodine Complexes of Benzylideneaniline and its Derivatives

By Nozomu EBARA

(Received July 31, 1959)

In the preceding paper the author proposed for benzylideneaniline a structure with the benzene ring of N side nearly perpendicular to the rest of the molecule. Then the non-bonding electron will migrate into the benzene ring to a large extent, and the ionization potential of the lone-pair electron will increase and its donor ability will decrease compared with the case where there is no interaction. To examine the validity of this assumption, the nature of the lone-pair electron is now investigated by means of the measurement of the equilibrium constant of iodine complex.

Iodine Complex.—The interaction between iodine molecule and aromatic compounds was firstly suggested by Benesi and Hildebrand[1] to be the acid-base type interaction, where the iodine molecule behaves as an acid and the aromatic molecule as a base. It has been shown by Mulliken[2] that this type of interaction is based upon charge-transfer resonance stablilization, and the new absorption band in the ultraviolet region, which was absent in both component molecules but now comes into appearence in the complex, can be interpreted as the charge-transfar band, for which this resonance interaction is responsible. This band was also explained by Kuboyama and Nagakura[3] from the LCMO treatment to be due to the electron transition from the perturbed higest filled orbital of the donor component to the lowest vacant σ_u MO of iodine component. Also the absorption band of I_2 shifts toward shorter wavelengths when a complex is formed, which again can be interpreted from the consideration that the σ_u MO of I_2 is raised while the π_g MO is not so much affected[1]. This phenomenon has been investigated extensively by many authors[2-7] for a large variety of compounds including as bases those with lone pair electrons or π-electrons, and the equilibrium constants, as well as heats and entropies of formation of these complexes have been measured[8-10].

Hastings, Franklin, Schiller and Matsen[11] and McConnell, Ham and Platt[12] correlated the positions of charge-transfer absorption maxima with the ionization potentials of the donor molecules and found an excellent agreement between theory and experiments.

When benzylideneaniline is used as the base, the donor orbital may be non-bonding orbital, π-orbital or both, and the position of the charge-transfer band will be the fingerpost for assuming the ionization potential of the donor orbital, and the equilibrium constant will serve as a criterion of the geometry of this molecule.

Results and Discussion

The spectra of the mixtures of iodine and benzylideneaniline in various concentrations in

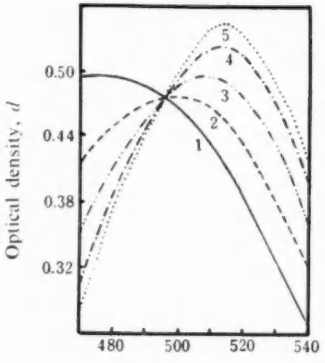

Fig. 1. Spectra of benzylideneaniline+I_2 in CCl_4; Base concentration: 1, —— 1.10; 2, ---- 0.55; 3, ·-·-· 0.275; 4, -·-· 0.138; 5, ····· 0.069 mol./l. I_2 concentration 1.74×10^{-4} mol./l.

1) H. A. Benesi and J. H. Hildebrand, *J. Am. Chem. Soc.*, **70**, 2832 (1948).
2) R. S. Mulliken, ibid., **72**, 600 (1950); **74**, 811 (1952); *J. Phys. Chem.*, **56**, 801 (1952).
3) A. Kuboyama anb S. Nagakura, *J. Chem. Soc. Japan, Pure Chem. Sec.* (*Nippon Kagaku Zasshi*), **75**, 1082 (1954).
4) S. Nagakura, *J. Am. Chem. Soc.*, **80**, 520 (1958).
5) H. A. Benesi and J. H. Hildebrand, ibid., **71**, 2703 (1949); **72**, 2273 (1950).
6) R. M. Keefer and L. J. Andrews, ibid., **74**, 458, 1891, 4500 (1952); **75**, 3561 (1953).
7) C. Reid and R. S. Mulliken, ibid., **76**, 3869 (1954).
8) R. M. Keefer and L. J, Andrews, ibid., **77**, 2164 (1955).
9) N. Ogimachi, L. J. Andrews and R. M. Keefer, ibid., **77**, 4205 (1955).
10) T. M. Cromwell, ibid., **72**, 3825 (1950).
11) S. H. Hastings, J. L. Franklin, J. C. Schiller and F. A. Matsen, ibid., **75**, 2900 (1953).
12) H. McConnell, J. S. Ham and J. R. Platt, *J. Chem. Phys.*, **21**, 66 (1953).

carbon tetrachloride in the visible region is shown in Fig. 1, the concentration of the former being constant. It shows an apparent isosbestic point, which proves the formation of 1 : 1 complex. Regrettably enough, as benzylideneaniline absorbs light considerably in the region below 400 mμ, and the equilibrium constant of the complex at the room temperature is found to be very small, no charge-transfer band could be observed on account of experimental difficulty. But the shift of I_2 band is considerable, from which the equilibrium constant could be calculated.

The equilibrium constant can be calculated by means of the equation

$$d = C_1\varepsilon_c + (C_1\varepsilon_i - d)/C_2K$$

where d is the optical density of the mixture solution at the measured wavelength, C_1 and C_2 are the concentrations of iodine and benzylideneaniline, respectively, ε_i and ε_c are the molar extinction coefficients of iodine and complex, respectively, at the wavelength, and K is the equilibrium constant. This equation can easily be derived from the law of mass action of 1 : 1 complex, with the consideration that the concentration of benzylideneaniline is actually not altered, as it is so high compared with that of iodine, and that the observed optical density is the sum of those of iodine and a complex. As the absorption due to benzylideneaniline can not be ignored, measurements were carried out with the benzylideneaniline solutions as references.

The values of d are plotted against $(C_1\varepsilon_i - d)/C_2$ (Fig. 2). They fall on straight lines which are parallel to each other, of which the slope indicates $1/K$.

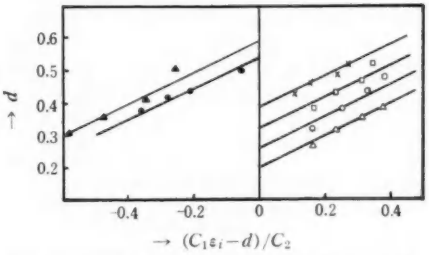

Fig. 2. Plots of d values against $(C_1\varepsilon_i - d)/C_2$.

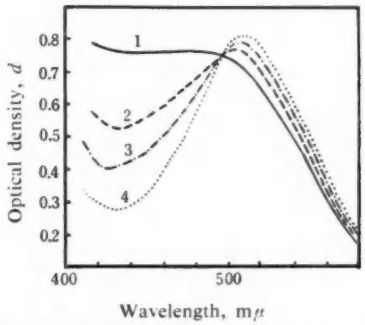

Fig. 3. Spectra of benzylidene-*p*-anisidine+I_2 in CCl_4; Base concentration: 1, —— 0.83; 2, ---- 0.42; 3, -·-· 0.21; 4, ····· 0.10 mol./l. I_2 concentration 2.68×10^{-4} mol./l.

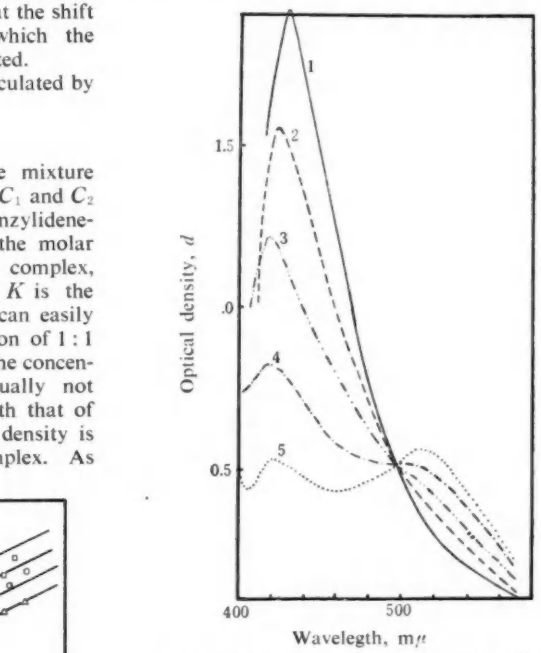

Fig. 4. Spectra of benzylidene-*o*-anisidine+I_2 in CCl_4; Base concentration: 1, —— 0.83; 2, ---- 0.42; 3, ·····0.21; 4, -·-· 0.10; 5, ····· 0.05 mol./l. I_2 concentration 1.93×10^{-4} mol./l.

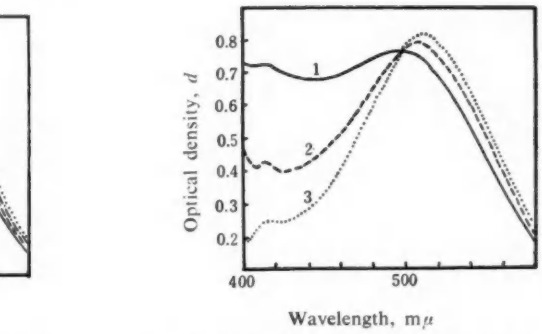

Fig. 5. Spectra of benzylidene-*o*-chloroaniline +I_2 in CCl_4; Base concentration: 1, —— 0.83; 2, ---- 0.42; 3, ····· 0.21 mol./l. I_2 concentration 2.68×10^{-4} mol./l.

The spectra of iodine complexes of benzylidene-*p*- and *o*-anisidine are shown in Figs. 3 and 4. There is a maximum near 420~430 mμ for the latter, which is too intense to be a perturbed iodine transition, and probably it is the charge-transfer band. For the former compound, this band seems to appear at shorter wavelength. The spectra of the chlorine derivatives also show the same peculiarity for the ortho-compound (Fig. 5).

The appropriate values are listed in Table I.

Table I. Equilibrium constants of iodine complexes of benzylideneanilines in CCl_4 at 11.0°C

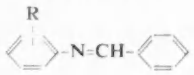

R	*K*
H	2.0
o-OCH_3	10.6
p-OCH_3	9.2
o-Cl	2.4
m-Cl	2.0
p-Cl	2.7

The positions of I_2 absorption maxima could not strictly be defined, as, at the shorter wavelengths, the absorption due to the free base and presumably due to the charge-transfer band becomes large and the exact calculations are not feasible. But the color of the solutions is bright golden yellow and the calculation shows that their positions should not be above 460 mμ. As the shifts of I_2 band in aromatic hydrocarbons are usually not more than 10~20 mμ, it can probably be safe to say that the iodine molecule attaches predominantly to the lone-pair orbital, which is to be more favored, if the steric requirement is fulfilled.

The influence of the methoxyl group in the aniline ring is remarkable. One explanation is that the iodine molecule attaches to the oxygen atom of the substituent, but this is not likely to be the case, because the increment of *K* is too large to be interpreted under this assumption. Moreover, it can not account for the larger values of *K* and longer wavelengths of the charge-transfer bands of ortho-derivatives.

If the proposed structure is assumed, it may be said that the methoxyl group will reduce the ionization potential of the lone-pair electron of the nitrogen atom and facilitate complex formation, and for *o*-methoxy-derivative, in addition to this, the two parallel and closely standing non-bonding orbitals with almost the same size will interact strongly with the iodine molecule and stabilize the complex. For the chlorine derivatives, the effects of the substituent would be small and the *K* values not much different from that of the unsubstituted molecule as expected, and for the *o*-chloro-compound, owing to the large size of chlorine atom, the steric hindrance will predominate over other factors affecting the equilibrium.

The equilibrium constant of benzylideneaniline is unexpectedly small and can be compared with those of the hydrocarbons. But for dimethylaniline, *K* is also small[13], and this is probably partly due to the increase of the ionization potential of the lone-pair electron caused by its migration into the benzene ring and partly due to the steric inhibition rather than to the complex formation with π-orbital as the donor, as other evidences tend to support the former model.

When the almost perpendicular structure is assumed, the hybridization of nitrogen-valence-orbitals will approach largely to the *sp*-type, then the non-bonding orbital will be almost of the *p*-type. Furthermore, as the interaction of the latter with the benzene ring is of the order of perturbation, it must retain largely its original *p* structure. This orbital is less concentrated along one direction than sp^2 orbital, and can not overlap well with I_2 orbital unless this comes nearer. This would cause the increase of steric hindrance and decrease the equilibrium constants.

Experimental

Preparations of benzylideneanilines were described in the previous paper. Iodine was sublimed two times from the G. R. grade commercial substance.

Absorption spectra were measured by a Cary self-recording spectro photometer model 14 M and a Hitachi EPU 2 type spectrophotometer using 1 cm. quartz cell. Measurements were made as soon as the solutions were prepared, so as to avoid the change due to the reaction. Reaction occurs in considerable extent when the mixture is left standing for a long time, but in the course of measurement no remarkable change was observed.

Summary

Absorption spectra of the mixtures of iodine with benzylideneanilines in various concentrations have been measured, and from the optical densities of the solutions the equilibrium constants have been calculated.

The equilibrium constants are unexpectedly small. But for methoxy-derivatives and especially for ortho-compound, the equilibrium constants are considerably large.

For *o*-methoxy- and *o*-chloro-derivatives, the charge-transfer bands appear at the longer wavelengths.

13) H. Tsubomura, Private communication to Professor S. Nagakura to whom the author is very much indebted for having been allowed to refer to it.

These experimental evidences are also adequately explained by the perpendicular structure of benzylideneaniline.

The author expresses his sincere thanks to Professor S. Nagakura for his kind help throughout this study.

Department of Chemistry
College of General Education
The University of Tokyo
Meguro-ku, Tokyo

Biochemical Studies on Pearl. IX. Amino Acid Composition of Conchiolin in Pearl and Shell

By Shozo TANAKA, Hiroyuki HATANO and Osamu ITASAKA*

(Received August 4, 1959)

An organic constituent of shells of molluscs was first named conchiolin by Frémy, and then it was recognized as a kind of protein by Schlossberger and Voit[1]. The amino acid constituents of this protein were studied by Krukenberg & Engel[1], Wetzel[2], Stary & Andratschke[3] and Friza[4]; and the presence of glycine, leucine, tyrosine, tryptophane and arginine was found in hydrolysates of conchiolin. Amino acid components of conchiolin prepared from different species of molluscs were also studied by Roche, Ranson & Eysseric-Lafon[5] and by Grégoire, Duchâteau & Florkin[6]. The composition of various kinds of conchiolin was reported to differ with the kinds of molluscs from which they were prepared. The authors have reported that about fifteen kinds of amino acids were found in hydrolysates of conchiolin prepared from the pearls and the shells of pearl oysters[7]. Halogen-containing amino acids, iodotyrosine and bromotyrosine, which are known as the peculiar components of screloproteins obtained from calciferous skeletons of marine invertebrata such as sponge and gorgonia, were not found in conchiolin of pearls and shells[7].

Electron-microscopic studies on conchiolin by Grégoire, Duchâteau & Florkin[6] and also by Grégoire[8] alone showed that the physical structure of conchiolin in the shells was reticulated unlike that of keratin or collagen which has fibrous structure. Conchiolin has been reported to be successfully fractionated into several preparations by suitable chemical reagents[6,9]. From chemical and crystallographical studies on the pearls and the shells of pearl oysters, the nacre of pearls was found to be identical with the nacreous layer of shells but quite different from the prismatic layer of shells[10]. These results may be of interest in studying the correlation between physical observations and chemical structures. This paper deals with the results of quantitative analyses of amino acids in the hydrolysates of conchiolin prepared from the pearl and the two layers of the shell of an oyster.

Experimental

Materials.—*The pearl and the shell of the pearl oyster.*—The pearls were harvested from the pearl oysters, *Pinctada martensii* (Dünker)**, which had been cultured in the pearl farm at Matoya Bay near Kashikojima during two winters after culture operations. The shells were obtained from the same pearl oysters. Both were rinsed thoroughly with tap water and with distilled water, and then dried at room temperature.

The nacreous substance of pearls.—This substance was obtained from crushed pearls, from which nuclei had been mechanically taken away.

The nacreous substance of shells.—This substance was obtained from shell valves by grinding off prismatic substances after removing the sea-weed

* Present address: School of Chemistry, Shiga University, Otsu.

1) E. Abderhalden, "Handbuch der Biologischen Arbeitsmethoden", Urban & Schwarzenberg, Berlin Bd. I-8, (1922), p. 554.
2) G. Wetzel, *Z. physiol. Chem.*, **29**, 386 (1900).
3) Z. Stary and I. Andratschke, *Z. physiol. Chem.*, **148**, 83 (1925).
4) F. Friza, *Biochem. Z.*, **246**, 29 (1932).
5) J. Roche, G. Ranson and M. Eysseric-Lafon, *Compt. rend. soc. biol.*, **145**, 1474 (1951).
6) C. Grégoire, G. Duchâteau and M. Florkin, *Ann. inst. oceanog., (Paris)*, **31**, 1 (1955).
7) S. Tanaka et al., *J. Chem. Soc. Japan, Pure Chem. Sec. (Nippon Kagaku Zasshi)*, **74**, 193 (1953).
8) C. Grégoire, *J. Biophys. Biochem. Cytol.*, **3**, 797 (1957).
9) S. Tanaka, H. Hatano and G. Suzue, *J. Biochem.*, 47, 117 (1960).
10) S. Tanaka, H. Hatano and O. Itasaka, This Bulletin, **33**, 182 (1960).

** The authors wish to express their hearty thanks to Mr. K. Isowa, the president of Nippon Pearl Co., for his kind donation of the pearls and the pearl oysters for this experiment.

and other adhering materials from the surface.

The prismatic substance of shells.—This substance was obtained from the thin posterior shell margins. All materials were crushed and pulverized into powder of about ten mesh, washed with tap water, and dried at room temperature.

Conchiolin.—Conchiolin was prepared from the above materials by the method described in the previous paper[2]. The materials were immersed in 1 N hydrochloric acid solutions, which were frequently renewed, until no more evolution of carbon dioxide was observed in vacuo. Insoluble matter was washed several times with distilled water and was dialyzed against running water until the chloride ion in the dialyzate became undetectable. The conchiolin prepared from the nacre of pearls and from the nacreous substance of shells had a faint yellowish color, but that from the prismatic layer of shells, had a reddish-brown tint.

Methods.—*Preparation of the conchiolin hydrolysates.*—About 50 mg. of pulverized conchiolin was hydrolyzed with 5 ml. of 6 N hydrochloric acid at 100°C in a sealed tube for 30 hr. After small amounts of humin formed were filtered off, the hydrochloric acid was evaporated in vacuo repeatedly. The hydrolysate was dissolved into a mixture of *n*-butanol, *n*-propanol, and 0.1 N hydrochloric acid (1 : 2 : 1, v/v).

Amino Acid Analysis.—The analyses were carried out chromatographically by Stein and Moore's method on starch columns[11-13]. The preparatory procedure of the columns of potato starch (150 mesh), the selection of solvents and also the procedure for chromatography followed the description by Stein and Moore[11-13]. Columns of 0.9 cm. × 40 cm. of starch containing 30% of water were prepared and were washed under pressure of 150 mmHg until the washings became negative to a ninhydrin test. The hydrolysate was poured on the columns under pressure of 150 mmHg. Two kinds of solvent were used for elution. Solvent I was a mixture of *n*-butanol, *n*-propanol, and 0.1 N hydrochloric acid (1 : 2 : 1, v/v) and Solvent II was composed of *n*-propanol and 0.5 N hydrochloric acid (2 : 1, v/v). The eluting rate had been controlled as 1.5 ml. of the effluent per hour at the optimum velocity.

Each 0.5 ml. of the effluent fractions was collected by an automatic fraction collector. The amount of amino acids in each effluent fraction was estimated by the colorimetric ninhydrin method[14]. A solution of 250 ml. of ethylcellosolve containing 5 ml. of 0.01 M potassium cyanate, a solution of 2.5 g. ninhydrin in 50 ml. of ethylcellosolve and a 0.2 M citrate buffer solution adjusted to pH 5.4 with 1 N sodium hydroxide, were mixed. After each 0.5 ml. of the effluent aliquot was adjusted to pH 5.4 with 1 N sodium hydroxide in the case of Solvent II, though the pH was not controlled in the case of Solvent I, 0.5 ml. of the citrate buffer solution and 0.5 ml. of the ninhydrin reagent were added to the effluent. The mixed solution was allowed to stand for 20 min. in a boiling water bath. By heating the definite volume of the reaction mixture (5 ml.) with 60% ethanol, violet color was developed. Colorimetric determination was carried out by measuring the optical density of the coloring solution at 570 mμ by using a Beckman model DU spectrophotometer. Only for proline, the measurement was done at 440 mμ. The color yield of each amino acid was determined by comparing it with that of pure amino acid, respectively.

11) W. H. Stein and S. Moore, *J. Biol. Chem.*, **176**, 337 (1948).
12) S. Moore and W. H. Stein, ibid., **176**, 367 (1948).
13) S. Moore and W. H. Stein, ibid., **178**, 53 (1949).
14) E. W. Yemm and E. C. Cocking, *Biochem. J.*, **58**, xii (1954); *Analyst*, **80**, 209 (1955).

Results and Discussion

The mensuration curves obtained with the hydrolysates of conchiolin from the nacre of pearls, the nacreous substance and the prismatic substance of shells, are shown in Fig. 1.

It was noticed that relatively large amounts of leucines, alanine, glycine, and cystine are contained in both conchiolin from the pearls and the shells. Proline was not recognized in conchiolin from the nacre of the pearl and the nacreous layer of the shell, while its existence was proved in conchiolin from the prismatic substance of the shell.

It is of interest that a relatively large amount of cystine is found in conchiolin. The fact may suggest a fibrous structure of conchiolin, like keratin in the hair and the skin which

TABLE I. AMINO ACID COMPOSITION OF CONCHIOLIN PREPARED FROM THE NACRE OF PEARLS, THE NACREOUS SUBSTANCE OF SHELLS AND THE PRISMATIC SUBSTANCE OF SHELLS*

Amino acid residue	Conchiolin**		
	Nacre of pearl	Nacreous substance of shell	Prismatic substance of shell
Leucines	9.2	13.6	9.0
Phenylalanine	1.1	0.0	16.9
Valine	2.1	0.5	1.0
Tyrosine	2.7	7.2	3.0
Methionine	0.4	0.4	0.0
Proline	0.0	0.0	7.9
Alanine	14.0	16.3	4.6
Glutamic acid	3.1	1.5	1.5
Threonine***	0.6	9.3	0.3
Aspartic acid	6.2	2.2	3.7
Serine***	5.4	2.1	3.5
Glycine	24.3	12.8	16.8
Ammonia	0.7	0.5	0.1
Arginine	7.2	15.3	10.2
Lysine	7.4	3.3	1.5
Histidine	0.5	0.0	1.0
Cystine/2	12.2	11.8	14.7

* Determined by chromatography of the acid hydrolysates on columns of starch.
** Presented as gram of amino acid residue per 100 g. of protein.
*** Corrected to the hydrolytic damage of threonine (5%) and serine (10%).

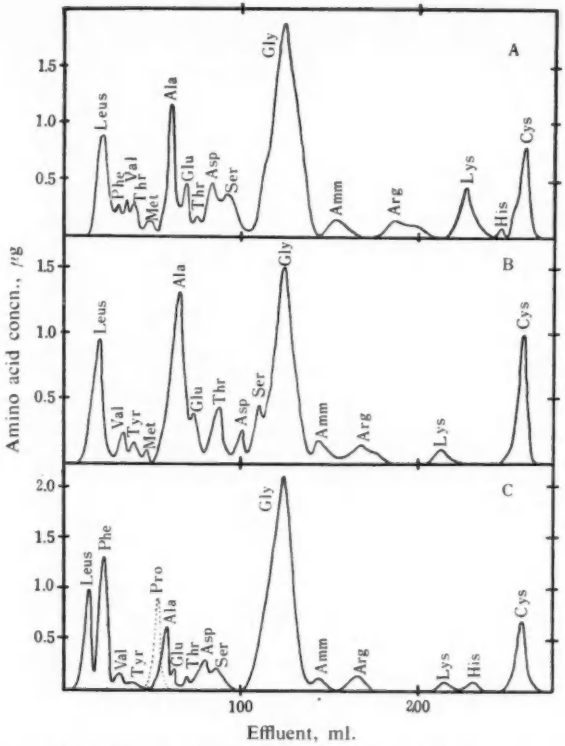

Fig. 1. Starch column chromatography of each 30 hr. hydrolysate of conchiolin prepared from the nacre of pearls (A), the nacreous substance of shells (B) and the prismatic substance of shells (C). Optical density at 570 mμ is plotted on the ordinate for the effluent fractions separated by a 0.9 cm. × 40 cm. column of starch, after treatment with the ninhydrin reagent. The values of optical densities have been corrected by baseline absorption.

causes the elasticity of the tissues. As shown in Table I, conchiolin in the nacreous layer of the shell and that in the pearl contain less phenylalanine and proline, and more alanine than that in the prismatic layer.

Summary

Conchiolin, a kind of screloprotein, was isolated from the pearl and the shell of the pearl oysters. The amino acid composition of conchiolin was determined by the chromatographic method with the starch column. Relatively large amounts of leucines, alanine, glycine and cystine were found in conchiolin.

Remarkable differences were found in the contents of phenylalanine, alanine and proline between conchiolin from the nacreous substance and that from the prismatic substance.

Department of Chemistry
Faculty of Science
Kyoto University
Sakyo-ku, Kyoto

Chemisorption of Hydrogen on Zinc Oxide. I. Rate of Desorption and Adsorption Isotherm

By Yutaka KUBOKAWA

(Received September 9, 1959)

The rate of adsorption and adsorption equilibrium have been measured for various chemisorption systems by many workers. As regards the rate of desorption, however, few quantitative measurements have been carried out with powdered catalysts[1]. For these catalysts the activation energy of desorption is usually taken as the sum of the activation energy of adsorption and the heat of adsorption obtained from the rate of adsorption and adsorption equilibrium, respectively. It is however frequently encountered in chemisorption that the slow attainment of equilibrium and the occurrence of bulk or surface diffusion process introduce considerable uncertainty in the values of the activation energy of adsorption and the heat of adsorption. If the activation energy of desorption is determined by direct measurements of the rate of desorption and compared with the activation energy of adsorption and the heat of adsorption, the information concerning the energy relation for a given chemisorption will be much improved. The present study was undertaken to present such an attempt for the chemisorption of hydrogen on zinc oxide. This paper reports the activation energies for desorption obtained from the rate of desorption at various temperatures, together with adsorption equilibrium data. The rate of adsorption and its relation to the results here reported, will be dealt with in a forthcoming paper.

Experimental

Materials.—For zinc oxide two samples, ZnO I and ZnO II were used. ZnO I was prepared as follows: Zinc oxalate was precipitated from the solutions of ammonium oxalate and zinc nitrate. The precipitate was washed, filtered, dried at 110°C and finally converted to the oxide by heating in air at 400°C. ZnO II was prepared from zinc nitrate and sodium carbonate by the method similar to ZnO I. The reagents were of Extra Pure grade. Hydrogen was obtained by the electrolysis of 30% solution of potassium hydroxide, purified by passing through heated palladium asbestos, phosphorus pentoxide, and finally, through a trap immersed in liquid nitrogen. Nitrogen was prepared by the thermal decomposition of sodium azide, and purified by passing through phosphorus pentoxide. Helium was obtained from commercial sources, and was used without further purification.

Apparatus and Procedure.—The adsorbed amount was determined by using a conventional constant volume apparatus, as shown in Fig. 1. The volume of the dead space was measured by the expansion of a known volume of helium over the whole range of temperatures and pressures employed. The mercury manometer M_1 and the Mcleod gauge M_2 covered a wide range of pressure from 10^{-5} to 70 mmHg.

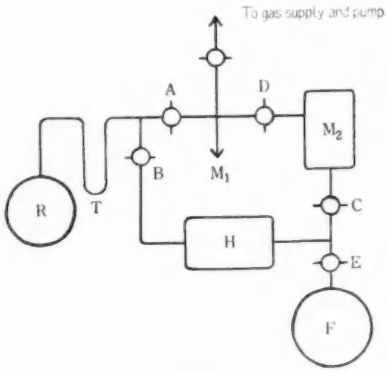

Fig. 1.

The rate of desorption was measured as follows: Before starting a measurement of desorption rate, the pressure in the adsorption vessel R was adjusted to a range of several mmHg by pumping out a known amount of gas through the Mcleod gauge M_2 and mercury manometer M_1. Then, stop-cocks A and D were closed, B and C opened, and the gas desorbed by mercury diffusion pump H was collected into M_2, whose pressure was followed at definite intervals. During a desorption experiment trap T was cooled to −78°C. By using the volume of H at its working state which was determined by an independent measurement, the rate of desorption was calculated from the pressure increase in M_2. When gas was accumulated in M_2 to such an extent that the rate of desorption might be affected by readsorption, the stopcock D was opened and C closed for a short time to pump out the gas in M_2, after which the measurement of desorption was continued. The pressure in the adsorption vessel R during the desorption experiment was measured

1) J. Weber and K. J. Laidler, *J. Chem. Phys.*, **19**, 1089 (1951); J. J. F. Scholten and P. Zwietering, *Trans. Faraday Soc.*, **53**, 1363 (1957); K. Tamaru and M. Boudart, "Advances in Catalysis", Vol. 9, Academic Press, Inc., New York (1957), p. 699.

by closing stopcock C, opening E, A and D, and leading the desorbed gas to flask F, instead of Mcleod gauge M_2.

The adsorption vessel was maintained at various required temperatures in the following manner; for the range above room temperature an electric furnace was used, with the constancy of $\pm 1°C$; for the range below room temperature, solid carbon dioxide in ethanol and melting chlorobenzene and bromobenzene were used; a bath for $-60°C$ was obtained by cooling acetone by the addition of a small amount of dry ice from time to time.

Preceding to the chemisorption experiment, the adsorbent was subjected to alternating evacuation and exposure to hydrogen at 400°C several times, and then evacuated for five hours at 420°C. The surface area of the adsorbents was determined by the B. E. T. method using nitrogen as an adsorbate with the following results; ZnO I, 6.6 m^2/g.; ZnO II, 5.2 m^2/g. The weight of the adsorbent was 14.64 g. (ZnO I) or 11.60 g. (ZnO II).

Results and Discussion

Rates and Activation Energies of Desorption at Various Coverages.—Since the observed rate of desorption is that substracted by the rate of the reverse process, i.e. readsorption, the activation energy of desorption can not be determined from the observed rates unless the rate of readsorption is negligible. As a test to decide whether this condition is satisfied, the following experiment was carried out. After measuring the pressure in adsorption vessel during desorption rate measurements, the pressure increase caused by isolating the adsorption vessel from the mercury diffusion pump was observed. Fig. 2 represents a typical experiment carried out at room temperature. Although adsorption equilibrium was not easily attained, the rapid pressure increase observed suggests that the pressure in the adsorption vessel at the moment when the diffusion pump was cut off would have been negligible compared with the equilibrium pressure corresponding to the adsorbed amount at that moment, and hence that the rate of readsorption was negligible compared with that of desorption. The same was also found to be the case for desorption under other experimental conditions.

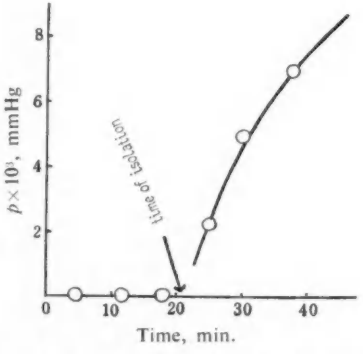

Fig. 2. Pressure increase on isolating the adsorption vessel from the mercury diffusion pump. Pressure in the adsorption vessel before the isolation was 1.3×10^{-4} mmHg.

After hydrogen was allowed to be adsorbed at about 300°C and 20~25 mmHg, the system was cooled down to 209 or 22°C, at which temperature the rate of desorption was measured with the results shown in Fig. 3. Fig. 4 represents the same results as the plots of the logarithm of desorption rate $\log R_{dep}$ against desorbed amount q. As to the data given in Fig. 3 a simple unimolecular or bimolecular rate law was found to be inapplicable. This results, together with the fact that the plot of $\log R_{dep}$ against q in Fig. 4 is nearly linear, will be explained by the increase of activation energy for desorption with decreasing amount

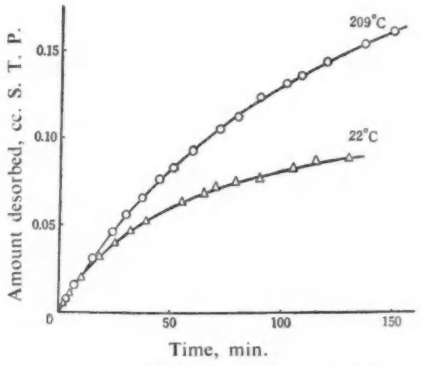

Fig. 3. Rates of desorption of hydrogen chemisorbed on ZnO II. The amount adsorbed at $t=0$ was 0.51 cc. at 209°C and 1.12 cc. at 22°C.

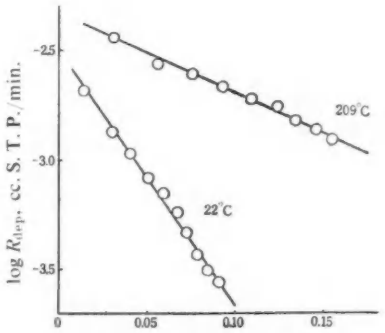

Fig. 4. Plots of $\log R_{dep}$ against the amount desorbed q for the data in Fig. 3.

adsorbed, and its quantitative relationship will also be shown later.

The activation energy of desorption was determined as a function of adsorbed amount by the following procedure: The temperature of desorption was lowered abruptly during the rate measurement, as shown in Fig. 5 (hydrogen chemisorption before the desorption experiment was carried out in a similar manner to that in Fig. 3); the plot of $\log R_{dep}$ against q for the curve before the temperature drop, such as shown in the figure, was extrapolated to a smaller amount adsorbed where the rate measurements after the temperature drop were carried out. Thus, the rates at the two different temperatures corresponding to the same amount adsorbed and, consequently, the activation energy of desorption were obtained.

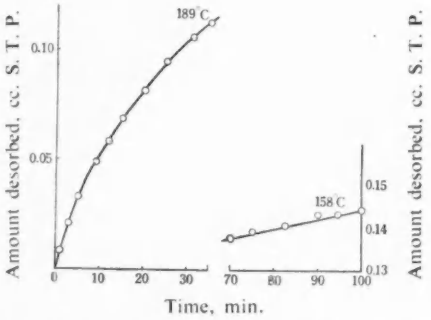

Fig. 5. Determination of the activation energy of desorption. The amount adsorbed at $t=0$ was 0.72 cc. The activation energy was estimated as 23.5 kcal./mol.

The initial admission of hydrogen was usually made at about 300°C and 30~40 mmHg, after which the temperature of the system was lowered to room temperature, and after about 10 hr. it was raised up to 400°C in stages, at each of which the activation energy of desorption was determined in the above mentioned manner. The results obtained with ZnO II are shown in Fig. 6. Fig. 7 shows similar results obtained with ZnO I[2] for a range of higher coverage where desorption was measurable at lower temperatures. It follows from the two figures that the activation energy of desorption increases with decreasing amount adsorbed, up to 31 kcal./mol., and thereafter remains nearly constant[3].

It may be noted that such behavior of the activation energy toward coverage is responsible for the fact that the slope of the plot $\log R_{dep}-q$ is smaller in the higher temperature range, as seen in Fig. 4.

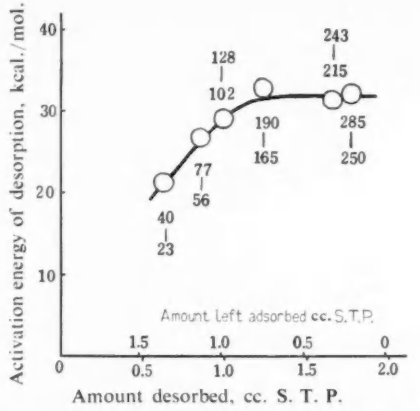

Fig. 6. Activation energies of desorption of hydrogen chemisorbed on ZnO II. The amount adsorbed before desorption at room temperature was 1.98 cc. Figures indicate the temperature interval where the activation energy was determined.

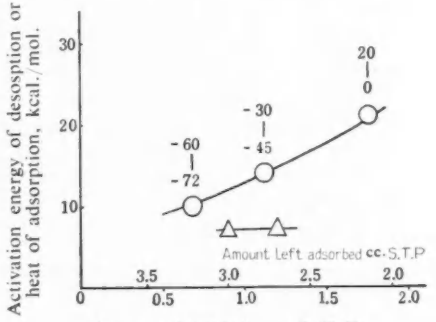

Fig. 7. Activation energies of desorption and heats of adsorption of hydrogen on ZnO I at high coverage. Figures indicate the temperature interval where the activation energy was determined. The amount adsorbed and the equilibrium pressure at room temperature before desorption were 3.90 cc. and 29.5 mmHg respectively. -○-, activation energy of desorption; -△-, heat of adsorption.

Adsorption Isotherms at Various Temperatures. —An adsorption isotherm obtained in the usual manner, i.e. by admitting a small amount of gas to an evacuated sample successively, was found to be different from that obtained in the reverse way, i.e. by successive withdrawals of the gas. These may be called the adsorption and the desorption branches of the isotherm, respectively. An example at 370°C is given in Fig. 8. This result was obtained with ZnO II

2) Results with ZnO II were similar.

3) The fact that a simple unimolecular or bimolecular rate law was not applicable to the data above 200°C, where the approximately constant activation energy was observed, appears to have resulted from a slight change of the activation energy with the amount desorbed, within the experimental error, ±2 kcal./mol.

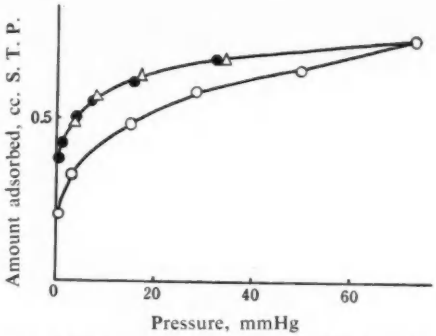

Fig. 8. Adsorption isotherms on the adsorption and desorption branch for the hydrogen chemisorption on ZnO II at 370°C. -○-, initial adsorption; -●-, desorption; -△-, readsorption.

which had been evacuated for five hours at 420°C. On the desorption branch the adsorption equilibrium was rapidly established and reproduced on decreasing or increasing pressure in the pressure range lower than the maximum pressure employed on the adsorption branch. It may therefore be concluded that the isotherm obtained on the desorption branch represents a true equilibrium. The isotherm at varied temperatures was obtained in the following way. After recording the equilibrium pressure at a particular temperature, the temperature was lowered and the new equilibrium pressure at a lower temperature was obtained; a certain amount of hydrogen was then pumped out and the measurements were repeated. The results obtained with ZnO II are shown in Fig. 9. It follows from this figure that the heat of adsorption is nearly constant and equal to 18 kcal./

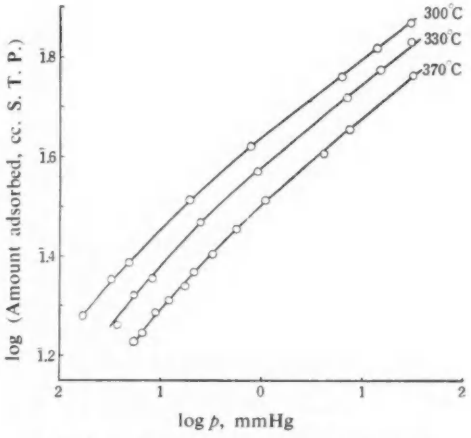

Fig. 9. Adsorption isotherms for hydrogen on ZnO II.

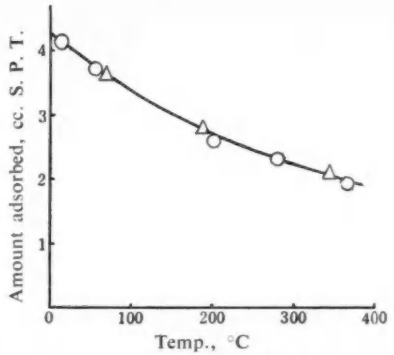

Fig. 10. Adsorption isobar for hydrogen on ZnO I in the pressure range 40~70 mmHg. -△-, on raising temperature; -○-, on lowering temperature.

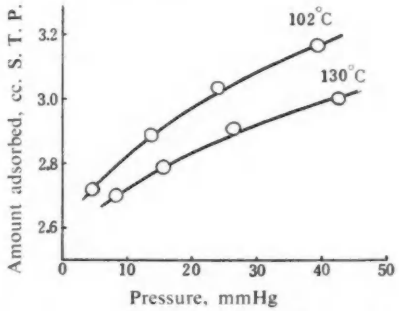

Fig. 11. Adsorption isotherms for hydrogen on ZnO I at 102 and 130°C. The amount adsorbed and the equilibrium pressure at room temperature were 3.76 cc. and 32.8 mmHg respectively.

mol. The same value of the heat of adsorption was obtained with ZnO I.

The adsorption isobar for this system was obtained in the following way: After hydrogen was allowed to be adsorbed at about 350°C, the temperature was lowered in stages down to room temperature and then raised again to 350°C. The results obtained with ZnO I are shown in Fig. 10. It is seen in the figure that the isobars obtained by lowering and raising the temperature nearly coincide, indicating that, once hydrogen is adsorbed at a high temperature, adsorption equilibrium is nearly attained even at considerably lower temperatures, and hence that approximate adsorption isotherms can also be obtained at such low temperatures. Fig. 11 represents such isotherms at 102 and 130°C obtained with ZnO I after hydrogen adsorption at about 300°C, determined in the manner already described for the higher temperature range. Though these low temperature isotherms may be less accurate, the heat of adsorption is

estimated from these as 6~8 kcal./mol.

The activation energy of adsorption may be estimated by combining the activation energy of desorption and the heat of adsorption. As described above, the maximum value of activation energy for desorption and the heat of adsorption are 31 and 18 kcal./mol., respectively. The maximum activation energy of adsorption is, therefore, estimated as 13 kcal./mol.

For the range where the activation energy of adsorption or desorption varies with the amount adsorbed, it seems necessary to take into account the fact that on a heterogeneous surface equal amounts adsorbed do not necessarily mean identical states of adsorption. As described in Figs. 7 and 11, however, adsorbed amount and equilibrium pressure at room temperature differs a little between these two runs, suggesting that in this case the states of hydrogen adsorbed to an equal amount may be compared. Thus, in Fig. 7, the values of the heat of adsorption in the low temperature range described above were shown as a function of the adsorbed amount, together with the activation energy of desorption. It follows from this figure that the activation energy of adsorption in this range is about 5~7 kcal./mol. This figure also suggests that most part of hydrogen chemisorption on zinc oxide is an activated adsorption, although it is doubtful whether the same argument is valid for the fraction which desorbs rapidly below −72°C.

Summary

The rate of desorption of hydrogen chemisorbed on zinc oxide was measured over a wide range of temperatures. The rate at a constant temperature was found to obey approximately the kinetics of the Elovich type. The activation energy of desorption was determined at various coverages, with the result that it increased with decreasing amount from at least about 10~31 kcal./mol. and then remained constant. The heat of adsorption obtained from adsorption isotherms in the temperature range 300~370°C was found to be 18 kcal./mol., being roughly constant. Meanwhile, from the isotherms at about 100°C, a heat of adsorption of 6~8 kcal./mol. was obtained. Comparison between the activation energy of desorption and the heat of adsorption suggests that most part of hydrogen chemisorption on zinc oxide involves an activation energy, its highest value being estimated as 13 kcal./mol.

The author wishes to express his sincere thanks to Professor O. Toyama for his guidance and encouragement throughout the course of this study.

Department of Applied Chemistry
College of Engineering
University of Osaka Prefecture
Sakai-shi, Osaka

Chemisorption of Hydrogen on Zinc Oxide. II. Rate of Chemisorption and Heterogeneity of the Surface of Zinc Oxide

By Yutaka KUBOKAWA

(Received September 9, 1959)

Taylor and coworkers[1], in a study of hydrogen chemisorption on zinc oxide and other catalysts, found a rapid desorption followed by a slow adsorption and explained these phenomena in terms of a heterogeneity of the surface. As pointed out by various workers[2], however, there are other possibilities leading to such phenomena, which, therefore, may not be regarded as a proof of the existence of any surface heterogeneity. As a proof in relation to this problem, it seems to be promising to investigate the behavior of desorption of the chemisorbed hydrogen in the manner described in a previous report[3], since surface heterogeneity may affect seriously its behavior. The purpose of the present work is to clarify the nature of slow chemisorption by measuring not only the rate of adsorption, but also that of desorption under various experimental conditions, and to obtain, on the basis of these results combined with those described in the previous paper[3], definite conclusions as to the heterogeneity of zinc oxide surface in hydrogen chemisorption.

1) H. S. Taylor and S. C. Liang, *J. Am. Chem. Soc.*, 69, 1306 (1947); H. S. Taylor, "Advances in Catalysis", Vol. I, Academic Press, Inc., New York (1948), p. 1.
2) J. H. de Boer, ibid., Vol. 8, (1956), p. 18; O. Beeck, ibid., Vol. 2, (1950), p. 151.
3) Y. Kubokawa, This Bulletin, 33, 546 (1960).

Experimental

The details of materials, apparatus and procedure were described in the previous paper[3].

Results and Discussion

Dependence of Chemisorption Rate on Pressure and Temperature.—In early experiments, the rate of chemisorption was measured in the usual manner, i.e. by admitting a known amount of hydrogen to an evacuated sample and measuring the pressure change in the system at a constant volume. Some examples of the results obtained at a constant temperature and various pressures are shown in Fig. 1[4]. It might be expected that comparison of the times required for the adsorption of a certain amount, determind from such plots, would give the pressure dependence of the rate at the given temperature. However,

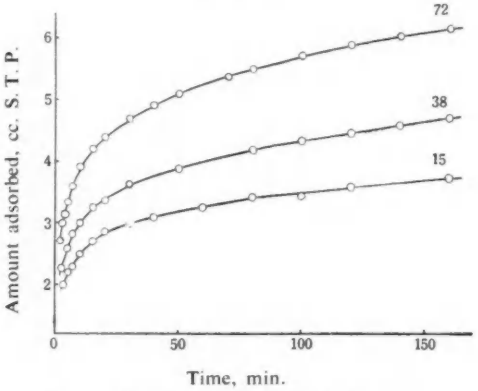

Fig. 1. Rate of adsorption of hydrogen on zinc oxide at 140°C. Figures indicate the initial pressures in mmHg. Different samples were used in these runs.

when the rate thus obtained is represented as proportional to p^n, it is found that not only the exponent n increases with the adsorbed amount, but is also greater than unity. The explanation for such unexpected behavior will be given below, according to which experiments such as shown in Fig. 1 do not reflect the true pressure dependence of the adsorption rate. From a similar argument, it will be shown that a series of rate measurements at a constant pressure and various temperatures does not give the true temperature dependence of the rate. Consequently, in the following experiments, the dependence of the rate on pressure or temperature was determined by observing the change in rate caused by an abrupt change of pressure or temperature during adsorption.

4) The pressure decrease due to adsorption was no more than 10~20% of the initial pressure.

The results concerning the pressure dependence are shown in Figs. 2 and 3. As seen in these figures, on increasing pressure an instantaneous adsorption followed by a slow process takes place. Hence, by extrapolation of the rates to the time when a sudden pressure change occurs, the rates at different pressures corresponding

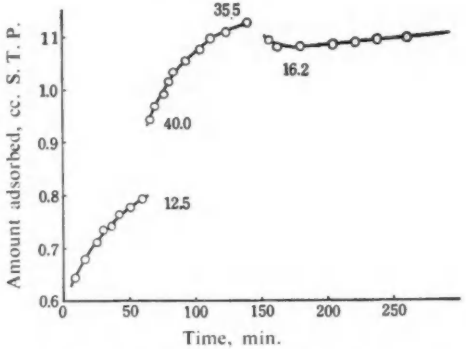

Fig. 2. Effect of the pressure change during adsorption on the rate of adsorption of hydrogen on ZnO II at 18°C. Pressure range, 10~40 mmHg. Figures indicate the pressure before and after the pressure change in mmHg.

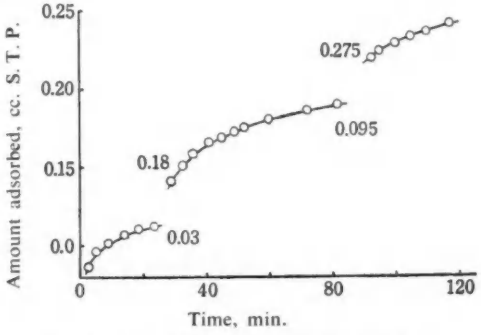

Fig. 3. Effect of the pressure change during adsorption on the rate of adsorption of hydrogen on ZnO I at 18°C. Pressure range, 0.03~0.30 mmHg. Figures indicate the pressure before and after the pressure change in mmHg.

Table I. Values of n in the expression, rate $\propto p^n$ for the data shown in Figs. 2 and 3

	Pressure before and after the pressure change	n
Fig. 2	12.5 → 40.0	1.0±0.1
	35.5 → 16.2	2.0±0.3
Fig. 3	0.03 → 0.18	1.1±0.1
	0.095 → 0.275	0.9±0.1

to equal amounts of slow chemisorption were evaluated. The results are shown in Table I, which shows that the rate is proportional to $p^{0.9\sim1.1}$ on increasing pressure. This relationship was found to be applicable in the whole temperature range studied. As seen in Table I, on decreasing pressure the rate decreases more markedly than is expected from the results obtained on increasing pressure.

The results concerning the temperature dependence obtained with ZnO I in the pressure range 50～70 mm Hg are represented in Fig. 4. It is seen in this figure that on an abrupt temperature change[5], as suggested by Taylor and Liang[1], a rapid desorption followed by a slow adsorption takes place. The activation energy for the slow process was determined in the same manner as for the pressure dependence, with the results shown in Table II. The activation energy

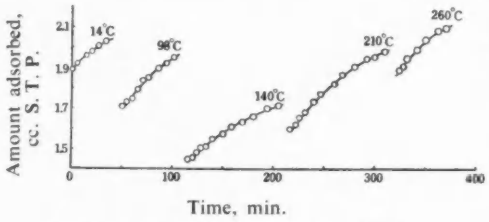

Fig. 4. Effect of the temperature elevation during adsorption on the rate of adsorption of hydrogen on ZnO I. Pressure range, 50～70 mmHg.

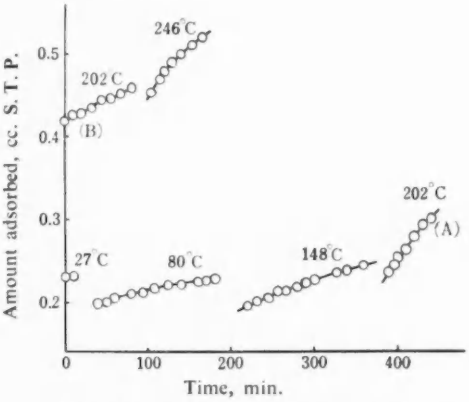

Fig. 5. Effect of the temperature elevation during adsorption on the rate of adsorption of hydrogen on ZnO I. Pressure range, 0.1～0.2 mmHg. Between the runs A and B, the sample was kept at room temperature for 10 hours.

5) A blank experiment carried out with helium in place of hydrogen showed that on such an abrupt temperature change the temperature equilibrium was attained in less than three minutes.

TABLE II. ACTIVATION ENERGIES OF ADSORPTION FOR THE DATA SHOWN IN FIGS. 4 AND 5

Pressure	Temp.	Activation energy
50～70 (Fig. 4)	14～ 98	5.5±1.5
	98～140	7.5±1.0
	140～210	11.0±1.5
	210～260	14.5±1.5
0.1～0.2 (Fig. 5)	80～148	6.3±1.0
	148～202	13.0±1.0
	202～246	15.0±1.0

increases steadily as the temperature becomes higher. As shown in Fig. 5 and Table II, the results obtained in the pressure range 0.1～0.2 mmHg are similar except for the smaller amount of rapid desorption on raising temperature.

In view of the occurrence of hydrogen-deuterium exchange reaction on zinc oxide and, in addition, from a comparison of the energy values for the system of hydrogen on zinc oxide described previously[3] with the information concerning the hydrogen chemisorption on metals given by Gomer and other workers[6], hydrogen chemisorption on zinc oxide at room temperature or above may be assumed to be a dissociative adsorption. Hence, if the rate-determining step of the slow process were a surface migration of the adsorbate, the exponent n in the rate expression Rate $\propto p^n$ would be lower than 0.5. Such expectation is evidently inconsistent with what was observed. It may therefore be concluded that the rate-determining step is not a sort of surface migration, but an adsorption.

As described above, the pressure dependence obtained by increasing pressure differs markedly from that by decreasing pressure. This suggests that desorption can not be neglected during adsorption[7]. Because of this effect, the pressure dependence obtained by increasing pressure, may be somewhat larger than the true value, although the difference may be small compared with that in the case of decreasing pressure.

Heterogeneity of the Surface of Zinc Oxide in Hydrogen Chemisorption.—The considerations given above indicate that the slow process is a chemisorption with an appreciable activation energy which increases with adsorbed amount, judged from the considerable change of the activation energy of desorption as described in

6) R. Gomer et al., *J. Chem. Phys.*, **26**, 1147 (1957); **27**, 1099 (1957); O. Beeck, loc. cit., etc.

7) Taking into account of desorption, the rate of dissociative adsoption on a homogeneous surface will be

$$kp(1-\theta)^2[1-(p_e/p)]$$

where p_e is the equilibrium pressure corresponding to a coverage θ. The term $1-(p_e/p)$ is a correction for desorption. This equation predicts such behavior as observed on an abrupt pressure change during the adsorption rate measurements: In the case where desorption takes place considerably during adsorption, the decrease in the value of $1-(p_e/p)$ on decreasing pressure will be markedly larger than its increase on increasing pressure.

the previous paper[3]. With respect to the behavior observed on raising temperature during adsorption, there are apparently two possible explanations, as the rate-determining step of the slow process is confined to adsorption; one is a heterogeneity of the surface emphasized by Taylor et al. and the other is the coexistence of two types of bonding on a homogeneous surface as frequently proposed by various workers[8]

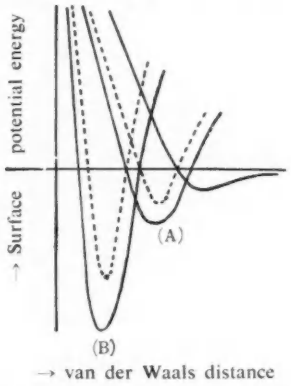

Fig. 6. Energy relation for the two types of chemisorption. Full line, for bared surface; broken line, for covered surface.

(Fig. 6). In the latter case the increase of activation energy of adsorption is attributed to the decrease of heat of adsorption with coverage. According to this model the chemisorption of type A has a low heat of adsorption and negligible activation energy, and hence the adsorption equilibrium is nearly realized throughout the course of slow adsorption, while that of type B involves an appreciable activation energy increasing with coverage and is responsible for the slow process. The behavior observed in this work on raising temperature might be explained by this model in terms of the rapid desorption of the A-type adsorbate followed by the slow adsorption of type B. On the other hand, as regards the rate of desorption, the observed slow process would solely be the desorption of the B-type adsorbate, since that of type A would be probably rapid; the rate of slow desorption would thus be determined only by the adsorbed amount at a given time, irrespective of other experimental conditions.

In order to examine if such a prediction is realized, the following experiments were carried out: At room temperature hydrogen was allowed to be left in contact with the adsorbent for 15 min. in one experiment and 16 hr. in the other one; after which, pumping out a known amount

8) E. Wicke, *Z. Elektrochem.*, **53**, 279 (1949); J. H. de Boer, loc. cit.; P. M. Gundry and F. C. Tompkins., *Trans. Faraday Soc.*, **52**, 1609 (1956); etc.

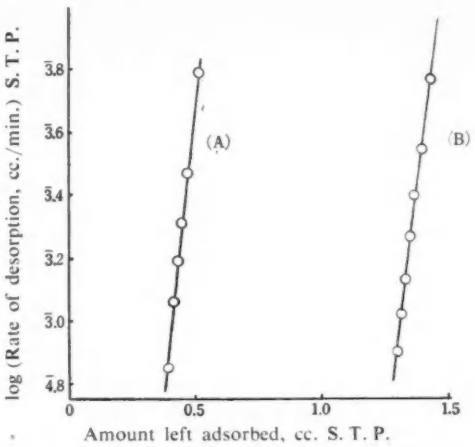

Fig. 7. Rate of desorption as a function of the amount left adorbed. Temp., 16°C.

	Time of contact	Amount adsorbed before desorption in cc.
Run A	15 min.	1.67
Run B	16 hr.	2.65

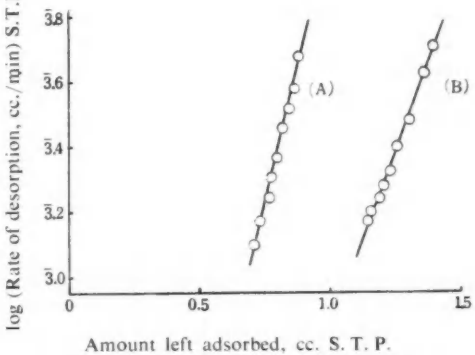

Fig. 8. Rate of desorption as a function of the amount left adsorbed. Temp., 188°C

	Time of contact	Amount adsorbed before desorption in cc.
Run A	15 min.	1.38
Run B	16 hr.	1.85

of hydrogen from the system, the rate of desorption was measured in the manner described in the previous paper[3]. The results are shown in Fig. 7, where, contrary to what has been predicted above, the desorption rates corresponding to equal amounts adsorbed differ markedly from each other, indicating that the postulate of two types of chemisorption can not be applied to this system. Similar results were obtained by the experiments at higher temperatures, an example at 188°C being given in Fig. 8.

Of the two alternatives given above, there remains now the postulate of heterogeneity of the surface to be accepted[9,10]. In view of the continuous variation of the activation energy of desorption with adsorbed amount, the pattern of this heterogeneity seems to be characterized by a continuous distribution function of sites with the heats of adsorption and the activation energies of adsorption varying in the same direction as proposed by Halsey[11]. According to this model, on the sites with a low activation energy, the heat of adsorption is also low and adsorption equilibrium will immediately be established after admission of hydrogen. Whilst, those with a high activation energy are covered by a slow process and the activation energy becomes higher as the adsorption proceeds. On raising the temperature during adsorption, a rapid desorption takes place on the sites with a low activation energy, but on the sites with a high activation energy the slow adsorption continues. In this way this model can explain the phenomena found by Taylor and Liang[1]. Furthermore, the observation such as the marked difference in the rates of desorption corresponding to equal amounts adsorbed in the two experiments with different times of contact with hydrogen and the unexpected pressure dependence of the rate of adsorption obtained in the usual manner may be explained as follows: under different experimental conditions, e.g. different times for adsorption or different initial pressures, different sets of sites may be covered to different extents. Hence, the states of equal amounts adsorbed are not necessarily comparable.

Activation Energy of Adsorption.—The temperature dependence of slow chemisorption given in Table II will give the true activation energy of adsorption, if desorption is negligible. As described above, this condition is not satisfied in this system. However, in view of the nature of surface heterogeneity given above, the situation before and after a temperature raise may be supposed as follows. Before the temperature raise adsorption proceeds mainly on the sites with a particular value of activation energy, since on those with a lower activation energy the adsorption equilibrium must be almost established, while those with a higher activation energy must be nearly bare. On raising temperature, coverage on these sites may become close to the equilibrium value. Hence, adsorption now proceeds mainly on those with a higher activation energy. Since the heat of adsorption changes in parallel with the activation energy, it seems unlikely that the effect of desorption is markedly altered on raising temperature. Thus, the temperature dependence obtained by extrapolating these rates to the time of a rapid temperature change will give the activation energy not greatly in error. In fact, as described in the previous report[5], the maximum value of the activation energy of adsorption estimated from the activation energy of desorption and the heat of adsorption is 13 kcal./mol., in agreement with 15 kcal./mol. obtained directly from the adsorption rate measurements.

9) An assumption of the coexistence of three or more types of bonding on a homogeneous surface in a limited temperature range might explain the observed behavior. It is, however, difficult to work out plausible physical models for such various types of bonding.

10) The experiments described above, of course, can not decide between the two possibilities, one-type and two-type chemisorption on a heterogeneous surface. As will be shown in a later paper, there is no convincing evidence to support the latter at present.

11) G. D. Halsey, *J. Phys. Chem.*, **55**, 21 (1951).

Summary

With respect to hydrogen chemisorption on zinc oxide, the dependence of adsorption rate on pressure and temperature was determined by an abrupt change of pressure or temperature during adsorption. The pressure dependence obtained on increasing pressure differed markedly from that on decreasing pressure, indicating that desorption can not be neglected. The apparent activation energy of slow chemisorption increased from 6 to 15 kcal./mol. as the temperature range becomes higher. Marked differences were found between the rates corresponding to equal amounts adsorbed in the two experiments where the times of contact with hydrogen were different. On the basis of these results, combined with the variation of activation energy of desorption with the amount adsorbed previously, it was shown that for this system the concept of the two types of chemisorption on a uniform surface can not be applied. Instead a postulate of a heterogeneous surface where the activation energy of adsorption and the heat of adsorption varies in the same direction was found to be able to explain all the results obtained.

The author wishes to express his sincere thanks to Professor O. Toyama for his guidance and encouragement throughout the course of this study.

Department of Applied Chemistry
College of Engineering
University of Osaka Prefecture
Sakai-shi Osaka

Carbon Monoxide Chemisorption on Zinc Oxide

By Yutaka KUBOKAWA

(Received September 9, 1959)

Carbon monoxide chemisorption on zinc oxide at room temperature has been investigated by Garner and coworker[1] who reported that the heat of adsorption obtained from the adsorption isotherms is 10~14 kcal./mol., and that the chemisorption is instantaneous and completely reversible at room temperature. Few studies[2] have hitherto been reported on the carbon monoxide chemisorption at high temperatures, which appears to play an important role in the reaction of carbon monoxide, e. g. the oxidation of carbon monoxide. The present work has therefore been undertaken to obtain quantitative information concerning this chemisorption over a wide temperature range by measuring the rate of adsorption and adsorption equilibrium as well as the rate of desorption in the manner described in previous papers[3,4]. Moreover, in this paper, the nature of surface heterogeneity in this system is discussed on the basis of the results obtained, and especially those of the desorption under various experimental conditions which proved to be useful in clarifying the nature of the heterogeneneity of zinc oxide surface in the hydrogen chemisorption[4].

Experimental

Materials.—Zinc oxide was prepared from zinc oxalate in a manner similar to that described in the previous paper[3]. The weight of adsorbent was 16.72 g. and the surface area determined by the B. E. T. method was 6.1 m^2/g. Carbon monoxide was prepared by the reaction of air-free formic acid and concentrated sulfuric acid, purified by passing through soda lime and phosphorus pentoxide, and finally through a trap immersed in liquid nitrogen.

Apparatus and Procedure.—Details of the apparatus and procedure were described in the previous paper[3]. Before a series of experiments, the pretreatment of the sample with carbon monoxide at 400°C followed by evacuation at this temperature were repeated several times.

Results and Discussion

Adsorption Isotherms at About Room Temperature.—According to the investigations by Garner et al.[1], carbon monoxide chemisorption at room temperature is instantaneous and involves no appreciable activation energy. The results obtained in the present study were similar to their results except for the occurrence of a slow uptake even at room temperature, though its amount was very small. The adsorption isotherm obtained by successive

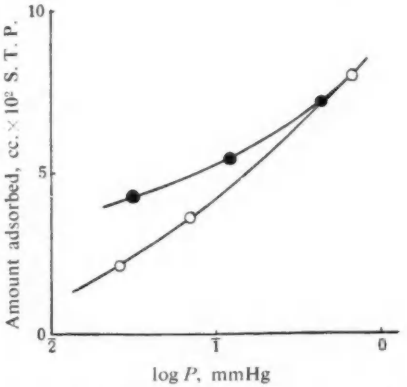

Fig. 1. Adsorption isotherms on the adsorption and desorption branches for the chemisorption of CO on ZnO at 22°C. -○-, on adsorption; -●-, on desorption.

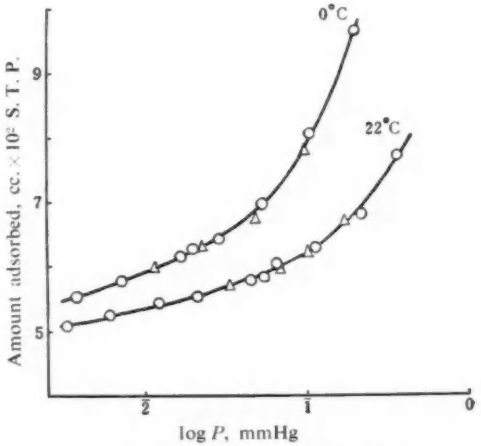

Fig. 2. Adsorption isotherms of CO on ZnO at 0 and 22°C. -○-, on decreasing pressure; -△-, on increasing pressure.

1) W. E. Garner and J. Maggs, *Trans. Faraday Soc.*, **32**, 1744 (1936).
2) R. L. Burwell and H. S. Taylor, *J. Am. Chem. Soc.*, **59**, 697 (1937); E. R. S. Winter, "Chemisorption", edited by W. E. Garner, Butterworths Scientific Publications, London (1957), p. 189.
3) Y. Kubokawa, This Bulletin, **33**, 546 (1960).
4) Y. Kubokawa, ibid., **33**, 550 (1960).

additions of the gas in the usual manner was found to be different from that obtained in the reverse way, i.e., by successive withdrawals of the gas, as shown in Fig. 1. However, the isotherms determined by the latter method were reproducible on increasing or decreasing pressure as found for the hydrogen chemisorption described in the previous paper[3]. Fig. 2 shows the results obtained, which give the heat of adsorption as 10~12 kcal./mol.

Dependence of the Rate of Adsorption on Pressure and Temperature.—Carbon monoxide was introduced at room temperature and its adsorption followed, the temperature being raised in stages up to about 300°C. The results obtained are shown in Fig. 3, which shows that the rate of slow uptake increases markedly with temperature, and that above 100°C only a slight rapid desorption takes place on raising the temperature, in contrast with the case of hydrogen chemisorption previously reported[4]. The pressure dependence of the slow process was obtained in a manner similar to that for hydrogen chemisorption, i.e. by comparison of the rates at equal amounts of slow chemisorption between before and after a rapid pressure change during the adsorption rate measurements. A typical result is shown in Fig. 4 and Table I. The rate is proportional to $p^{0.8\sim0.9}$ on both increasing and decreasing pressures, indicating that desorption is negligible during adsorption.

The temperature dependence of the slow process was obtained by a comparison of the rates corresponding to the equal amounts of slow chemisorption at different temperatures. The results evaluated from Fig. 3 are shown

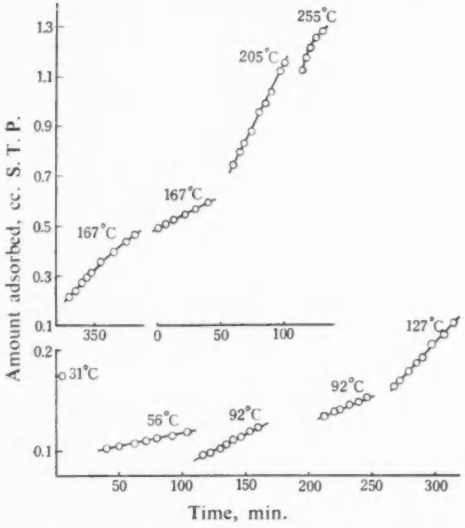

Fig. 3. Effect of the temperature change during adsorption on the rate of chemisorption of CO on ZnO. Pressure, 0.2~0.4 mmHg. Runs at 92 and 167°C were interrupted by reducing pressure or temperature.

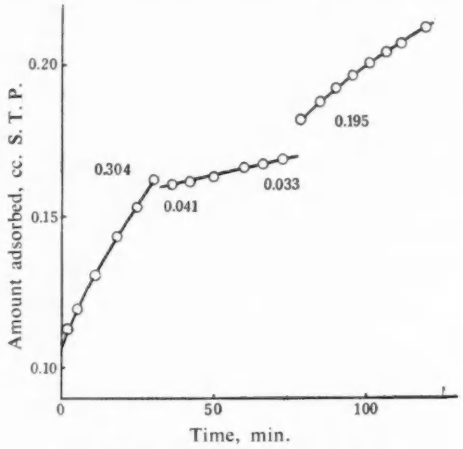

Fig. 4. Effect of the pressure change during adsorption on the rate of chemisorption of CO on ZnO. Temp., 120°C. Figures indicate the pressure before and after the pressure change in mmHg.

TABLE I. VALUES OF n IN THE EXPRESSION, RATE $\propto P^n$ FOR THE DATA IN FIG. 4

Pressure before and after the pressure change, mmHg	n
0.304 → 0.041	0.89±0.06
0.033 → 0.195	0.86±0.06

TABLE II. ACTIVATION ENERGIES OF ADSORPTION FOR THE DATA IN FIG. 3

Temp. range, °C	Activation energy kcal./mol.
56~ 92	5.5±1.0
92~127	7.5±1.0
127~167	11.5±0.7
167~205	16.5±0.7

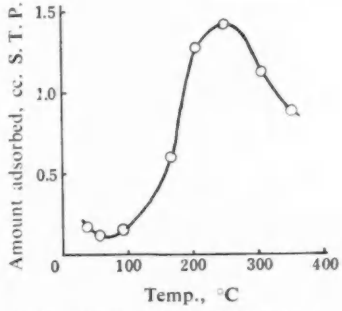

Fig. 5. Adsorption isobar of CO on ZnO at 0.2~0.4 mmHg.

in Table II, which indicates that the activation energy of the slow process increases as the temperature range becomes higher.

The adsorption isobar at approximately constant pressure 0.2~0.4 mmHg was obtained from the amount adsorbed after 1 hour at each temperature. Fig. 5 illustrates this isobar which shows a minimum at about 70°C and a maximum at about 250°C.

Activation Energies of Desorption at Various Coverages.—The temperature of the adsorbent which had already adsorbed carbon monoxide at about 300°C was raised from −72 to about 400°C in stages, at each of which the activation energy of desorption was determined in the manner described in the previous paper[3]. The variation of the activation energy for desorption with the amount desorbed is shown in Fig. 6. As seen in this figure, the curve of activation energy of desorption against the desorbed amount is composed of two parts, one corresponding to the desorption below room temperature with the activation energy of 2.5 kcal./mol., and the other to that above 200°C with the activation energy of approximately 40 kcal./mol. The former value is essentially the same as the heat of adsorption derived from the isotherms around room temperature, indicating that the chemisorption at room temperature involves no activation energy, as may be expected. In the latter case, the activation energy of desorption increases somewhat with decreasing coverage.

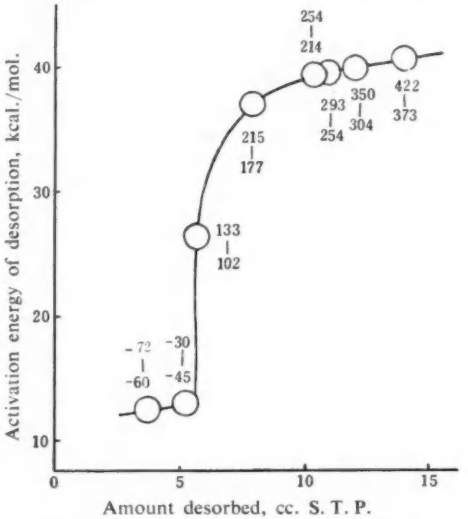

Fig. 6. Activation energies of desorption of CO chemisorbed on ZnO. Figures indicate the temperature interval where the activation energy was determined. The amount adsorbed at room temperature before desorption was 15.81 cc.

This conclusion is based on the assumption that the measured rate of desorption is not affected by the reverse reaction. This was confirmed in the manner previously described[3], i.e., by observing the pressure increase caused by isolating the adsorption vessel from the mercury diffusion pump. In the temperature range above room temperature the observed behavior was almost the some as that of the hydrogen chemisorption previously[3] described, indicating that adsorption is negligible during the desorption rate measurement. Whilst in the temperature range below room temperature, somewhat different behavior was observed as represented in Fig. 7. This shows that an equilibrium pressure P_e is here easily attained, and moreover that the pressure in the adsorption vessel during the desorption experiment P, is now comparable to P_e. However, the ratio P_e/P was found not to vary seriously by an abrupt change of temperature. From the data given in Fig. 7 this ratio was estimated to be 3.5 at −30°C, while the similar measurements at −45°C following these experiments gave the value of 2.6. The error introduced in the activation energy of desorption by this difference in P_e/P was estimated to be at most 1 kcal./mol. It may therefore be concluded that the activation energy of desorption obtained below room temperature is also nearly equal to the true value.

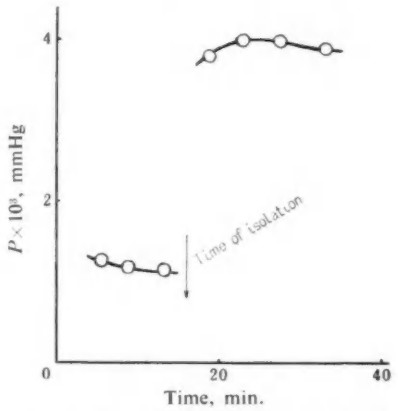

Fig. 7. Results obtained by isolating the adsorption vessel from the mercury diffusion pump. Temp., −30°C.

In order to confirm the reversibility of chemisorption the content of carbon dioxide in the desorbed gas was examined by immersing the trap attached to the MacLeod gauge in liquid nitrogen. The absence of carbon dioxide was confirmed below 350°C, while above this temperature its content amounted to the fraction 1/3~1/2 of the desorbed gas.

Adsorption Isotherms at Higher Temperature[5]. —The adsorption isotherms in temperature 300~370°C were determined by successive withdrawals of the gas as described for low temperature isotherms. These isotherms are strictly reproduced on increasing or decreasing pressure, as shown in Fig. 8. Fig. 9 represents the fact that the heat of adsorption derived from these isotherms decreases with the increasing amount adsorbed from 38 to 25 kcal./mol.

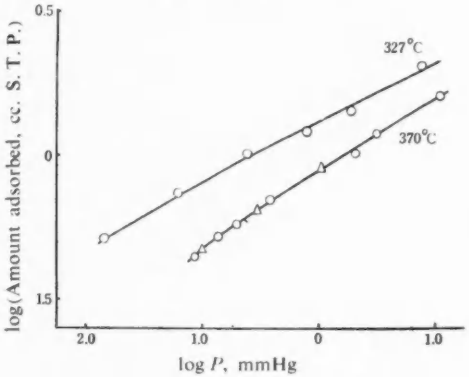

Fig. 8. Adsorption isotherms of CO on ZnO at 327 and 370°C. -○-, on decreasing pressure; -△-, on increasing pressure.

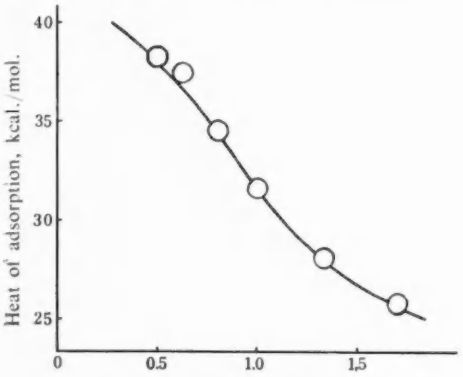

Fig. 9. Heats of adsorption of CO on ZnO.

Two Types of Carbon Monoxide Chemisorption on Zinc Oxide.—The plots of the activation energy for desorption against the amount adsorbed shown in Fig. 6, together with the adsorption isobar shown in Fig. 5, suggest that the two types of chemisorption are operating, one being a non-activated type predominating at a lower temperature, and the other an activated type occurring at a higher temperature. Moreover, not only the former, but also a considerable fraction of the latter is reversible, i.e. desorbed as such. Such behavior of the high temperature chemisorption appears to be inconsistent with the investigations by Garner and coworkers[6], who report that on a number of oxide catalysts the high temperature chemisorption takes place on the oxygen ion and the desorbed gas consists of carbon dioxide. However, the exchange reaction of the oxygen atom between carbon monoxide and the oxide surfaces have recently been investigated by Winter[2], who shows that the high temperature chemisorption does not necessarily lead to the desorption of carbon dioxide, in agreement with the results in the present work.

On the other hand, as described above, there is a slow uptake at room temperature which seems to imply that the chemisorption with the lower activation energy occurs even at room temperature. The phenomena of hysteresis observed at room temperature may then be accounted for, since the high temperature type is considered to be irreversible at this temperature.

Nature of Heterogeneity of the Surface.—The problem was dealt with in the same manner as previously reported for the hydrogen chemisorption[1]: At 192°C a known amount of carbon monoxide was left in contact with the adsorbent for fifteen minutes in one case and for fifteen hours in the other case; then, by pumping out a known amount of the gas from the system, the desorption rates in the two cases were compared with the results shown in Fig. 10, where curves A and B represent desorption rates after fifteen minute and fifteen hour contacts, respectively. After desorption B a certain amount of carbon monoxide was further pumped out at a higher temperature until the remaining amount adsorbed became comparable to that left after desorption A; thereupon, the temperature was lowered down to 192°C, and desorption rate measurements were carried out. Their results, denoted by C, are also shown in Fig. 10. It follows from this figure that the rate of desorption is greater on the surface where the larger amount is adsorbed, and is determined by the remaining amount adsorbed alone, independent of the conditions employed for the adsorption, in contrast with the behavior of hydrogen described in the previous paper[1].

These results might be explained in terms of the concept that the increase of the activation

5) During the adsorption isotherm measurements, the formation of carbon dioxide was negligibly small and darkening of zinc oxide was not observed, suggesting that the reaction $2CO \rightarrow C+CO_2$ scarcely takes place at all, in disagreement with the results obtained by Taylor and Burwell[2]. Such discrepancy appears to be explained by the severe carbon monoxide treatment in the present work, since the authors cited above reported a marked decrease in the activity toward this reaction after the carbon monoxide treatment.

6) W. E. Garner, *J. Chem. Soc.*, **1947**, 1239.

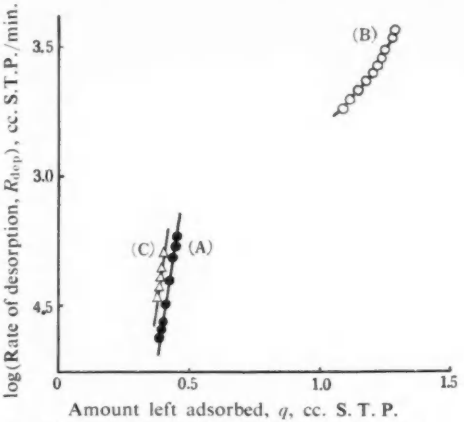

Fig. 10. Rate of desorption as a function of the amount left adsorbed. Temp, 192°C.

energy of adsorption with the adsorbed amount is due to the decrease of the heat of adsorption with coverage, without the concept of an *a priori* heterogeneity. However, the fact that the value of $d \log R_{dep}/dq$ differs markedly between the two runs, A and B, as shown in Fig. 10, can not be explained in terms of the induced heterogeneity[7] above mentioned, because there is no marked difference in the coverage θ between these two runs, considering that the adsorbed amount at $\theta=1$ estimated from Fig. 8 is about 10 cc. With respect to this problem, the following experimental results may be mentioned. From the plots of $\log R_{dep}-q$ at varied temperatures which were determined for the purpose of determining the activation energy of desorption at various coverages, the values of $d \log R_{dep}/dq$ at different adsorbed amount were estimated as shown in Fig. 11. This considerable change[8] can not be expected from the concept of induced heterogeneity. It may therefore be concluded that in this system again the variation of the heat of adsorption

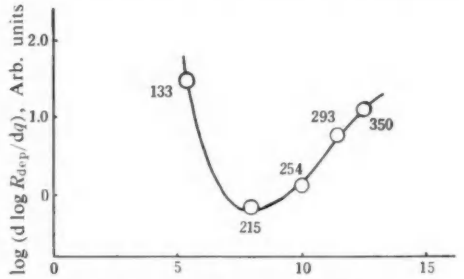

Fig. 11. Values of $d(\log R_{dep})/dq$ at various amounts adsorbed. Figures indicate the temperature in °C where the rate of desorption was measured.

with the adsorbed amount will arise mainly from *a priori* heterogeneity, the nature of which is such that the activation energy of adsorption and the heat of adsorption varies conversely to each other, in contrast with hydrogen chemisorption. Such a correlation between the activation energy of adsorption and the heat of adsorption requires that the maximum activation energy of adsorption 16 kcal./mol. should correspond to the minimum activation energy of desorption 37 kcal./mol. and the minimum of the former 5 kcal./mol. to the maximum of the latter 41 kcal./mol. This gives as the heats of adsorption 36 and 21 kcal./mol. in fair agreement with the values directly obtained from the adsorption isotherms[9].

Summary

The rates of adsorption and desorption, and the adsorption equilibrium for carbon monoxide chemisorption on zinc oxide were measured over a wide range of temperatures as in the previous study of hydrogen chemisorption on zinc oxide. The behavior of desorption indicated the existence of two types of chemisorption; the non-activated type and the activated type. For the former type the heat of adsorption was estimated as 10~12 kcal./mol. from the adsorption isotherms, in agreement with the activation energy of desorption. The considerable fraction of the latter type was reversible, i.e. desorbed as such. For this type, the activation energy of adsorption increased with the adsorbed amount from 5 to 16 kcal./mol., and the rate was proportional to $P^{0.8\sim0.9}$. Moreover, the heat of adsorption obtained from the adsorption isotherms ranged from 25 to 38 kcal./mol., in fair agreement with those estimated from the activation energy of adsorption and desorption. The behavior of desorption suggested the predominance of surface heterogeneity, the nature of which was such that the activation energy of adsorption and the heat of adsorption varied conversely to each other.

The author wishes to express his sincere thanks to Professor O. Toyama for his guidance and encouragement throughout the course of this study.

Department of Applied Chemistry
College of Engineering
University of Osaka Prefecture
Sakai-shi, Osaka

7) M. Boudart, *J. Am. Chem. Soc.*, **74**, 3556 (1952).

8) It will be shown in a forthcoming paper that this considerable change inevitably arises on a surface where *a priori* heterogeneity is predominating.

9) In Figs. 3, 6 and 9, the states of the carbon monoxide adsorbed to an equal amount can not be be compared, since the surface has a heterogeneous character, and moreover the observed amount of adsorption includes the irreversible one, the extent of which varies with the experimental conditions.

SHORT COMMUNICATIONS

Formation of Mullite from Kaolin Minerals at Low Temperature

By Hiroshi OKUDA

(Received February 27, 1960)

Mechanism of the mullite formation has not been explained completely, and there is a widespread disagreement concerning the formation temperature in the literatures[1-4]. It was reported that the formation of mullite from well-crystallized kaolinite occurs above 950°C and the formation of mullite from poorly crystallized kaolinite and halloysite occurs at a higher temperature[5,6]. Colegrave and Rigby[7] showed that traces of mullite were formed, when kaolinite was mixed with 2% of boric oxide and heated at 900°C. for 200 hr. No literature reported that the formation of mullite from kaolin minerals occured below 900°C.

During the course of an investigation of the effects of additive on the mullite formation of kaolin minerals[8], it was found that fluoride of alkali and alkaline earth elements promoted the formation and lithium fluoride was most effective. The present experiment has been carried out to find the effect of additive lithium fluoride on the temperature of mullite formation.

A well-crystallized kaolinite from Kampaku, Tochigi Prefecture, Japan and halloysite from Korea were used. The dried minerals were mixed with 2.5, 5 and 10% of lithium fluoride. The mixtures were heated for 5 hr. at 500, 550, 600, 700, 800 and 900°C. The heated samples were examined by an X-ray diffractometer, and the results are shown in Fig. 1 and Table I.

When 2.5% of lithium fluoride was added to kaolin, mullite and β-spodumene started to be formed at 800°C. The kaolin mixed with 5% of lithium fluoride was converted into β-spodumene above 600°C and into mullite above 700°C. It was found that β-spodumene was formed at 500°C and a small amount of mullite was formed at 550°C, when kaolin was mixed with 10% of lithium fluoride.

It is concluded that by the addition of lithium fluoride the kaolin minerals form mullite at a extremely lower temperature than that reported in the literature. Further experiment, however,

TABLE I. PHASE FOR KAOLIN MINERALS CONTAINING LITHIUM FLUORIDE HEATED AT VARIOUS TEMPERATURES FOR 5 HR.

Sample	Temp. (°C)					
	500	550	600	700	800	900
Halloysite +2.5% LiF	halloysite	metakaolin	metakaolin	metakaolin	β-sp. mull.	β-sp. mull.
Halloysite +5% LiF	halloysite	metakaolin	β-sp.	β-sp. mull.	β-sp. mull.	β-sp. mull.
Halloysite +10% LiF	halloysite β-sp.	β-sp. mull.	β-sp. mull.	β-sp. mull.	β-sp. mull.	β-sp. mull.
Kaolinite +2.5% LiF	kaolinite	metakaolin	metakaolin	metakaolin	β-sp. mull.	β-sp. mull.
Kaolinite +5% LiF	kaolinite	metakaolin	β-sp.	β-sp. mull.	β-sp. mull.	β-sp. mull.
Kaolinite +10% LiF	kaolinite β-sp.	β-sp. mull.	β-sp. mull.	β-sp. mull.	β-sp. mull.	β-sp. mull.

β-sp. : β-spondumene, mull. : mullite

1) A. H.Jay, *Trans. Brit. Ceram. Soc.*, **38**, 455 (1939).
2) H. M. Richardson and F. G. Wilde, ibid., **51**, 387 (1952).
3) G. W. Brindley and K. Hunter, *Mineralog. Mag.*, **30**, 574 (1955).
4) G. W. Brindley and M. Nakahira, *J. Am. Ceram. Soc.*, **42**, 311 (1959).
5) W. D. Johns, *Mineralog. Mag.*, **30**, 186 (1953).
6) H. D. Glass, *Am. Mineralogist*, **39**, 193 (1954).
7) E. B. Colegrave and G. R. Rigby, *Trans. Brit. Ceram. Soc.*, **51**, 355 (1952).
8) H. Okuda, M. Haga and S. Kato, *Reports of the Government Industrial Research Institute, Nagoya* (Nagoya Kogyogijutsu-shikenjo Hokoku), **6**, 60 (1957); ibid., **7**, 74 (1958).

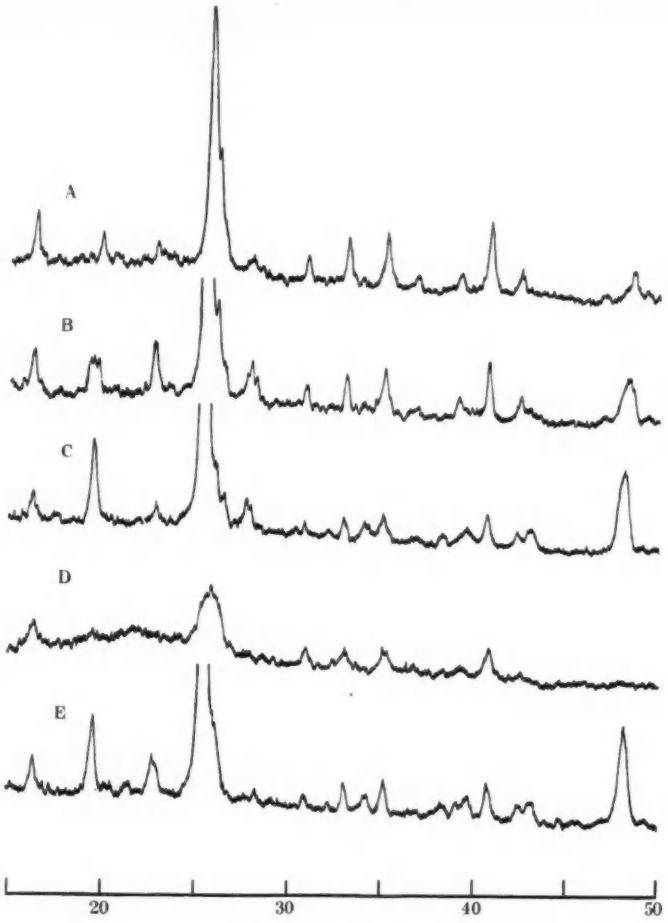

Fig. 1. X-ray diffraction patterns of kaolin minerals containing lithium fluoride.
A, is for the mixture of halloysite and 2.5% LiF heated at 800°C: B, the mixture of halloysite and 5% LiF heated at 700°C: C, the mixture of halloysite and 10% LiF heated at 550°C: D, the mixture of kaolinite and 2.5% LiF heated at 800°C: and E, the mixture of kaolinite and 10% LiF heated at 550°C. Heating period is 5 hr. in all cases.

is necessary to understand the mechanism of the mullite formation and to explain the effect of the addition of lithium fluoride on the formation.

Government Industrial Research Institute
Kita-ku, Nagoya

A New Application of Neutron Activation Analysis to the Polarography of Holmium

By Hiroshi HAMAGUCHI, Jinzo HASHIMOTO, Kyoichi HOSOHARA and Yoshio NARUSAWA

(Received February 16, 1960)

In general, two stepped reduction waves are observed in the polarograms of lanthanide elements. Conflicting explanations for the mechanism of electrode reaction have been reported as summarized in Table 1.

The present authors introduced a new method for the study of the electrode reduction process of holmium by utilizing a neutron activation technique. Assuming the electrode reaction of holmium to be $Ho^{3+}_{aq} + 3e + Hg \rightarrow Ho(Hg)$, the amount of holmium m(μg.) amalgamated in one drop of mercury is calculated by

$$m = i_1 \cdot \tau \cdot 164.94/3F$$

where i_1 is the limiting current (microamp.), τ the drop time (sec.), 164.94 the atomic weight of holmium and F the Faraday constant. In the case of the experimental condition shown in Fig. 1, the amount of holmium that would be deposited is calculated as 0.022 μg. (τ=3.08 sec.) for the first wave and 0.023 μg. (τ=2.67 sec.) for the second wave. These amounts are well above the sensitivity limit of the activation analysis of the element[9].

One drop of mercury taken up immediately after electrode reaction* was sealed in a vinyl bag, and irradiated for two days with a neutron flux of $\sim 10^{11}$ $n/cm^2/sec.$ in the JRR-1 reactor. After irradiation, the induced radionuclide ^{166}Ho was purified by going through decontamination chemistry, and the amount of holmium was then determined by comparing the β activity of holmium from the sample with that of the monitor.

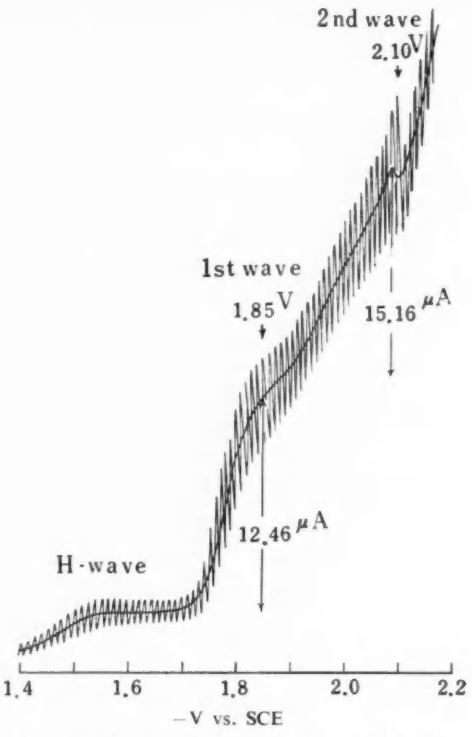

Fig. 1. Polarogram of 2.32×10^{-3} mol./l. Ho^{3+}, aq. in 0.1 N LiCl soln. containing 0.01% gelatine. Temp. 25.0±0.01 °C.
The 1st wave: Number of electron 3(pH< 3.1), temp. coeff. 3.0%, linear relationship between wave height and concentration is obtained. Reversible at pH<3.10, quasi-reversible at 3.10<pH<3.90, irreversible at pH>3.90 are explained by Matsuda-Ayabe's theory. $E_{1/2}$ shifts toward more negative with decreasing of pH.
The 2nd wave: Followed by a maximum wave, no linear relation between wave height and concentration is obtained, although the correlation between them is held. The ratio of wave height of the 2nd to that of the 1st is not 2 : 1.

Contrary to the earlier reports that had suggested a reduction of lanthanides to the metallic state, extremely smaller amount of holmium than was expected was found at both reduction steps as shown in Table II.

In the light of the above data and of the polarographic behavior shown in Fig. 1, it should reasonably be considered that the polarographic reduction of holmium is not the reduction of the holmium aquo-complex ion to a metallic state but the discharge of hydrogen ions

1) W. Noddack and A. Brukle, *Angew. Chem.*, **50**, 362 (1937).
2) L. Holleck, *Z. Elektrochem.*, **46**, 69 (1940).
3) I. M. Kolthoff and J. J. Lingane, "Polarography", Vol. II, Interscience Publisher, New York (1952), p. 435.
4) G. Glockler et al., *J. Am. Chem. Soc.*, **70**, 1342, 1345 (1948); **71**, 1641 (1949).
5) S. Misumi and A. Iwase, ibid., **76**, 1231 (1955), **77**, 640 (1956).
6) A. Purushottam and B. H. S. V. Raghava Rao, *Anal. Chim. Acta*, **12**, 589 (1955).
7) A. Iwase, *J. Chem. Soc. Japan, Pure Chem. Sec.* (*Nippon Kagaku Zasshi*), **78**, 114 (1957).
8) H. Hamaguchi, J. Hashimoto and Y. Narusawa, *J. Chem. Soc. Japan, Pure Chem. Sec.* (*Nippon Kagaku Zasshi*), **80**, 43 (1959).
9) H. Hamaguchi, *J. Japanese Chem.* (*Kagaku-no-Ryoiki*), **13**, 316 (1959).

* The method of collecting a drop of mercury is the same as that by J. J. Lingane and I. M. Kolthoff, *J. Am. Chem. Soc.*, **61**, 825 (1939).
In the present communication the re-dissolution of the deposited metal into the regulating solution, though possible, has not been taken into consideration.

TABLE 1. PROPOSED EXPLANATIONS FOR ELECTRODE REACTIONS OF LANTHANIDE ELEMENTS AT A DROPPING MERCURY ELECTRODE

Element studied	First wave	Second wave	Investigators
Sc, Y, La, etc.	$M^{3+}+e \rightarrow M^{2+}$	$M^{2+}+2e \rightarrow M^0$	Noddack, Bruckle[1,2]
Lanthanides except Eu, Yb	Hydrogen wave	$M^{3+}+3e \rightarrow M^0$	Kolthoff, Lingane[3]
La, Pr, Nd, Sm, Gd	$M^{3+}+3e \rightarrow M^0$	?	Glocker, et al.[4,5]
	$M^{3+}+e \rightarrow M^{2+}$ $M^{2+}+H_2O \rightarrow M^{3+}+OH^-+H^0$	$M^{2+}+2e \rightarrow M^0$	Purushottum, Raghava Rao[6]
Sm	$M(OH)^{2+}+3e \rightarrow M^0+OH^-$	?	Iwase[7]
Y	$M(OH_2)_6^{3+}+3e \rightarrow M(OH)_3(OH_2)_3+3H^0$	?	Authors[8]

TABLE II. THE AMOUNT OF HOLMIUM (μg.) FOUND IN A DROP OF MERCURY*

First wave		Second wave	
m_{Ho}(found)	m_{Ho}(calcd.)	m_{Ho}(found)	m_{Ho}(calcd.)
0.0050	0.0218	0.0010	0.0230

* Values are corrected for the blank (0.0050 μg. Ho) in a drop of mercury.

produced by the dissociation of the aquo-complex ion. Details will be published later.

We are indebted to the members of the radiochemistry division, Japan Atomic Energy Research Institute for their co-operation with the irradiation. A part of the expense was defrayed from a grant from the Ministry of Education.

Department of Chemistry
Faculty of Science
Tokyo University of Education
Bunkyo-ku, Tokyo

Transport Behavior of Ferric, Aluminum and Cupric Ions across the Alginate and the Other Membranes

By Manabu SENŌ, Tazuko SAITŌ and Takeo YAMABE

(Received January 26, 1960)

Recently many attempts have been undertaken to separate various species of ions by the electrodialyses using the ion-selective membranes, but there is no report as to the selective permeability of heavy metal ions. One of the objects of this study is to describe the transport behavior of ferric, aluminum and cupric ions across the ion-selective membranes. Another is to examine the permeability of ferric ion across the alginate membrane which is prepared from alginic acid. It is known that alginic acid adsorbs preferentially the ferric ion[1].

The electrodialyses were carried out at the constant current densities, $(0.33 \sim 2.50) \times 10^{-2}$ amp./cm^2, for one hour, using a five-compartment cell which was schematically Shown in Fig. 1.

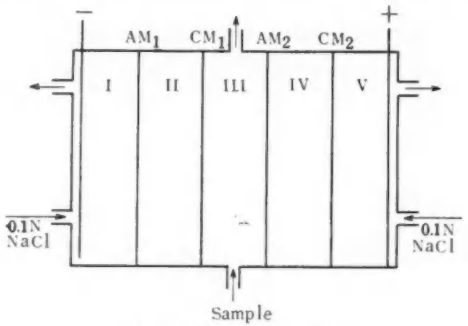

AM$_1$, SAM ; CM$_2$, SCM

Fig. 1. A five-compartment cell for the electrodialyses.

Into the central compartment, the solution containing 5~10 meq./l. of ferric and aluminum chloride or ferric and cupric chloride and being adjusted to be about pH 1.3 (ca. 0.05N HCl) were fed at the flow-rate of about 1 l./hr. The amounts of ions transferred to the adjacent compartments, which were filled with the same solution beforehand, across the ion-selective membranes were measured. The analyses were done by the simultaneous colorimetric methods[2]. The ion-selective membranes were heterogeneous and were prepared from Amberlite resins in the authors' laboratory*. The alginate membrane

1) M. Senō and T. Yamabe, This Bulletin, to be published.

2) R. E. Kitson, *Anal. Chem.*, 22, 664 (1950); K. Motojima, *J. Chem. Soc. Japan, Pure Chem. Sec.* (*Nippon Kagaku Zasshi*), 76, 903 (1955).

* From the four kinds of Amberlite resins, IR-120, IRC-50, IRA-400 and IR-4B, the corresponding ion exchange membranes were prepared. These are a strongly and a weakly dissociated cation-selective membrane and a strongly and a weakly dissociated anion-selective membrane, which are abbreviated as SCM, WCM, SAM and WAM. Similarly the alginate membrane is designated as ACM in Table II.

was prepared from polyvinylchloride and alginic acid crosslinked with formaldehyde[3], using cyclohexanone as a mixing agent. The obserbed membrane potentials of these membranes are 80~90% of the theoretical (S.C.E. | 0.1N KCl | memb. | 0.01N KCl | S.C.E.).

A part of the experimental results was given in Tables I and II. The following facts are to be noticed.

TABLE I. PERMEABILITIES OF HYDROGEN, FERRIC, ALUMINUM AND CUPRIC IONS ACROSS A STRONGLY DISSOCIATED CATION-SELECTIVE MEMBRANE

Current densities	Concentration ratios* Fe-Al system			Fe-Cu system		
amp./cm^2×10^2	H	Fe	Al	H	Fe	Cu
0.33	1.99	0.84	0.79	1.88	0.78	0.72
0.83	2.60	1.02	1.26	2.41	1.13	1.78
1.67	3.36	1.15	1.39	4.28	2.18	3.28
2.50	4.90	2.26	2.49	4.70	2.41	4.30

* These are ratios of concentrations of a given ion in the compartment II before and after electrodialysing.

TABLE II. PERMSELLCTIVITY COEFFICIENTS ACROSS THE VARIOUS ION-SELECTIVE MEMBRANES AT 0.0083 amp./cm^2

Ion-selective membrane system (CM1-AM2)	Permselectivity coefficients* T_{Fe}^{Al}	T_{Fe}^{Cu}	T_{Fe}^{H}	
SCM-SAM	1.23	1.57	2.55	2.13
WCM-SAM	1.27	1.32	2.49	2.00
WCM-WAM	1.07	1.30	2.06	2.35
ACM-SAM	1.03	1.70	1.72	2.50
ACM-WAM	1.01	1.51	1.75	2.06

* $T_A^B = \dfrac{[B]_f[A]_i}{[B]_i[A]_f}$

where $[A]_i$, $[B]_i$; concentration of A or B ion in the initial solution filling the compartment II, respectively; $[A]_f$, $[B]_f$; concentration of ion A or B in the final (concentrated) solution in the compartment II, respectively.

** In the first column, the values obtained for Fe-Al system were shown and in the second column, those for Fe-Cu system were presented.

(1) The order of permeabilities of these cations across the cation-selective membranes is as follows; $Fe^{3+} < Al^{3+} < Cu^{2+} < H^+$, excepting the case at the lowest current density**.

(2) This order remains invariable, independently of the various combinations of the ion-selective membranes. The permeability of the ferric ion across the alginate membrane is nearly the same as that in the other membrane systems. There is no parallel relationship between the selectivity in the ion exchange equilibria[1] and the permselectivity in this experiment, of the various ion-selective membranes.

(3) Some amount of the ferric ion transports across the anion-exchange membranes and this behavior seems to be due to the formation of a complex anion. A further investigation is carried out now, for the experimental error of this research prevents from giving a final conclusion to this problem.

The full data will be presented in the near future.

The authors wish to express their thanks to Professor T. Takahashi for his continuous advice, and to the Ministry of Education for grand-in-aid.

Institute of Industrial Science
The University of Tokyo
Yayoi-cho, Chiba

3) T. Yamabe, Y. Tanka and M. Senō, *Industrial Science (Seisan Kenkyu)*, **9**, 476 (1959).

** This order does not depend on the current density higher than 0.0083 amp./cm^2. The diffusion of ions through membrane and the migration of water due to the electro-osmosis make a contribution to the transport behavior to some extent. On this account, the concentration ratio of the metal ions shown in Table I is smaller than unity at the current density, 0.0033 amp./cm^2. When the current density is high enough and the same membrane used as AMI, the permselectivity coefficient T_A^B defined in Table II is considered to be a relative measure of the permeabilities of the cations across the cation-exchange membrane CMI.

Two Types of Antifoamers and their Cooperating Action

By Satiko OKAZAKI and Tsunetaka SASAKI

(Received February 18, 1960)

The present authors pointed out[1] that attention should he drawn to two factors, foam stability and foam producing power, to explain the phenomena of foam formation, and also that two factors should be taken into account, i. e., foam breaking action and foam inhibiting action, to elucidate the phenomena of antifoaming. In this relation we have already shown[2] that when an aqueous solution of saponin which is marked for its foam stabilizing action is mixed with an aqueous solution of alcohol which is marked for its foam producing power, a pronounced foam formation, presumably due to their cooperative or syergistic action, can be observed even in such a dilute solution as they can exhibit only

1) T. Sasaki and S. Okazaki, *Kolloid-Z.*, **159**, 11 (1958).
2) T. Sasaki, This Bulletin., **15**, 449 (1940).

TABLE I. ACTION OF ANTIFOAMERS TOWARDS AQUEOUS SAPONIN AND SODIUM DODECYL SULFATE FOAMS

Saponin Foam (0.5% aqueous solution)

Antifoamers	Before addition (foam height in cm.)	10 sec. after addition (foam height in cm.)	3 sec. after shaken again (foam height in cm.)
Silicone	10	9.4	0
i-Amyl alcohol	10	1.7	10
i-Amyl alcohol +silicone*	10	2.2	0
Ethyl acetate	10	5.5	10.6
Ethyl acetate +silicone*	10	5.6	0
Ethanol	10	7.3	11
Ethanol +silicone*	10	6.8	0

Sodium dodecyl sulfate foam (10^{-2} mol./l. aqueous solution)

Antifoamers	Before addition (Foam height in cm.)	10 sec. after addition (Foam height in cm.)	3 sec. after shaken again (Foam height in cm.)
Silicone	12	7.0	0
i-Amyl alcohol	12	0.7	12
i-Amyl alcohol +silicone*	12	2.0	0.6
Ethyl acetate	12	4.3	12
Ethyl acetate +silicone*	12	3.3	0.3
Ethanol	12	8.7	12
Ethanol +silicone*	12	6.7	0.8

* Composition of mixtures being 1 : 1 in weight. Room temperature : 16°C

a poor foam formation when each of them exists separately.

Now we can demonstrate a similar experiment also in the case of antifoaming. As we have shown,[1] silicone oil antifoamer is a well-known excellent foam inhibitor but is not always a good foam breaker, while *i*-amyl alcohol is a strong foam breaker but is not a good foam inhibitor* when added in a small amount. Now, when these two antifoamers of rather mutually opposite in the types of their actions are mixed together and a drop of the mixture is appleid onto the aqueous saponin and sodium dodecyl sulfate foams, a remarkable foam breaking action and foam inhibiting action are observed simultaneously. The results of these experiments are shown in Table 1. Similar instances may be shown for other pairs of antifoamers of the same relation. In this table we can also confirm a slight difference in antifoaming action of a given antifoamer towards different types of foams, i. e., saponin and sodium dodecyl sulfate foams. Anyhow, we can confirm distinctly the existence of two different types of antifoaming actions, i. e., foam breaking and foam inhibiting ones which have been reported merely qualitatively in many literatures,[3] and also confirm their cooperating action, though actually we can only make a rough distinction between two types of antifoamers according to these actions.

* Detailed behavior of antifoamers will be reported elsewhere.

The authors thank the Ministry of Education for the Scientific Research Expenditure given to T. Sasaki.

Department of Chemistry
Faculty of Science
Tokyo Metropolitan University
Setagaya-ku, Tokyo

3) For instance, S. Ross and J. W. McBain, *Ind. Eng. Chem.*, **36**, 570 (1944).

Preparation of a New Phototropic Substance

By Taro HAYASHI and Koko MAEDA

(Received March 1, 1960)

Under the investigation of the mechanism of chemiluminescence which occurred when lophine (2, 4, 5-triphenyl-imidazole) was oxidized in an ethanol solution of potassium hydroxide with an oxidizing agent, there was isolated a new phototropic substance which was considerd to be an imidazole derivative. To the solution of lophine (1 g.) in a solution of potassium hydroxide (12 g.) in ethanol (100 cc.), 450 cc. of 1% potassium ferricyanide aqueous solution was added during a period of 1.5 hr. with stirring by a stream of oxygen at room temperature. The violet color of the solution, which initially appeared, gradually disappeared and white precipitates, having a tinge of pale violet, separated out. When the oxidation was carried out in a dark place, a weak greenish blue chemiluminescence was observed. The precipitates were filtered and then washed with water repeatedly until the washing showed no reaction of ferricyanide ion. The precipitates, dried in vacuo (0.9g.) were dissolved in benzene to yield a deep red violet solution. When the solution was concentrated under reduced pressure, a lemon yellow crystalline substance separated out. It was recrystallized from ethanol as lemon yellow prisms, m. p. 199~201°C.

Found: C, 85.20; H, 5.50; N, 9.41. Calcd. for $C_{21}H_{15}N_2$: C, 85.38; H, 5.11; N, 9.49%.

The molecular weight in benzene solution was determined to be about 290 by a cryoscopic method. Although this compound had the composition nearly equal to that of lophine, properties of these compounds were different from each other, showing that this compound was different from lophine. This compound was soluble in ordinary solvents, giving a pale yellow or almost colorless solution. Its ultraviolet absorption spectrum showed an absorption maximum at ca 267 mμ in ethanol. This compound was also obtained by the oxidation of lophine with an ethanol solution of bromine. In this case, the bromine solution was mixed in benzene with a solution of lophine in ethanolic potassium hydroxide. A mixture of ethanol solution of this compound with 4% aqueous solution of potassium ferrocyanide, which yielded white precipitates, was warmed in a water bath for 1 hr. and then water was added until white precipitates dissolved in a solution. The solution was evaporated to give white precipitates which were recrystallized from ethanol and identified to be lophine.

This compound showed a marked phototropy; when it was irradiated with sun light or light of mercury lamp in a solution of organic solvent as well as in solid at room temperature, it rapidly turned red violet, both in air and in vacuo. The absorption spectrum of the red violet solution showed absorption maxima at 350 and 550 mμ in benzene. In solid the red violet color faded slowly at room temperature but rapidly when the colored substance was warmed in a water bath. In solution the color faded rather rapidly even at room temperature. When the benzene solution of this phototropic substance was irradiated, no change of the molecular weight was observed. When nitrogen oxide gas was passed through the red violet benzene solution, the color immediately disappeared. This fact shows that the red violet coloration is due to the formation of a free radical. Electron spin resonance absorption was detected with this red violet substance in benzene solution as well as in solid[1]. The solution of this compound exhibited thermochromism.

From the results mentioned above, it is considered that the red violet form is an oxidation product of lophine which is a free radical $C_{21}H_{15}N_2$ (I), while the lemon yellow form may be a rather labile meso ionic form.

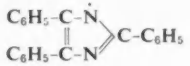

(I)

1) The results of the investigation by electron spin resonance absorption and spectroscopic methods will be published in the near future, T. Hayashi and K. Maeda, *J. Chem. Phys.*, in press.

Department of Chemistry
Faculty of Science
Ochanomizu University
Bunkyo-ku, Tokyo.

Hydrogenation and Hydrogenolysis. III[1]. *Rhodium-Platinum Oxide as a Catalyst for the Hydrogenation of the Aromatic Nucleus*

By Shigeo NISHIMURA

(Received March 10, 1960)

It has been shown in these two decades that rhodium is useful as a catalyst for the hydrogenation of various organic compounds[2], and recently that it is specially effective for the hydrogenation of the aromatic nucleus[3-5]. However, most of the works on rhodium catalysts are concerned with the use of colloidal or supported rhodium, and none with the use of rhodium oxide of Adams' type. It seem that this is because of the difficulty of reducing rhodium oxide to the metal form under mild conditions[6].

The present author prepared a useful catalyst consisting of rhodium oxide and platinum oxide in a ratio of 3:1 by the weights of the metals, by fusion of the mixture of rhodium chloride and chloroplatinic acid or ammonium chloroplatinate with sodium nitrate exactly in the same way as in the preparation of Adams platinum oxide[7]. This rhodium-platinum oxide[8] can be reduced with hydrogen to rhodium-platinum

1) Part II of this series: S. Nishimura, This Bulletin, 32, 1155 (1959).
2) For earlier literatures, see Refs. 3 and 5.
3) L. D. Freedman, G. O. Doak and E. L. Petit, *J. Am. Chem. Soc.*, 77, 4262 (1955).
4) H. A. Smith and R. G. Thompson, "Advances in Catalysis", Vol. 9, Academic Press Inc., New York (1957), p. 727.
5) G. Gilman and G. Cohn, ibid., p. 733.
6) Cf. Ref. 4, p. 732. This difficulty was also confirmed by the present author.
7) R. Adams, V. Voorhees and R. L. Shriner, "Organic Syntheses", Col. Vol. I, 2nd Ed., John Wiley & Sons, Inc., New York (1941), p. 463.
8) The mixed oxide thus prepared, is not identical with the mere mixture of rhodium oxide and platinum oxide, the former being reduced with hydrogen much more rapidly and uniformly than the latter.

TABLE I. HYDROGENATION OF AROMATIC COMPOUNDS WITH RHODIUM-PLATINUM OXIDE AND PLATINUM OXIDE AS CATALYSTS AT THE ORDINARY TEMPERATURE AND PRESSURE[a]

Compound	Amount, g.	Catalyst, g.	Hydrogen uptake, mol./mol.	Time for complete hydrogenation, min.
Methylphenylcarbinol	0.611	Rh-Pt, 0.05	3.04	36
〃	〃	Pt, 0.20	3.87	80
Benzhydrol	0.553	Rh-Pt, 0.05	6.03	105
〃	〃	Pt, 0.20	6.73	120
Phenol	0.471	Rh-Pt, 0.05	3.04	14
〃	〃	Pt, 〃	3.35	40
Anisole[b]	0.541	Rh-Pt, 〃	3.04	18
〃	〃	Pt, 〃	3.45	85
Cinnamyl alcohol[c]	1.342	Rh-Pt, 〃	1.04	11
〃	〃	Pt, 〃	1.31	26
Benzene[d]	0.781	Rh-Pt, 〃	2.99	20
〃	〃	Pt, 〃	2.99	80
Ethyl benzoate	0.751	Rh-Pt, 〃	3.02	21
〃	〃	Pt, 〃	3.00	120

a) 20 cc. of glacial acetic acid was used as solvent.
b) Smith and Thompson (Ref. 4) reported that anisole absorbed 3.06 mol. of hydrogen with 5% rhodium on alumina and 3.40 mol. with Adams platinum oxide in acetic acid at 30°C under initial hydrogen pressures of 40–60 p. s. i.
c) Reduction to 3-phenyl-1-propanol and propylbenzene.
d) Gilman and Cohn (Ref. 5) reported that 5 ml. of benzene was hydrogenated four times as rapidly with 1 g. of 5% rhodium on alumina as with 1 g. of 5% platinum on alumina in acetic acid under ordinary conditions.

black in neutral ethanolic or acetic acid suspension at the ordinary temperature and pressure. The reduction begins in about twenty minutes and completes in about forty minutes in acetic acid at 25°C. The rhodium-platinum black thus prepared is an excellent catalyst in the hydrogenation of various aromatic compounds in acetic acid under ordinary conditions as shown in Table I. With this catalyst, methylphenylcarbinol, benzhydrol, phenol, anisole and cinnamyl alcohol are reduced rapidly and quantitatively to the corresponding saturated compounds with far less portions of hydrogenolysis than with Adams platinum oxide as indicated by the moles of hydrogen absorbed. The catalyst is four and six times as active as Adams platinum oxide in the hydrogenation of benzene and ethyl benzoate, respectively, where the hydrogen uptake is equally 3 mol. with both catalysts. Thus the results show that the rhodium-platinum catalyst retains to a large extent the nature of pure rhodium catalysts and is substantially superior to Adams platinum oxide both in activity and in selectivity in the hydrogenation of the aromatic nucleus. Details will follow.

The author wishes to express his hearty thanks to Professor Y. Urushibara for his continued encouragement.

Department of Chemistry
Faculty of Science
The University of Tokyo
Hongo, Tokyo

The Synthesis of the Pterocarpin Ring System[1]

By Hiroshi SUGINOME and Tsukasa IWADARE

(Received March 1, 1960)

The structures of pterocarpin and homopterocarpin, the minor principles of *pterocarpus santalinus*, were elucidated in 1940 by Robertson and Whalley and by Späth and Schläger[2] as III, R_1=R_4=OMe, R_2, R_3=–O–CH_2–O–, and III, R_1=R_3=OMe, R_2=R_4=H, respectively. However, the syntheses of pterocarpin and homopterocarpin have not been hitherto completed.

This paper presents the syntheses of the

1) Oxygen heterocycles. (II). Previous paper in this series, Hiroshi Suginome, *J. Org. Chem.*, **24**, 1655 (1959).
2) A. Robertson and W. B. Whalley, *J. Chem. Soc.*, **1940**, 787; **1954**, 1440; E. Späth and J. Schläger, *Chem. Ber.*, **73**, 1 (1940).

simple core of pterocarpin, III, R_1=R_2=R_3=R_4=H, and compound V, as shown in the annexed chart, which establish a synthetic route to DL-pterocarpin and DL-homopterocarpin or their isomers.

In view of a possible biogenetic link[1,3,4] of pterocarpin and homopterocarpin to naturally occurring 2'-hydroxyisoflavonoids, the synthetic sequence, I→II→III, is of particular interest.

Mild acid hydrolysis of 2,2'-bis(methoxymethoxy) benzoin, m. p. 104~104.5°[5]. (Found: C, 64.79; H, 5.59. Calcd. for $C_{18}H_{20}O_6$: C, 65.09; H, 6.02%) afforded 2,2'-dihydroxybenzoin, m. p. 161~163°C[6] (Found: C, 68.48; H, 5.02. Calcd. for $C_{14}H_{12}O_4$: C, 68.84; H, 4.95%), accompanied by a small amount of an unidentified substance, m. p. 156~157°C, I. R. bands at 1627 cm^{-1} (conjugated carbonyl) and 3200 cm^{-1} (broad hydroxyl band).

2,2'-Dihydroxydesoxybenzoin, m. p. 102~103°C, readily prepared from above 2,2'-dihydroxybenzoin and from the unidentified substance, m. p. 156~157°C, by zinc-alkali reduction, was converted into 2'-hydroxyisoflavone (I), m. p. 153°C (Found: C, 75.67; H, 4.45. Calcd. for $C_{15}H_{10}O_3$: C, 75.62; H, 4.23%), I. R. bands at 1621 cm^{-1} (γ-pyrone carbonyl) and 3187 cm^{-1} (phenolic hydroxyl), with ethyl formate and sodium. No isomeric 3-benzoylcoumarone (VI) could be isolated from the reaction mixture. The isoflavone (I) was reduced to an amorphous stereoisomeric mixture of 2' hydroxyisoflavan-4-ol (U. V. spectrum: λ_{max}(ethanol) 275 mμ) by $NaBH_4$[7] or $LiAlH_4$.

The successful intramolecular dehydrocyclization of this amorphous diol by mild treatment in acidic medium, led to compound III, R_1=R_2=R_3=R_4=H, m. p. 125~126.5° (Found: C, 79.83; H, 5.49. Calcd. for $C_{15}H_{12}O_2$: C, 80.33; H, 5.39%) (U. V. spectrum; λ_{max}(ethanol) 278 mμ(ε; 3260). I. R. No band in the region 3000~3500 cm^{-1}), without any proof of stereochemical assignment of B/C ring junction.

On the other hand, catalytic hydrogenation of 2'-hydroxyisoflavone (I) in glacial acetic acid with Adams's platinum oxide as a catalyst, gave the corresponding 2'-hydroxyisoflavanone, m. p. 118~122°C. I. R. bands at 1660 cm^{-1} (conjugated carbonyl) and 3297 cm^{-1} (associated phenolic hydroxyl), which was converted into anhydro-compound V,[1] m. p. 80~83°, U. V. spectrum; λ_{max}(ethanol) 331, 299, 286, and 239 mμ (ε; 11190, 7350, 7240, and 11740), in a good yield by treatment in acidic medium.

The synthesis of homopterocarpin along the above synthetic line is now in progress.

Full details of this work will appear shortly.

The authors are grateful to Professors Toshi Irie, Takeshi Matsumoto and Tadashi Masamune for their interest and encouragement in this work.

Department of Chemistry
Faculty of Science
Hokkaido University
Sapporo

3) W. B. Whalley, *J. Chem. Soc.*, **1956**, 3224.
4) Also cf. R. Robinson, "The Structural Relations of Natural Products", Oxford Univ. Press, London (1955), p. 41.
5) F. B. Laforge, *J. Am. Chem. Soc.*, **55**, 3040 (1933). F. B. Laforge records b. p. 200~210°C/1 mmHg.
6) F. B. Laforge records m. p. 142~149°C. (Ref. 4).
7) M. Miyano and M. Matsui, *Chem. Ber.*, **91**, 2044 (1958).